Resource Planning Committee

June 4, 2020 Hearings

Additional Materials

Thomas Jordan

Conditional Use Permit Hearing

Correspondence in Favor

Regarding a Conditional Use Permit allowing non-metallic mining for Parcel #0280432343033B.

May 14, 2020

Dear members of WIZAP and the Washington Island Town Board,

We would appreciate it if we could add the following updates to the letter we emailed to you on May 12, 2020, a copy of which is also included below this letter.

The updates, and the paragraphs of the letter to which they apply are as follows:

Under #1. Dust - Also, as required by the Door County Soil and Water Conservation Department and as specified in our engineering site plans, the dirt driveway will be removed and a new stone driveway will be installed, further reducing dust issue possibilities.

Under #6. Hours - We would reduce hours to the following: We would limit the hours in which we would access the mine for product to between 8:00 am and 5:00 pm, Monday - Friday. The only exception to this would be when, should a company from the Mainland be hired to crush, we would follow Town / County working hours guidelines. Again, as stated in the attached letter below, if we hire a company to crush, we expect an interval of years between each time this would occur.

Under # 7. Estimated Material Usage - Based on past usage by the concrete plant, we are estimating usage to be 1500 cubic yards +/- per year meaning the 7800 to 8500 cubic yard amount could last 5+ years.

Thank you very much. Please contact either of us should you have any questions concerning this additional information.

Best Regards,

Tom Jordon (920)559-0134

Julian Hagen (920)559-2356

Letter sent May 12, 2020

Regarding a Conditional Use Permit allowing non-metallic mining for Parcel #0280432343033B.

6. Hours - We would limit the hours in which we would access the mine for product to between 8:00 am and 5:00 pm on week days, from 9:00 am to 12:00 noon on Saturday, and would be closed for operation on Sunday. The only exception to this would be when, should a company from the Mainland be hired to crush, we would follow Town / County working hours guidelines. Again, as stated, if we hire a company to crush, we expect an interval of years between each time this would occur.

7. Estimated Material Usage: For the sake of perspective, one foot deep times the mine site area would represent almost 6500 cubic yards of material. When rock is crushed to a smaller size, spaces are created between the stones causing this 6500 cubic yards to increase in volume 20% to 30%, to between 7800 to 8500 cubic yards.We are estimating usage to be 1500+/- cubic yards per year.

8. We are aware that additional noise pollution will have an impact and we will be aware of this. We will also attempt to keep the use of our truck's Jake brake to a minimum.

In closing, we hope this helps give clarity to the questions and concerns. Do not hesitate to email us if you have any questions. If calling is preferred, please feel free to call either of us at the following numbers: Tom at (920)535-0134 or Julian at (920)559-2356.
Thank you.

Best regards,

Tom Jordon

Julian Hagen

Thomas Jordan
Conditional Use Permit Hearing
Correspondence in Opposition

Riemer, Linda

From: Leif Thoreson <dualtyme6@aol.com>
Sent: Tuesday, June 2, 2020 11:53 AM
To: Riemer, Linda
Subject: 04June20 Resource planning meeting

RECEIVED
JUN 02 2020
DOOR COUNTY
LAND USE SERVICES DEPARTMENT

Leif S. Thoreson
Norma E Thoreson
1292 East Side Rd
Washington Island, WI 54246
608-449-5053
dualtyme6@aol.com

Thank you for allowing us to voice our concerns concerning a CUP that Tom Jordan requests for a non-metallic mine at 1342 East Side Rd. Washington Island, WI. Section 32, Town 34 North, Range 30 East and in a General Agricultural (GA) zoning district.

We have concerns about the noise, dust, decreased property values, and increased traffic on Town Line Rd and East Side Rd. Please remember that East Side Road is heavily traveled during "dump" days, as the dump is also on that road. And lets not forget the environmental issues and concerns as well. Granted, this is not a subdivision you would see in a town setting, but still, we are a residential neighborhood nonetheless. We value our quiet, our peaceful surroundings, and our fresh air.

We moved to this Island for the purpose of the peace and tranquility that we experienced when we visited here during the summer of 2018. We went back home to Janesville, put our homes on the market and decided to make Washington Island our home. We brought my parents here so we could care for them in their golden years. They both have compromised immune systems, and the great air quality was a plus in bringing them here to the Island, as was the quiet.

My concern with the traffic, because it was stated in their original assessment that East Side Rd was a lightly traveled road. That is not true. With the dump days Monday, Wednesday, and Saturday, and now in the summer Friday as well. East Side Road and Town Line Roads get very busy. Sometimes a steady stream of traffic, at times like being on Highway 42/57 in the County. We live on the corner, so we do see traffic coming from all directions. I can't tell you the number of near-miss accidents I've seen on the corner on dump days. Now lets add dump trucks into the equation.

The noise: Just two weekends ago Mr. Jordan was working over on his property and the winds were out of the Northeast, which is where they are most prevalent for the past few years strange as that may be, but it pushed all the noise they were making right into our yard where we were outside working. The endless beeping of the back-up alarm on his equipment, the banging of the bucket up and down on his equipment was nerve wracking. We had no peace while we were outside trying to enjoy our surroundings. That noise continued until well after 2:00 in the afternoon...Not why we moved here!!

Another operation similar to the one Mr. Jordan wants was recently given approval. Do you really think its necessary for yet another mine to be here on the Island? What value does it bring us? What economic gain does it gain anyone here on this Island? We feel that it is going to bring nothing but resentment to those of us living around the site of this proposed mine because of all the noise, dust, traffic, and environmental impact. We all feel it will bring our property values down. Ask them how they would like a mine and all the noise associated with it to be right next to their homes.

This letter is for those of you who do not live here and do not realize how much we cherish our quality of life we are grateful for and respect. WIZAP did the right thing voting against this and the town board only passed this measure by one vote. We plead with you to vote against this CUP so that we can retain our quality of life, our property values, and safety.

We thank you greatly for listening to our concerns.

Sincerely,
Leif and Norma Thoreson

RECEIVED

MAY 28 2020

DOOR COUNTY
LAND USE SERVICES DEPARTMENT

JUST THE FAX

Washington Island Ferry Line
P.O. Box 39
Washington Island, WI 54246

wisferry.com

Phone: 800-223-2094
Fax: 920-847-2807

Date: 05-26-20

To: RESOURCE PLANNING Committee
Attn: DAVID ENGIL

Number of Pages: 3

From: Jeannette Hansen
1361 East Side Road

Remarks:

For the resource committee vote on June 4th per a mine permit for Mr. Jordan and Mr. Hagen on East Side Road Washington Island

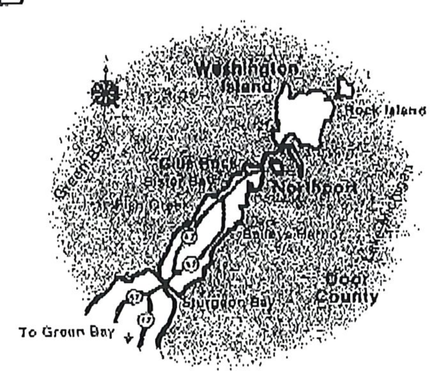

SWEET MOUNTAIN FARM

David Enigl, Chairman
Door County Resource Planning Committee
c/o Door County Land Use Services Department
421 Nebraska Street
Sturgeon Bay, WI 54235

May 27, 2020

Dear Mr. Enigl:

The quarry placement on Gunnglusson Road, Washington Island does not have my support for four significant reasons. A quarry is harmful to my health, apiary business, ongoing research, and the peaceful environment I moved here to enjoy.

Asthma is a debilitating condition. Clean air is critical to my quality of life.

Sweet Mountain Farm, LLC raises and sells over 100 Russian honeybee nucleus colonies each year on its 18 acre farm and keeps between 120-170 colonies for breeding and research. The business began eleven years ago. The land was selected for its pristine environment conducive to raising a highly sought after local, cold hardy, mite resistant honeybee. Beekeeping is my livelihood. Colonies are sold to beekeepers throughout Wisconsin. A healthy environment is needed to breed healthy honeybees. Vibration causes aggressive bees and disrupts larval development. Dust adheres to thousands of tiny hairs found on the bee's body. Dust particles are transferred back to the hive and stored along with the pollen. This is one cause of colony collapse given the dust laden pollen is fed to the queen and the brood.

Working with the Department of Consumer Trade and Consumer Protection (DATCP), research proposals are submitted on the effects lavender has on honeybee health as well as a project on Russian honeybees being more effective cold weather pollinators. This research would end given a change in environmental factors that could potentially affect the outcome.

If you have any questions about my objections to situating a quarry in close proximity to my land, please let me know so we can discuss this further.

Sincerely,

Sue A. Dompke

Sue A. Dompke
Sweet Mountain Farm, LLC
1402 Mountain Road
Washington Island, WI 54246
920-847-2337
www.sweetmountainfarm.com
info@sweetmountainfarm.com

RECEIVED

MAY 2 8 2020

DOOR COUNTY
LAND USE SERVICES DEPARTMENT

Zoning meeting June 4th

To Mr. Rick Brauer and members of the Door County Zoning committee.

I would like to express my opposition to the conditional use permit on East Side Road you are going to vote on for Washington Island.

Our Island zoning committee voted NO to the application yet our town board said yes. I live directly across the road from the property in question. I believe this will damage our land quality and have the possibility to ruin wells and or foundations once the blasting starts. Makes me wonder if you have all come to the Island to look this land over? Yes , they say it most likely will not do any damage to wells or foundations but what if ?

The negative impact this could have here is great! There will be records kept on truck traffic , pollutants, heavy equipment, dust and noise correct ? I feel very strict guidelines need to be in place. Please make this happen.Who can the neighbors call or write when rules are broken ? Will the DNR come to look and have records about the Heinz Emerald Dragon Fly ? Such a shame you can allow them to ruin this beautiful road here not to mention what will happen with the dragon fly.

Once again , does Washington Island 35 square miles, REALLY need two mines? Please give this your consideration before you vote to approve this mine which most are opposed to happening. And think of the well being of the Island as a whole if you let this take place.

Thanks for your time.
Jeannette Hanlin

Jeannette Hanlin

Brauer, Rick

From: Carol Johnson <magotsrus@yahoo.com>
Sent: Sunday, May 31, 2020 11:34 AM
To: Brauer, Rick
Subject: Non-metalic mining permit for Jordan/Hagan tax parcel #0280432343033B

Sir,
My name is George Johnson and I have been a summer resident on Washington Island for over thirty years. I live on East Side Road and understand that Tom Jordan has purchased property on this same road, not too far from me. He has applied for a Conditional Use Permit on Tax Parcel #0280432343033B to operate a gravel pit where MINING, BLASTING, and CRUSHING will take place. East Side road is not only residential, but is zoned GA and "light industry", but I have a hard time believing that MINING, BLASTING, and CRUSHING gravel would be considered "light industry. Washington Island is approximately four miles by eight miles and already has three operating gravel pits. Do we really need another???
East Side Road is traveled by more than half of the Islanders at least one or two times a week on their way to the town dump. Again...this is a residential road where we have enjoyed peace, quiet, and clean air, which will all change if this endeavor is allowed to happen. Imagine the NOISE, DUST, and the added TRAFFIC of heavy trucks going back and forth on a daily basis.
I also can't help feeling that this "light industry" is going to lower the value of my property and that of all the other residents in the area, possibly fracturing our foundations, and/or fracture our wells contaminating our water. If you do choose to issue this permit I would ask that there is a condition stipulated that Mr. Jordan will purchase a certificate of additional insurance naming residents that will be affected, covering structural damage, contamination of water supply, and damage to wells and septic systems, all of which are in very good working order at this time.
This area is also a habitat for the Hine's Emerald Eyed Dragonfly, which was considered extinct and is now federally protected as an endangered species. Of the four states that are currently known to habitat these dragonflies, Door County has the largest population, which will be compromised.
In closing, I doubt very much that any one of you board members would choose to live this close to a business that you could not only HEAR but TASTE because of the dust hanging in our once clean air EVERY DAY! I strongly urge you to DENY the issuance of a permit of any kind for this business in a residential area.

George Johnson
1427 East Side Rd.
Washington Island Wi.

RECEIVED
JUN -2 2020
DOOR COUNTY
LAND USE SERVICES DEPARTMENT

MAY 24, 2020

SCOT LACE - DENNIS BUETTNER
1362 MOUNTAIN ROAD P.O. BOX 236
WASHINGTON ISLAND WI 54246
920.421.8000

TO THE DOOR COUNTY RESOURCE PLANNING COMMITTEE
DAVID ENIGL, CHAIR
VINNI CHOMEAU, ROY ENGLEBERT, KEN FISHER
AND RICHARD VIRLEE - MEMBERS.

RE: JUNE 4, 2020 - AGENDA ITEM 6.2
CONDITIONAL USE PERMIT APPLICATION.
THOMAS JORDAN, ESTABLISH NONMETALLIC MINE
ON 3.94 ACRES OF 10.17 ACRE PARCEL, DIRECTLY
NORTH OF 1342 EAST SIDE ROAD; GENERAL
AGRICULTURAL (GA) ZONING DISTRICT, WASHINGTO[N]

AS RESIDENTIAL OWNERS OF 5 ACRES - 1362 MOUNTAIN ROAD - LOCATED DUE WEST OF 1342 EAST SIDE ROAD, WE HAVE NUMEROUS AND SERIOUS CONCERNS REGARDING MR. JORDANS REQUEST.

THE LOCATION - PARCEL #028-04-32343033, IN QUESTION IS LOCATED IN AN EXISTING <u>RESIDENTIAL AREA</u>. THE PROPOSED NON-METALLIC MINE IS NOT APPROPRIATE IN ITS

PROXIMITY TO ESTABLISHED RESIDENCES,

WITHOUT QUESTION, OUR QUALITY OF LIFE WILL BE IMPACTED NEGATIVELY BY EXCESSIVE NOISE FROM MINING OPERATIONS - DYNAMITE BLASTING, CRUSHING, LOADING AND HAULING.

OUR AIR QUALITY WILL BE NEGATIVELY REDUCED BY EXCESSIVE DUST GENERATED BY MINING OPERATIONS.

THE POSSIBILITY OF OUR WATER QUALITY DETERIORATING BY WELL CONTAMINATION EXACERBATED BY FRACTURING OF THE DOLOMITE DUE TO DYNAMITE BLASTING.

AS RESIDENTIAL LAND OWNERS WE ARE VERY MUCH OPPOSED TO THIS REQUEST FOR USE AND CONCERNED ABOUT THE NEGATIVE IMPACT ON OUR QUALITY OF LIFE AND POTENTIAL LOSS OF VALUE OF OUR PROPERTY.

RESPECTFULLY, SCOTT LACE

[signature]

DENNIS R. BUETTNER

Dennis R. Buettner

Brauer, Rick

From:	Juliann B.Gardner <juliann@onesmallgarden.com>
Sent:	Friday, May 29, 2020 9:28 AM
To:	Riemer, Linda
Cc:	Brauer, Rick
Subject:	June 4th Zoning Board
Attachments:	WiWi EastSide mining ltr_26May20.pdf; ATT00001.htm

Linda:

Attached please find my letter to the Door County Zoning Board in reference to the Jordan/Hagan Nonmetallic mine proposal on Washington Island,WI. Please enter into the records packet for the June 4th meeting.

There are certainly other issues regarding this proposal that I plan on bringing up at the meeting.

Thank you,

Ted Gardner
1096 Townline Road, Washington, WI 54246
513.497.7245 e: tedstoystore@zoomtown.com

May 27, 2020

Rick Brauer, Zoning Administrator
Door County Government Center
421 Nebraska Street
Sturgeon Bay, WI 54235

E: rbrauer@co.door.wi.us

Town of Washington
c/o Valerie Carpenter
P.O. Box 220
Washington Island, WI 54246

E: townoffice@washingtonisland-wi.gov

Re: Washington Island CUP, Parcel ##0280432343033B

Dear Door County Board members:

I am writing regarding your consideration of the Conditional Use Permit application for rock mining on Washington Island, applicants Jordan and Hagan. Like other residents and property owners of Washington Island, we have previously submitted our objections to this permit and listed the negative impacts of this proposed blasting, mining and crushing operation. Please distribute this letter to those with authority to consider or grant the subject permit.

Our residential property is situated in the northeast quadrant of Town Line and East Side Roads, immediately south of the proposed mining site. My wife Juliann and I have been improving our island home over the past year with the intent of moving in as soon as practical. We and our neighbors are concerned about issues such as public safety and community well-being, environmental quality (air, water, noise, visual), increased truck traffic, and other negative impacts.

If a mining / processing permit is allowed, we ask that you consider the following suggestions for mandatory requirements to reduce negative impacts on the immediate area and the community:

1. Maximum amounts of rock extraction and processing should be spelled out (e.g. X cu. yd. per month or year);

2. Maximum hours of operation should be 9:00am – 5:00pm weekdays only;

3. A professionally prepared site plan should be required, fully illustrating the allowable area boundaries for rock extraction, required setbacks and visual / acoustic buffers, locations of proposed rock-crushing, material storage, vehicle maintenance and hazardous materials storage, perimeter earth berms with landscaping, etc.;

4. The use of adjacent parcels for mining-related activity should not be allowed (i.e. mining equipment or vehicles, material processing and storage, offices or employee facilities, etc.;

5. Any rock mining activities, including drilling for explosive charges, should adhere to a prescribed schedule that is made available to the public;

6. Water quality monitoring and reporting protocols should be enacted to assure no negative impacts on quantity and quality of subsurface and/or surface water;

7. Air scrubbers, site watering and other measures should be mandated to reduce dust transmission and assure no negative impacts on the area's air quality;

8. Commercial traffic into, within, and out of the subject site should be limited to 9:00am – 5:00pm weekdays only, monitored and enforced. The use of truck air brakes should be strictly prohibited. Site entry drive turning lanes and intersection improvements at Town Line and East End may be warranted. Earth berms should be required to help reduce the off-site impacts of back-up warning horns of mining and transport operating equipment;

9. The primary quarry / process plant access (East Side Road) should be direct into the parcel and <u>not</u> on the existing Jordan property dirt road, which is immediately adjacent to our shared property line ±60 feet north of our residence.

10. Applicant's site plan should show the existing and proposed topography and vegetation at all perimeter areas of the subject site. This should include large earth berms and planting schemes to provide visual and acoustic screening of the site prior to operations commencing. A site remediation plan should be required to show how the land will be brought into acceptable condition as various extracted areas are depleted in phases or abandoned; final site conditions and proposed land use should be delineated.

There may be other supporting conditions proposed by our neighbors on Washington Island, and we sincerely appreciate your time and consideration of these important factors. Please feel free to contact me directly if we can discuss these matters in further detail.

With best regards,

Ted Gardner
513.497.7245

To whom it may concern:

We are neighbors to the proposed nonmetallic mine on East Side Road and are concerned about the impact this would have to our home directly across the street, and to the neighborhood we live in.

This road is already a busy one on days the Island dump is open, to add further traffic and debris to the area would exacerbate this issue. We have young children and like to walk on our road.

Will a mine going in across the street affect our property value? Could blasting affect our homes structure as well, or the quality of our well. We know that blasting won't be an every day event, or hauling for that matter, but feel it still will be impactful.

If you haven't been up to the Island to see the proposed site, it's hard to understand the area. There are many homes and families in very close proximity. It's not in the midst of an industrial area. When I take a walk, the vehicles that pass are my neighbors, not dump trucks or mixers. We are a residential neighborhood, and the addition of a mine could affect the natural beauty and feel of where we live.

We understand the island's need for gravel, and were glad to hear when another gravel pit was recently approved in a much more appropriate location. Why could this latest mine not be in a similar location away from homes.

We fear this will be opening the door to more noise, mess, and disruption. Thank you for taking the time to consider our concerns.

Sincerely,
Pete and Lydia Nikolai

RECEIVED
JUN 3 2020
DOOR COUNTY
LAND USE SERVICES DEPARTMENT

Brauer, Rick

From: jim lind <jimllind@yahoo.com>
Sent: Wednesday, June 3, 2020 2:43 PM
To: Brauer, Rick
Subject: Conditional Use Permit / nonmetallic mine June 3, 2020

Dear Resource Board, This letter is concerning the conditional use permit requested by Thomas Jordan for a nonmetallic mine on Washington Island. To give a little backround I own the 5 acres directly across the road from the proposed mine and I strongly oppose this attempt at destroying the land for personal gain. I had originally planned on building my retirement home on this property but if this is allowed to proceed I will have to scrap my plans. Now for the facts and information, because of the town dump being a half mile down the road traffic on dump days is already extremely heavy now with the addition of Mr. Jordans construction business on the adjacent lot to the mine property there is constant truck and equipment traffic noise and dust all day. Next for surface water drainage, for 3 days straight Mr. Jordan hauled truckloads of manure and dumped it at the proposed mine site now there is a pile as big as a house on which he grinds with a big noisy machine creating an actual manure dust storm. That has to be very unhealthy for anyone in the vicinity its a good thing I already have a mask, my son wont bring my grandchildren over to the property anymore because of the dust,noise and smell. What happens when it rains? Where does the runoff go? There is no containment in place and with the land being mostly rock this sewage runoff can go a long ways. The land does not perk for a conventional septic so what will happen to our wells? Why is manure needed for a mine? So many questions so few answers. As far as potential change in natural vegetation and topography this land has already been clear-cut to about 90% it actually looks like a war zone not a tree or bush standing. There is no visual harmony of buildings with the neighborhood because he already built 2 giant storage buildings on the adjacent property and no one knows whats in store for the proposed mine property. Of course this has been very detrimental to the property values. I had a standing offer to purchase my property if I ever wanted to sell which was recently rescinded. They said with all this going on they had lost interest and who could blame them? What with a proposed mine, a giant smelly manure pile, constant construction traffic noise dust and dirt directly across the street I ask you can it get any worse? How can this even be considered in what was a beautiful neighborhood with families living here this is definitely not compatible.

Finally I plead with the RPC to carefully consider all the negative aspects this proposed conditional use permit will bring and deny it once this door is opened its too late. Nothing good can come from this its just a man wanting to make money by destroying the land and his neighbors. Thank You, James D. Lindgren

Riemer, Linda

From: James Smith <james@doorcounty.attorney>
Sent: Wednesday, June 3, 2020 3:29 PM
To: Riemer, Linda
Subject: Re: RPC Meeting 6/4/2020
Attachments: Effect of Rock Mining on Local Residential Property Values within 1 Mile of Proposed Mine.pdf; Crushed Limestone Safety Data Sheet.pdf; Karst Map.pdf; The Value-Undermining Effects of Rock Mining on Nearby Residential Property.pdf; Delineation of areas contributing groundwater to springs and wetlands supporting the Hine's Emerald Dragonfly, Door County, Wisconsin.pdf; Potential Environmental Impacts of Quarrying Stone in Karst - A Literature Review.pdf; US Study on the Impact of Pits Quarries on Home Prices.pdf

Good Afternoon Linda,

Please find attached hereto documents to which I will be referring during my testimony in front of the RPC tomorrow.

If you have any questions or concerns, please do not hesitate to contact me.

Best regards,

James

THE LAW OFFICE OF JAMES R. E. SMITH, S.C.
Sturgeon Bay, WI 54235
(920) 724-1754
www.doorcounty.attorney

On Wed, Jun 3, 2020 at 12:19 PM James Smith <james@doorcounty.attorney> wrote:

> Much appreciated, Linda!
>
> THE LAW OFFICE OF JAMES R. E. SMITH, S.C.
> Sturgeon Bay, WI 54235
> (920) 724-1754
> www.doorcounty.attorney
>
>

prohibited. If you have received this transmission in error, please destroy it and notify us immediately at 920-724-1754.

On Wed, Jun 3, 2020 at 12:19 PM Riemer, Linda <lriemer@co.door.wi.us> wrote:

Thanks Jim. I will put you down to speak in opposition.

Enjoy your day.

Linda Riemer

Door County Land Use Services Department

Door County Government Center

421 Nebraska Street |Sturgeon Bay, WI 54235

(P) 920-746-2323 | (Fax) 746-2387

Email: lriemer@co.door.wi.us | Website: https://www.co.door.wi.gov/164/Land-Use-Services

From: James Smith <james@doorcounty.attorney>
Sent: Wednesday, June 3, 2020 12:00 PM
To: Riemer, Linda <lriemer@co.door.wi.us>
Subject: RPC Meeting 6/4/2020

To Whom It May Concern:

Please be advised that I intend to provide live oral testimony regarding the CUP for mining on Washington Island at the RPC meeting tomorrow, June 4, 2020.

Name: James R. E. Smith

Addres: 1236 Bluebird St, Sturgeon Bay, WI 54235

Cell: 920-724-1754

I wish to speak in opposition to the granting of the CUP.

Sincerely,

James

This is a transmission from The Law Office of James R. E. Smith, S.C. and may contain information which is privileged, confidential, and protected by the attorney-client privilege or attorney work product privilege. If you are not the addressee, note that any disclosure, copying, distribution or use of the contents of this message is prohibited. If you have received this transmission in error, please destroy it and notify us immediately at 920-724-1754.

EFFECT OF ROCK MINING ON LOCAL RESIDENTIAL PROPERTY VALUES WITHIN 1 MILE OF PROPOSED MINE				
STREET ADDRESS	**OWNER**	**EFMV**	**3.7% of EFMV***	**14.5% of EFMV****
1462 RANGE LINE RD	BARBER	$273,513	**$10,120**	**$39,659**
1544 RANGE LINE RD	GRAHAM	$117,400	**$4,344**	**$17,023**
1602 RANGE LINE RD	WALLMAN	$336,843	**$12,463**	**$48,842**
1703 MOUNTAIN RD	HERSCHBERGER	$237,100	**$8,773**	**$34,380**
1271 JACKSON HARBOR RD	HENKEL	$320,500	**$11,859**	**$46,473**
1740 MOUNTAIN RD	MUNAO	$194,303	**$7,189**	**$28,174**
1724 MOUNTAIN RD	WOLD	$162,100	**$5,998**	**$23,505**
1702 MOUNTAIN RD	GILBERTSON	$189,700	**$7,019**	**$27,507**
1680 MOUNTAIN RD	FLASCH	$181,986	**$6,733**	**$26,388**
1662 MOUNTAIN RD	NIKOLAI	$296,200	**$10,959**	**$42,949**
1641 MOUNTAIN RD	HERSCHBERGER	$279,900	**$10,356**	**$40,586**
1610 MOUNTAIN RD	ELLEFSON	$186,714	**$6,908**	**$27,074**
1592 MOUNTAIN RD	ELLEFSON	$167,000	**$6,179**	**$24,215**
1554 MOUNTAIN RD	JOHNSON	$292,400	**$10,819**	**$42,398**
1538 MOUNTAIN RD	ELLEFSON	$272,500	**$10,083**	**$39,513**
1463 MOUNTAIN RD	HUFFMAN	$212,300	**$7,855**	**$30,784**
1403 MOUNTAIN RD	JORGENSON	$212,900	**$7,877**	**$30,871**
1402 MOUNTAIN RD	DOMPKE	$166,674	**$6,167**	**$24,168**
1384 MOUNTAIN RD	SHAUSKE	$333,200	**$12,328**	**$48,314**
1362 MOUNTAIN RD	BUETTNER	$82,423	**$3,050**	**$11,951**
972 EAST SIDE	VAN HOWE	$243,400	**$9,006**	**$35,293**
1076 MICHIGAN RD	DANFORTH	$217,500	**$8,048**	**$31,538**
1216 MICHIGAN RD	BONNIN	$355,500	**$13,154**	**$51,548**
1234 MICHIGAN RD	SCHULTZ	$251,400	**$9,302**	**$36,453**
1256 MICHIGAN RD	BRENNAN	$151,800	**$5,617**	**$22,011**
1259 MICHIGAN RD	CORNELL	$353,600	**$13,083**	**$51,272**
1314 MICHIGAN RD	MILLER	$608,800	**$22,526**	**$88,276**
1394 MICHIGAN RD	MURRAY	$287,000	**$10,619**	**$41,615**
987 TOWN LINE RD	ERVIN	$477,500	**$17,668**	**$69,238**
847 TOWN LINE RD	RICHMOND	$230,600	**$8,532**	**$33,437**
851 TOWN LINE RD	HOUSE	$316,400	**$11,707**	**$45,878**
823 TOWN LINE RD	RUNYAN	$168,200	**$6,223**	**$24,389**
779 TOWN LINE RD	FLESVIG	$263,805	**$9,761**	**$38,252**
904 TOWN LINE RD	CORNELL	$341,700	**$12,643**	**$49,547**
1361 EAST SIDE RD	HANLIN	$181,294	**$6,708**	**$26,288**
1377 EAST SIDE RD	NIKOLAI	$243,300	**$9,002**	**$35,279**
1329 MOUNTAIN RD	JORGENSON	$273,577	**$10,122**	**$39,669**
TOTAL PROPERTY LOSS IN VALUE			**$350,798**	**$1,374,750**

*Based on an average 2.3-5.1% reduction in value as determined in the paper *The Value-Undermining Effects of Rock Mining on Nearby Residential Property: A Semiparametric Spatial Quantile Autoregression.*

**Based on the estimated reduction in value for homes located within a mile radius of mine as provided for in *An Assessment of the Economic Impact of the Proposed Stoneco Gravel Mine Operation on Richland Township.*

Safety Data Sheet

Solms Crushed Limestone (Crushed Rock, Limestone, Base Rock, Scrubber Stone, Agg-Lime)

Section 1: Identification

MANUFACTURER'S NAME & ADDRESS: Capitol Aggregates Inc.
2330 North Loop 1604 West.
San Antonio, Texas 78248

PRODUCT NAME:	**Solms Crushed Limestone**

EMERGENCY TELEPHONE NUMBER: (210) 871-6111
SDS INFORMATION OR ASSISTANCE: (210) 871-7247
COMPANY PHONE NUMBER: (210) 871 7260
CHEMICAL NAME: Solms Crushed Limestone
CAS NUMBER: N/A
TRADE NAME or SYNONYMS: (Crushed Rock, Limestone, Base Rock, Scrubber Stone, Agg-Lime)
PRODUCT USE: Construction Aggregates, Soil Amendment

Section 2: Hazards Identification

WARNING! CRUSHED LIMESTONE IS NOT A KNOWN HEALTH HAZARD. HOWEVER CRUSHED LIMESTONE MAY BE SUBJECTED TO VARIOUS NATURAL OR MECHANICAL FORCES THAT PRODUCE SMALL PARTICLES (DUST), WHICH MAY CONTAIN RESPIRABLE CRYSTALLINE SILICA (PARTICLES LESS THAN 10 MICROMETERS IN AERODYNAMIC DIAMETER).REPEATED INHALATION OF RESPIRABLE CRYSTALLINE SILICA (QUARTZ) MAY CAUSE DAMAGE TO LUNGS THROUGH PROLONGED OR REPEATED EXPOSURE AND MAY CAUSE LUNG CANCER.

Classification of the substance or mixture:

CARCINOGENICITY/INHALATION — Category 1A

SPECIFIC TARGET ORGAN TOXICITY
(REPEATED EXPOSURE) — Category 2

CAPITOL AGGREGATES INC

GHS label elements

Hazard pictograms:

Signal word: **Danger**

Hazard statements: **Harmful if swallowed. May cause cancer (inhalation). May cause damage to lungs with prolonged or repeated exposure (inhalation).**

EMERGENCY OVERVIEW:

Appearance/Odor: Loose granular rock, gravel, and silt mixture of varying size and color. No odor.

Carcinogen, Acute & Chronic Toxin Warning:

- This product contains greater than 0.1% crystalline silica. Crystalline silica has been linked to cancer, silicosis, and other lung problems in conditions of prolonged airborne over-exposure. Repeated inhalation of respirable crystalline silica (quartz) may cause lung cancer according to IARC and NTP; ACGIH states that it is a suspected cause of cancer. Other forms of RCS (e.g. Tridymite and Cristobalite) may also be present or formed under certain industrial processes.
- Carcinogen- Acute & Chronic. Product contains crystalline silica quartz. The International Agency for Research on Cancer (IARC) classifies respirable crystalline silica as Group I – Known Human Carcinogen. The National Toxicology Program (NTP) lists respirable crystalline silica as a Known Human Carcinogen. The American Conference of Governmental Industrial Hygienists (ACGIH) lists respirable crystalline silica as a Suspected Human Carcinogen (A-2).

OSHA REGULATORY STATUS:

This product is considered HAZARDOUS by the OSHA Hazard Communication Standard (29 CFR 1910.1200).

POTENTIAL HEALTH EFFECTS:

LIKELY ROUTES OF EXPOSURE: Inhalation

TARGET ORGAN(S): Lungs

EYE

- Avoid eye contact. Exposure to dust may be irritating to the eyes and may impair visibility. These effects are transient similar to nuisance dust and recovery should follow.

SKIN

- Avoid prolonged and repeated skin contact. Do not handle until all safety precautions have been read and understood. Wear protective gloves, protective clothing, eye protection and face protection. Wash hands thoroughly after handling.

INHALATION

- Avoid prolonged and repeated inhalation of dust. Acute and chronic exposure to dusts may be irritating to the respiratory tract by frictional action, and may provoke bronchoconstriction in hyper-susceptible individuals.
- Respirable dusts can cause bothersome deposits in the nasal passages. Nuisance dusts cause toxicity from physical overloading of the respiratory clearance mechanisms.
- Significant deterioration of pulmonary function and chronic bronchitis can develop with prolonged overexposure to dusts in excess of established limits (See Section 8).
- Continued overexposure to silica dust can result in silicosis, a chronic, progressive and sometimes fatal lung disease that is characterized by the presence of typical nodulation of the lungs leading to fibrosis. Silicosis can develop in weeks with high exposures and after years of lower exposure. Symptoms and signs of silicosis include cough, shortness of breath, wheezing, decreased pulmonary function, and changes in chest X-rays.

INGESTION

- Minute amounts accidentally ingested during industrial handling are not likely to cause injury.

MEDICAL CONDITIONS AGGRAVATED BY EXPOSURE

- Chronic exposure to nuisance dusts may enhance susceptibility to respiratory tract infections.
- Silica can cause silicosis which, in turn, increases the risk of pulmonary tuberculosis infection.
- Smoking may increase the risk of developing lung disorders associated with silicosis.

Section 3: Composition / Information on Ingredients

Component	CAS No.	Wt.%	Hazardous?	GHS-US
Calcium Carbonate	1317-65-3	> 85	No	Not Classified
Crystalline Silica Quartz (a component of crushed stone)	14808-60-7	< 6	Yes	Acute Tox. 4 (Oral), H302 Carc. 1A, H350 STOT RE 1, H372

Crystalline Silica is reported as total silica and not just the respirable fraction.

Any concentration shown as a range is to protect confidentiality of trade secret information or is due to process variation.

Section 4: First Aid Measures

Description of necessary first aid measures

EYE CONTACT
Limestone dust: Immediately flush eyes with large amounts of water and continue flushing for 15 minutes. Remove contact lenses, if worn. Occasionally lift the eyelid(s) to ensure thorough rinsing. Beyond rinsing, do not attempt to remove material from the eye(s). Get medical attention if irritation develops or persists.

SKIN CONTACT
Limestone dust: Wash contaminated area thoroughly with soap and water. If redness or irritation occurs and persists, seek medical attention.

INHALATION
Limestone dust: Remove to fresh air. If breathing is difficult keep at rest in a position comfortable for breathing and get medical attention.

INGESTION
Limestone dust: If swallowed, do NOT induce vomiting unless directed to do so by medical personnel. Never give anything by mouth to an unconscious person. Give large quantity of water and get medical attention if distress develops.

MOST IMPORTANT SYMPTOMS/EFFECTS, ACUTE and DELAYED POTENTIAL ACUTE HEALTH EFFECTS

Eye contact: May cause eye irritation due to abrasion if crushed limestone particles become entrapped in the eyes. Symptoms may include discomfort or pain, excess blinking and tear production, with marked redness and swelling of the conjunctiva.

Inhalation: May cause respiratory tract irritation. Symptoms may include sneezing or coughing similar to inhalation of nuisance dust particles if sand or gravel particles are inhaled. Inhaling sand and gravel may cause discomfort in the chest, shortness of breath and coughing.

Skin contact: Symptoms may include skin abrasion or redness if sand and gravel particles collide forcefully with the skin.

Ingestion: Harmful if swallowed. May cause stomach distress, nausea, choking, and vomiting if sand or gravel is swallowed.

OVER-EXPOSURE SIGNS/SYMPTOMS

Eye contact: Adverse symptoms may include the following: pain, watering and redness

Inhalation: Adverse symptoms may include the following: respiratory tract irritation and coughing. Prolonged inhalation may cause chronic health effects. This product contains crystalline silica. Prolonged or repeated inhalation of respirable crystalline liberated from silica can cause silicosis and may cause cancer.

Skin contact: Adverse symptoms may include skin abrasion and redness.

Ingestion: Adverse symptoms may include stomach distress, nausea, vomiting, or choking if crushed stone is swallowed.

NOTES TO PHYSICIAN
Ensure that medical personnel are aware of the materials involved, and take precautions to protect themselves. Pre-existing medical conditions that may be aggravated by exposure include disorders of the eye, skin and lung (including asthma and other breathing disorders).If addicted to tobacco, smoking will impair the ability of the lungs to clear themselves of dust.

Section 5: Fire Fighting Measures

FLAMMABLE PROPERTIES:
Noncombustible and not explosive.

EXTINGUISHING MEDIA:
Suitable extinguishing media: Crushed Limestone is not flammable. Use fire extinguishing media appropriate for surrounding materials.
Unsuitable extinguishing media: None known.

SPECIFIC HAZARDS ARISING FROM THE CHEMICAL
No specific fire or explosion hazard. Not a combustible dust.

THERMAL DECOMPOSITION PRODUCTS
None specific however contact with powerful oxidizing agents and acids may cause fire and/or explosions (See section 10 of this safety data sheet).

PROTECTION OF FIREFIGHTERS:
No special precautions use protective equipment appropriate for surrounding materials.

Section 6: Accidental Release Measures

PERSONAL PRECAUTIONS:
Use personal protective equipment (PPE) specified in Section 8 (Exposure Controls/Personal Protection). Also see Section 3 (Hazards Identification), Section 7 (Handling & Storage), and Section 10 (Stability & Reactivity).

ENVIRONMENTAL PRECAUTIONS:
Do not allow spilled material to enter sewers or waterways.

METHODS OF CONTAINMENT:
Wet suppression can be used to minimize dust levels

METHODS FOR CLEAN-UP:
Clean up quickly and avoid generating dust. Spilled material where dust is generated, may overexpose cleanup personnel to respirable crystalline silica-containing dust. Do not dry sweep or

use compressed air for clean-up. Wetting of spilled material and/or use of respiratory protection equipment may be necessary.

OTHER INFORMATION:
Notify appropriate local authorities of spills into sewers or waterways. See section 8 for further information on protective clothing and equipment, section 13 for advice on waste disposal.

Section 7: Handling and Storage

HANDLING:
Do not handle until all safety precautions have been read and understood. Keep formation of airborne dusts to a minimum. Provide appropriate exhaust ventilation at places where dust is formed. Do not breathe dust. Avoid prolonged and repeated exposure to dusts. Wet suppression can be used to minimize dust exposure. Provide adequate ventilation. Wear appropriate personal protective equipment. Observe good industrial hygiene practices. Avoid contact with eyes. Do not swallow. Avoid generating and breathing dust. Good housekeeping is important to prevent accumulation of dust. The use of compressed air for cleaning clothing, equipment, etc, is not recommended. DO NOT use product for sand blasting. Blasting breaks down natural silica and creates freshly fractured respirable crystalline silica which may lead to silica-related disease in persons exposed at levels exceeding occupational exposure limits.

ADVICE FOR GENERAL OCCUPATIONAL HYGIENE
Eating, drinking and smoking should be prohibited in areas where this material is handled, stored and processed. Workers should wash hands and face before eating, drinking and smoking. Remove contaminated clothing and protective equipment before entering eating areas. See also Section 8 for additional information on hygiene measures.

STORAGE:
No special storage procedures are necessary. Avoid dust formation or accumulation. Keep workers off large piles of product to minimize dust levels or engulfment hazards. Do not enter a silo or other enclosure containing bulk quantities of these products without using all appropriate safety precautions as engulfment or suffocation may occur. Crushed Stone may form a surface crust which appears solid but may not support the weight of humans. Accordingly, do not stand on crushed stone without using all appropriate safety precautions, including, without limitation, properly employed harnesses, lifelines and all other necessary safety equipment.

OTHER:

Also see Section 8 (Exposure Controls/Personal Protection)

Section 8: Exposure Controls / Personal Protection

EXPOSURE GUIDELINES:

Component	CAS No.	Exposure Limits					
		OSHA		MSHA		ACGIH	
		respirable dust	total dust	respirable dust	total dust	respirable dust	total dust
Crushed Limestone (as Particulates Not Otherwise Regulated or Nuisance Dusts)	SEQ250	PEL 8hr-TWA: 5 mg/m^3	PEL 8hr-TWA: 15 mg/m^3	PEL 8hr-TWA: 5 mg/m^3	PEL 8hr-TWA: 10 mg/m^3	TLV 8hr-TWA: 3 mg/m^3	TLV 8hr-TWA: 10 mg/m^3
Crystalline Silica Quartz	14808-60-7	PEL 8hr-TWA: 10 mg/m^3 /(%SiO_2+2)	PEL 8hr-TWA: 30 mg/m^3 /(%SiO_2+2)	PEL 8hr-TWA: 10 mg/m^3 /(%SiO_2+2)	PEL 8hr-TWA: 30 mg/m^3 /(%SiO_2+3)	TLV 8hr-TWA: 0.025 mg/m^3	N/A

APPROPRIATE ENGINEERING CONTROLS:
Good general ventilation (typically 10 air changes per hour indoors) should be used. Ventilation rates should be matched to conditions. If applicable, use process enclosures, local exhaust ventilation, or other engineering controls to maintain airborne levels below recommended exposure limits. If exposure limits have not been established, maintain airborne levels to an acceptable level.

PERSONAL PROTECTIVE EQUIPMENT (PPE):

EYE/FACE PROTECTION
Wear safety glasses or goggles.

SKIN PROTECTION
Wear standard work gloves (leather, cotton, coated cotton, etc.) as needed to prevent abrasion. Wear clothes with sleeve rolled down and collars buttoned, and trousers gathered at the ankles to minimize skin contact.

RESPIRATORY PROTECTION
When handling or performing work with crushed limestone that produces dust or respirable crystalline silica, a NIOSH approved respirator is recommended in poorly ventilated areas or when permissible exposure limits may be exceeded. Wear a NIOSH approved respirator that is properly fitted and is in good condition. Respirator selection must be based on known or anticipated exposure levels, the hazards of the product and the safe working limits of the selected respirator. All respirators must be NIOSH-certified.

GENERAL HYGIENE CONSIDERATIONS

Practice good housekeeping and hygiene practices to minimize generating and spreading airborne dust. Always wash areas of the body (hands, face, arms, etc.) that have come in contact with the product. Always wash hands and face with soap and water before eating, drinking, or smoking.

Section 9: Physical and Chemical Properties

Physical State: Solid. [Granular, Pebbles to Boulders]

Color: White/Grayish White/ or Tan

Odor: Odorless.

Odor threshold: No data available.

pH: As Calcium Carbonate 8-9.

Melting point: No data available.

Boiling point: No data available

Flash point: Non-combustible.

Burning time: Not available.

Burning rate: Not available.

Evaporation rate: Not applicable.

Flammability (solid, gas): Not applicable

Lower and upper explosive (flammable) limits: Not applicable.

Vapor pressure: Not applicable.

Vapor density: Not applicable.

Relative density: > 2.0

Solubility: Insoluble in water.

Solubility in water: Not applicable

Partition coefficient: n-octanol/water: Not applicable.

Auto-ignition temperature: Not applicable.

Decomposition temperature: Not applicable.

SADT: Not available.

Viscosity: Not applicable.

Section 10: Stability and Reactivity

REACTIVITY

Product is stable and non-reactive under normal conditions of use but reacts vigorously with acids to form CO2. Ignites on contact with Fluorine.

CHEMICAL STABILITY:

Material is stable under normal conditions but reacts vigorously with acids to form CO2. Ignites on contact with Fluorine.

POSSIBILITY OF HAZARDOUS REACTIONS:

Avoid contact with strong oxidizers such as acids which will react vigorously and form CO2.

CONDITIONS TO AVOID:
Avoid generation of dusts. Avoid contact with strong oxidizers such as acids which will react vigorously and form CO2. Crushed Limestone should not be mixed or stored with Fluorine, Ammonium Salts, Aluminum, Hydrogen, Magnesium, or Acids.

INCOMPATIBLE MATERIALS:
Contact with powerful oxidizing agents such as Fluorine, Chlorine Tri-Fluoride, Manganese Trioxide, Oxygen Di-Fluoride, Ammonium Salts, Aluminum, Hydrogen, Magnesium, or Acids.

HAZARDOUS DECOMPOSITION PRODUCTS:
Silica-containing respirable dust particles may be generated if dust is generated. Limestone decomposes at 1742 degrees Farenheit to produce calcium oxide.

OTHER INFORMATION
See also additional precautions Section 5 (Fire Fighting Measures), Section 6 (Accidental Release Measures) and Section 7 (Handling & Storage).

Section 11: Toxicological Information

INFORMATION ON TOXICOLOGICAL EFFECTS

Acute toxicity: Not classified. Limestone LD50/LC50 of >6000mg/Kg (Rat, oral). Limestone is not listed by MSHA, OSHA, or IARC as a carcinogen but this product may contain trace amounts of crystalline silica, which has been classified by IARC as a carcinogenic to humans when inhaled in the form of quartz or Crystobalite.

Harmful if swallowed. May cause stomach distress, nausea, or vomiting

Irritation/Corrosion:

Skin: Not applicable.
Eyes: Not applicable.
Respiratory: May cause respiratory tract irritation.
Sensitization: Not applicable.

Carcinogenicity – May Cause Cancer
A; General Product Information:
The Occupational Safety and Health Administration (OSHA), the National Toxicology Program (NTP) and the International Agency for Research on Cancer (IARC) have not listed crushed limestone as a carcinogen.

B: Component Carcinogenicity Nuisance Dust-Crystalline Silica Dust

This product, however, may contain a constituent which is listed by IARC and NTP as carcinogen. Respirable crystalline silica in the form of quartz or cristobalite from occupational sources is listed by the International Agency for Research on Cancer (IARC) and National

Toxicology Program (NTP) as a lung carcinogen. Prolonged exposure to respirable crystalline silica has been known to cause silicosis, a lung disease, which may be disabling. While there may be a factor of individual susceptibility to a given exposure to respirable silica dust, the risk of contracting silicosis and the severity of the disease is clearly related to the amount of dust exposure and the length of time (usually years) of exposure.

Chronic Toxicity

Specific target organ toxicity – (repeated/extended exposure), Crystalline Silica is considered hazardous by inhalation. IARC has classified silica as a Group 1 substance, carcinogenic to humans. This classification is based on the findings of laboratory animal studies (inhalation and implantation) and epidemiology studies that were considered sufficient for carcinogenicity. NTP has also classified respirable crystalline silica as a known carcinogen. Excessive exposure to crystalline silica can cause silicosis, a chronic, progressive and sometimes fatal lung disease which, in turn, increases the risk of pulmonary tuberculosis infection.

Mutagenicity: There are no data available.

Reproductive Toxicity : Not applicable

Specific target organ toxicity (single exposure): Not Applicable

Specific target organ toxicity (repeated exposure)

Name	Category	Route of Exposure	Target Organs
Quartz	1	Inhalation	Respiratory tract and kidneys

Aspiration Hazard: There are no data available

INFORMATION ON LIKELY ROUTES OF EXPOSURE

Symptoms related to the physical, chemical and toxicological characteristics:

Eye contact: Limestone dust: May cause irritation through mechanical abrasion. Discomfort in the chest, shortness of breath, coughing. Adverse symptoms associated with eye contact with particle debris include the following: discomfort, excess blinking, tear production, watering, marked redness and swelling of the conjunctiva.

Inhalation: Limestone dust: May cause respiratory tract irritation. Adverse symptoms may include respiratory tract irritation and coughing. Prolonged inhalation may cause chronic health effects. This product contains crystalline silica. Prolonged or repeated inhalation of respirable crystalline silica liberated from this product can cause silicosis, a fibrosis (scarring) of the lungs, and may cause cancer.

Skin contact: Limestone dust: Adverse symptoms may include skin abrasion and redness.

Ingestion: Limestone dust: Harmful if swallowed. Adverse symptoms may include stomach distress, nausea, or vomiting.

Section 12: Ecological Information

ECOTOXICITY
Not expected to be harmful to aquatic organisms. Discharging crushed stone, sand, dust and fines into waters may increase total suspended particulate (TSP) levels that can be harmful to certain aquatic organisms.

PERSISTENCE and DEGRADABILITY
Not Applicable

BIOACCUMULATIVE POTENTIAL
Not Applicable

MOBILITY IN SOIL
Not Applicable

OTHER ADVERSE EFFECTS
No other adverse environmental effects (e.g. ozone depletion, photochemical ozone creation potential, global warming potential) are expected from this component.

Section 13: Disposal Considerations

Recover or recycle if possible.

REGULATORY INFORMATION
Disposal must comply with all applicable federal, state and local regulations.

WASTE DISPOSAL METHODS
The generation of waste should be avoided or minimized wherever possible. Disposal of this product should comply with the applicable requirements of environmental protection and waste disposal legislation and any regional local authority applicable requirements. Dispose of surplus and non-recyclable products via a licensed waste disposal contractor. Do not allow fine particulate matter to drain into sewers/water supplies. Do not contaminate ponds, waterways or ditches with fine particulates. Waste packaging should be recycled. Incineration or landfill should only be considered when recycling is not feasible. This material and its container must be disposed of in a safe manner. Care should be taken when handling empty containers that have not been cleaned or rinsed out. Empty containers or liners may retain some product residues. Avoid dispersal of spilled material and runoff, and contact with soil, waterways, drains and sewers. Dispose of waste materials only in accordance with applicable federal, state, and local laws and regulations.

HAZARDOUS WASTE CODE
Not Regulated. Crushed Limestone is used in many soil and construction applications, waste material does not meet the criteria of a hazardous waste as defined under the Resource Conservation And Recovery Act (RCRA), 40 CFR 261. Dispose of residual products and empty containers responsibly and lawfully.

Section 14: Transport Information

UN NUMBER
Not Applicable

UN PROPER SHIPPING NAME
Not Applicable

BASIC SHIPPING DESCRIPTION:
U.S. Department of Transportation (DOT) Highway/Rail (Bulk): Not classified
U.S. Department of Transportation (DOT) Highway/Rail (Non-bulk): Not classified

ADDITIONAL INFORMATION:

The DOT description is provided to assist in the proper shipping classification of this product and may not be suitable for all required shipping descriptions. Many local communities and jurisdictions regulate the transporting of Crushed Stone in open vehicles or trailers requiring tarps, covering, or other protections of the load.

Section 15: Regulatory Information

OSHA:
This product is considered Hazardous by the OSHA Hazard Communication Standard (29 CFR 1910.1200) and should be included in employers' hazardous communication programs.

TSCA:
Crushed Limestone is not listed on TSCA (Toxic Substances Control Act) inventory, however a component Quartz (CAS 14808-60-7) is listed on the United States Toxic Substances Control Act inventory.

CERCLA:
This product in not listed as a CERCLA hazardous substance

CLEAN AIR ACT

Clean Air Act Section 112 (b): Hazardous Air Pollutants (HAPs) — Not listed
Clean Air Act Section 602: Class I Substances — Not listed
Clean Air Act Section 602: Class II Substances — Not listed

DEA

DEA List I Chemicals: (Precursor Chemicals) — Not listed
DEA List II Chemicals: (Essential Chemicals) — Not listed

SAFE DRINKING WATER ACT
Not Listed

SARA TITLE III:

Hazard categories:
Immediate Hazard – No
Delayed Hazard – Yes
Fire Hazard – No
Pressure Hazard – No
Reactivity Hazard - No

Section 302:
This product is not and does not contain an Extremely Hazardous Substance

Section 311/312:
The following materials are reportable under the Tier II rules:
Crystalline Silica Quartz

Section 313:
The following TRI chemicals are present in this product:

Chemical Name	CAS No.	Wt%
None		

INTERNATIONAL REGULATIONS
Not applicable since not shipped internationally.

US STATE REGULATIONS:

California Proposition 65:
This product contains the following chemicals known to the State of California to cause cancer:

Name	CAS Number
Crystalline Silica	14808-60-7

California law requires the manufacturer to give the above warning in the absence of definitive testing to prove that the defined risks do not exist.

Massachusetts Right To Know Substance List
Crystalline Silica (Quartz) (CAS 14808-60-7)
Respirable Tridymite and Cristobalite (other forms of crystalline silica) (CAS Mixture)

New Jersey Worker and Community Right-to-Know Act
Crystalline Silica (Quartz) (CAS 14808-60-7)
Respirable Tridymite and Cristobalite (other forms of crystalline silica) (CAS Mixture)

Pennsylvania Worker and Community Right-to-Know Law
Crystalline Silica (Quartz) (CAS 14808-60-7)
Respirable Tridymite and Cristobalite (other forms of crystalline silica) (CAS Mixture

Rhode Island Right To Know Substance List
Not regulated.

CAPITOL AGGREGATES INC

Section 16: Other Information

NFPA Ratings:

Health: 1
Flammability: 0
Reactivity: 0
0 = minimal hazard, 1 = slight hazard, 2 = moderate hazard, 3 = severe hazard, 4 = extreme hazard

Capitol Aggregates Inc.
2330 North Loop 1604 West.
San Antonio, Texas 78248
(210)-871-6111

PRECAUTIONARY WARNING!
CRUSHED LIMESTONE, (SOLMS CRUSHED LIMESTONE), IS NOT A KNOWN HEALTH HAZARD. ALTHOUGH CRUSHED LIMESTONE MAY BE SUBJECTED TO VARIOUS NATURAL OR MECHANICAL FORCES THAT PRODUCE SMALL PARTICLES (DUST), WHICH MAY CONTAIN RESPIRABLE CRYSTALLINE SILICA (PARTICLES LESS THAN 10 MICROMETERS IN AERODYNAMIC DIAMETER).REPEATED INHALATION OF RESPIRABLE CRYSTALLINE SILICA (QUARTZ) MAY CAUSE DAMAGE TO LUNGS THROUGH PROLONGED OR REPEATED EXPOSURE AND MAY CAUSE SILICOSIS A FORM OF LUNG CANCER. DO NOT USE PRODUCT FOR SAND BLASTING. BLASTING BREAKS DOWN NATURAL SILICA AND CREATES FRESHLY FRACTURED RESPIRABLE CRYSTALLINE SILICA WHICH MAY LEAD TO SILICA-RELATED DISEASE IN PERSONS EXPOSED AT LEVELS EXCEEDING OCCUPATIONAL EXPOSURE LIMITS. BEFORE USING, ALSO READ THE SAFETY DATA SHEET FOR THIS PRODUCT FOUND AT WWW.CAPITOLAGGREGATES.COM.

KEEP OUT OF THE REACH OF CHILDREN (Poison Control No. 1-800-222-1222)

Product Identifier:
SOLMS CRUSHED LIMESTONE
CAS NO. N/A

Hazard Statement **DANGER**
Harmful if swallowed. May cause damage to lungs with prolonged or repeated exposure (inhalation). May cause cancer, (inhalation).

CAPITOL AGGREGATES INC

ABBREVIATIONS

ACGIH	American Conference of Governmental Industrial Hygienists
CAS	Chemical Abstract Service
CERCLA	Comprehensive Environmental Response, Compensation, and Liability Act
CFR	Code of Federal Regulations
DOT	Department of Transportation
IARC	International Agency for Research on Cancer
m^3	Cubic meter
mg	Milligram
SDS	Safety Data Sheet (formerly known as MSDS)
MSHA	Mine Safety and Health Administration
N/A	Not applicable
NFPA	National Fire Protection Association
NIOSH	National Institute for Occupational Safety and Health
NTP	National Toxicology Program
OSHA	Occupational Safety and Health Administration
PEL	Permissible Exposure Limit
PPE	Personal Protective Equipment
RQ	Reportable Quantity
TLV	Threshold Limit Value
TRI	Toxic Release Inventory
TSCA	Toxic Substance Control Act

NOTE: This SDS attempts to describe as accurately as possible the potential exposures associated with normal use of this product. Health and safety precautions on this data sheet may not be adequate for all individuals and/or situations. Users have the responsibility to evaluate and use this product safely and to comply with all applicable environmental, health, and safety laws and regulations.

Prepared in August 2015
Supersedes any and all previous versions (extensive revisions were made)

Disclaimer of Warranty:

While the information provided herein is believed to provide a useful summary of the hazards of different types of Crushed Limestone designated above as commonly used, this SDS cannot anticipate and provide all of the information that might be needed by every individual in every situation. Inexperienced users should obtain proper training prior to using any Crushed Limestone product and no one should use any Crushed Limestone product without following all applicable safety laws and regulations related to its storage, handling, use and disposal and without first understanding the potential hazards of Crushed Limestone. This SDS does not cover such potential hazards.

The information provided in this SDS is believed by Capitol Aggregates, Inc. to be accurate at the time it was prepared or it was prepared from sources then believed to be reliable. It is the responsibility of the user independently to investigate and understand other pertinent sources of information and to comply with all laws, regulations and procedures applicable to the safe storage, handling, use and disposal of Crushed Limestone. It is also the responsibility of the user to independently determine the suitability or fitness of any of the products covered by this SDS for their intended uses.

CAPITOL AGGREGATES, INC. MAKES NO REPRESENTATIONS OR WARRANTIES, EXPRESS OR IMPLIED, BY OR THROUGH THIS SDS CONCERNING THE PRODUCTS COVERED HEREBY OR THEIR FITNESS FOR ANY PARTICULAR USE. LIKEWISE CAPITOL AGGREGATES, INC. MAKES NO REPRESENTATIONS OR WARRANTIES REGARDING THE ACCURACY OR COMPLETENESS OF THE INFORMATION SET FORTH HEREIN. THE PROVISION OF THE SUCH INFORMATION IS NOT INTENDED TO BE, AND SHOULD NOT BE CONSTRUED AS LEGAL OR OTHER ADVICE, OR AS ENSURING COMPLIANCE WITH ANY PARTICULAR LAWS AND REGULATIONS.

CAPITOL
AGGREGATES INC

Dear Customer

Whether you are a long term customer or a new contractor, we would like to thank you for purchasing Capitol Aggregates Products. We are a Texas owned Company and produce all of our products in the State of Texas. This Safety Data Sheet (SDS), provided for the product you purchased or intend to use is a revision and replaces any previous versions formerly known as Material Safety Data Sheets or (MSDS). We are providing you this SDS as required by the Mine Safety & Health Administration's (MSHA), or the Occupational Safety & Health Administration, OSHA, and any applicable State Right-To –Know laws. The requirements applicable to the OSHA and MSHA Hazard Communication Standards can be found at 29 CFR 1910.1200 for OSHA and 30 CFR 47 for MSHA.

It is an important responsibility for you as a customer or contractor to communicate this information to your employees, customers, and contractors who may use, contact, or be exposed to this product. It is also an important consideration and responsibility for you to follow any applicable laws that require you to forward a copy of this SDS to your customers or end users. Please direct this SDS to the person responsible for safety and health compliance at your company as they may be able to assist you with any of the necessary requirements. If you need additional copies or have questions about this SDS please contact 210-871-6111, or visit us at www.capitolaggregates.com .

Spanish language versions will be available in the near future at www.capitolaggregates.com .

Sincerely

Chuck Ross
Director of Safety

EXPLANATION OF MAP UNITS

Humid climate region (>30 inches (in.) average annual precipitation)

Dry climate region (≤30 in. average annual precipitation)

Approximate maximum extent of Pleistocene ice

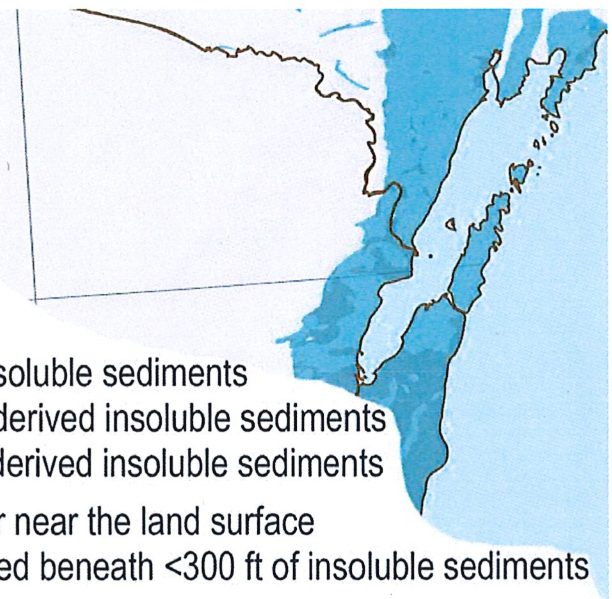

Humid Climate Karst

- Carbonate rocks at or near the land surface
- Carbonate rocks buried beneath <300 feet (ft) of insoluble sediments
- Carbonate rocks buried beneath ≤50 ft of glacially derived insoluble sediments
- Carbonate rocks buried beneath >50 ft of glacially derived insoluble sediments

- Unconsolidated calcareous or carbonate rocks at or near the land surface
- Unconsolidated calcareous or carbonate rocks buried beneath <300 ft of insoluble sediments

- Evaporite rocks at or near the land surface
- Evaporite rocks buried beneath ≤50 ft of glacially derived insoluble sediments
- Evaporite rocks buried beneath >50 ft of glacially derived insoluble sediments

- Quartz sandstone buried beneath ≤50 ft of glacially derived insoluble sediments
- Quartz sandstone buried beneath >50 ft of glacially derived insoluble sediments

The Value-Undermining Effects of Rock Mining on Nearby Residential Property: A Semiparametric Spatial Quantile Autoregression*

EMIR MALIKOV[1] YIGUO SUN[2] DIANE HITE[1]

[1]Auburn University, United States
[2]University of Guelph, Canada

This Draft: August 15, 2017

Abstract

Rock mining operations, including limestone and gravel production, have considerable adverse effects on residential quality of life due to elevated noise and dust levels resulting from dynamite blasting and increased truck traffic. This paper provides the first estimates of the effects of rock mining—an environmental disamenity—on local residential property values. We focus on the relationship between a house's price and its distance from nearby rock mine. Our analysis studies Delaware County, Ohio which, given its unique features, provides a natural environment for the valuation of property-value-suppressing effects of rock mines on nearby houses. We improve upon the conventional approach to valuating adverse effects of environmental disamenities based on hedonic house price functions. Specifically, in a pursuit of robust estimates, we develop a novel (semiparametric) partially linear spatial quantile autoregressive model which accommodates unspecified nonlinearities, distributional heterogeneity as well as spatial dependence in the data. We derive the consistency and normality limit results for our estimator as well as propose a consistent model specification test. We find statistically and economically significant property-value-suppressing effects of being located near an operational rock mine which gradually decline to insignificant near-zero values at a roughly ten-mile distance. Our estimates suggest that, all else equal, a house located a mile closer to a rock mine is priced, on average, at about 2.3–5.1% discount, with more expensive properties being subject to larger markdowns.

Keywords: Environmental Disamenity, Hedonic Model, Partially Linear, Quantile Regression, Rock Mines, SAR, Semiparametric, Spatial Lag

JEL Classification: C14, C21, R30, Q51

*Email: emalikov@auburn.edu (Malikov), yisun@uoguelph.ca (Sun), hitedia@auburn.edu (Hite).

1 Introduction

This paper provides the first estimates of the effects of rock mining—an environmental disamenity—on local residential property values. Rock mining operations, including limestone rock blasting and gravel mining, have considerable adverse effects on residential quality of life primarily due to elevated noise and dust levels resulting from blasting and increased truck traffic. Exacerbating matters, residential building activity and rock mining are also both pro-cyclical. Further, mining operations naturally seek to minimize their transportation costs by locating closer to their consumers in populated areas (Jaeger, 2006) thus increasing opportunities for opposition from local homeowners and citizen groups due to negative externalities associated with the former.

To valuate the effects of rock mining, we estimate Rosen's (1974) first-stage hedonic house price gradient which has long been used to estimate implicit prices of non-marketable local public goods or, as in our case, public bads from the housing market data. To this end, we focus on the relationship between a house's price and its distance from nearby rock mine. This distance effectively represents environmental amenity/quality, with better quality occurring at farther distances from mines as customarily presumed in hedonic studies. Our analysis focuses on Delaware County, Ohio which, given its unique features, provides a natural environment for the valuation of property-value-suppressing effects (if any) of rock mines on nearby houses. According to the U.S. Census Bureau, Delaware County has been among the two fastest growing counties in the state for the past twenty years. At the same time, given its geology, the county has rich limestone formations that have long been exploited as surface mines.[1] Consequently, residential and commercial expansion in the county has been in conflict with traditional land uses: farming and, especially, rock mining.

In our analysis, we seek to improve upon the conventional approach to valuating adverse effects of environmental disamenities based on hedonic house price functions. Specifically, in a pursuit of robust estimates of property-value effects of rock mines located in the vicinity of residential real estate, we estimate a house valuation function via novel (semiparametric) partially linear spatial quantile autoregressive model. The motivation for developing our model is threefold.

First, our partially linear model allows the distance from a house to nearby rock mine to enter the hedonic house price function in a completely unspecified nonparametric fashion thereby accommodating any potential nonlinearities in the relationship between property values and disamenity. This constitutes a significant improvement over prior studies most of which assume linearity and hence a constant marginal effect of the environmental disamenity on house prices. Few exceptions in earlier work include Harrison & Rubenfeld (1978), Kohlhase (1991), Leggett & Bockstael (2000), Hite et al. (2001), Cohen & Coughlin (2008) and Zabel & Guignet (2012) who model the disamenity quadratically, logarithmically or as a series of range-based dummy variables. In contrast to the latter studies, ours however does not assume the form of nonlinearity *a priori* and instead lets the data determine the nature of functional dependence between the distance to rock mine and house prices. Furthermore, by having the price of a house vary with its distance to mine nonparametrically, one no longer needs to *pre*specify the distance threshold beyond which the disamenity is presumed to have a zero effect on property values. Motivated by the argument that the effects of local disamenities are *local* in nature, the latter is usually done by fixing a spatial radius around a given disamenity thereby defining a circular area to be included in the analysis (e.g., Nelson et al., 1992; Reichert et al., 1992; Hite et al., 2001). In practice, the need to prespecify the radius is oftentimes dictated by the fact that one is more likely to find counterintuitive results if "irrelevant" data from far distances are included in the estimation of a parametric model that inherently cannot accommodate unknown nonlinearities in the property-value effects of disamenities, unless correctly

[1]Source: Ohio Department of Natural Resources.

prespecified. Our model is far more robust to this problem since it assumes no particular form of nonlinearity in the relationship between property values and disamenity.

Second, it is well-known in the real estate literature that environmental disamenities are likely to have heterogeneous impacts on residential property values with larger effects expected in more expensive upscale neighborhoods and more modest effects in less expensive areas (e.g., Reichert et al., 1992; Gayer, 2000). Nonetheless, virtually all earlier attempts at measuring the impact of environmental disamenities on property values have done so by estimating a hedonic house price function at the conditional *mean*. Such an approach delivers the marginal effect on the average house price, which can be rather uninformative from a policy perspective even after controlling for neighborhood characteristics because an "average" may not be representative of actual properties within the same locality, especially in the presence of thick tails of the house price distribution. In order to accommodate heterogeneous effects, we therefore assess the property-value impact of rock mines at different conditional *quantiles* of the house price distribution. We accomplish the latter by estimating a quantile regression model which, besides being more robust to the error distributions including the presence of outliers, allows for *distributional* heterogeneity of the effects of rock mines on property values.

Third, our model explicitly allows for spatial dependence in property values. By estimating a spatially autoregressive hedonic price function, we are able to indirectly control for *unobserved* neighborhood characteristics and shared local amenities (e.g., parks, playgrounds, traffic, air quality, crime, etc.) that affect property values. The spatial lag measuring the average price of neighboring houses serves as a good proxy for these unobserved neighborhood-wide attributes because, owing to their shared nature, they are also priced into the *observed* values of neighboring properties. While these characteristics can be partly controlled for using locality fixed effects, such an approach may be unsatisfactory since it does not let characteristics of neighboring houses affect the price of a given house (Anselin & Lozano-Gracia, 2009). However, by including the spatial lag in a hedonic house pricing function, we are able to accommodate such cross-neighbor effects as can be seen from a reduced form of our model whereby the conditional quantile of house price depends not only on its own attributes but also on its neighbors'. Perhaps more importantly, the spatial lag also contains information about (and thus can proxy for) unobserved *property*-specific attributes such as curb appeal because a given property's value, which is already reflective of its unobserved characteristics, affects its neighboring house's price through the "sales comparison approach" to a real estate appraisal whereby real estate agents base their appraisals of properties on the sale price information for houses in the neighborhood (see the references in Small & Steimetz, 2012). Thus, our spatially autoregressive hedonic model is significantly more robust to the omitted variable bias problem, which the overwhelming majority of housing-market-based valuations of adverse effects of environmental disamenities suffer from (Chay & Greenstone, 2005; Bajari et al., 2012). Prior papers that have also employed spatial hedonic models are largely limited to Gawande & Jenkins-Smith (2001), Brasington & Hite (2005) and Cohen & Coughlin (2008) although, unlike us, these studies of environmental disamenities focus on more restrictive parametric conditional mean models.

Our econometric model itself is a stand-alone contribution to the literature. It constitutes a practically useful fusion of semi/nonparametric quantile methods with models of spatial dependence. While the econometric literature has recently seen a rapid development in the theory of nonparametric estimation of quantile models (e.g., He & Shi, 1996; Yu & Jones, 1998; He & Liang, 2000; Lee, 2003; Honda, 2004; Kim, 2007), most such papers however do not allow endogenous explanatory variables as well as rule out any cross-sectional dependence by focusing on the case of *i.i.d.* data. In this paper, we consider quantile regression in the presence of endogeneity-inducing spatial dependence in the outcome variable. Our model nests several special cases that have been studied in the literature with Su & Yang (2011) and Su & Hoshino (2016) being the two most closely related papers [see Section 2 for more discussion]. Building on Chernozhukov & Hansen (2006), we propose estimating our model via a two-step nonparametric sieve instrumental variable (IV) quantile estimator. Under fairly mild regularity conditions, we show that our estimator is consistent and asymptotically normal. Furthermore, given that our partially linear model nests a more traditional *fully* linear spatial autoregressive model as a special case, one may naturally wish to formally discriminate between the two. To do so, we propose a bootstrap model specification test statistic which provides a vehicle for testing for a fully parametric specification of the spatial autoregression as well as an overall relevancy of some covariates in the model. The motivation for our test statistic comes from Ullah's (1985) nonparametric likelihood-ratio test formulated for a conditional mean model[2] which we extend to the quantile framework along the lines of Koenker & Machado (1999). We show the proposed is a consistent test.

We find statistically and economically significant property-value-suppressing effects of being located near an operational rock mine which gradually decline to insignificant near-zero values at a roughly ten-mile distance. For residential property in the middle of the price distribution, our estimates suggest that, all else equal, a house located a mile closer to a rock mine is predicted to be priced, on average, at about 3.1% discount. The analogous average discounts for houses in the first and third quartiles of price distribution are around 2.3 and 3.4%, respectively. For upscale property in the 0.95th quantile, it is at an astounding 5.1%. As a back-of-the-envelope welfare calculation, the above discount estimates imply the average loss in property value associated with the house being located a mile closer to a rock mine ranging from \$3,691 to \$10,970 for houses within the interquartile range of price distribution. For more expensive neighborhoods in the 0.95th quantile, such losses can be, on average, as high as \$28,410. Applying the estimated statistically significant discounts to house prices at each observation lying within a 10-mile radius from the mine to predict an increase in each property's value if it were moved from its actual location to a (counterfactual) 10-mile distance from the mine, we find the aggregate property value loss associated with rock mining in the area to be \$68.4 million at the median. Overall, using our specification test, we find that the proximity to rock mines *does* matter for residential property values.

The rest of the paper unfolds as follows. We first introduce our econometric model in Section 2, where we outline a two-step estimation methodology for it as well as provide its large-sample statistical properties. Section 3 presents a model specification test. (We study the finite-sample performance of our proposed estimator and the test statistic in a small set of Monte Carlo simulations in Appendix B.) We discuss the data in Section 4. The empirical results are reported in Section 5. Section 6 concludes.

2 A Partially Linear Spatial Quantile Autoregression

Following Jenish & Prucha (2012) and Qu & Lee (2015), we study spatial processes located on a (possibly) uneven lattice space $D \subseteq R^d$ for some $d \geq 1$. Let $\mathcal{Z}_n = \{(y_{i,n}, \mathbf{x}_{i,n}, \mathbf{z}_{i,n}, u_{i,n}, \varepsilon_{i,n}) : \boldsymbol{l}(i) \in D_n, n \geq 1\}$ be a triangular array of random fields defined on a probability space $(\Omega, \mathcal{F}, P)$ with $D_n \subset D$, where D_n is a finite subset of D, and $\boldsymbol{l}(i)$ refers to the location of the ith spatial unit in D, which is equipped with some distance metric $\varrho(i,j)$. For instance, we can let $\varrho(i,j) = \|\boldsymbol{l}(i) - \boldsymbol{l}(j)\|$ be a Euclidean distance between location $\boldsymbol{l}(i)$ and $\boldsymbol{l}(j)$. Also, let $|U|$ denote the cardinality of a finite subset $U \subset D$. We consider the increasing domain asymptotics as described in the following assumption.

[2]Also see Fan et al. (2001) and Lee & Ullah (2003).

Assumption 1 *The lattice D is infinitely countable with $|D_n| = n$, and $\varrho(i,j) > \varrho_0 > 0$ for any $i \neq j$.*

We consider the following PLSQAR model for a given quantile index τ:

$$y_{i,n} = \rho_{\tau,0} \sum_{j \neq i} w_{ij,n} y_{j,n} + \mathbf{x}'_{i,n} \boldsymbol{\beta}_{\tau,0} + \alpha_{\tau,0}(\mathbf{z}_{i,n}) + u_{i,n} \quad \forall\, \tau \in (0,1), \tag{2.1}$$

where $y_{i,n}$ is the (scalar) outcome variable of interest; $\mathbf{x}_{i,n}$ and $\mathbf{z}_{i,n}$ are $d_x \times 1$ and $d_z \times 1$ vectors of exogenous covariates, respectively; $\sum_{j \neq i} w_{ij,n} y_{j,n}$ is the endogeneity-inducing spatial lag with $w_{ij,n}$ being the (i,j)-th element of an $n \times n$ non-stochastic spatial weighting matrix $\mathbf{W}_n$ such that $w_{ii,n} = 0$ for all i and $\max_{1 \leq i \leq n} |\lambda_i \{\mathbf{W}_n\}| \leq 1$ where $\lambda_i\{\mathbf{A}\}$ is the ith eigenvalue of some $n \times n$ matrix $\mathbf{A}$; $\rho_{\tau,0} \in (-1,1)$ is a scalar varying spatial lag parameter function; $\boldsymbol{\beta}_{\tau,0}$ is a $d_x \times 1$ vector of constant slope parameters; and $\alpha_{\tau,0}(\cdot)$ is a scalar nonparametric function of $\mathbf{z}_{i,n}$. For identification purposes, $\mathbf{x}_{i,n}$ is assumed to include non-constant regressors only, and hence function $\alpha_{\tau,0}(\cdot)$ subsumes a traditional constant intercept parameter. Therefore, we refer to $\alpha_{\tau,0}(\cdot)$ as the "intercept function". Lastly, $u_{i,n}$ is the quantile error term such that

$$\Pr[u_{i,n} \leq 0 | \mathbf{X}_n, \mathbf{Z}_n, \mathbf{M}_n] = \tau \quad \text{a.s.} \quad \forall\, i = 1, \ldots, n, \tag{2.2}$$

where $\mathbf{X}_n = (\mathbf{x}_{1,n}, \ldots, \mathbf{x}_{n,n})'$ and $\mathbf{Z}_n = (\mathbf{z}_{1,n}, \ldots, \mathbf{z}_{n,n})'$ are $n \times d_x$ and $n \times d_z$ data matrices, respectively; and $\mathbf{M}_n = (\mathbf{m}_{1,n}, \ldots, \mathbf{m}_{n,n})'$ is an $n \times d_m$ instrument matrix with $\mathbf{m}_{i,n}$ being a $d_m \times 1$ vector of valid instruments for the endogenous spatial lag $\sum_{j \neq i} w_{ij,n} y_{j,n}$.

Letting $\mathbf{y}_n = (y_{1,n}, \ldots, y_{n,n})'$ and $\mathbf{u}_n = (u_{1,n}, \ldots, u_{n,n})'$, we can rewrite our model (2.1) in the matrix form as follows

$$\mathbf{y}_n = \rho_{\tau,0} \mathbf{W}_n \mathbf{y}_n + \mathbf{X}_n \boldsymbol{\beta}_{\tau,0} + \boldsymbol{\alpha}_{\tau,0}(\mathbf{Z}_n) + \mathbf{u}_n, \tag{2.3}$$

where $\boldsymbol{\alpha}_{\tau,0}(\mathbf{Z}_n) = (\alpha_{\tau,0}(\mathbf{z}_{1,n}), \ldots, \alpha_{\tau,0}(\mathbf{z}_{n,n}))'$. From (2.3), it is evident that, by assuming that the eigenvalues of $\mathbf{W}_n$ do not exceed one in absolute magnitude[3] and that the spatial lag parameter lies within the unit circle, we ensure the non-singularity of $\mathbf{I}_n - \rho_{\tau,0}\mathbf{W}_n$ necessary to guarantee the existence of the reduced form for our model:

$$\mathbf{y}_n = [\mathbf{I}_n - \rho_{\tau,0} \mathbf{W}_n]^{-1} \left(\mathbf{X}_n \boldsymbol{\beta}_{\tau,0} + \boldsymbol{\alpha}_{\tau,0}(\mathbf{Z}_n) + \mathbf{u}_n \right). \tag{2.4}$$

The appeal of our proposed semiparametric PLSQAR model in (2.1) is at least two-fold. First, not only does it accommodate heterogeneity in the spatial relationship by allowing some covariates in the model (namely, $\mathbf{z}_{i,n}$) to affect the outcome variable in a completely unspecified way thereby admitting any potential unit-specific nonlinearities but it also allows for *distributional* heterogeneity of the effects of $\mathbf{X}_n$ and $\mathbf{Z}_n$ on $\mathbf{y}_n$. The latter is accomplished by separate measurements of the spatial relationship at different points of a response distribution. Second, unlike more conventional conditional mean models of spatial dependence, our quantile model is more robust to the error distributions including the presence of outliers.

Model (2.1) nests several special cases of quantile regressions that have been studied in the literature. Perhaps, the two most closely related models are those by Su & Yang (2011) and Su & Hoshino (2016). Specifically, if nonparametric intercept function $\alpha_{\tau,0}(\cdot)$ does not vary with $\mathbf{z}_{i,n}$ and is constant for any given quantile index τ, i.e., when $\alpha_{\tau,0}(\mathbf{z}_{i,n}) = \alpha_{\tau,0}$ for all $\mathbf{z}_{i,n}$, our model becomes a (more restrictive) *fully* parametric linear spatial quantile autoregression (SQAR) considered by

[3]Which is satisfied if one standardizes a raw spatial weighting matrix by dividing all of its elements by its largest eigenvalue in absolute value.

Su & Yang (2011). On the other hand, our model can also be viewed as a special case of Su & Hoshino's (2016) varying-coefficient quantile regression where all parameter functions, except for the intercept, are forced to be constant. However, while their model also features endogenous regressors, it rules out any cross-sectional dependence by focusing on the case of *i.i.d.* data. In contrast, our PLSQAR model relaxes the *i.i.d.* assumption by allowing the spatial dependence in $\mathbf{y}_n$. In the case when the outcome variable exhibits no spatial dependence and hence $\rho_{\tau,0} = 0$, our model is no longer subject to endogeneity and essentially becomes an ordinary partially linear quantile regression which has been rather extensively studied for *i.i.d.* data (e.g., He & Shi, 1996; He & Liang, 2000; Lee, 2003). If one further restricts $\boldsymbol{\beta}_{\tau,0} = \mathbf{0}_{d_x}$, the model collapses to a fully nonparametric quantile regression studied by Yu & Jones (1998). In case of exogenous regressors only, some other closely related models include a varying coefficient quantile regression studied by Honda (2004) and Kim (2007) for *i.i.d.* data and Cai & Xu (2008) for the time-series case.

2.1 Sieve IV Quantile Estimator

Our estimation strategy relies on Chernozhukov & Hansen's (2006) idea whereby the solution to the instrument-based quantile restriction (2.2) is essentially equivalent to the search for $\left(\rho_{\tau,0}, \boldsymbol{\beta}'_{\tau,0}, \alpha_{\tau,0}(\mathbf{z}_{i,n})\right)'$ such that zero is the solution to the usual quantile regression of $y_{i,n} - \rho_{\tau,0}\sum_{j\neq i} w_{ij,n}y_{j,n} - \mathbf{x}'_{i,n}\boldsymbol{\beta}_{\tau,0} - \alpha_{\tau,0}(\mathbf{z}_{i,n})$ on exogenous $(\mathbf{x}_{i,n}, \mathbf{z}_{i,n}, \mathbf{m}_{i,n})$, i.e.,

$$0 \in \arg\min_{f\in\mathcal{H}} \mathbb{E}\left[\zeta_\tau\left\{\left(y_{i,n} - \rho_{\tau,0}\sum_{j\neq i} w_{ij,n}y_{j,n} - \mathbf{x}'_{i,n}\boldsymbol{\beta}_{\tau,0} - \alpha_{\tau,0}(\mathbf{z}_{i,n})\right) - f(\mathbf{x}_{i,n}, \mathbf{z}_{i,n}, \mathbf{m}_{i,n})\right\}\right], \tag{2.5}$$

where $\zeta_\tau\{u\} \equiv u(\tau - \mathbb{1}\{u < 0\})$ for some $u \in R$ is the so-called "check function" with $\mathbb{1}\{\cdot\}$ being the indicator function, and $f(\cdot) \in \mathcal{H}$ is some measurable function.

Chernozhukov & Hansen (2006) pioneered this "instrumental variable quantile regression" approach for a parametric (fully linear) constant-coefficient model. Recently, it has been extended to a broader class of semiparametric varying-coefficient models by Su & Hoshino (2016). Both papers however assume *i.i.d.* data, which is certainly *not* the case in our paper given the spatial dependence in $\mathbf{y}_n$. We show that, under some regularity conditions, the approach nonetheless remains valid even for the spatial data. Different from Su & Yang (2011) who study the fully parametric special case of our model, we do so using the Law of Large Numbers (LLN) and Central Limit Theorem (CLT) for spatial near-epoch dependent (NED) processes derived in Jenish & Prucha (2012). In what follows, we outline the estimation methodology for our PLSQAR model. The asymptotic results along with the necessary assumptions to support them are discussed in Section 2.2.

We approximate unknown nonparametric function using sieves [for an excellent review of the sieve methods, see Chen (2007)]. Specifically, let $\{\phi_1(\cdot), \phi_2(\cdot), \ldots\}$ be a sequence of B-spline series (or the tensor product thereof). Then, for each z, we approximate the unknown intercept function $\alpha_{\tau,0}(z)$ by $\boldsymbol{\phi}_{L_n}(z)' \mathcal{A}_{\tau,0}$ where, for any integer $\kappa > 0$, we denote a $\kappa \times 1$ vector of known basis functions $\boldsymbol{\phi}_\kappa(u) = (\phi_1(u), \ldots, \phi_\kappa(u))'$, and the unknown parameter vector $\mathcal{A}_{\tau,0}$ is of dimension L_n. Hence, we can now rewrite our model in (2.1) as follows

$$y_{i,n} \approx \rho_{\tau,0}\sum_{j\neq i} w_{ij,n}y_{j,n} + \mathbf{x}'_{i,n}\boldsymbol{\beta}_{\tau,0} + \boldsymbol{\phi}_{L_n}(\mathbf{z}_{i,n})' \mathcal{A}_{\tau,0} + u_{i,n} \quad \forall\, \tau \in (0,1). \tag{2.6}$$

Following Chernozhukov & Hansen (2006), we also restrict $\mathcal{H}$ to the following class of linear functions:

$$\mathcal{H} = \left\{f(\mathbf{x}_{i,n}, \mathbf{z}_{i,n}, \mathbf{m}_{i,n}) = \mathbf{m}'_{i,n}\gamma\right\}, \tag{2.7}$$

where γ is a $d_m \times 1$ vector of constant parameters.

The sample counterpart of the objective function in the population instrumental variable quantile regression (2.5) then takes the following form:

$$\mathbb{Q}_{n,\tau}(\rho, \beta, \mathcal{A}, \gamma) \equiv \frac{1}{n}\sum_{i=1}^{n} \zeta_\tau \left\{ y_{i,n} - \rho \sum_{j \neq i} w_{ij,n} y_{j,n} - \mathbf{x}'_{i,n}\beta - \phi_{L_n}(\mathbf{z}_{i,n})' \mathcal{A} - \mathbf{m}'_{i,n}\gamma \right\}. \tag{2.8}$$

Based on the rationale behind (2.5), one is to expect the estimate of γ_τ to be close to zero when the estimate of $\left(\rho_{\tau,0}, \beta'_{\tau,0}, \alpha_{\tau,0}(\cdot)\right)'$ is close to the true population value. Building on this intuition, we can estimate unknown $\left(\rho_{\tau,0}, \beta'_{\tau,0}, \alpha_{\tau,0}(\cdot)\right)'$ in two steps.

Step 1. For a given value of ρ, we estimate the usual quantile regression of $\dot{y}_{i,n}(\rho) \equiv y_{i,n} - \rho \sum_{j \neq i} w_{ij,n} y_{j,n}$ on exogenous covariates $\mathcal{X}_{i,n} = \left(\mathbf{x}'_{i,n}, \mathbf{m}'_{i,n}, \phi_{L_n}(\mathbf{z}_{i,n})'\right)'$ to obtain the "profiled" estimates of $\boldsymbol{\theta}_{\tau,0}(\rho) = \left(\beta_{\tau,0}(\rho)', \gamma_{\tau,0}(\rho)', \mathcal{A}_{\tau,0}(\rho)'\right)'$:

$$\widehat{\boldsymbol{\theta}}_\tau(\rho) = \underset{\boldsymbol{\theta}(\rho) \in \Theta}{\arg\min} \frac{1}{n}\sum_{i=1}^{n} \zeta_\tau \left\{ \dot{y}_{i,n}(\rho) - \mathcal{X}'_{i,n}\boldsymbol{\theta}(\rho) \right\}, \tag{2.9}$$

where $\boldsymbol{\theta}_{\tau,0}(\rho)$ is an interior point of Θ, a compact subset of $R^{1+d_x+d_m+L_n}$, and is the unique solution to the population counterpart of (2.9):

$$\boldsymbol{\theta}_{\tau,0}(\rho) = \underset{\boldsymbol{\theta}_0(\rho) \in \Theta}{\arg\min}\ \mathbb{E}\left[\zeta_\tau \left\{ \dot{y}_{i,n}(\rho) - \mathcal{X}'_{i,n}\boldsymbol{\theta}_0(\rho) \right\}\right]. \tag{2.10}$$

Step 2. We minimize the weighted norm of $\widehat{\gamma}_\tau(\rho)$ estimated in the first step with respect to ρ to obtain our estimator of $\rho_{\tau,0}$:

$$\widehat{\rho}_\tau = \underset{\rho}{\arg\min}\ \widehat{\gamma}_\tau(\rho)' \mathbf{V}_n \widehat{\gamma}_\tau(\rho), \tag{2.11}$$

where $\mathbf{V}_n$ is some $d_m \times d_m$ symmetric positive-definite weighting matrix. Correspondingly, the estimators of $\beta_{\tau,0}$ and $\mathcal{A}_{\tau,0}$ are respectively given by

$$\widehat{\beta}_\tau = \widehat{\beta}_\tau(\widehat{\rho}_\tau) \quad \text{and} \quad \widehat{\mathcal{A}}_\tau = \widehat{\mathcal{A}}_\tau(\widehat{\rho}_\tau). \tag{2.12}$$

Hence, for any given $\mathbf{z}$, the sieve estimator of the unknown intercept function $\alpha_{\tau,0}(\mathbf{z})$ is

$$\widehat{\alpha}_\tau(\mathbf{z}) = \phi_{L_n}(\mathbf{z})' \widehat{\mathcal{A}}_\tau. \tag{2.13}$$

The implementation of our estimator warrants three remarks. First, assuming that $\mathbf{x}_{i,n}$ and $\mathbf{z}_{i,n}$ are strictly exogenous and relevant, a selection of linearly independent variables from $\mathbf{W}_n\mathbf{X}_n, \mathbf{W}_n\mathbf{Z}_n, \mathbf{W}_n^2\mathbf{X}_n, \mathbf{W}_n^2\mathbf{Z}_n, \ldots$ provides a set of good instruments for the endogenous spatial lag $\mathbf{W}_n\mathbf{y}_n$. Since we only seek to obtain a consistent nonparametric IV estimator without pursuing optimality, we use $\mathbf{m}_{i,n} = \left[(\mathbf{W}_n\mathbf{X}_n)'_i, (\mathbf{W}_n\mathbf{Z}_n)'_i\right]'$ as our instruments, having removed any redundant terms, where $(\mathbf{W}_n\mathbf{A})_i = \sum_{j \neq i} w_{ij,n} a_j$ for $\mathbf{A} = \mathbf{X}_n, \mathbf{Z}_n$. Second, the outlined two-step estimation methodology can be operationalized in the form of a grid search or, alternatively, both steps can be estimated jointly via an automatic numerical search. In either case, it is imperative to impose appropriate box constraints on ρ to ensure that it lies within the unit circle. Third, in the second-step estimation, an obvious practical choice for $\mathbf{V}_n$ is an identity matrix, as suggested by Chernozhukov & Hansen (2006) and Su & Yang (2011). In fact, when $d_m = 1$ and our model is exactly identified, we can show that the limiting distribution of our estimator is expectedly invariant to the choice of $\mathbf{V}_n$. In the case of an over-identified model, one however could improve asymptotic efficiency by weighing $\widehat{\gamma}_\tau(\rho)$ using the inverse of its asymptotic covariance matrix, which obviously would first need to be consistently estimated. For tractability purposes, in our paper we set $\mathbf{V}_n = \mathbf{I}_{d_m}$.

2.2 Asymptotic Properties

The derivation of limit results for our proposed estimator requires the following assumptions.

Assumption 2 *(i)* $\{(\mathbf{x}_{i,n}, \mathbf{z}_{i,n})\}$ *is non-stochastic and uniformly bounded in absolute values; (ii)* $u_{i,n} = b_{i,n}(\mathbf{X}_n, \mathbf{Z}_n, \boldsymbol{\varepsilon}_n)$ *is a function of* $\mathbf{X}_n$, $\mathbf{Z}_n$ *and* $\boldsymbol{\varepsilon}_n$ *such that* $\Pr(u_{i,n} \leq 0) = \tau$ *holds almost surely for all* i, *and* $\boldsymbol{\varepsilon}_n = (\varepsilon_{1,n}, \ldots, \varepsilon_{n,n})$ *is an* $n \times 1$ *vector of errors with uniformly bounded variances; (iii)* $\{u_{i,n}, \boldsymbol{l}(i) \in D_n\}$ *is uniformly* L_2*-NED on* $\{\varepsilon_{j,n}, \boldsymbol{l}(i) \in D_n\}$ *with the NED coefficients of* $\psi(s) = O(s^{-\varsigma})$ *for some* $\varsigma > d$, *and the* α*-mixing coefficients of* $\{\varepsilon_{i,n}\}$ *satisfy* $\alpha(k,l,r) \leq (k+l)^{\upsilon}\,\widehat{\alpha}(r)$ *for some* $\upsilon \geq 0$ *and* $\sum_{r=1}^{\infty} r^{d(\upsilon+1)-1}\widehat{\alpha}(r) < \infty$, *where the NED concept is defined over* $\mathcal{F}_{i,n}(s) = \sigma(\varepsilon_{j,n}, \boldsymbol{l}(j) \in D_n, \varrho(i,j) \leq s)$, *the smallest* σ*-field generated by* $\{\varepsilon_{i,n}\}$ *located in the* s*-neighborhood of the spatial unit* i.

Assumption **2(i)**, also used by Qu & Lee (2015), permits a simple exposition of our assumptions without loss of generality and can be relaxed to allow stochasticity with bounded moment conditions. Under Assumption **2(ii)–(iii)**, $\{u_{i,n}, \boldsymbol{l}(i) \in D_n\}$ is a weakly dependent spatial process with heteroskedasticity. To conserve space, we refer the reader to Jenish & Prucha (2009, 2012) for definition of the spatial α-mixing and NED process including $\alpha(k,l,r)$ and $\widehat{\alpha}(r)$. Since $\mathbf{X}_n$ and $\mathbf{Z}_n$ are non-stochastic, the stochastic property of $u_{i,n}$ is determined solely by its location $\boldsymbol{l}(i)$ and a nonlinear moving average of $\boldsymbol{\varepsilon}_n$. According to Jenish & Prucha (2012), Assumption **2(iii)** holds if $\max_{1\leq i \leq n} \mathbb{E}[\varepsilon_{i,n}^2] < M < \infty$ and the overall contributions (i.e., weights) of $\{\varepsilon_{i,n}\}$ in absolute values are ignorable among far-away spatial units. The convergence speeds of the mixing coefficients and the NED coefficients to zero are the same as those in Jenish (2016).

To see the validity of Assumption **2(iii)**, consider an example of $u_{i,n} = \sigma_{i,n}\varepsilon_{i,n}$, where $\{\varepsilon_{i,n}\}$ is an *i.i.d.* error with finite variance and $\sigma_{i,n} = \lambda_0 + \lambda_1 \sum_{j \neq i} w_{ij,n} y_{j,n} + \mathbf{x}_{i,n}'\boldsymbol{\lambda}_2 + \lambda_3(\mathbf{z}_{i,n})$. Combining with (2.3)–(2.4), we have that

$$\boldsymbol{\sigma}_n = \lambda_0 \mathbf{i}_n + \mathbf{X}_n \boldsymbol{\lambda}_2 + \boldsymbol{\lambda}_3(\mathbf{Z}_n) + \lambda_1 \mathbf{G}_n \mathbf{X}_n \boldsymbol{\beta}_{\tau,0} + \lambda_1 \mathbf{G}_n \boldsymbol{\alpha}_{\tau,0}(\mathbf{Z}_n) + \lambda_1 \mathbf{G}_n \mathcal{E}_n \boldsymbol{\sigma}_n, \tag{2.14}$$

where $\boldsymbol{\sigma}_n = (\sigma_{1,n}, \ldots, \sigma_{n,n})'$, $\mathcal{E}_n = \operatorname{diag}\{\varepsilon_{1,n}, \ldots, \varepsilon_{n,n}\}$, and $\mathbf{i}_n$ is an $n \times 1$ vector of ones. Furthermore, letting $\mathbf{S}_n(\rho) = \mathbf{I}_n - \rho \mathbf{W}_n$ and $\mathbf{G}_n(\rho) = \mathbf{W}_n \mathbf{S}_n(\rho)^{-1}$, we define $\mathbf{S}_n = \mathbf{S}_n(\rho_{\tau,0})$ and $\mathbf{G}_n = \mathbf{G}_n(\rho_{\tau,0})$ the latter of which has a typical element $g_{ij,n}$. If the random matrix $\mathbf{I}_n - \lambda_1 \mathbf{G}_n \mathcal{E}_n$ is invertible almost surely,[4] $\sigma_{i,n}$ is an MA(∞) spatial process of $\{\varepsilon_{i,n}\}$. Roughly speaking, $\{\sigma_{i,n}, \boldsymbol{l}(i) \in D_n\}$ is L_2-NED on $\{\varepsilon_{j,n}, \boldsymbol{l}(i) \in D_n\}$ by Proposition 1 in Jenish & Prucha (2012) if $\lim_{s\to\infty} \sup_{n, \boldsymbol{l}(i) \in D_n} \sum_{\boldsymbol{l}(j) \in D_n, \varrho(i,j) > s} |g_{ij,n}| = 0$. Consequently, $\{u_{i,n}, \boldsymbol{l}(i) \in D_n\}$ is L_2-NED on $\{\varepsilon_{j,n}, \boldsymbol{l}(i) \in D_n\}$.

[4]Let $e(\mathbf{A})$ be the largest eigenvalue of $\mathbf{A}$ in the absolute value, where $\mathbf{A}$ is an $n \times n$ matrix with a typical element a_{ij}. Then, $e(\mathbf{A}) \leq \|\mathbf{A}\|_1$, where $\|\mathbf{A}\|_1 = \max_{1 \leq j \leq n} \sum_{i=1}^{n} |a_{ij}|$ by Seber (2008, Property 4.68). Now, $\|\mathbf{I}_n - \lambda_1 \mathbf{G}_n \mathcal{E}_n\|_1 \leq |1 - \lambda_1 g_{jj,n}\varepsilon_{j,n}| + |\lambda_1| \max_{1 \leq j \leq n} \sum_{i \neq j} |g_{ij}|\,|\varepsilon_{jn}| < 1$ holds almost surely if $\|\mathbf{G}_n\|_1 < M < \infty$, $\{\varepsilon_{in}\}$ has a compact support, and λ_1 is small enough (Seber, 2008, p.472), where $\|\mathbf{G}_n\|_1 < M < \infty$ is a regularity assumption commonly imposed in the spatial autoregressive literature (e.g., Kelejian & Prucha, 2010).

Assumption 3 *(i)* $\mathbf{S}_n(\rho)$ *is a nonsingular matrix over* $\rho \in \Lambda_\rho$*, and* $\rho_{\tau,0}$ *is an interior point of* Λ_ρ*, a compact subset of R; (ii) there exists a positive integer N such that both* $\mathbf{W}_n$ *and* $\mathbf{S}_n^{-1}(\rho)$ *have finite row- and column-sum matrix norms for all* $n > N$ *and* $\rho \in \Lambda_\rho$*; (iii)* $|w_{ij,n}| \leq c_1 \varrho(i,j)^{-c_2 d}$ *for some positive constants* c_1 *and* $c_2 > \varsigma/d$*.*

Assumption **3(i)–(ii)** are the regularity conditions (e.g., Kelejian & Prucha, 2010). Assumption **3(iii)** deviates from Qu & Lee (2015) by assuming gradually decaying spatial weights as the distance between two spatial units grows, which includes the case when $|w_{ij,n}| = 0$ if $\varrho(i,j)$ is greater than some threshold value.

Assumption 4 *(i) There exists an* $L_n \times 1$ *vector* $\mathcal{A}_{\tau,0}$ *such that*

$$\sup_{\mathbf{z}\in\mathcal{S}_\mathbf{z}} \left|\alpha_\tau(\mathbf{z}) - \mathcal{A}'_{\tau,0}\phi_{L_n}(\mathbf{z})\right| \leq M L_n^{-\xi} \tag{2.15}$$

for any $\rho \in \Lambda_\rho$ *and some* $\xi > 2$ *as* $L_n \to \infty$*; (ii)* $\{\phi_l(\cdot)\}$ *is uniformly bounded over all l such that* $\|\phi_{L_n}\| = \sup_\mathbf{z} \sqrt{\sum_{l=1}^{L_n} \phi_l(\mathbf{z})} = O\left(\sqrt{L_n}\right)$.

Since $\mathcal{S}_z$ is a compact set, B-spline tensors can be used to construct the basis functions. Hence, Assumption **4** holds if $\alpha_\tau(\cdot)$ is p-smooth with uniformly bounded derivatives up to order p for some $p > \xi$.

Assumption 5 *Define* $\mathbf{v}_n(\rho) = [\mathbf{I}_n + (\rho_{\tau,0} - \rho)\mathbf{G}_n]\mathbf{u}_n$ *and let* $v_{i,n}(\rho)$ *be its ith element. (i)* $v_{i,n}(\rho)$ *has cdf* $F_{v_{i,n}(\rho)}(v)$ *and pdf* $f_{v_{i,n}(\rho)}(v)$*, and* $f_{v_{i,n}(\rho)}(v)$ *is continuously differentiable and uniformly bounded up to its first derivative with respect to* $v \in R$ *and* $\rho \in \Lambda_\rho$*; (ii) there exists two finite constants* $\underline{c}$ *and* $\bar{c}$ *such that* $0 < \underline{c} \leq \lambda_{\min}\{\mathbf{\Sigma}_\tau(\rho)\} \leq \lambda_{\max}\{\mathbf{\Sigma}_\tau(\rho)\} \leq \bar{c} < \infty$ *uniformly over* $\rho \in \Lambda_\rho$*; (iii)* $\mathcal{A}_2$ *is a nonsingular matrix, where* $\mathbf{\Sigma}_\tau(\rho)$ *and* $\mathcal{A}_2$ *are respectively defined in* (A.6) *and* (A.9) *in Appendix A.*

Since $v_{i,n}(\rho)$ is a linear combination of $\{u_{i,n}\}$, applying our earlier arguments and under Assumptions **2–3**, in Lemma 1 in Appendix A we show that $\{v_{i,n}(\rho), \boldsymbol{l}(i) \in D_n\}$ is also an L_2-NED on $\{\varepsilon_{i,n}, \boldsymbol{l}(i) \in D_n\}$ with the NED coefficients of $\psi(s) = O(s^{-\varsigma})$. Assumption **5(ii)** ensures the existence of the estimator calculated in Step 1, while Assumption **5(iii)** ensures the existence of the second-step estimator.

Assumption 6 *As* $n \to \infty$*,* $L_n \to \infty$*,* $nL_n^{1-2\xi} \to 0$ *and* $L_n^2/n \to 0$*.*

Assumption **6** is an assumption on the smoothing parameter L_n to ensure the consistency of our proposed estimator. Specifically, letting $L_n = cn^q$ for some $c > 0$Assumption **6** implies that $0 < 1/(2\xi - 1) < q < 1/2$.

Assumption 7 $F_{u_{i,n}}(u|\bar{u}_{i,n})$ *and* $f_{u_{i,n}}(u|\bar{u}_{i,n})$ *are, respectively, conditional cdf and pdf of* $u_{i,n} = u$ *conditional on* $\bar{u}_{i,n} = \sum_{j\neq i} g_{ij,n}u_{j,n}$*, and* $f_{u_{i,n}}(u|\bar{u}_{i,n})$ *is uniformly bounded and continuous up to the second-order derivatives with respect to u.*

Assumptions **1–6** are used to show the consistency of our first-step estimator, whereas Assumption **7** is used to derive the asymptotic normality results of the second-step estimator.

Theorem 1 *Under Assumptions **1–6**, we have that* $\max_{\rho\in\Lambda_\rho}\left\|\widehat{\boldsymbol{\theta}}_\tau(\rho) - \boldsymbol{\theta}_{\tau,0}(\rho)\right\| = O_p\left(\sqrt{L_n/n}\right)$.

Theorem 2 *Under Assumptions 1–7, we have*

$$\sqrt{n}\boldsymbol{\Sigma}_n^{-1/2}\begin{pmatrix}\widehat{\rho}_\tau - \rho_{\tau,0}\\ \widehat{\boldsymbol{\beta}}_\tau - \boldsymbol{\beta}_{\tau,0}\\ \widehat{\gamma}_\tau\end{pmatrix} \xrightarrow{d} \mathbb{N}\left(\mathbf{0}, \mathbf{I}_{1+d_x+d_m}\right) \quad and \quad \sqrt{n/\omega_{n,\tau}}\left(\widehat{\alpha}_\tau(\mathbf{z}) - \alpha_{\tau,0}(\mathbf{z})\right) \xrightarrow{d} \mathbb{N}(0,1),$$

where $\boldsymbol{\Sigma}_n$ *and* $\omega_{n,\tau}$ *are defined in the proof of this theorem in Appendix A.*

From the proof of this theorem, we see that $\boldsymbol{\Sigma}_n$ is a nonsingular matrix under Assumption **5(ii)–(iii)** and that $\omega_{n,\tau} = O\left(\sqrt{L_n}\right)$.

Remark 1. We study the finite-sample performance of our proposed two-step estimator in a small set of Monte Carlo simulations, the discussion of which is relegated to Appendix B. Overall, the results are encouraging, and simulation experiments support our asymptotic results.

3 Specification Testing

We next consider a model specification test which permits testing several useful hypotheses. Specifically, for a τth spatial quantile autoregression written as

$$y_{i,n} = q\left(\sum_{j\neq i} w_{ij,n}y_{j,n}, \mathbf{x}_{i,n}, \mathbf{z}_{i,n}, \tau\right) + u_{i,n} \equiv q_i(\tau) + u_{i,n}, \tag{3.1}$$

we consider the following null hypotheses about the form of its conditional quantile function $q_i(\tau)$:

$$\mathrm{H}_0(\mathrm{i}): \quad q_i(\tau) = \rho_{\tau,0}\sum_{j\neq i} w_{ij,n}y_{j,n} + \mathbf{x}_{i,n}'\boldsymbol{\beta}_{\tau,0} + (1, \mathbf{z}_{i,n})'\boldsymbol{\delta}_{\tau,0} \tag{3.2}$$

$$\mathrm{H}_0(\mathrm{ii}): \quad q_i(\tau) = \rho_{\tau,0}\sum_{j\neq i} w_{ij,n}y_{j,n} + \mathbf{x}_{i,n}'\boldsymbol{\beta}_{\tau,0} + \delta_{\tau,0}, \tag{3.3}$$

against the alternative (the PLSQAR model):

$$\mathrm{H}_1: \quad q_i(\tau) = \rho_{\tau,0}\sum_{j\neq i} w_{ij,n}y_{j,n} + \mathbf{x}_{i,n}'\boldsymbol{\beta}_{\tau,0} + \alpha_{\tau,0}(\mathbf{z}_{i,n}). \tag{3.4}$$

Alternatively, the above null and alternative hypotheses can be rewritten as follows: $\mathrm{H}_0(\mathrm{i})$: $\Pr\left[\alpha_{\tau,0}(\mathbf{z}_{i,n}) = (1, \mathbf{z}_{i,n})'\boldsymbol{\delta}_{\tau,0}\right] = 1$ for some $\boldsymbol{\delta}_{\tau,0} \in R^{1+d_z}$ against $\mathrm{H}_1: \Pr\left[\alpha_{\tau,0}(\mathbf{z}_{i,n}) = (1, \mathbf{z}_{i,n})'\boldsymbol{\delta}_\tau\right] < 1$ for any $\boldsymbol{\delta}_\tau \in R^{1+d_z}$, and $\mathrm{H}_0(\mathrm{ii})$: $\Pr\left[\alpha_{\tau,0}(\mathbf{z}_{i,n}) = \delta_{\tau,0}\right] = 1$ for some $\delta_{\tau,0} \in R$ against H_1 : $\Pr\left[\alpha_{\tau,0}(\mathbf{z}_{i,n}) = \delta_\tau\right] < 1$ for any $\delta_\tau \in R$. The null in (3.2) is meant to test for linearity of the conditional quantile function in $\mathbf{z}_{i,n}$. In practice, one may choose any desired *parametric* specification for the intercept function $\alpha_{\tau,0}(\cdot)$ to test against the nonparametric alternative in (3.4). The second null in (3.3) is essentially the test of overall relevancy of $\mathbf{z}_{i,n}$.

To test these hypotheses, we essentially propose a nonparametric likelihood-ratio test based on the comparison of the restricted and unrestricted models. The motivation for our test statistic comes from Ullah's (1985) nonparametric test that compares residual sums of squares under the null and the alternative (also see Fan et al., 2001; Lee & Ullah, 2003). The idea behind this test, which is formulated for a conditional mean model, can be extended to the conditional quantile framework along the lines of Koenker & Machado (1999) whereby the estimated residual sum of check functions effectively plays the role of the residual sum of squares. Specifically, for any given quantile index τ, we consider the following residual-based test statistic:

$$T_n = \frac{RSC_{0,\tau} - RSC_{1,\tau}}{RSC_{1,\tau}}, \tag{3.5}$$

where $RSC_{0,\tau}$ is the residual sum of check functions under H_0 computed as $RSC_{0,\tau} = \sum_{i=1}^{n} \zeta_\tau\{\widetilde{u}_{i,n}\}$ with $\widetilde{u}_{i,n} = y_{i,n} - \widetilde{q}_i(\tau)$ being the quantile residual defined as the difference between $y_{i,n}$ and the consistent estimate of $q_i(\tau)$ under either of the two null hypotheses in (3.2)–(3.3); and $RSC_{1,\tau}$ is the residual sum of check functions under H_1 computed as $RSC_{1,\tau} = \sum_{i=1}^{n} \zeta_\tau\{\widehat{u}_{i,n}\}$, where $\widehat{u}_{i,n}$ is the residual from our second-step estimator, i.e., $\widehat{u}_{i,n} = y_{i,n} - \widehat{q}_i(\tau) = y_i - \widehat{\rho}_\tau \sum_{j \neq i} w_{ij,n} y_{j,n} - \mathbf{x}_{i,n}' \widehat{\boldsymbol{\beta}}_\tau - \widehat{\alpha}_\tau(\mathbf{z}_{i,n})$. Residuals under H_0 can be obtained via Su & Yang's (2011) estimator.

Theorem 3 *Under Assumptions 2–5, under H_0 we have that $T_n \xrightarrow{p} 0$, while under H_1 we have* $\Pr[T_n \geq M_n] \to 0$ *for any non-stochastic, positive sequence M_n.*

See Appendix A for the proof. Thus, T_n is a consistent test. Intuitively, the test statistic is expected to converge to zero under the null and is positive under the alternative. Hence, the test is one-sided. We suggest using bootstrap for approximating the null distribution of T_n, especially given that residual-based nonparametric tests are well-known to perform rather poorly in finite samples when relying on asymptotic critical values. Bootstrap methods however offer a means to improve their finite-sample performance. For fixed $\tau \in (0, 1)$, we use the following wild (residual) bootstrap procedure modified to suit the asymmetric loss function used in the quantile estimation:[5]

(1) Estimate the restricted model under either of the two nulls in (3.2)–(3.3) to obtain residuals $\{\widetilde{u}_{i,n};\ i = 1, \ldots, n\}$.

(2) Generate two-point wild bootstrap errors by setting $u_{i,n}^* = \omega_1 \times |\widetilde{u}_{i,n}|$ with probability $(1 - \tau)$ and $u_{i,n}^* = \omega_2 \times |\widetilde{u}_{i,n}|$ with probability τ, where $\omega_1 = 2(1 - \tau)$ and $\omega_2 = -2\tau$.

(3) Construct the bootstrap sample $\{y_{i,n}^*, \sum_{j \neq i} w_{ij,n} y_{j,n}^*, \mathbf{x}_{i,n}, \mathbf{z}_{i,n};\ i = 1, \ldots, n\}$, where $y_{i,n}^*$ is generated from the restricted model under the appropriate null:

$$\mathbf{y}_n^* = \begin{cases} [\mathbf{I}_n - \widetilde{\rho}_\tau \mathbf{W}_n]^{-1} \left(\mathbf{X}_n \widetilde{\boldsymbol{\beta}}_\tau + [\mathbf{i}_n, \mathbf{Z}_n] \widetilde{\boldsymbol{\delta}}_\tau + \mathbf{u}_n^* \right) & \text{for } \mathrm{H}_0(\mathrm{i}) \\ [\mathbf{I}_n - \widetilde{\rho}_\tau \mathbf{W}_n]^{-1} \left(\mathbf{X}_n \widetilde{\boldsymbol{\beta}}_\tau + \mathbf{i}_n \widetilde{\delta}_\tau + \mathbf{u}_n^* \right) & \text{for } \mathrm{H}_0(\mathrm{ii}), \end{cases} \tag{3.6}$$

where $\mathbf{y}_n^* = (y_{1,n}^*, \ldots, y_{n,n}^*)'$ and $\mathbf{u}_n^* = (u_{1,n}^*, \ldots, u_{n,n}^*)'$.

(4) Reestimate both the restricted and unrestricted models using the bootstrap sample from step (3) to obtain bootstrap residuals $\{\widetilde{u}_{i,n}^*;\ i = 1, \ldots, n\}$ and $\{\widehat{u}_{i,n}^*;\ i = 1, \ldots, n\}$ under H_0 and H_1, respectively.

(5) Compute the bootstrap test statistic $T_n^* = \left(RSC_{0,\tau}^* - RSC_{1,\tau}^* \right) / RSC_{1,\tau}^*$, where $RSC_{0,\tau}^* = \sum_{i=1}^{n} \zeta_\tau\{\widetilde{u}_{i,n}^*\}$ and $RSC_{1,\tau}^* = \sum_{i=1}^{n} \zeta_\tau\{\widehat{u}_{i,n}^*\}$.

[5] Feng et al. (2011) show that a traditional wild bootstrap procedure is invalid for quantile estimators due to nonlinear score functions associated with the check-function-based objective function. Alternatively, Sun (2006) introduces a modified wild bootstrap method applicable to testing in the quantile regression framework.

(6) Repeat steps (2)–(5) B times. Use the empirical distribution of $B+1$ bootstrap statistics, where the first bootstrap test statistic equals the test statistic calculated from the raw data, to obtain the upper $a \times 100$th percentile value c_a for a given $a \in (0,1)$. Use this c_a to approximate the upper percentile (critical) value of the test statistic T_n under H_0. We wil reject H_0 if the bootstrap test statistic is greater than c_a.

Monte Carlo simulations (discussed in Appendix B) show that the bootstrap T_n test has quite an accurate size and exhibits superb power which rises with the sample size, as expected.

4 Data

Our data come from Delaware County Auditor's Office and were obtained in the form of ArcGIS parcel shapefiles. Each parcel record contains information about house and other property characteristics such as house and lot size, number of rooms, etc. (see Table 1 for a full self-descriptive list of variables). Based on land-use codes, we retain only records containing arm's length single-family home transactions. We do so because hedonic models require competitive housing markets with buyers and sellers whose willingnesses to pay and accept are formed based on property characteristics only. Our operational sample includes 5,500 sale transactions that took place in the county during the 2009:1–2011:3 period (roughly, two years).

There are four rock mines in the county, three of which are no longer operational. All are surface mines. They were located from geographic coordinates of parcels owned by the mining companies (Ohio Department of Natural Resources, 2010, 2011) and were further verified using Google Earth. The only operational mine (state mine number: Del-5) also happens to be the largest of all by an order of magnitude. It is located in the Southwestern part of the county near the city of Delaware and is about 510 acres large,[6] which is almost triple the size of an average farm in the county (187 acres). In the case of Delaware County, all mines are limestone (but colloquially called gravel mines) and thus are subject to dynamite blasting which creates a far greater nuisance than other types of mines such as composite mines. Given that other mines in the county were no longer in operation by the period of our study and hence did not generate noise, dust and traffic, in our analysis we solely focus on the operational Del-5 mine, which is not only very large but is also located in an area of high urban growth.

Because our data are explicitly georeferenced, we use a standard software routine to calculate straight-line distances from each property to the mine centroid. This distance proxies environmental amenity associated with rock mining, with better quality occurring at farther distances from mines. We opt for such a measure over the alternative measures of environmental quality associated with disamenities such as the number of disamenities within a certain distance of a property because, in our case, we have a single occurrence of a large disamenity spread widely throughout the area. Further, since our econometric model allows environmental impacts to be nonlinear, the use of straight-line distances as a measure of environmental quality does not appear that problematic.

We also match our data with the neighborhood-specific demographic variables at the Census block level from the U.S. Census Bureau. Specifically, we include the black[7] population share, median income and the property tax rate in the neighborhood. We use these variables as observable controls for neighborhood characteristics (in addition to the spatial lag term as discussed in the introduction). We opt for these continuous measures of neighborhood characteristics over discrete

[6]Based on Google Earth Pro measurements.

[7]Variables for other non-white population groups have been consistently found to be insignificant, and their exclusion has affected the results in no material way.

Table 1. Data Summary Statistics

Variable	Units	Mean	5th Perc.	Median	95th Perc.
House Price	thousands $	258.42	64.00	232.49	552.50
Distance to Rock Mine	thousands ft.	49.12	12.92	51.14	80.27
Square Footage	$ft.^2$	2,452.99	1,188.00	2,360.00	4,054.05
Acreage	acres	0.78	0.15	0.30	3.18
Age	years	20.42	0	10	108
Story Height	cardinal number	1.79	1	2	2
# of Bedrooms	cardinal number	3.58	3	4	4
# of Bathrooms	cardinal number	2.95	1	3	5
# of Fireplaces	cardinal number	0.83	0	1	1
Garage Capacity	cardinal number	1.29	0	2	3
Attached Garage	binary indicator	0.551			
Full Basement	binary indicator	0.447			
Partial Basement	binary indicator	0.457			
Attic	binary indicator	0.095			
Central A/C	binary indicator	0.885			
Black Population Share	% pt.	3.27	0.00	1.88	11.11
Median Income	thousands $	80.04	36.40	81.20	113.00
Property Tax Rate	% pt.	1.87	1.39	1.92	2.23

The last three variables are at the Census block group level.

locality fixed effects primarily out of computational considerations because quantile estimation is known to performs rather poorly in the presence of multiple binary covariates.

5 Empirical Results

We estimate the hedonic house valuation function in the form of our PLSQAR model in (2.1), where we let the distance to nearby rock mine enter the function nonparametrically as a "z" variable with the rest of hedonic attributes included parametrically as "x" variables. All right-hand-side covariates appear in levels except for square footage and acreage to which we apply the logarithmic transformation. In the case of the number of bedrooms, bathrooms and age, we also include quadratic terms. Following the literature, we take the logarithm of the left-hand-side house price (the "y" variable) thereby facilitating the interpretation of marginal effects in terms of percentages, allowing for nonlinearities and ensuring the outcome variable can take any real value.

Given the highly uneven distribution of houses in space, we use a distance-based k-nearest-neighbor type of spatial weighting matrices to model spatial relationship across properties. The latter helps ensure that each house gets neighbors whose prices are deemed "relevant" (by getting relatively large weights) in predicting its value. The use of alternative distance-based weighting matrices, where the spatial weights are decaying functions of distance, leads to an undesirable situation when houses in highly urbanized localities have multiple "relevant" neighbors that are assigned large weights and houses in a sparsely populated countryside hardly have any such "relevant" neighbors, which obviously is inaccurate because appraisers are willing to look far for comparable properties when valuating houses in rural areas. We select the number of nearest neighbors that minimizes the AIC criterion for the median model. The data favor $k = 5$, which we use throughout.

When estimating the model, we approximate the unknown nonparametric intercept function $\alpha_{\tau,0}(\cdot)$ via cubic B-spline sieves, the order of approximation for which (in this case, the number of knots) is also selected by minimizing AIC. Throughout, we use spatial lags of continuous house-specific attributes (log square footage and log acreage) as our instruments. We do not include lags of other exogenous attributes into the instrument set because they are discrete and lead to severe multicollinearity and convergence problems.

Since the objective of our paper is to assess property-value-suppressing effects of rock mines on nearby property (and in order to conserve space), in what follows we primarily focus on the results concerning the relationship between a house's price and its distance from the mine. Consistent with the notion that rock mines are an environmental disamenity that creates negative externalities such as dust, noise and additional traffic, our expectation is the *positive* relationship between the two variables implying that the houses located farther from mines would be appraised at higher values. (The results pertaining to other house attributes are relegated to Appendix C.)

As discussed earlier, most studies pursuing the housing-market-based valuation of adverse welfare effects of environmental disamenities estimate a linear hedonic price function, which rather restrictively assumes constant marginal impact of the disamenity on house prices. Few papers that do explore potential nonlinearities have largely favored a quadratic form (e.g., Kohlhase, 1991; Hite et al., 2001) which, given its reliance on an *a priori* functional form assumption, is still subject to potential misspecification. We circumvent these problems by letting the distance between the house and a rock mine (z) enter the house valuation function in a nonparametric fashion [through an unspecified intercept function $\alpha_{\tau,0}(\cdot)$] thereby accommodating any potential nonlinearities in the relationship between (log) property values and the distance to the mine. We first examine the sensitivity of empirical results to potential functional-form misspecification of $\alpha_{\tau,0}(\cdot)$. To do so, in addition to our semiparametric PLSQAR model of house prices, we also estimate a *fully* parametric SQAR model under the following two specifications of the intercept function: (i) $\alpha_{\tau,0}(z) = a_{0,\tau} + a_{1,\tau}z + a_{2,\tau}z^2$ and (ii) $\alpha_{\tau,0}(z) = a_{0,\tau} + a_{1,\tau}z$. These specifications imply quadratic and linear functional forms of the relationship between the log price and z, respectively. Comparing the results from our flexible PLSQAR model, which lets the data determine the shape of $\alpha_{\tau,0}(\cdot)$, to those from a parametric model under these two specifications enables us to empirically assess the extent to which the hedonic estimates of property-value-suppressing effects of rock mines on nearby houses are sensitive to "correct" functional form specification of the house price function. Such a comparison is especially interesting given the wide popularity of linear and quadratic parameterizations in the literature. The parametric model under both specifications of $\alpha_{\tau,0}(\cdot)$ is estimated via a two-step procedure following Su & Yang (2011). To conserve space, we focus on the median quantile ($\tau = 0.50$) when comparing these alternative models.

Figure 1 plots the estimated intercept function across the three models. Our preferred PLSQAR model, which estimates $\alpha_{\tau,0}(z)$ nonparametrically, points to a rather steep relationship between the house price and its distance to the mine when the house is located in a close vicinity from a mine (smaller values of z) with a diminishing gradient that ultimately plateaus at around a 10-mile mark.[8] Such a shape is remarkably consistent with one's expectation that the property-value effects of environmental disamenities are a *local* phenomenon and that rock mines would not impact values of *distant* properties (with larger values of z). The latter can also be seen from Figure 2, which graphs the estimated gradient of the intercept function along with its 95% confidence bounds. The figure is indicative of a significant positive effect of z on the log house price within roughly a 10-mile radius of the mine that eventually decreases to a statistically insignificant gradient.

Comparing our model to its parametric alternatives, we expectedly find that parametric models are more susceptible to a functional-form misspecification. While the quadratic model does successfully find a decreasing gradient of $\alpha_{\tau,0}(z)$ in a close proximity from the mine, it is however unable

[8] Just above $z = 50$ thousand feet.

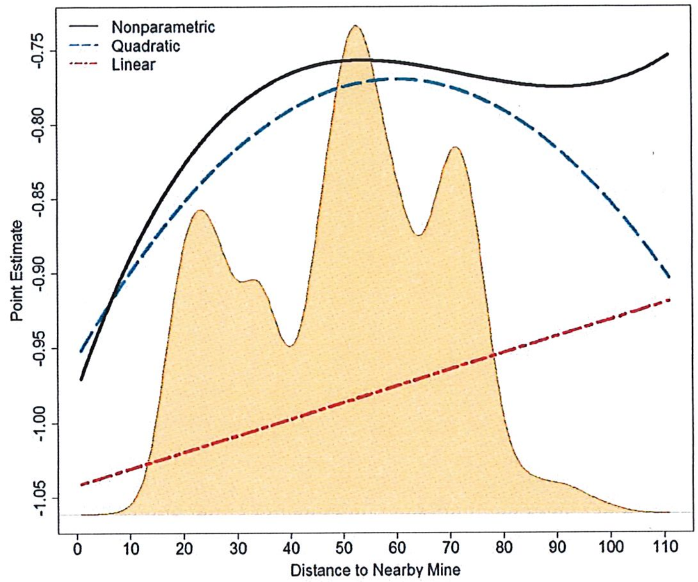

Figure 1. Estimated Intercept Functions of the Distance to Rock Mine for the Conditional Median Model [*Note:* Shaded is the kernel density of the distance variable]

to detect that rock mines appear to become rather irrelevant for the (median) price of houses lying outside their 10-mile radius zone. In fact, a parabolic relationship estimated by the quadratic model rather counter-intuitively suggests a negative (and statistically significant) relationship between the two for large values of z [see Figures 1 and 2]. This illustrates the sensitivity of parametric models (due to their inflexibility) to the inclusion of data on properties that are located farther from the disamenities and thus are less, if at all, impacted by negative environmental externalities they generate. To avoid this problem, researchers employing parametric specifications therefore usually have to prespecify a spatial radius of potential impact around the disamenity (e.g., Nelson et al., 1992; Reichert et al., 1992; Hite et al., 2001). However, such an *a priori* choice of the radius is oftentimes *ad hoc* in nature; whereas our model, owing to its nonparametric approach to modeling the distance to disamenity, essentially detects the radius of non-zero impact directly from the data. Lastly, fitting a linear SQAR model mitigates the problem but at a cost of producing a linear relationship characterized by a rather misleading "average" gradient. The latter can be vividly seen in Figure 2 which shows that, due to its inherent inability to allow for nonlinearities and hence heterogeneity across units, the linear SQAR model tends to grossly under-estimate the gradient.

However, the gradient estimates of $\alpha_{\tau,0}(z)$ plotted in Figure 2 cannot be interpreted as representing marginal partial effects of z on (median) house prices due to the appearance of spatial lag of house prices on the right-hand side of the estimated quantile function. Hence, to obtain partial effects, we consider a reduced form of the fitted outcome variable at the τth quantile: $\widehat{\mathbf{y}}_\tau = [\mathbf{I}_n - \widehat{\rho}_\tau \mathbf{W}_n]^{-1} \left(\mathbf{X}_n \widehat{\boldsymbol{\beta}}_\tau + \widehat{\boldsymbol{\alpha}}_\tau(\mathbf{Z}_n)\right)$, from where we have the following $n \times n$ matrices of marginal effects:

$$\frac{\partial \widehat{\mathbf{y}}_\tau}{\partial \mathbf{Z}_n'} = [\mathbf{I}_n - \widehat{\rho}_\tau \mathbf{W}_n]^{-1} \times \operatorname{diag}\left\{ \frac{\partial \widehat{\alpha}_\tau(z_{1,n})}{\partial z_{1,n}}, \ldots, \frac{\partial \widehat{\alpha}_\tau(z_{n,n})}{\partial z_{n,n}} \right\}, \tag{5.1}$$

$$\frac{\partial \widehat{\mathbf{y}}_\tau}{\partial \mathbf{x}_{j,n}'} = [\mathbf{I}_n - \widehat{\rho}_\tau \mathbf{W}_n]^{-1} \times \widehat{\beta}_{\tau,j} \qquad \forall\, j = 1, \ldots, d_x, \tag{5.2}$$

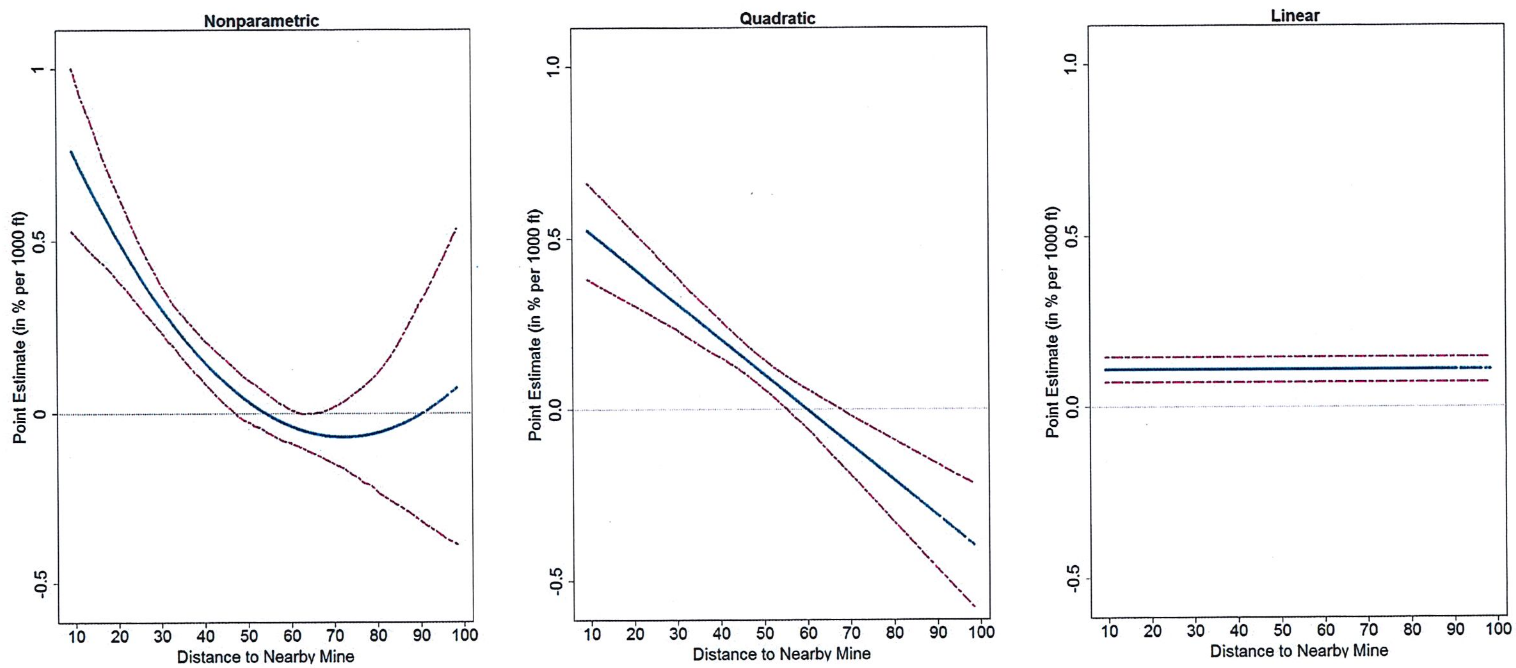

Figure 2. Estimated Gradients of Intercept Functions of the Distance to Rock Mine for the Conditional Median Model
(with the 95% bootstrap confidence bounds)

Table 2. Summary of Statistically Significant Point Estimates of ME of the Distance to Rock Mine on Conditional Median of Property Value

	Entire Sample			*Within 10-Mile Radius*		
	TME	DME	IME	TME	DME	IME
			Nonparametric			
5th Perc.	−0.0853	−0.0597	−0.0257	0.1192	0.0831	0.0363
25th Perc.	0.1477	0.1037	0.0433	0.2946	0.2030	0.0885
50th Perc.	0.4629	0.3243	0.1396	0.5810	0.4046	0.1751
75th Perc.	0.8023	0.5581	0.2403	0.8560	0.5957	0.2575
95th Perc.	1.0740	0.7520	0.3227	1.0793	0.7566	0.3245
Mean	0.4836	0.3379	0.1456	0.5768	0.4031	0.1737
			Quadratic			
5th Perc.	−0.3221	−0.2263	−0.0943	0.1271	0.0897	0.0372
25th Perc.	−0.1506	−0.1071	−0.0439	0.2044	0.1449	0.0599
50th Perc.	0.1836	0.1300	0.0535	0.4338	0.3065	0.1272
75th Perc.	0.5108	0.3572	0.1508	0.6130	0.4332	0.1789
95th Perc.	0.7199	0.5063	0.2110	0.7395	0.5226	0.2167
Mean	0.1964	0.1386	0.0577	0.4146	0.2929	0.1217
			Linear			
5th Perc.	0.1646	0.1113	0.0505	0.1646	0.1113	0.0506
25th Perc.	0.1646	0.1124	0.0508	0.1646	0.1113	0.0506
50th Perc.	0.1646	0.1131	0.0514	0.1646	0.1131	0.0515
75th Perc.	0.1646	0.1137	0.0521	0.1646	0.1137	0.0522
95th Perc.	0.1646	0.1140	0.0533	0.1646	0.1140	0.0533
Mean	0.1646	0.1129	0.0516	0.1646	0.1129	0.0517

The reported estimates are in % per 1,000 ft.

where $\mathbf{x}_{j,n} = (x_{j,1}, \ldots, x_{j,n})'$ is the jth column of $\mathbf{X}_n$. In the spirit of LeSage & Pace (2009), we refer to the diagonal elements of the gradient matrices of $\widehat{\mathbf{y}}_\tau$ in (5.1)–(5.2) as direct marginal effects (DMEs) and to the off-diagonal elements as indirect marginal effects (IMEs). We analyze marginal effects row-by-row which implies a "*to* a house" interpretation, i.e., how the change in a given covariate across *all* houses affects the price of the ith house. Hence, the summation of elements in the ith row of the gradient matrices in (5.1)–(5.2) provides a measure of the total marginal effect (TME) on the ith house. Also note that, because by design the maximum-eigenvalue-standardized k-nearest-neighbor spatial weights matrix employed in the estimation is in fact row-stochastic, TMEs of covariates that have *constant* gradients (i.e., all "x" variables and, in the case of a linear parametric SQAR model, also variable z) are the same across all observations and are equal to the corresponding gradient times $(1 - \widehat{\rho}_\tau)^{-1}$.

The point estimates of total, direct and indirect marginal effects of the distance to nearby mine onto the median (log) house price across the three models are summarized in Table 2. Given that insignificant estimates are statistically indistinguishable from zero (implying no effect), here and henceforth, we focus on statistically significant estimates of marginal effects only. For inference within each model, we use the 95% bootstrap percentile confidence bounds.[9] As expected, the results are starkly different across the models, with parametric specifications consistently under-estimating the magnitude of marginal effects of the distance to rock mine on the property value. When considering the entire sample, we find that, in part due to the presence of a large number of

[9]We use 499 bootstrap replications throughout.

houses for which negative marginal effects were estimated, the quadratic model produces estimates of marginal effects on median house values that, on average, are about 59% smaller than those obtained from our semiparametric PLSQAR model. The results from a linear model are even more timid (smaller by 66% on average). Focusing on the more economically relevant results confined to a 10-mile radius zone around rock mines, we find that our PLSQAR model suggests the average TME of the distance to the mine on median house prices at around 0.57% per 1,000 feet, 0.40% points of which are the direct effect. The quadratic and linear models however yield significantly smaller estimates with the corresponding average TMEs of about 0.42% and 0.17% per 1,000 feet, which are 28% and 71% smaller than their nonparametric counterpart, respectively. The marked difference across our semiparametric model and its two parametric alternatives is apparent not only at the average values of marginal effects but along their entire distributions across houses.

Our comparison of the results from the proposed semiparametric model and those from its two parametric counterparts, until now, have largely been casual. However, given that both the linear and quadratic specifications are the special cases of our PLSQAR model, we can formally discriminate between the models by means of a specification test described in Section 3. Namely, both parametric median SQAR models can be cast as restricted models under the null of the first type $\mathrm{H}_0(\mathrm{i})$ given in (3.2) to be tested against our unrestricted PLSQAR model. We reject the null in favor of our proposed model in both cases with the bootstrap p-value no larger than 0.032. We also entertain a third specification for the parametric SQAR model whereby $\alpha_{\tau,0}(z) \equiv \alpha_{0,\tau}$ for all z, which effectively assumes that z is an irrelevant hedonic attribute that has no effect on the house price. This "constant in z" model serves an auxiliary purpose and is estimated solely in order to facilitate the test of overall relevancy of the house's proximity to a rock mine for its value. In terms of the types of null hypothesis described in Section 3, this restricted model falls under the second type of nulls $\mathrm{H}_0(\mathrm{ii})$ given in (3.3), which we test against our PLSQAR model. The corresponding bootstrap p-value is 0.038 suggesting that the proximity to rock mines *does* matter for residential property values.

Given the data lend strong support to our more flexible semiparametric model of house prices, in what follows, we therefore report the results from our PLSQAR model only. Furthermore, in the light of our earlier findings, we focus on the results confined to a local 10-mile radius zone around the mine (2,956 observations) which appear to be the most economically relevant.[10]

Table 3 summarizes statistically significant (house-specific) point estimates of marginal effects of the distance to nearby rock mine on the 0.25th, 0.50th, 0.75th and 0.95th conditional quantiles of the house price from our PLSQAR model. (We caution the reader against confusing quantiles τ of the house price distribution for which model is estimated with quantiles of the fitted distribution of observation-specific marginal effects for *each* τ.) By looking at different quantiles of the house value distribution, we are able to investigate the potentially heterogeneous impact of rock mining on residential property of *different values* thereby looking beyond the results for properties of a "typical" value delivered by standard conditional mean models. Given the tendency of quantile models to be noisier when fitted far in the tails of the distribution, in our analysis we therefore primarily focus on the interquartile range of the conditional house price distribution (setting $\tau = \{0.25, 0.50, 0.75\}$) which should give us sufficient insights into distributional effects, if any, of rock mines on house prices. That said, motivated by the proposition oftentimes claimed in the literature whereby environmental disamenities have significantly larger effects on expensive upscale properties (Reichert et al., 1992; Gayer, 2000), we also estimate our model at the 0.95th quantile to examine if the negative effects of rock mines are especially amplified when located near the most expensive houses. Overall, the results in Table 3 lend strong support to heterogeneous distributional value-

[10]To improve accuracy and to achieve better convergence rates, we still use the full sample during the estimation.

Table 3. Summary of Statistically Significant Semiparametric Estimates of ME of the Distance to Rock Mine on Conditional Quantiles of Property Value within 10-Mile Radius

	TME	DME	IME	TME	DME	IME
	0.25th Q. of Property Value			**0.75th Q. of Property Value**		
25th Perc.	0.3252	0.2182	0.1057	0.3565	0.2676	0.0887
50th Perc.	0.4781	0.3221	0.1571	0.6788	0.5105	0.1688
75th Perc.	0.5645	0.3803	0.1839	0.9979	0.7457	0.2491
Mean	0.4442	0.2993	0.1450	0.6493	0.4875	0.1618
	0.50th Q. of Property Value			**0.95th Q. of Property Value**		
25th Perc.	0.2946	0.2030	0.0885	0.5150	0.3893	0.1256
50th Perc.	0.5810	0.4046	0.1751	0.9952	0.7505	0.2437
75th Perc.	0.8560	0.5957	0.2575	1.3304	1.0048	0.3268
Mean	0.5768	0.4031	0.1737	0.9739	0.7354	0.2385

Reported are the estimates (in % per 1,000 ft) from the PLSQAR model.

suppressing effects of rock mines on the prices of nearby houses, the magnitude of which increase with the value of these houses, as expected. This distributional heterogeneity in the marginal effects can be seen even more vividly in Figure 3 which plots the distribution of the TME estimates across quantiles of the house price distribution. The figure also points to an increase in variability (i.e., a higher degree of heterogeneity across individual houses) of the TME estimates as house prices rise.

As we move from the first to third quartile of the house price distribution, we find that the average estimate of TME of the distance to nearby rock mine on house prices significantly increases from 0.44% to 0.65% per 1,000 feet [see Table 3]. When we focus on the most expensive properties at the 0.95th quantile, the TME goes up even further with the corresponding *median* estimate of about 1% and a half of point estimates being even larger than that; the mean estimate is 0.97% per 1,000 feet. For residential property in the middle of the price distribution ($\tau = 0.50$), our estimates suggest that, between two identical houses, the one located a mile closer to a rock mine is predicted to be priced, on average, at about 3.1% discount.[11] The analogous average discounts for houses in the first and third quartiles of price distribution are around 2.3 and 3.4%, respectively. For upscale property in the 0.95th quantile, it is at an astounding 5.1%. This is rather expected because of income sorting whereby higher income households have higher ability to pay for better environmental quality: in this case, distance from a disamenity. Conversely, households with lower incomes and less expensive homes are perhaps more willing to substitute environmental quality for other, more necessary, house characteristics. As a back-of-the-envelope welfare calculation using unconditional sample quantiles of house values corresponding to the fitted quantile functions,[12] the above discount estimates imply the average loss in property value associated with the house being located a mile closer to a rock mine ranging from \$3,691 to \$10,970 for houses within the interquartile range of price distribution. For more expensive neighborhoods in the 0.95th quantile, such losses can be, on average, as high as \$28,410. We can further extend the welfare analysis to obtain aggregate property value losses due to the houses' proximity to rock mine by applying the estimated discounts to actual house prices at each observation in order to predict increase in each property's value if it were moved from its actual location to a (counterfactual) 10-mile distance from

[11] 5.28 thousand feet times the mean estimate of 0.58% per 1,000 feet. The average discount estimates for other quantiles of house price are obtained similarly.

[12] And assuming a constant marginal willingness to pay.

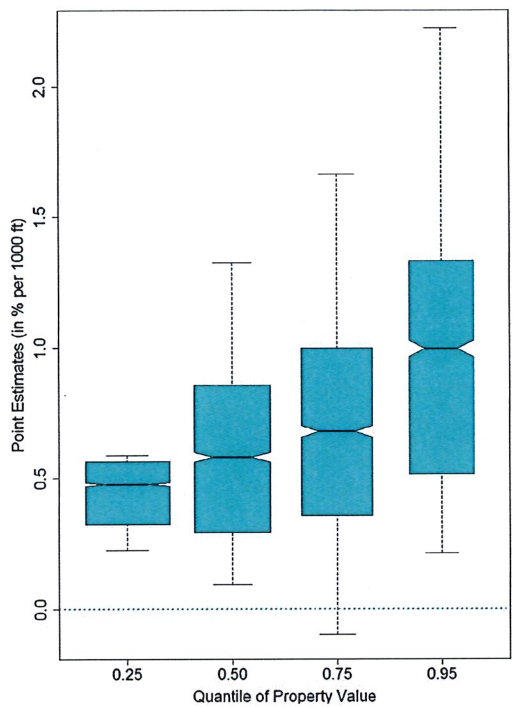

Figure 3. Statistically Significant Semiparametric Estimates of TME of the Distance to Rock Mine on Conditional Quantiles of Property Value within 10-Mile Radius across Quantiles

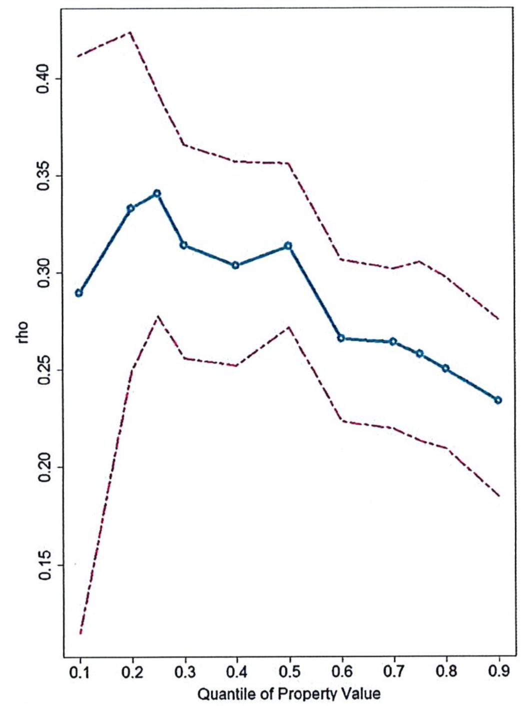

Figure 4. Semiparametric Estimates of the SAR Parameter across Quantiles (with the 95% bootstrap confidence bounds)

the mine. Applying this method to properties with statistically significant total marginal effects[13] of the distance lying within a 10-mile radius from the mine, we find a total property value loss of $68.4 million at the median, which would have a significant impact on public goods expenditures in the county, especially on schools, because of lost tax revenue amounting to approximately $1.3 million per annum.

Our estimates of marginal effects also indicate a decreasing (relative) importance of IMEs for residential properties of higher values. While the indirect effects working through neighbors, on average, contribute 37.8% to the TME of z_i on the log house price at the first quartile of the property value distribution, their average contribution falls quite dramatically to 26.6% for the houses at the third quartile. A plausible explanation for this is that less expensive properties may have very different interior quality levels resulting in more unobserved heterogeneity as compared to higher priced houses. Thus, in more expensive neighborhoods, the adverse effects of nearby rock mines are "priced in" directly during the valuation as opposed to via a spillover comparison to neighboring properties. In other words, we find that spatial dependence in house prices decreases as the value of property rises. To see this, consider the estimates of spatial autoregressive parameter which measures spatial dependence in the data. We summarize the estimates of $\rho_{\tau,0}$, along with their confidence bounds, across different τ of the conditional house price distribution in Figure

[13]Thereby conservatively assuming that the value of houses with insignificant marginal effects of the distance wound not increase.

4. It is evident that the SAR coefficient declines as we move from the left to the right tail of the distribution implying that neighborhood effects are more pronounced in less expensive areas. This result is similar to Liao & Wang's (2012), who estimate a fully parametric hedonic quantile model (however, with no environmental disamenities considered) and also find that the spatial autoregressive parameter declines between the 30th and 70th quantiles. Nonetheless, our estimated spatial effects are statistically significant throughout the entire house price distribution thereby indicating that the failure to account for spatial dependence, as usually done in the literature on housing-market-based valuations of adverse effects of environmental disamenities, would likely yield inconsistent estimates. This substantiates our spatial-econometric approach to hedonic modeling.

6 Conclusion

This paper provides the first estimates of the effects of rock mining—an environmental disamenity—on local residential property values. We estimate the relationship between a house's price and its distance from nearby rock mine in Delaware County, Ohio. We improve upon the conventional approach to valuating adverse effects of environmental disamenities based on hedonic house price functions by developing a novel (semiparametric) partially linear spatial quantile autoregressive model which accommodates unspecified nonlinearities, distributional heterogeneity as well as provides a means to indirectly control for unobservable house and neighborhood characteristics using the spatial dependence in the data. Our model constitutes a practically useful fusion of semi/nonparametric quantile methods with models of spatial dependence. We estimate it via a two-step nonparametric sieve IV quantile estimator. We also propose a model specification test.

We find statistically and economically significant property-value-suppressing effects of being located near an operational rock mine which gradually decline to insignificant near-zero values at a roughly ten-mile distance. Our estimates suggest that, *ceteris paribus*, a house located a mile closer to a rock mine is priced, on average, at about 2.3–5.1% discount, with more expensive properties being subject to larger markdowns. As a back-of-the-envelope welfare calculation, the above discount estimates imply the average loss in property value associated with the house being located a mile closer to a rock mine ranging from \$3,691 to \$10,970 for houses within the interquartile range of price distribution. For more expensive neighborhoods in the 0.95th quantile, such losses can be, on average, as high as \$28,410. Applying the estimated statistically significant discounts to house prices at each observation lying within a 10-mile radius from the mine to predict an increase in each property's value if it were moved from its actual location to a (counterfactual) 10-mile distance from the mine, we find the aggregate property value loss associated with rock mining in the area to be \$68.4 million at the median.

Appendix

A Brief Mathematical Proofs

For any $x \neq 0$ and y, we have

$$\zeta_\tau\{x-y\} - \zeta_\tau\{x\} = y\varphi_\tau\{y\} + \int_0^y \left(\mathbb{I}\{x \le t\} - \mathbb{I}\{x \le 0\}\right) dt, \tag{A.1}$$

where $\varphi_\tau\{u\} = \tau - \mathbb{I}\{u < 0\}$.

Lemma 1 *(i) Under Assumption 3, we have* $\sup_{n,\boldsymbol{l}(i)\in D_n}\sum_{\boldsymbol{l}(j)\in D_n,\varrho(i,j)>s}|g_{ij,n}|\leq Ms^{-c_2 d}$*; (ii) under Assumptions 2–3,* $\{v_{i,n}(\rho),\boldsymbol{l}(i)\in D_n\}$ *is uniformly* L_2*-NED on* $\{\varepsilon_{in},\boldsymbol{l}(i)\in D_n\}$ *with the NED coefficients of* $\psi(s)=O(s^{-\varsigma})$*; (iii)*

$$\frac{1}{n}\sum_{i=1}^{n}\left\{f_{v_{i,n}(\rho)}(\eta_{i,n}(\rho))-\mathbb{E}\left[f_{v_{i,n}(\rho)}(\eta_{i,n}(\rho))\right]\right\}\mathcal{X}_{i,n}\mathcal{X}_{i,n}'\xrightarrow{p}\mathbf{0}_{1+d_x+d_m+L_n},\tag{A.2}$$

where $\eta_{i,n}(\rho)=(\rho-\rho_{\tau,0})\sum_{j=1}^{n}g_{ij,n}\left[\mathbf{x}_{j,n}'\beta_{\tau,0}+\alpha_{\tau,0}(\mathbf{z}_{j,n})\right]+\mathbf{x}_{i,n}'\left[\boldsymbol{\beta}_\tau(\rho)-\boldsymbol{\beta}_{\tau,0}\right]+\alpha_\tau^*(\mathbf{z}_{i,n},\rho)-\alpha_{\tau,0}(\mathbf{z}_{i,n})+\mathbf{m}_{i,n}'\gamma_\tau(\rho)$ *and* $\alpha_\tau^*(\mathbf{z}_{i,n},\rho)=\phi_{L_n}(\mathbf{z}_{i,n})'\mathcal{A}_\tau(\rho)$.

Proof. (i) Under Assumption **3**, we have $\mathbf{G}_n\equiv\mathbf{W}_n\mathbf{S}_n^{-1}=\mathbf{W}_n\sum_{k=0}^{\infty}(\rho_{\tau,0}\mathbf{W}_n)^k=\mathbf{W}_n+\rho_{\tau,0}\mathbf{W}_n^2+\rho_{\tau,0}^2\mathbf{W}_n^3+\ldots$, and hence we have

$$\begin{aligned}g_{ij,n}&=w_{ij,n}+\rho_{\tau,0}\sum_{l\neq i}w_{il,n}w_{lj,n}+\rho_{\tau,0}^2\sum_{l_2\neq i}w_{il_2,n}\left(\sum_{l_1\neq l_2}w_{l_2l_1,n}w_{l_1j,n}\right)+\rho_{\tau,0}^3\sum_{l_3\neq i}w_{il_3,n}\sum_{l_2\neq l_3}w_{l_3l_2,n}\\&\quad\times\left(\sum_{l_1\neq l_2}w_{l_2l_1,n}w_{l_1j,n}\right)+\ldots+\rho_{\tau,0}^k\sum_{l_k\neq i}\sum_{l_{k-1}\neq l_k}\cdots\sum_{l_1\neq l_2}w_{il_k,n}w_{l_kl_{k-1},n}\cdots w_{l_2l_1,n}w_{l_1j,n}+\ldots.\end{aligned}$$

For all j such that $\boldsymbol{l}(j)\in D_n$ and $\varrho(i,j)>s$, we have

$$\begin{aligned}\sum_{\boldsymbol{l}(j)\in D_n,\varrho(i,j)>s}|g_{ij,n}|&\leq c_1\sum_{k=1}^{\infty}\rho_{\tau,0}^{k-1}\left(\frac{s}{k}\right)^{-c_2d}\leq\frac{c_1s^{c_2d}}{\rho_{\tau,0}}\int_1^{\infty}\rho_{\tau,0}^{x}x^{[c_2d]+1}dx\\&=-\frac{c_1s^{-c_2d}}{(\ln\rho_{\tau,0})^{[c_2d]+2}}\sum_{k=0}^{[c_2d]+1}\frac{([c_2d]+1)!}{([c_2d]+1-k)!}(-\ln\rho_{\tau,0})^{[c_2d]+1-k},\end{aligned}$$

where $[a]$ is the largest integer smaller than $a>0$. This completes the proof of (i).

(ii) By definition, $v_{i,n}(\rho)=u_{i,n}+(\rho_{\tau,0}-\rho)\sum_{j=1}^{n}g_{ij,n}u_{j,n}$. Applying Minkowski's and conditional Jensen's inequalities yields

$$\begin{aligned}\|v_{i,n}(\rho)-\mathbb{E}[v_{i,n}(\rho)|\mathcal{F}_{i,n}(s)]\|_2&\leq\|u_{i,n}-\mathbb{E}[u_{i,n}|\mathcal{F}_{i,n}(s)]\|_2+|\rho_{\tau,0}-\rho|\sum_{j=1}^{n}|g_{ij,n}|\,\|u_{j,n}-\mathbb{E}[u_{j,n}|\mathcal{F}_{i,n}(s)]\|_2\\&\leq M\psi(s)+2|\rho_{\tau,0}-\rho|\sum_{\{j:\varrho(i,j)>s\}}|g_{ij,n}|\,\|u_{j,n}\|_2.\end{aligned}$$

This completes the proof of (ii).

(iii) Given the above results, applying Theorem 1 in Jenish & Prucha (2012) yields (A.2). ■

Proof of Theorem 1. Denote $\widehat{\boldsymbol{\vartheta}}_\tau(\rho)=\sqrt{n}\left[\widehat{\boldsymbol{\theta}}_\tau(\rho)-\boldsymbol{\theta}_{\tau,0}(\rho)\right]$, $Y_{i,n}^*(\rho)=y_{i,n}-\rho\sum_{j\neq i}w_{ij,n}y_{j,n}-\mathcal{X}_{i,n}'\boldsymbol{\theta}_{\tau,0}(\rho)=v_{i,n}(\rho)-\eta_{i,n}$ and $Y_{i,n}(\rho)=Y_{i,n}^*(\rho)-n^{-1/2}\mathcal{X}_{i,n}'\boldsymbol{\vartheta}_\tau(\rho)$. Then, for any given $\rho\in\Lambda_\rho$, $\widehat{\boldsymbol{\vartheta}}_\tau(\rho)$ minimizes

$$Q_n(\boldsymbol{\vartheta}_\tau(\rho))=\frac{1}{n}\sum_{i=1}^{n}\left(\zeta_\tau\{Y_{i,n}(\rho)\}-\zeta_\tau\{Y_{i,n}^*(\rho)\}\right),\tag{A.3}$$

which is convex in $\boldsymbol{\vartheta}_\tau(\rho)$. We can show that, under Assumptions **2** and **5**,

$$\Pr\left[\sum_{i=1}^{n}\mathbb{I}\left\{Y_{i,n}^{*}(\rho)=0\right\}=O(1)\right]=1 \quad \text{almost surely over all } \rho\in\Lambda_\rho. \tag{A.4}$$

We consider

$$Q_n(\boldsymbol{\vartheta}_\tau(\rho))=\mathbb{E}\left[Q_n(\boldsymbol{\vartheta}_\tau(\rho))\right]+\frac{\boldsymbol{\vartheta}_\tau(\rho)'}{n^{3/2}}\sum_{i=1}^{n}\mathcal{X}_{i,n}\left(\varphi_\tau\left\{Y_{i,n}^{*}(\rho)\right\}-\mathbb{E}\left[\varphi_\tau\left\{Y_{i,n}^{*}(\rho)\right\}\right]\right)+R_n(\vartheta_\tau(\rho)).$$

Denoting $t_{i,n}=n^{-1/2}\mathcal{X}_{i,n}'\boldsymbol{\vartheta}_\tau(\rho)$ and applying (A.1) and (A.4), we obtain

$$\begin{aligned}
\mathbb{E}\left[Q_n(\boldsymbol{\vartheta}_\tau(\rho))\right] &= \frac{1}{n}\sum_{i=1}^{n}\mathbb{E}\left[\zeta_\tau\left\{Y_{i,n}^{*}(\rho)-n^{-1/2}\mathcal{X}_{i,n}'\boldsymbol{\vartheta}_\tau(\rho)\right\}-\zeta_\tau\left\{Y_{i,n}^{*}(\rho)\right\}\right]\\
&\approx \frac{\boldsymbol{\vartheta}_\tau(\rho)'}{n^{3/2}}\sum_{i=1}^{n}\mathcal{X}_{i,n}\mathbb{E}\left[\varphi_\tau\left\{Y_{i,n}^{*}(\rho)\right\}\right]+\frac{1}{n}\sum_{i=1}^{n}\int_0^{t_{i,n}}\mathbb{E}\left[\mathbb{I}\left\{Y_{i,n}^{*}(\rho)\le t\right\}-\mathbb{I}\left\{Y_{i,n}^{*}(\rho)\le 0\right\}\right]dt\\
&= \frac{\boldsymbol{\vartheta}_\tau(\rho)'}{n^{3/2}}\sum_{i=1}^{n}\mathcal{X}_{i,n}\mathbb{E}\left[\varphi_\tau\left\{Y_{i,n}^{*}(\rho)\right\}\right]+\frac{1}{n}\sum_{i=1}^{n}\int_0^{t_{i,n}}\left[F_{v_{i,n}(\rho)}(\eta_{i,n}(\rho)+t)-F_{v_{i,n}(\rho)}(\eta_{i,n}(\rho))\right]dt\\
&= \frac{\boldsymbol{\vartheta}_\tau(\rho)'}{n^{3/2}}\sum_{i=1}^{n}\mathcal{X}_{i,n}\mathbb{E}\left[\varphi_\tau\left\{Y_{i,n}^{*}(\rho)\right\}\right]+\\
&\qquad \frac{\boldsymbol{\vartheta}_\tau(\rho)'}{2n^2}\sum_{i=1}^{n}f_{v_{i,n}(\rho)}(\eta_{i,n}(\rho))\mathcal{X}_{i,n}\mathcal{X}_{i,n}'\boldsymbol{\vartheta}_\tau(\rho)+O_p\left(\left(\frac{L_n}{\sqrt{n}}\right)^{3/2}\right),
\end{aligned}$$

where $F_{v_{i,n}(\rho)}(\eta_{i,n}(\rho)+t)-F_{v_{i,n}(\rho)}(\eta_{i,n}(\rho))=f_{v_{i,n}(\rho)}(\eta_{i,n}(\rho))\,t+f_{v_{i,n}(\rho)}'(\bar{\eta}_{i,n}(\rho))\,t^2/2$ with $\bar{\eta}_{i,n}(\rho)$ lying between $\eta_{i,n}(\rho)$ and $\eta_{i,n}(\rho)+t$, and

$$\left|\frac{1}{n}\sum_{i=1}^{n}\int_0^{t_{i,n}}f_{v_{i,n}(\rho)}'(\bar{\eta}_{i,n}(\rho))\,t^2dt\right|\le\frac{M}{3n^{5/2}}\sum_{i=1}^{n}\left|\mathcal{X}_{i,n}'\boldsymbol{\vartheta}_\tau(\rho)\right|^3=O_p\left(n^{-3/2}L_n^3\right)=o_p(1)$$

under Assumptions **5**–**6**.

Next, we consider $R_n(\boldsymbol{\vartheta}_\tau(\rho))=n^{-1}\sum_{i=1}^{n}(Q_{i,n}(\rho)-\mathbb{E}[Q_{i,n}(\rho)])$, where

$$\begin{aligned}
Q_{i,n}(\rho) &= \zeta_\tau\left\{Y_{i,n}(\rho)\right\}-\zeta_\tau\left\{Y_{i,n}^{*}(\rho)\right\}-n^{-1/2}\boldsymbol{\vartheta}_\tau(\rho)'\mathcal{X}_i\varphi_\tau\left\{Y_{i,n}^{*}(\rho)\right\}\\
&= \int_0^{t_{i,n}}\left[\mathbb{I}\left\{v_{i,n}(\rho)\le\eta_{i,n}(\rho)+t\right\}-\mathbb{I}\left\{v_{i,n}(\rho)\le\eta_{i,n}(\rho)\right\}\right]dt.
\end{aligned}$$

Since $Q_{i,n}(\rho)$ is a function of $v_{i,n}(\rho)$, $\{Q_{i,n}(\rho),\boldsymbol{l}(i)\in D_n\}$ is uniformly L_2-NED on $\{\varepsilon_{i,n},\boldsymbol{l}(i)\in D_n\}$ with the same NED mixing coefficients as those for $\{v_{i,n}(\rho),\boldsymbol{l}(i)\in D_n\}$. It is readily seen that $\sum_{s=1}^{\infty}s^{d-1}\psi(s)\le M\sum_{s=1}^{\infty}s^{d-\varsigma-1}<M$ because $\varsigma>d$, and $\mathbb{E}\left[|Q_{i,n}(\rho)|^{2+\delta}\right]\le\mathbb{E}\left[|t_{i,n}|^{2+\delta}\right]\le Mn^{-(2+\delta)/2}L_n^{2+\delta}\to 0$ for any $\delta>0$ as $n\to\infty$ under Assumption **6**. By Lemma A.3(a) in Jenish & Prucha (2012), we obtain $\mathbb{V}\mathrm{ar}\left[R_n(\boldsymbol{\vartheta}_\tau(\rho))\right]\le ML_n^3/n^{3/2}$ under Assumption **2(iii)**. Hence, we obtain $R_n(\boldsymbol{\vartheta}_\tau(\rho))=O_p\left((L_n/\sqrt{n})^{3/2}\right)$.

Combining the above results gives

$$Q_n(\boldsymbol{\vartheta}_\tau(\rho))=\frac{\boldsymbol{\vartheta}_\tau(\rho)'}{n^{3/2}}\sum_{i=1}^{n}\mathcal{X}_{i,n}\varphi_\tau\left\{Y_{i,n}^{*}(\rho)\right\}+\frac{1}{2n}\boldsymbol{\vartheta}_\tau(\rho)'\,\boldsymbol{\Sigma}_\tau(\rho)\,\boldsymbol{\vartheta}_\tau(\rho)+o_p(1) \tag{A.5}$$

under Assumption **6**, and this result holds uniformly over $\rho \in \Lambda_\rho$ by the convexity lemma of Pollard (1991), where

$$\boldsymbol{\Sigma}_\tau(\rho) = \lim_{n\to\infty} n^{-1} \sum_{i=1}^{n} \mathbb{E}\left[f_{v_{i,n}(\rho)}(\eta_{i,n}(\rho))\right] \mathcal{X}_{i,n}\mathcal{X}_{i,n}' \tag{A.6}$$

by Lemma **1(iii)**. It then follows that

$$\widehat{\boldsymbol{\vartheta}}_\tau(\rho) = -\frac{\boldsymbol{\Sigma}_\tau^{-1}(\rho)}{\sqrt{n}} \sum_{i=1}^{n} \mathcal{X}_{i,n}\varphi_\tau\left\{Y_{i,n}^*(\rho)\right\} + o_p(1) \tag{A.7}$$

holds uniformly over $\rho \in \Lambda_\rho$. So, we obtain

$$\sqrt{n}\left[\widehat{\boldsymbol{\theta}}_\tau(\rho) - \boldsymbol{\theta}_{\tau,0}(\rho)\right] = -\frac{\boldsymbol{\Sigma}_\tau^{-1}(\rho)}{\sqrt{n}} \sum_{i=1}^{n} \left[\tau - \mathbb{I}\left\{v_{i,n}(\rho) \le \eta_{i,n}(\rho)\right\}\right] \mathcal{X}_{i,n} + o_p(1). \tag{A.8}$$

Applying Lemma **1(ii)** and the CLT of Jenish & Prucha (2012, Theorem 2), we obtain that $n^{-1/2}\sum_{i=1}^{n}\left(\mathbb{I}\left\{v_{i,n}(\rho) \le \eta_{i,n}(\rho)\right\} - \mathbb{E}\left[\mathbb{I}\left\{v_{i,n}(\rho) \le \eta_{i,n}(\rho)\right\}\right]\right)\mathcal{X}_{i,n} = O_p(1)$ element by element, where $n^{-1}\sum_{i=1}^{n}\left\{\tau - \mathbb{E}\left[\mathbb{I}\left\{v_{i,n}(\rho) \le \eta_{i,n}(\rho)\right\}\right]\right\}\mathcal{X}_{i,n} = 0$ since this term is the first-order condition of $\max_{\boldsymbol{\vartheta}_\tau(\rho)} \mathbb{E}\left[Q_n(\boldsymbol{\vartheta}_\tau(\rho))\right]$. Hence, under Assumption **5(iii)**, we obtain $\left\|\widehat{\boldsymbol{\theta}}_\tau(\rho) - \boldsymbol{\theta}_{\tau,0}(\rho)\right\| = O_p\left(\sqrt{L_n/n}\right)$ uniformly over ρ. This completes the proof of this theorem. ■

Proof of Theorem 2. In Step 2, we calculate $\widehat{\rho}_\tau = \arg\min_\rho \widehat{\gamma}_\tau(\rho)'\mathbf{V}_n\widehat{\gamma}_\tau(\rho)$, where $\widehat{\gamma}_\tau(\rho) = \gamma_{\tau,0}(\rho) + o_p(1)$ uniformly over ρ by Theorem **1**. Since $\widehat{\gamma}_\tau(\rho)$ is continuous in ρ and $\gamma_{\tau,0}(\rho)'\mathbf{V}_n\gamma_{\tau,0}(\rho)$ has a minimum value at $\rho_{\tau,0}$, we obtain $\widehat{\rho}_\tau \xrightarrow{p} \rho_{\tau,0}$ by Theorem 2.1 in Newey & McFadden (1994). Since $\boldsymbol{\theta}_{\tau,0}(\rho)$ is continuous in ρ, we have $\left\|\widehat{\boldsymbol{\theta}}_\tau - \boldsymbol{\theta}_{\tau,0}\right\| = o_p(1)$.

When $\rho = \rho_{\tau,0}$, we have $v_{i,n}(\rho_{\tau,0}) = u_{i,n}$, $\eta_{i,n}(\rho_{\tau,0}) = \alpha_{\tau,0}^*(\mathbf{z}_{i,n}) - \alpha_{\tau,0}(\mathbf{z}_{i,n})$, and

$$\boldsymbol{\Sigma}_\tau = \boldsymbol{\Sigma}_\tau(\rho_{\tau,0}) = \lim_{n\to\infty} n^{-1} \sum_{i=1}^{n} f_{u_{i,n}}(0)\,\mathcal{X}_i\mathcal{X}_i' \quad \text{by (2.15) and (A.6).}$$

Let ρ_n be a constant satisfying $\rho_n = \rho_{\tau,0} + o(1)$, and denote $\widehat{Y}_{i,n}(\rho_n) = y_{i,n} - \rho_n\sum_{j\neq i} w_{ij,n}y_{j,n} - \mathcal{X}_{i,n}'\widehat{\boldsymbol{\theta}}_\tau(\rho_n) = Y_{i,n}^*(\rho_n) + \mathcal{X}_{i,n}'\left(\boldsymbol{\theta}_{\tau,0}(\rho_n) - \widehat{\boldsymbol{\theta}}_\tau(\rho_n)\right)$. By Lemma A.2 in Ruppert & Carroll (1980), we have $o_p(1) = n^{-1/2}\sum_{i=1}^{n}\varphi_\tau\left\{\widehat{Y}_{i,n}(\rho_n)\right\}\mathcal{X}_{i,n}$. Let $\chi_{i,n}(\rho,\boldsymbol{\theta}) = \varphi_\tau\left\{y_{i,n} - \rho\sum_{j\neq i} w_{ij,n}y_{j,n} - \mathcal{X}_{i,n}'\boldsymbol{\theta}(\rho)\right\}\mathcal{X}_{i,n}$ and $\mathbb{E}\left[\chi_{i,n}\left(\rho_n, \widehat{\boldsymbol{\theta}}_\tau(\rho_n)\right)\right] = \mathbb{E}\left[\chi_{i,n}(\rho,\boldsymbol{\theta}(\rho))\right]_{(\rho,\boldsymbol{\theta}(\rho))=(\rho_n,\widehat{\boldsymbol{\theta}}_\tau(\rho_n))}$ and decompose

$$\begin{aligned}\frac{1}{\sqrt{n}}\sum_{i=1}^{n}\varphi_\tau\left\{\widehat{Y}_{i,n}(\rho_n)\right\}\mathcal{X}_{i,n} &= \frac{1}{\sqrt{n}}\sum_{i=1}^{n}\left[\chi_{i,n}\left(\rho_n,\widehat{\boldsymbol{\theta}}_\tau(\rho_n)\right) - \mathbb{E}\left[\chi_{i,n}\left(\rho_n,\widehat{\boldsymbol{\theta}}_\tau(\rho_n)\right)\right]\right] \\ &\quad + \frac{1}{\sqrt{n}}\sum_{i=1}^{n}\mathbb{E}\left[\chi_{i,n}\left(\rho_n,\widehat{\boldsymbol{\theta}}_\tau(\rho_n)\right)\right].\end{aligned}$$

First, since $\mathbb{E}\left[\chi_{i,n}(\rho,\boldsymbol{\theta}_\tau(\rho))\right] = \mathbb{E}\left[\tau - \mathbb{I}\left\{v_{i,n}(\rho) \le \eta_{i,n}(\rho)\right\}\right]\mathcal{X}_{i,n}$, we have

$$\mathbb{E}\left[\tau - \mathbb{I}\left\{v_{i,n}(\rho) \le \eta_{i,n}(\rho)\right\}\right] = \mathbb{E}\left[F_{u_{i,n}}(0|\bar{u}_{i,n}) - F_{u_{i,n}}\left(\frac{(\rho_{\tau,0}-\rho)\,\bar{u}_{i,n} + \eta_{i,n}(\rho)}{1 + (\rho_{\tau,0}-\rho)\,g_{ii,n}}\,\middle|\,\bar{u}_{i,n}\right)\right]$$

$$= -\mathbb{E}\left[\bar{u}_{i,n} f_{u_{i,n}}\left(\bar{c}_{i,n}|\bar{u}_{i,n}\right)\right] \frac{\rho_{\tau,0}-\rho}{1+\left(\rho_{\tau}-\rho\right) g_{ii,n}}$$
$$-\mathbb{E}\left[f_{u_{i,n}}\left(\bar{c}_{i,n}|\bar{u}_{i,n}\right)\right] \frac{\eta_{i,n}(\rho)}{1+\left(\rho_{\tau,0}-\rho\right) g_{ii,n}}$$

if $1+\left(\rho_{\tau,0}-\rho\right) g_{ii,n}>0$, where $\bar{c}_{i,n}$ lies between 0 and $\left[\left(\rho_{\tau,0}-\rho\right) \bar{u}_{i,n}+\eta_{i,n}(\rho)\right]\left[1+\left(\rho_{\tau,0}-\rho\right) g_{ii,n}\right]^{-1}$. Therefore, if $\lim_{n \rightarrow \infty} \inf_{1 \leq i \leq n}\left[1+\left(\rho_{\tau,0}-\rho_{n}\right) g_{ii,n}\right]=c_{g}>0$, we obtain

$$\frac{1}{\sqrt{n}} \sum_{i=1}^{n} \mathbb{E}\left[\chi_{i,n}\left(\rho_{n}, \widehat{\boldsymbol{\theta}}_{\tau}\left(\rho_{n}\right)\right)\right] \approx-\mathcal{A}_{1} \sqrt{n}\left(\rho_{\tau,0}-\rho_{n}\right)-\mathcal{A}_{2} \sqrt{n}\left(\boldsymbol{\theta}_{\tau,0}\left(\rho_{n}\right)-\widehat{\boldsymbol{\theta}}_{\tau}\left(\rho_{n}\right)\right),$$

where

$$\begin{aligned}
\mathcal{A}_{1} &= \lim_{n \rightarrow \infty} \frac{1}{n} \sum_{i=1}^{n}\left[1+\left(\rho_{\tau,0}-\rho_{n}\right) g_{ii,n}\right]^{-1} \mathbb{E}\left[f_{u_{i,n}}\left(0|\bar{u}_{i,n}\right)\left(\bar{u}_{i,n}+\sum_{j=1}^{n} g_{ij,n}\left[\mathbf{x}_{j,n}^{\prime} \boldsymbol{\beta}_{\tau,0}+\alpha_{\tau,0}\left(\mathbf{z}_{j,n}\right)\right]\right)\right] \mathcal{X}_{i,n}, \\
\mathcal{A}_{2} &= \lim_{n \rightarrow \infty} \frac{1}{n} \sum_{i=1}^{n}\left[1+\left(\rho_{\tau,0}-\rho_{n}\right) g_{ii,n}\right]^{-1} \mathbb{E}\left[f_{u_{i,n}}\left(0|\bar{u}_{i,n}\right)\right] \mathcal{X}_{i,n} \mathcal{X}_{i,n}^{\prime}. \qquad \text{(A.9)}
\end{aligned}$$

Second, Jenish (2016) has proven the stochastic equicontinuity result of an empirical process for the smooth function of a NED spatial process and finite parameters. Applying Theorem 5 in Jenish (2016), we obtain that the equicontinuity result also holds for $\Delta_{n}(\rho, \boldsymbol{\theta}(\rho))$ here, i.e.,

$$\left\|\Delta_{n}\left(\rho_{n}, \widehat{\boldsymbol{\theta}}_{\tau}\left(\rho_{n}\right)\right)-\Delta_{n}\left(\rho_{\tau,0}, \boldsymbol{\theta}_{\tau,0}\left(\rho_{\tau,0}\right)\right)\right\|=o_{p}(1), \qquad \text{(A.10)}$$

where

$$\mathcal{A}_{n,0} \equiv \Delta_{n}\left(\rho_{\tau,0}, \boldsymbol{\theta}_{\tau,0}\left(\rho_{\tau,0}\right)\right)=\frac{1}{\sqrt{n}} \sum_{i=1}^{n}\left(\varphi_{\tau}\left\{Y_{i,n}^{*}\left(\rho_{\tau,0}\right)\right\}-\mathbb{E}\left[\varphi_{\tau}\left\{Y_{i,n}^{*}\left(\rho_{\tau,0}\right)\right\}\right]\right) \mathcal{X}_{i,n}. \qquad \text{(A.11)}$$

Third, combining the above results yields

$$\sqrt{n}\left(\widehat{\boldsymbol{\theta}}_{\tau}\left(\rho_{n}\right)-\boldsymbol{\theta}_{\tau,0}\left(\rho_{n}\right)\right)=-\mathcal{A}_{2}^{-1} \mathcal{A}_{n,0}+\mathcal{A}_{2}^{-1} \mathcal{A}_{1} \sqrt{n}\left(\rho_{\tau,0}-\rho_{n}\right).$$

Partition below matrix/vector conformably with 1, 2 and 3 corresponding to $\mathbf{x}_{i,n}$, $\mathbf{m}_{i,n}$ and $\phi_{L_{n}}\left(\mathbf{z}_{i,n}\right)$, respectively:

$$\mathcal{A}_{1}=\left[\begin{array}{l}
\mathcal{A}_{1,1} \\
\mathcal{A}_{1,2} \\
\mathcal{A}_{1,3}
\end{array}\right], \quad \mathcal{A}_{2}^{-1}=\left[\begin{array}{lll}
\mathcal{A}_{2}^{11} & \mathcal{A}_{2}^{12} & \mathcal{A}_{2}^{13} \\
\mathcal{A}_{2}^{21} & \mathcal{A}_{2}^{22} & \mathcal{A}_{2}^{23} \\
\mathcal{A}_{2}^{31} & \mathcal{A}_{2}^{32} & \mathcal{A}_{2}^{33}
\end{array}\right]=\left[\begin{array}{l}
\mathcal{A}_{2}^{1} \\
\mathcal{A}_{2}^{2} \\
\mathcal{A}_{2}^{3}
\end{array}\right] \text{ and } \mathcal{A}_{n,0}=\left[\begin{array}{l}
\mathcal{A}_{n,0,1} \\
\mathcal{A}_{n,0,2} \\
\mathcal{A}_{n,0,3}
\end{array}\right].$$

Then, we have

$$\sqrt{n}\left(\begin{array}{c}
\widehat{\boldsymbol{\beta}}_{\tau}\left(\rho_{n}\right)-\boldsymbol{\beta}_{\tau,0}\left(\rho_{n}\right) \\
\widehat{\boldsymbol{\gamma}}_{\tau}\left(\rho_{n}\right)-\boldsymbol{\gamma}_{\tau,0}\left(\rho_{n}\right)
\end{array}\right)=-\left[\begin{array}{l}
\mathcal{A}_{2}^{1} \\
\mathcal{A}_{2}^{2}
\end{array}\right] \mathcal{A}_{n,0}+\left[\begin{array}{l}
\mathcal{A}_{2}^{1} \\
\mathcal{A}_{2}^{2}
\end{array}\right] \mathcal{A}_{1} \sqrt{n}\left(\rho_{\tau,0}-\rho_{n}\right). \qquad \text{(A.12)}$$

In addition, from Step 2, we have $\widehat{\rho}_{\tau}=\arg\min_{\rho_{n}} \widehat{\boldsymbol{\gamma}}_{\tau}^{\prime}\left(\rho_{n}\right) \mathbf{V}_{n} \widehat{\boldsymbol{\gamma}}_{\tau}\left(\rho_{n}\right)$. Applying the CLT of Jenish & Prucha (2012) gives

$$\mathbf{e}_{j}^{\prime} \mathcal{A}_{n,0} \xrightarrow{d} \mathbb{N}\left(\mathbf{0}, \mathbf{e}_{j}^{\prime} \boldsymbol{\Omega}_{\tau} \mathbf{e}_{j}\right)$$

with

$$\boldsymbol{\Omega}_{\tau}=\lim_{n\to\infty}n^{-1}\sum_{i=1}^{n}\sum_{j=1}^{n}\mathcal{X}_{i,n}\mathbb{C}\text{ov}\left[\varphi_{\tau}\left\{u_{i,n}\right\},\varphi_{\tau}\left\{u_{j,n}\right\}\right]\mathcal{X}_{jn}'=O\left(1\right)$$

by Lemma A.3 in Jenish & Prucha (2012), where $\mathbf{e}_j$ is any one of the column vectors of $\mathbf{I}_{d_x+d_m+L_n}$. It follows that $\sqrt{n}\left\|\widehat{\gamma}_{\tau}\left(\rho_n\right)-\gamma_{\tau,0}\left(\rho_n\right)\right\|=O_p\left(1\right)$, which implies that $\sqrt{n}\left(\rho_{\tau,0}-\rho_n\right)=O\left(1\right)$. Consequently, we obtain

$$\sqrt{n}\left(\widehat{\rho}_{\tau}-\rho_{\tau,0}\right)=\left[\mathcal{A}_1'\left(\mathcal{A}_2^2\right)'\mathbf{V}_n\mathcal{A}_2^2\mathcal{A}_1\right]^{-1}\mathcal{A}_1'\left(\mathcal{A}_2^2\right)'\mathbf{V}_n\mathcal{A}_2^2\mathcal{A}_{n,0}\equiv\mathcal{M}_{\rho}\mathcal{A}_{n,0}.$$

Therefore we have

$$\sqrt{n}\left(\begin{array}{c}\widehat{\boldsymbol{\beta}}_{\tau}\left(\rho_n\right)-\boldsymbol{\beta}_{\tau,0}\left(\rho_n\right)\\ \widehat{\gamma}_{\tau}\left(\rho_n\right)-\gamma_{\tau,0}\left(\rho_n\right)\end{array}\right)=\left[\begin{array}{c}\mathcal{A}_2^1\\ \mathcal{A}_2^2\end{array}\right]\left(\mathcal{A}_1\mathcal{M}_{\rho}-\mathbf{I}_{d_x+d_m+L_n}\right)\mathcal{A}_{n,0},$$

so that we obtain

$$\sqrt{n}\boldsymbol{\Sigma}_n^{-1/2}\left[\begin{array}{ccc}\widehat{\rho}_{\tau}-\rho_{\tau,0} & \widehat{\boldsymbol{\beta}}_{\tau}'-\boldsymbol{\beta}_{\tau,0}' & \widehat{\gamma}_{\tau}'\end{array}\right]'\overset{d}{\to}\mathbb{N}\left(\mathbf{0},\mathbf{I}\right),$$

where $\boldsymbol{\Sigma}_n=\mathcal{P}\boldsymbol{\Omega}_{\tau}\mathcal{P}'$ with $\mathcal{P}=\left[\mathcal{M}_{\rho}',\boldsymbol{\Psi}'\left[\left(\mathcal{A}_2^1\right)',\left(\mathcal{A}_2^2\right)'\right]\right]'$ and $\boldsymbol{\Psi}=\mathcal{A}_1\mathcal{M}_{\rho}-\mathbf{I}_{d_x+d_m+L_n}$.

Lastly, we have

$$\sqrt{n}\left[\widehat{\alpha}_{\tau}\left(\mathbf{z}\right)-\alpha_{\tau,0}\left(\mathbf{z}\right)\right]=\sqrt{n}\boldsymbol{\phi}_{L_n}\left(\mathbf{z}\right)'\left(\widehat{\mathcal{A}}_{\tau}-\mathcal{A}_{\tau,0}\right)=\boldsymbol{\phi}_{L_n}\left(\mathbf{z}\right)'\mathcal{A}_2^3\left[\mathcal{A}_1\mathcal{M}_{\rho}-\mathbf{I}_{d_x+d_m+L_n}\right]\mathcal{A}_{n,0},$$

and hence obtain

$$\sqrt{n/\omega_{n,\tau}}\left[\widehat{\alpha}_{\tau}\left(\mathbf{z}\right)-\alpha_{\tau,0}\left(\mathbf{z}\right)\right]\overset{d}{\to}\mathbb{N}\left(0,1\right),$$

where $\omega_{n,\tau}=\boldsymbol{\phi}_{L_n}\left(\mathbf{z}\right)'\mathcal{A}_2^3\boldsymbol{\Psi}\boldsymbol{\Omega}_{\tau}\boldsymbol{\Psi}'\left(\mathcal{A}_2^3\right)'\boldsymbol{\phi}_{L_n}\left(\mathbf{z}\right)$. This completes the proof of this theorem. ■

Proof of Theorem 3. By definition, $RSC_{0,\tau}=\sum_{i=1}^{n}\zeta_{\tau}\{\widetilde{u}_{i,n}\}$ and $RSC_{1,\tau}=\sum_{i=1}^{n}\zeta_{\tau}\{\widehat{u}_{i,n}\}$ with

$$\begin{aligned}\widetilde{u}_{i,n}&=y_{i,n}-\widetilde{\rho}_{\tau}\sum_{j\neq i}w_{ij,n}y_{j,n}-\mathbf{x}_{i,n}'\widetilde{\boldsymbol{\beta}}_{\tau}-\mathbf{z}_{i,n}'\widetilde{\boldsymbol{\delta}}_{\tau}=Y_{i,n,0}\left(\widetilde{\rho}_{\tau}\right)+\mathbf{m}_i'\widetilde{\gamma}_{\tau},\\ \widehat{u}_{i,n}&=y_{i,n}-\widehat{\rho}_{\tau}\sum_{j\neq i}w_{ij,n}y_{j,n}-\mathbf{x}_{i,n}'\widehat{\boldsymbol{\beta}}_{\tau}-\widehat{\alpha}_{\tau}(\mathbf{z}_{i,n})=Y_{i,n}\left(\widehat{\rho}_{\tau}\right)+\mathbf{m}_i'\widehat{\gamma}_{\tau},\end{aligned}$$

where $Y_{i,n,0}^{*}\left(\rho\right)=y_{i,n}-\rho\sum_{j\neq i}w_{ij,n}y_{j,n}-\mathbf{x}_{i,n}'\boldsymbol{\beta}_{\tau,0}\left(\rho\right)-\mathbf{z}_{i,n}'\boldsymbol{\delta}_{\tau,0}\left(\rho\right)-\mathbf{m}_{i,n}'\gamma_{\tau,0}\left(\rho\right)$, $Y_{i,n}^{*}\left(\rho\right)$ is defined the same as in the proof of Theorem 1 and, to simplify notation, we let $\mathbf{z}_{i,n}$ include 1 in the model under the null. Denoting $\chi_{i,n}=\left[\mathbf{x}_{i,n}',\mathbf{z}_{i,n}',\mathbf{m}_{i,n}'\right]'$ and $Y_{i,n,0}\left(\rho\right)=Y_{i,n,0}^{*}\left(\rho\right)-\chi_i'\left[\widetilde{\boldsymbol{\theta}}_{\tau}\left(\rho\right)-\boldsymbol{\theta}_{\tau,0}\left(\rho\right)\right]$, we have

$$\begin{aligned}n^{-1}RSC_{0,\tau}&=n^{-1}\sum_{i=1}^{n}\zeta_{\tau}\left\{Y_{i,n,0}\left(\widetilde{\rho}_{\tau}\right)+\mathbf{m}_{i,n}'\widetilde{\gamma}_{\tau}\right\}\\ &=n^{-1}\sum_{i=1}^{n}\left[\zeta_{\tau}\left\{Y_{i,n,0}\left(\widetilde{\rho}_{\tau}\right)\right\}-\zeta_{\tau}\left\{Y_{i,n,0}^{*}\left(\widetilde{\rho}_{\tau}\right)\right\}\right]+n^{-1}\sum_{i=1}^{n}\zeta_{\tau}\left\{Y_{i,n,0}^{*}\left(\widetilde{\rho}_{\tau}\right)\right\}+\\ &\quad n^{-1}\sum_{i=1}^{n}\left[\zeta_{\tau}\left\{Y_{i,n,0}\left(\widetilde{\rho}_{\tau}\right)+\mathbf{m}_{i,n}'\widetilde{\gamma}_{\tau}\right\}-\zeta_{\tau}\left\{Y_{i,n,0}\left(\widetilde{\rho}_{\tau}\right)\right\}\right]\end{aligned}$$

$$
\begin{aligned}
&= Q_{n,0}\left(\widetilde{\boldsymbol{\theta}}_{\tau}\left(\widetilde{\rho}_{\tau}\right)\right) + n^{-1}\sum_{i=1}^{n}\zeta_{\tau}\left\{Y_{i,n,0}^{*}\left(\widetilde{\rho}_{\tau}\right)\right\} + n^{-1}\sum_{i=1}^{n}\left[\zeta_{\tau}\left\{Y_{i,n,0}\left(\widetilde{\rho}_{\tau}\right) + \mathbf{m}_{i,n}^{\prime}\widetilde{\gamma}_{\tau}\right\} - \zeta_{\tau}\left\{Y_{i,n,0}\left(\widetilde{\rho}_{\tau}\right)\right\}\right] \\
&\approx -\frac{1}{2n^{2}}\left[\sum_{i=1}^{n}\chi_{i,n}\varphi_{\tau}\left\{u_{i,n}\right\}\right]^{\prime}\boldsymbol{\Sigma}_{\tau,0}^{-1}\left[\sum_{i=1}^{n}\chi_{i,n}\varphi_{\tau}\left\{u_{i,n}\right\}\right] + n^{-1}\sum_{i=1}^{n}\zeta_{\tau}\left\{u_{i,n}\right\} + o_{p}\left(n^{-1}\right),
\end{aligned}
$$

where, following the proof of Theorem 1, we have $Q_{n,0}\left(\boldsymbol{\vartheta}_{\tau}(\rho)\right) = n^{-1}\sum_{i=1}^{n}\left[\zeta_{\tau}\left\{Y_{i,n,0}(\rho)\right\} - \zeta_{\tau}\left\{Y_{i,n,0}^{*}(\rho)\right\}\right]$, and $\boldsymbol{\Sigma}_{\tau,0} = \lim_{n\to\infty} n^{-1}\sum_{i=1}^{n} f_{u_{i,n}}(0)\,\chi_{i}\chi_{i}^{\prime}$. In addition, we obtain

$$
\begin{aligned}
n^{-1}RSC_{1,\tau} &= n^{-1}\sum_{i=1}^{n}\zeta_{\tau}\left\{Y_{i,n}\left(\widehat{\rho}_{\tau}\right) + \mathbf{m}_{i,n}^{\prime}\widehat{\gamma}_{\tau}\right\} \\
&= Q_{n}\left(\widehat{\boldsymbol{\theta}}_{\tau}\left(\widehat{\rho}_{\tau}\right)\right) + n^{-1}\sum_{i=1}^{n}\zeta_{\tau}\left\{Y_{i,n}^{*}\left(\widehat{\rho}_{\tau}\right)\right\} + n^{-1}\sum_{i=1}^{n}\left[\zeta_{\tau}\left\{Y_{i,n}\left(\widehat{\rho}_{\tau}\right) + \mathbf{m}_{i,n}^{\prime}\widehat{\gamma}_{\tau}\right\} - \zeta_{\tau}\left\{Y_{i,n}\left(\widehat{\rho}_{\tau}\right)\right\}\right] \\
&\approx -\frac{1}{2n^{2}}\left[\sum_{i=1}^{n}\mathcal{X}_{i,n}\varphi_{\tau}\left\{u_{i,n}\right\}\right]^{\prime}\boldsymbol{\Sigma}_{\tau}^{-1}\left[\sum_{i=1}^{n}\mathcal{X}_{i,n}\varphi_{\tau}\left\{u_{i,n}\right\}\right] + n^{-1}\sum_{i=1}^{n}\zeta_{\tau}\left\{u_{i,n}\right\} + o_{p}\left(n^{-1}\right)
\end{aligned}
$$

by the proof of Theorem **1.**

Therefore, under H_0, we obtain

$$
RSC_{0,\tau} - RSC_{1,\tau} \approx \left(\mathcal{B}_{n,1}^{\prime}\boldsymbol{\Sigma}_{\tau}^{-1}\mathcal{B}_{n,1} - \mathcal{B}_{n,0}^{\prime}\boldsymbol{\Sigma}_{\tau,0}^{-1}\mathcal{B}_{n,0}\right)/2,
$$

where $\mathcal{B}_{n,0} = n^{-1/2}\sum_{i=1}^{n}\chi_{i,n}\varphi_{\tau}\left\{u_{i,n}\right\}$ and $\mathcal{B}_{n,1} = n^{-1/2}\sum_{i=1}^{n}\mathcal{X}_{i,n}\varphi_{\tau}\left\{u_{i,n}\right\}$. By Seber (2008, Property 20.17), $\mathcal{B}_{n,1}^{\prime}\boldsymbol{\Sigma}_{\tau}^{-1}\mathcal{B}_{n,1}$ can be rewritten as a linear combination of $d_x + d_m + L_n$ independent chi-squared random variables and $\mathcal{B}_{n,0}^{\prime}\boldsymbol{\Sigma}_{\tau,0}^{-1}\mathcal{B}_{n,0}$ can be rewritten as a linear combination of $d_x + d_m + d_z$ independent chi-squared random variables. Since $n^{-1}RSC_{1,\tau} = n^{-1}\sum_{i=1}^{n}\zeta_{\tau}\left\{u_{i,n}\right\} + o_p(1) \xrightarrow{p} n^{-1}\sum_{i=1}^{n}\mathbb{E}\left[\zeta_{\tau}\left\{u_{i,n}\right\}\right]$ by the LLN derived in Jenish & Prucha (2012), we obtain that

$$
T_n = \frac{RSC_{0,\tau} - RSC_{1,\tau}}{RSC_{1,\tau}} \approx \frac{\left(\mathcal{B}_{n,1}^{\prime}\boldsymbol{\Sigma}_{\tau}^{-1}\mathcal{B}_{n,1} - \mathcal{B}_{n,0}^{\prime}\boldsymbol{\Sigma}_{\tau,0}^{-1}\mathcal{B}_{n,0}\right)/2}{\sum_{i=1}^{n}\mathbb{E}\left[\zeta_{\tau}\left(u_{i,n}\right)\right]} = O_p\left(\frac{L_n}{n}\right).
$$

Under H_1, following the proof of Theorem **1**, we can show that there exists parameter $\boldsymbol{\theta}_{\tau}(\rho_{\tau}) = (\rho_{\tau}, \boldsymbol{\delta}_{\tau}^{\prime}, \gamma_{\tau}^{\prime})^{\prime} \neq \boldsymbol{\theta}_{\tau,0}$ such that $\widetilde{\rho}_{\tau} - \rho_{\tau} = O_p\left(n^{-1/2}\right)$ and $\widetilde{\boldsymbol{\theta}}_{\tau}(\rho) - \boldsymbol{\theta}_{\tau}(\rho) = O_p\left(n^{-1/2}\right)$ uniformly over $\rho \in \Lambda_{\rho}$. Then, it follows that

$$
n^{-1}RSC_{0,\tau} = n^{-1}\sum_{i=1}^{n}\zeta_{\tau}\left\{Y_{i,n,0}^{*}\left(\widetilde{\rho}_{\tau}\right) + \mathbf{m}_{i,n}^{\prime}\widetilde{\gamma}_{\tau}\right\} \approx n^{-1}\sum_{i=1}^{n}\zeta_{\tau}\left\{Y_{i,n,0}^{*}\left(\widetilde{\rho}_{\tau}\right)\right\} = O_p(1),
$$

because $Y_{i,n,0}^{*}\left(\widetilde{\rho}_{\tau}\right) = y_{i,n} - \widetilde{\rho}_{\tau}\sum_{j\neq i} w_{i,nj}y_{j,n} - \mathbf{x}_{i,n}^{\prime}\boldsymbol{\beta}_{\tau}\left(\widetilde{\rho}_{\tau}\right) - \mathbf{z}_{i,n}^{\prime}\boldsymbol{\delta}_{\tau}\left(\widetilde{\rho}_{\tau}\right) - \mathbf{m}_{i,n}^{\prime}\gamma_{\tau}\left(\widetilde{\rho}_{\tau}\right) = u_{i,n} + \left(\rho_{\tau,0} - \widetilde{\rho}_{\tau}\right)\sum_{j\neq i} w_{ij,n}y_{j,n} + \mathbf{x}_{i,n}^{\prime}\left(\boldsymbol{\beta}_{\tau,0} - \widetilde{\boldsymbol{\beta}}_{\tau}\left(\widetilde{\rho}_{\tau}\right)\right) + \alpha_{\tau,0}\left(\mathbf{z}_{i,n}\right) - \mathbf{z}_{i,n}^{\prime}\widetilde{\boldsymbol{\delta}}_{\tau}\left(\widetilde{\rho}_{\tau}\right) - \mathbf{m}_{i,n}^{\prime}\gamma_{\tau}\left(\widetilde{\rho}_{\tau}\right) = u_{i,n} + O_p(1)$ uniformly over i. Hence, we obtain

$$
T_n = \frac{RSC_{0,\tau} - RSC_{1,\tau}}{RSC_{1,\tau}} \approx \frac{n^{-1}\sum_{i=1}^{n}\left[\zeta_{\tau}\left\{Y_{i,n,0}^{*}\left(\widetilde{\rho}_{\tau}\right)\right\} - \zeta_{\tau}\left\{u_{i,n}\right\}\right]}{n^{-1}\sum_{i=1}^{n}\mathbb{E}\left[\zeta_{\tau}\left\{u_{i,n}\right\}\right]} = O_p(1).
$$

■

B Monte Carlo Simulations

In this section, we evaluate the finite-sample performance of our proposed estimator and the test statistic in a small set of Monte Carlo simulations.

B.1 Estimator

We generate the data using a random-coefficient "rendition" of our model in (2.1). Specifically, our PLSQAR model can be motivated by the following random-coefficient partially linear model:

$$y_{i,n} = \rho_0^*(v_{i,n}) \sum_{j \neq i} w_{ij,n} y_{j,n} + \mathbf{x}'_{i,n} \beta_0^*(v_{i,n}) + \alpha_0^*(\mathbf{z}_{i,n}, v_{i,n}), \tag{B.1}$$

where $v_{i,n} \perp (\mathbf{X}_n, \mathbf{Z}_n, \mathbf{M}_n)$ is the scalar random disturbance. In the structural framework, $v_{i,n}$ can be interpreted as capturing heterogeneity in the outcome variable $y_{i,n}$ due to some unobserved factors. Further, if following Chernozhukov & Hansen (2005, 2006) one were to assume that $v_{i,n} \sim$ *i.i.d.* $\mathbb{U}(0,1)$ and that the so-called structural quantile function of interest

$$q\left(\sum_{j \neq i} w_{ij,n} y_{j,n}, \mathbf{x}_{i,n}, \mathbf{z}_{i,n}, \tau\right) = \rho_0^*(\tau) \sum_{j \neq i} w_{ij,n} y_{j,n} + \mathbf{x}'_{i,n} \beta_0^*(\tau) + \alpha_0^*(\mathbf{z}_{i,n}, \tau) \tag{B.2}$$

is such that $\partial q(\cdot, \tau)/\partial \tau > 0$, the event $\{y_{i,n} \leq \rho_0^*(\tau) \sum_{j \neq i} w_{ij,n} y_{j,n} + \mathbf{x}'_{i,n} \beta_0^*(\tau) + \alpha_0^*(\mathbf{z}_{i,n}, \tau)\}$ becomes equivalent to the event $\{v_{i,n} \leq \tau\}$. Then, it is straightforward to establish the following quantile restriction:

$$\Pr[u_{i,n}^* \leq 0 | \mathbf{X}_n, \mathbf{Z}_n, \mathbf{M}_n] = \tau, \tag{B.3}$$

where, in an analogy to our model in (2.1), the new quantile error term is defined as $u_{i,n}^* \equiv y_{i,n} - \rho_0^*(\tau) \sum_{j \neq i} w_{ij,n} y_{j,n} - \mathbf{x}'_{i,n} \beta_0^*(\tau) - \alpha_0^*(\mathbf{z}_{i,n}, \tau)$. Clearly, (B.1) and (B.3) are respectively analogous to (2.1) and (2.2).

Thus, we use the following process to generate the data:

$$y_i = \rho_0(v_i) \sum_{j \neq i} w_{ij} y_j + x_i \beta_0(v_i) + \alpha_0(z_i, v_i) \quad \forall\, i = 1, \ldots, n, \tag{B.4}$$

where the variables are randomly drawn as follows: $z_i \sim$ *i.i.d.* $\mathbb{U}(-1,1)$, $x_i = 0.5 z_i + \xi_i$ with $\xi_i \sim$ *i.i.d.* $\mathbb{N}(0,1)$, and $v_i \sim$ *i.i.d.* $\mathbb{U}(0,1)$. Following Kelejian & Prucha (1999) and Jin & Lee (2015), we choose a circular "1 ahead and 1 behind" structure of $\mathbf{W}_n$, where a given spatial unit is related to one neighbor immediately ahead and one neighbor immediately behind it in a row. Each of these two neighbors are assigned an equal non-zero weight of 0.5. When specifying parameter functions, we consider the following two data-generating processes:

$$\rho_{\tau,0} \equiv \rho_0(v)\big|_{v=\tau} = 0.5 + 0.15\Phi^{-1}(v) \qquad \text{[DGP \#1 \& DGP \#2]} \tag{B.5}$$

$$\beta_{\tau,0} \equiv \beta_0(v)\big|_{v=\tau} = 0.2 + 0.15\Phi^{-1}(v) \qquad \text{[DGP \#1 \& DGP \#2]} \tag{B.6}$$

$$\alpha_{\tau,0}(z) \equiv \alpha_0(z,v)\big|_{v=\tau} = \sin(1 + 1.5z) + \begin{cases} 0.15\Phi^{-1}(v) & \text{[DGP \#1]} \\ 0.15\exp\{-z^2\}\Phi^{-1}(v). & \text{[DGP \#2]} \end{cases} \tag{B.7}$$

We conduct the experiments at three different quantiles $\tau = \{0.25, 0.50, 0.75\}$ for each of which the considered sample sizes are $n = \{125, 250, 500, 1000\}$. For each τ-n pair, we simulate the model

Table B.1. Simulation Results for the Estimator

	$\tau = 0.25$				$\tau = 0.50$				$\tau = 0.75$			
	$n = 125$	$n = 250$	$n = 500$	$n = 1000$	$n = 125$	$n = 250$	$n = 500$	$n = 1000$	$n = 125$	$n = 250$	$n = 500$	$n = 1000$
DGP #1												
$\rho_{\tau,0}$												
RMSE	0.09081	0.05811	0.03928	0.03009	0.07679	0.04391	0.02859	0.01985	0.09293	0.06012	0.04155	0.03029
MAE	0.07137	0.04556	0.03069	0.02390	0.05766	0.03437	0.02279	0.01604	0.07194	0.04590	0.03239	0.02375
$\beta_{\tau,0}$												
RMSE	0.04177	0.03045	0.02350	0.01875	0.03216	0.02130	0.01384	0.00957	0.04470	0.03095	0.02391	0.01870
MAE	0.03327	0.02442	0.01922	0.01602	0.02545	0.01633	0.01103	0.00755	0.03594	0.02429	0.01956	0.01614
$\alpha_{\tau,0}(z_i)$												
RMSE	0.09774	0.06333	0.04378	0.03327	0.08292	0.05015	0.03516	0.02609	0.10699	0.06757	0.04813	0.03567
MAE	0.08657	0.05511	0.03720	0.02803	0.07254	0.04297	0.02950	0.02160	0.09426	0.05938	0.04223	0.03096
DGP #2												
$\rho_{\tau,0}$												
RMSE	0.08516	0.05320	0.03979	0.03214	0.06697	0.03983	0.02548	0.01764	0.08204	0.06030	0.04401	0.03259
MAE	0.06624	0.04195	0.03135	0.02622	0.05068	0.03155	0.02020	0.01411	0.06500	0.04661	0.03396	0.02602
$\beta_{\tau,0}$												
RMSE	0.04265	0.03385	0.02706	0.02329	0.02942	0.01964	0.01359	0.00893	0.04494	0.03330	0.02731	0.02329
MAE	0.03460	0.02804	0.02320	0.02089	0.02351	0.01511	0.01092	0.00708	0.03652	0.02689	0.02354	0.02104
$\alpha_{\tau,0}(z_i)$												
RMSE	0.08686	0.05677	0.04213	0.03400	0.06861	0.04342	0.03016	0.02260	0.09372	0.06687	0.04929	0.03864
MAE	0.07716	0.04990	0.03660	0.02943	0.06023	0.03738	0.02550	0.01864	0.08333	0.05970	0.04379	0.03396

Table B.2. Simulation Results for the T_n Statistic with $\tau = 0.50$

	Estimated Size			*Estimated Power*		
Signif. Level	$n = 100$	$n = 200$	$n = 400$	$n = 100$	$n = 200$	$n = 400$
Case of $\mathrm{H}_0(i)$						
		DGP #1			DGP #3	
1%	0.020	0.016	0.014	0.892	0.981	1.000
5%	0.059	0.059	0.053	0.975	1.000	1.000
10%	0.122	0.106	0.094	0.993	1.000	1.000
20%	0.232	0.194	0.196	1.000	1.000	1.000
Case of $\mathrm{H}_0(ii)$						
		DGP #2			DGP #3	
1%	0.028	0.016	0.014	0.719	0.880	0.993
5%	0.085	0.070	0.070	0.941	0.996	1.000
10%	0.128	0.110	0.122	0.985	1.000	1.000
20%	0.239	0.196	0.232	0.998	1.000	1.000

Note: The reported are the rejection frequencies over 500 simulations.

500 times. We use cubic B-splines to approximate unknown function $\alpha_0(\cdot)$. For simplicity, we set $L_n = 3$ in our experiments for all sample sizes since the range of n is not that large. We compute the root mean squared error (RMSE) and the mean absolute error (MAE) for each fixed coefficient across 500 iterations. For a varying nonparametric intercept function, RMSE and MAE are first computed for each simulation iteration; reported are their averages computed over 500 iterations.

The results are reported in Table B.1. Consistent with our theory, performance of the estimator improves with an increase in the sample size across all quantiles. As one would normally expect, it performs better for "middle" quantiles (median, in our case): RMSE and MAE somewhat worsen when we estimate the model closer to tails of the response distribution.

B.2 Specification Tests

We next examine the small-sample performance of our proposed specification test statistic. To conserve space, we only consider $\tau = 0.50$. The sample sizes are $n = \{100, 200, 400\}$, and the number of simulation replications is 500. Residuals under H_1 are obtained via our proposed PLSQAR model using cubic B-splines to approximate the unknown function $\alpha_0(\cdot)$. Residuals under H_0 are obtained via Su & Yang's (2011) estimator. Given the sample size, for each simulation, we calculate our test statistic from the simulated data plus 199 bootstrap test statistics. Then, from the 200 test statistic values, we obtain the 1%, 5%, 10% and 20% upper percentile (critical) values.

To assess power and size of the test, we consider the following four experimental designs for the data-generating process given in (B.4):

(1) The null in (3.2) is true: $\rho_{\tau,0} \equiv \rho_0(v)\big|_{v=\tau} = 0.5 + 0.15\Phi^{-1}(v)$, $\beta_{\tau,0} \equiv \beta_0(v)\big|_{v=\tau} = 0.2 + 0.15\Phi^{-1}(v)$ and $\alpha_{\tau,0}(z) \equiv \alpha_0(z,v)\big|_{v=\tau} = 0.5 + 0.5z + 0.15\Phi^{-1}(v)$;

(2) The null in (3.3) is true: $\rho_{\tau,0} \equiv \rho_0(v)\big|_{v=\tau} = 0.5 + 0.15\Phi^{-1}(v)$, $\beta_{\tau,0} \equiv \beta_0(v)\big|_{v=\tau} = 0.2 + 0.15\Phi^{-1}(v)$ and $\alpha_{\tau,0}(z) \equiv \alpha_0(z,v)\big|_{v=\tau} = 0.5 + 0.15\Phi^{-1}(v)$ for all z;

(3) The alternative in (3.4) is true: $\rho_{\tau,0} \equiv \rho_0(v)\big|_{v=\tau} = 0.5 + 0.15\Phi^{-1}(v)$, $\beta_{\tau,0} \equiv \beta_0(v)\big|_{v=\tau} = 0.2 + 0.15\Phi^{-1}(v)$ and $\alpha_{\tau,0}(z) \equiv \alpha_0(z,v)\big|_{v=\tau} = \sin(1 + 1.5z) + 0.15\Phi^{-1}(v)$.

The results presented in Table B.2 show that the test has quite an accurate size across all null

Table C.1. Semiparametric Estimates of Constant Parameters on House Attributes in the Conditional Quantile Regression of Property Value across Quantiles

	Quantiles of Property Value			
	0.25th	0.50th	0.75th	0.95th
Log Sq. Footage	**0.59100**	**0.58160**	**0.59024**	**0.58871**
	(0.53217; 0.64599)	(0.53713; 0.62548)	(0.54446; 0.63067)	(0.49993; 0.74361)
Log Acreage	**0.04253**	**0.06913**	**0.08138**	**0.09038**
	(0.01883; 0.06745)	(0.04775; 0.08817)	(0.06252; 0.09893)	(0.02675; 0.11778)
Story Height	**−0.05092**	**−0.09042**	**−0.09235**	**−0.13096**
	(−0.09016; −0.00927)	(−0.11479; −0.06307)	(−0.11880; −0.06453)	(−0.18673; −0.05093)
# Bedrooms	−0.00629	−0.01029	−0.02846	−0.14829
	(−0.14271; 0.10882)	(−0.11146; 0.08000)	(−0.11103; 0.06366)	(−0.35613; 0.20943)
# Bedrooms^2	−0.00420	−0.00227	0.00006	0.01576
	(−0.02006; 0.01373)	(−0.01471; 0.01206)	(−0.01374; 0.01176)	(−0.03296; 0.04323)
# Bathrooms	0.06181	**0.06611**	0.00290	−0.03061
	(−0.00550; 0.12941)	(0.01357; 0.11258)	(−0.05774; 0.05336)	(−0.14870; 0.09881)
# Bathrooms^2	−0.00041	0.00180	**0.01322**	**0.02173**
	(−0.00877; 0.00853)	(−0.00366; 0.00784)	(0.00655; 0.02102)	(0.00243; 0.03575)
Full Basement	**0.17764**	**0.11541**	**0.10999**	0.07606
	(0.12002; 0.23109)	(0.07540; 0.15296)	(0.08254; 0.14185)	(−0.01222; 0.22164)
Partial Basement	**0.14850**	**0.07297**	**0.06104**	0.01918
	(0.09096; 0.20614)	(0.03693; 0.11070)	(0.03572; 0.09072)	(−0.06952; 0.15137)
Attic	0.02001	0.00833	**0.02287**	0.01788
	(−0.00580; 0.04998)	(−0.01016; 0.02775)	(0.00395; 0.04785)	(−0.03912; 0.08237)
Attached Garage	0.02530	0.01621	−0.03072	−0.11543
	(−0.03024; 0.07103)	(−0.01856; 0.04644)	(−0.07117; 0.00431)	(−0.23245; 0.04623)
Garage Capacity	**0.02446**	**0.02412**	**0.02613**	0.03682
	(0.00620; 0.04629)	(0.01226; 0.03812)	(0.01350; 0.04132)	(−0.02873; 0.07669)
# Fireplaces	**0.05920**	**0.05461**	**0.03577**	0.02552
	(0.03759; 0.08208)	(0.03640; 0.07530)	(0.01886; 0.05363)	(−0.02504; 0.08159)
Central A/C	**0.13311**	**0.11955**	**0.08045**	0.01313
	(0.06906; 0.19630)	(0.05463; 0.17715)	(0.03524; 0.13024)	(−0.09633; 0.11826)
Age	**−0.00603**	**−0.00464**	**−0.00258**	−0.00108
	(−0.00793; −0.00372)	(−0.00611; −0.00313)	(−0.00400; −0.00120)	(−0.00490; 0.00250)
Age^2	**0.00001**	**0.00001**	**0.00001**	0.00001
	(0.00000; 0.00003)	(0.00000; 0.00003)	(0.00000; 0.00002)	(−0.00002; 0.00003)

Reported are the estimates from a semiparametric PLSQAR model. The 95% bootstrap (percentile) confidence bounds in parentheses. Statistically significant estimates are in bold.

hypotheses regardless of n. Furthermore, the test exhibits superb power which increases with the sample size, as expected.

C Additional Results

In this section, we briefly comment on the results corresponding to hedonic attributes other than the distance to rock mine included in the estimated house price function. Their fixed parameter estimates (with bootstrap confidence bounds) across quantiles of the house price distribution are reported in Table C.1. For the estimates of median marginal effects of statistically significant covariates, see Table C.2. Among these non-distance variables, log square footage of house, log acreage and story height are the only ones consistently found to be significant across all estimated quantiles of the house price distribution. Interestingly, no other house attribute has a significant

Table C.2. Semiparametric Estimates of Median ME of Selected House Attributes on Conditional Quantiles of Property Value across Quantiles

	Quantiles of Property Value			
	0.25th	0.50th	0.75th	0.95th
Log Sq. Footage				
TME	0.8961	0.8467	0.7950	0.7882
Median DME	0.6048	0.5928	0.5976	0.5958
Median IME	0.2914	0.2540	0.1974	0.1925
Log Acreage				
TME	0.0645	0.1007	0.1096	0.1210
Median DME	0.0435	0.0705	0.0824	0.0915
Median IME	0.0210	0.0302	0.0272	0.0295
Story Height				
TME	–0.0772	–0.1316	–0.1244	–0.1753
Median DME	–0.0521	–0.0922	–0.0935	–0.1325
Median IME	–0.0251	–0.0395	–0.0309	–0.0428
Full Basement				
TME	0.2694	0.1680	0.1481	0.1018
Median DME	0.1818	0.1176	0.1114	0.0770
Median IME	0.0876	0.0504	0.0368	0.0249
Partial Basement				
TME	0.2252	0.1062	0.0822	0.0257
Median DME	0.1520	0.0744	0.0618	0.0194
Median IME	0.0732	0.0319	0.0204	0.0063
Garage Capacity				
TME	0.0371	0.0351	0.0352	0.0493
Median DME	0.0250	0.0246	0.0265	0.0373
Median IME	0.0121	0.0105	0.0087	0.0120
# Fireplaces				
TME	0.0898	0.0795	0.0482	0.0342
Median DME	0.0606	0.0557	0.0362	0.0258
Median IME	0.0292	0.0238	0.0120	0.0083
Central A/C				
TME	0.2018	0.1741	0.1084	0.0176
Median DME	0.1362	0.1219	0.0814	0.0133
Median IME	0.0656	0.0522	0.0269	0.0043

Reported are the medians of point estimates of MEs from the PLSQAR model estimated for a given conditional quantile of property value.

impact on property values in the 0.95th quantile. Houses in this top quantile include older (historic) houses in Delaware City as well as recently built McMansion-style houses. More generally, we find that the number of bedrooms and bathrooms in the house, the presence of an attic and the garage being attached to the main house are largely statistically insignificant across all quantiles which likely is due to property heterogeneity inherent with rapid urbanization. Among the statistically significant house attributes, the square footage has by far the largest marginal effect on the property value with its magnitude declining as the house price rises. We document a similar declining marginal effects (across quantiles) for the basement variables, the number of fireplaces and the presence of central air-conditioning system in the house. From Table C.2, it appears that garage capacity is equally valued by all home buyers regardless of the property value, whereas the lot size exhibits increasing importance for buyers of higher priced houses. The estimates of the total marginal effects of story height are negative across all quantiles with larger (absolute) magnitudes estimated at the higher house price quantiles. This likely is an artifact of changing consumer preferences as well as building trends in the area given that single-story houses have become more common in recent years.

References

Anselin, L. & Lozano-Gracia, N. (2009). Errors in variables and spatial effects in hedonic house price models of ambient air quality. *Empirical Economics*, *34*, 5–34.

Bajari, P., Fruehwirth, J. C., Kim, K. I., & Timmins, C. (2012). A rational expectations approach to hedonic price regressions with time-varying unobserved product attributes: The price of pollution. *American Economic Review*, *102*, 1898–1926.

Brasington, D. M. & Hite, D. (2005). Demand for environmental quality: A spatial hedonic analysis. *Regional Science and Urban Economics*, *35*, 57–82.

Cai, Z. & Xu, X. (2008). Nonparametric quantile estimation for dynamic smooth coefficient models. *Journal of the American Statistical Association*, *103*, 1595–1608.

Chay, K. Y. & Greenstone, M. (2005). Does air quality matter? Evidence from the housing market. *Journal of Political Economy*, *113*, 376–424.

Chen, X. (2007). Large sample sieve estimation of semi-nonparametric models. In J. J. Heckman & E. E. Leamer (Eds.), *Handbook of Econometrics*, volume 6B. North Holland.

Chernozhukov, V. & Hansen, C. (2005). An IV model of quantile treatment effects. *Econometrica*, *73*, 245–261.

Chernozhukov, V. & Hansen, C. (2006). Instrumental quantile regression inference for structural and treatment effect models. *Journal of Econometrics*, *132*, 491–525.

Cohen, J. P. & Coughlin, C. C. (2008). Spatial hedonic models of airport noise. *Journal of Regional Science*, *48*, 859–878.

Fan, J., Zhang, C., & Zhang, J. (2001). Generalized likelihood ratio statistics and Wilks phenomenon. *Annals of Statistics*, *29*, 153–193.

Feng, X., He, X., & Hu, J. (2011). Wild bootstrap for quantile regression. *Biometrika*, *98*, 995–999.

Gawande, K. & Jenkins-Smith, H. (2001). Nuclear waste trasport and residential property values: Estimating the effects of perceived risks. *Journal of Environmental Economics and Management*, *42*, 207–233.

Gayer, T. (2000). Neighborhood demographics and the distribution of hazardous waste risks: An instrumental variables estimation. *Journal of Regulatory Economics*, *17*, 131–155.

Harrison, D. & Rubenfeld, D. L. (1978). Hedonic housing prices and the demand for clean air. *Journal of Environmental Economics and Management*, *5*, 81–102.

He, X. & Liang, H. (2000). Quantile regression estimates for a class of linear and partially linear errors-in-variables models. *Statistica Sinica*, *10*, 129–140.

He, X. & Shi, P. (1996). Bivariate tensor-product B-splines in a partly linear model. *Journal of Multivariate*

Analysis, *58*, 162–181.

Hite, D., Chern, W., Hitzhusen, F., & Randall, A. (2001). Property-value impacts of an environmental disamenity: The case of landfills. *Journal of Real Estate Finance and Economics*, *22*, 185–202.

Honda, T. (2004). Quantile regression in varying coefficient models. *Journal of Statistical Planning and Inferences*, *121*, 113–125.

Jaeger, W. (2006). The hidden costs of relocating sand and gravel mines. *Resources Policy*, *31*, 146–164.

Jenish, N. (2016). Spatial semiparametric model with endogenous regressors. *Econometric Theory*, *32*, 714–739.

Jenish, N. & Prucha, I. (2009). Central limit theorems and uniform law of large numbers for arrays of random fields. *Journal of Econometrics*, *150*, 86–98.

Jenish, N. & Prucha, I. (2012). On spatial processes and asymptotic inference under near-epoch dependence. *Journal of Econometrics*, *170*, 178–190.

Jin, F. & Lee, L.-f. (2015). On the bootstrap for Moran's *I* test for spatial dependence. *Journal of Econometrics*, *184*, 295–314.

Kelejian, H. H. & Prucha, I. R. (1999). A generalized moment estimator for the autoregressive parameter in a spatial model. *International Economic Review*, *40*, 509–533.

Kelejian, H. H. & Prucha, I. R. (2010). Specification and estimation of spatial autoregressive models with autoregressive and heteroskedastic disturbances. *Journal of Econometrics*, *157*, 53–67.

Kim, M.-O. (2007). Quantile regression with varying coefficients. *Annals of Statistics*, *35*, 92–108.

Koenker, R. & Machado, J. A. F. (1999). Goodness of fit and related inference processes for quantile regression. *Journal of the American Statistical Association*, *94*, 1296–1310.

Kohlhase, J. E. (1991). The impact of toxic waste sites on housing values. *Journal of Urban Economics*, *30*, 1–26.

Lee, S. (2003). Efficient semiparametric estimation of a partially linear quantile regression model. *Econometric Theory*, *19*, 1–31.

Lee, T.-H. & Ullah, A. (2003). Nonparametric bootstrap specification testing in econometric models. In D. E. Giles (Ed.), *Computer-Aided Econometrics* (pp. 451–477). NY: CRC Press.

Leggett, C. G. & Bockstael, N. E. (2000). Evidence of the effects of water quality on residential land prices. *Journal of Environmental Economics and Management*, *39*, 121–144.

LeSage, J. & Pace, R. K. (2009). *Introduction to Spatial Econometrics.* Boca Raton: Taylor & Francis CRC Press.

Liao, W.-C. & Wang, X. (2012). Hedonic house prices and spatial quantile regression. *Journal of Housing Economics*, *21*, 16–27.

Nelson, A. C., Genereux, J., & Genereux, M. (1992). Price effects of landfills on house values. *Land Economics*, *68*, 359–365.

Newey, W. K. & McFadden, D. (1994). Large sample estimation and hypothesis testing. In R. Engle & D. McFadden (Eds.), *Handbook of Econometrics*, volume IV chapter 36, (pp. 2111–2245). Elsevier Science B.V.

Ohio Department of Natural Resources (2010). *2009 Report on Ohio Mineral Industries: An Annual Summary of the State's Economic Geology.* Division of Geological Survey. Compiled by Mark E. Wolfe.

Ohio Department of Natural Resources (2011). *2010 Report on Ohio Mineral Industries: An Annual Summary of the State's Economic Geology.* Division of Geological Survey. Compiled by Mark E. Wolfe.

Pollard, D. (1991). Asymptotics for least absolute deviation regression estimators. *Econometric Theory*, *7*, 186–199.

Qu, X. & Lee, L.-f. (2015). Estimating a spatial autoregressive model with an endogeneous spatial weight matrix. *Journal of Econometrics*, *184*, 209–232.

Reichert, A. K., Small, M., & Mohanty, S. (1992). The impact of landfills on residential property values. *Journal of Real Estate Research*, *7*, 297–314.

Rosen, S. (1974). Hedonic prices and implicit markets: Product differentiation in pure competition. *Journal of Political Economy*, *82*, 34–55.

Ruppert, D. & Carroll, R. J. (1980). Trimmed least squares estimation in the linear model. *Journal of the*

American Statistical Association, *75*, 828–838.

Seber, G. A. F. (2008). *A Matrix Handbook for Statisticians.* Wiley Series in Probability and Statistics. John Wiley & Sons, Inc.

Small, K. A. & Steimetz, S. S. C. (2012). Spatial hedonics and the willingness to pay for residential amenities. *Journal of Regional Science*, *52*, 635–647.

Su, L. & Hoshino, T. (2016). Sieve instrumental variable quantile regression estimation of functional coefficient models. *Journal of Econometrics*, *191*, 231–254.

Su, L. & Yang, Z. (2011). Instrumental variable quantile estimation of spatial autoregressive models. Working Paper, Singapore Management University.

Sun, Y. (2006). A consistent nonparametric equality test of conditional quantile functions. *Econometric Theory*, *22*, 614–632.

Ullah, A. (1985). Specification analysis of econometric models. *Journal of Quantitative Economics*, *1*, 187–209.

Yu, K. & Jones, M. C. (1998). Local linear quantile regression. *Journal of the American Statistical Association*, *93*, 228–237.

Zabel, J. E. & Guignet, D. (2012). A hedonic analysis of the impact of LUST sites on house prices. *Resource and Energy Economics*, *34*, 549–564.

Wisconsin Geological and Natural History Survey
3817 Mineral Point Road
Madison, Wisconsin 53705-5100
TEL 608/263.7389 FAX 608/262.8086
http://www.uwex.edu/wgnhs/

James M. Robertson, Director and State Geologist

Delineation of areas contributing groundwater to springs and wetlands supporting the Hine's Emerald Dragonfly, Door County, Wisconsin

Kenneth R. Bradbury
Michael K. Cobb

2008

Open-File Report 2008-04

34 p. [17 b/w + 17 color]

Delineation of areas contributing groundwater to springs and wetlands supporting the Hine's Emerald Dragonfly, Door County, Wisconsin

Final report to the Wisconsin Coastal
Management Program

May, 2008

By

Michael K. Cobb
Kenneth R. Bradbury

Wisconsin Geological and Natural History Survey, University of Wisconsin-Extension

Delineation of areas contributing groundwater to springs and wetlands supporting the Hine's Emerald Dragonfly, Door County, WI

Abstract

The coastal springs and wetlands of Door County, Wisconsin, provide rich habitat for the highly endangered Hine's emerald dragonfly. Understanding the source of groundwater discharging at the springs is critical to evaluating how local land-use decisions might impact the springs and to future efforts at groundwater and spring protection. This study delineated surface areas contributing groundwater to eleven sites understood to be critical Hine's habitat in Door County. Delineations used a combination of soil water-balance modeling and simple groundwater flow modeling to determine contributing areas. Contributing areas ranged in size from 0.2 to 11.4 square miles. Shallow groundwater flows through a fractured dolomite aquifer. Predicted groundwater velocities are extremely high (up to 40 ft/day) and residence times can be quite short (less than two years at most sites). Geochemical and isotopic data collected at several springs are consistent with model results. The scope of the project did not allow detailed study at any one site, but instead focused on an overview study of many sites. The results represent a starting point for more refined studies at specific critical sites.

Introduction

Background

The coastal springs and wetlands of Door County, Wisconsin, provide rich habitat for the highly endangered Hine's emerald dragonfly. The U.S. Fish and Wildlife Service, Wisconsin Department of Natural Resources, the Nature Conservancy, and biologists from the University of South Dakota are all actively engaged in research and other actions to better understand and protect the Hine's emerald. Despite these efforts, a significant risk to the Hines emerald has remained poorly understood. Development and disturbance in upgradient recharge areas has the potential to alter groundwater flow to the springs and wetlands that provide habitat for the Hine's emerald. Understanding, maintaining, and protecting groundwater flow to these coastal areas is essential for protection of the species. Delineating areas contributing water to the springs is the first step in this process.

This study has developed preliminary estimates of the areas contributing groundwater recharge that may affect eleven different Hine's emerald dragonfly habitats in Door County (Figure 1). Recharge-area delineations include a combination of water-balance and groundwater-flow modeling supported with field measurements of water levels and baseflows. We estimated groundwater recharge rates using a GIS-linked soil-water budget model. Contributing-area delineations were made using a series of relatively simple groundwater flow models calibrated to field measurements of surface water and groundwater levels and surface-water discharges. Measurements of spring chemistry, temperature, and isotopic indicators assisted in verifying model results and will provide baseline data currently lacking at the Hine's emerald sites.

Dragonfly ecology

The Hine's emerald dragonfly was federally listed as an endangered species in 1995. It is currently known to exist in only four states (Illinois, Michigan, Missouri, and Wisconsin) and was recently found in Ontario. Its habitat is largely restricted to spring-fed wetlands in areas of dolomite bedrock. The survival of the species has been threatened by habitat destruction, degradation and fragmentation.

Adult female dragonflies lay eggs in water or mud. When the eggs hatch the larvae spend up to five years in small streams and wetlands. Only after this multi-year period as larvae dwelling in shallow surface water do they transform into adults that are recognizable as dragonflies. This adult stage is comparatively brief, lasting no more than six weeks in a period from June through August. They capture prey in flight, feeding actively during daylight hours. Adults require complex wetlands with a forest edge and cool shallow water for foraging, roosting, and reproducing.

Acknowledgments

This study would not have been possible without assistance and advice from a project advisory committee. The committee met periodically to develop the proposal, review progress, advise on next steps, and to facilitate the project. Members of the project advisory committee were as follows.

Cathy Carnes, U S Fish and Wildlife Service, Green Bay Field Office, WI
Dr. Daniel Soluk, University of South Dakota, Vermillion, SD
Dr. Ron Stieglitz, University of Wisconsin-Green Bay, Green Bay, WI
Mike Grimm, The Nature Conservancy, Sturgeon Bay, WI
William Schuster, Door County Soil and Water Conservation, Sturgeon Bay, WI
Bill Smith, Wisconsin Department of Natural Resources, Madison, WI

The project was funded by a grant from the Wisconsin Coastal Management Program. The following organizations provided in-kind matching assistance for carrying out the project:

The Nature Conservancy
Door County
University of South Dakota, Vermillion
University of Wisconsin-Green Bay
Wisconsin Geological and Natural History Survey
Wisconsin Department of Natural Resources

We also thank private land owners in Door County who provided access to their land and allowed water-level measurements in private wells.

Hydrogeology

Door County's principal aquifer is composed of fractured, solution-weathered Silurian age dolomite. Extensive research has been conducted on the hydrogeology of the aquifer (e.g., Sherrill, 1978; Bradbury, 1989; Bradbury and Muldoon, 1992; Muldoon and others, 2001). The dolomite strata dip gently to the east, thickening from just tens of feet in the extreme southwest on the Green Bay shore to as much as 500 ft along Lake Michigan in the northeast of the county. Soil cover over the dolomite is frequently very thin, particularly in upland areas, and rainfall and snowmelt can infiltrate rapidly. Soil thicknesses increase in occasional buried bedrock valleys, particularly along the Lake Michigan shoreline. North of Sturgeon Bay, springs, streams and wetlands are typically restricted to these depressions in the bedrock surface.

The dolomite is very permeable but has relatively little storage. Recharge is conducted rapidly into the aquifer by vertical joints. Groundwater moves laterally along bedding plane fractures, many of which have been enlarged by rock dissolution. Muldoon and others (2001) showed that discrete near-horizontal zones of high permeability may be continuous over distances of as much as 10 miles.

Groundwater discharge occurs in springs, wetlands and into Lake Michigan and Green Bay. The majority of springs in Door County occur as focused discharge though a loose cover of sediment into a spring pool or stream bed. The visible turbulence in the sand or peat is commonly called a boil. Door County's springs have not been studied in detail, though it is assumed that most occur where highly permeable bedding plane fractures or joints intersects the bedrock surface. In many of the Hine's emerald habitats, we infer that a bedding plane fracture opens to a buried depression in the bedrock surface. The nature and volume of these springs suggests that they are not regional discharge points receiving far-field recharge transported as deeply circulating groundwater. We consider it more likely that most identified springs receive relatively local recharge conveyed in the shallower intervals of the dolomite aquifer.

Study Methods

Site selection

This study focused on eleven wetlands in Door County that are either confirmed or probable habitats for the Hine's emerald dragonfly (Figure 1). Other suspected habitats occur in Door County but were not included in this study. The physical bounds of each site were determined by the Wisconsin Department of Natural Resources and Dr. Daniel Soluk of the University of South Dakota. The sites vary in size from discrete spring complexes of several hundred square feet, to many mile-square wetland complexes known to include numerous breeding sites. Each site is described in more detail later in this report.

We divided the habitats in this study into two tiers based on site importance (Table 1). The bulk of field data collection and project resources were allocated to the first tier sites. The field data permitted more detailed model design and calibration, therefore contributing area estimates for these sites carry more confidence. Modeling of second tier sites made the best use of available data resources, but are in general less rigorously calibrated and therefore carry less confidence.

Table 1 Studied Habitats in Door County

First Tier Sites	Second Tier Sites
Mink River Estuary	Big Marsh/Washington Island
Three Springs Creek	Ephraim Swamp
North Bay Marsh	Arbter Lake
Reiboldts Creek/Ridges Sanctuary	Kellner Fen
Baileys Harbor Swamp	Gardner Swamp
Piel Creek	

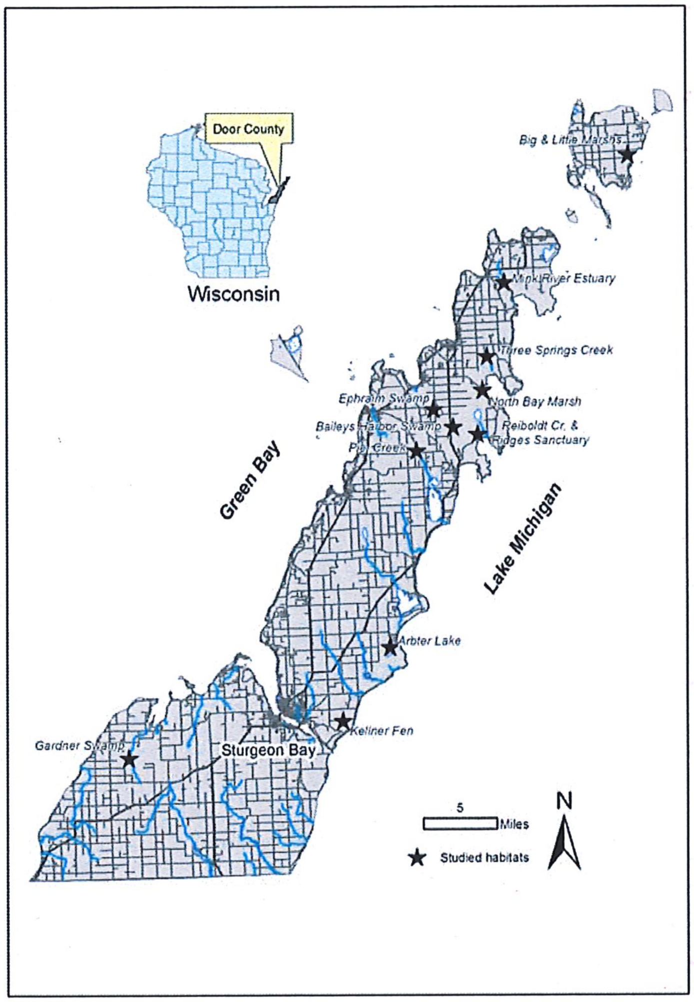

Figure 1. Locations of Hine's emerald dragonfly sites investigated in Door County.

Field investigations
We carried out a variety of field investigations designed to assist in model design and calibration, and to improve our understanding of the hydrogeologic system at the HED habitats. The major field tasks included habitat reconnaissance, stream-flow gauging, groundwater-level measurement, and spring sampling. Stream gauging and water-level measurement were focused near the first tier sites in northern Door County. Gauging was completed using an electromagnetic flow-meter. Water-level measurements were taken using a sonic water-level probe. The sonic probe allowed easy measurement of private water wells without the risks of contamination and tangling associated with a tape.

Laboratory samples were collected at only three HED habitats where focused spring discharge made it feasible to collect samples of discharge water and not standing surface water. Samples from these locations (Mink River, Three Springs Creek and upper Reiboldt Creek) were collected in both late November/early December and in early April. Samples were submitted to the University of Wisconsin Soil & Plant Analysis Lab in Madison for analysis of major ions, and to the Environmental Isotope Laboratory at the University of Waterloo, Ontario, for analysis of tritium, oxygen-18 and deuterium.

The WGNHS also completed a geophysical survey near the Reihboldts Creek habitat in the vicinity of Old Lime Kiln Road, in order to better understand the nature of the bedrock surface beneath the wetland habitat. The geophysical study is discussed in an appendix to this report.

Files relating to the field investigations have been archived at the WGNHS as a product of this study and are available for use by others. The files include further explanation and detailed results.

Recharge estimation
To estimate the quantity and spatial distribution of recharge we applied a soil-water balance model divided into daily time steps across a spatial grid (Dripps and Bradbury, 2007). The model uses common GIS coverages as inputs: soil hydrologic group, available water storage, land use, and overland flow direction. The flow-direction input was derived from a highly detailed digital elevation model that we generated using LIDAR (LIght Detection And Ranging) data furnished by Door County. We ran the model for the entire county on a 50-foot grid spacing, simulating recharge with daily precipitation and temperature data for four different years that approximated the median annual precipitation (2 different years), and the first and third quartiles (1 year each). Climatic data were acquired from the Wisconsin State Climatology Office in Madison. The model output for each run predicted cumulative monthly and annual and groundwater recharge for each cell. The two median model runs were averaged for the results and maps presented in this report. The accuracy of the predicted recharge values remains uncertain and are suspected to be biased low (i.e., more recharge is occurring than predicted). However, the model output is useful at identifying spatial trends and regions of preferential recharge. For ease of use by the public, the numerical recharge results have been simplified into a three-level system of recharge potential: low (0-3.75 in/year), medium (3.75 - 4.75 in/year) and high (greater than 4.75 in/year). The

statistical distribution of recharge predicted by the model is biased by numerous unreasonably high values (a model defect). However, the qualitative high/medium/low designations approximately divide the predicted recharge into thirds by area.

The recharge model files have been archived at the WGNHS as a product of this study and are available for use by others. The files include further explanation of model design and implementation.

Groundwater modeling

To estimate the contributing area for each Hine's emerald dragonfly habitat, we developed a series of groundwater flow models constructed using the GFLOW groundwater modeling code. GFLOW (http://www.haitjema.com/) simulates steady groundwater flow in two dimensions using mathematical analytic elements (linesinks) to represent hydrologic features such as wells, streams, wetlands, and springs.

To simulate groundwater flow in Door County, we constructed four different models representing: 1) Washington Island, 2) northern Door County from the Piel Creek habitat north to the Mink River habitat, 3) central Door County encompassing the Arbter Lake and Kelner Fen habitats, and 4) southern Door County encompassing Gardner Swamp. The northern Door County model included each of the first-tier sites, and was the most detailed in construction and calibration.

Models included streams and lakes as line sinks, digitized as a simplified map-view of the study area. Line sinks are assigned elevations, extracted from the digital elevation model, or interpreted from USGS 7.5 minute topographic maps. Models were divided into zones (termed inhomogeneities in the GFLOW environment) in order to vary hydraulic parameters. Zone areas were generally defined to reflect distinct terrains such as wetlands and uplands where recharge and aggregate hydraulic conductivity would be expected to differ.

Models were calibrated to match head and surface-water flux targets. Head targets included water-level data gathered for this study, data extracted from investigation reports of various contaminated sites in the county, and data reported by the USGS in their online database. The majority of surface water flux targets were based on field measurements made for this study in the late summer and fall of 2006. Additional gauging data was acquired from the WDNR's *2003-2004 Door Peninsula Baseline Monitoring Report.*

GFLOW models are powerful tools; however, they require great simplification of the true hydrogeologic complexity and assume steady-state flow. Door County's groundwater system has significant seasonal transience and vastly more heterogeneity than a computer model can represent, particularly at a regional scale. It should be recognized that no single groundwater model can be relied on to fully represent a hydrogeologic system. For this project, a confident estimate of contributing areas required multiple scenarios, not just one model. For each model area, a dry season and wet season model were created to bracket potential seasonal fluctuations. For the first-tier habitats, we completed three dry season and three wet season models, each considered a reasonable representation of the groundwater system. The differences between the model estimates in the various scenarios represent both seasonal variation and uncertainty in the model design and calibration.

The models were calibrated using the automated parameter estimation routine PEST (Dougherty, 2004). Several realizations were completed for each model. For the northern Door County model, three different low-season calibrations were performed with varying bounds set on allowable recharge. To simulate wet-season conditions, recharge was raised in each simulation in increments until wet-season head calibration targets were reached. Because far fewer reliable calibration targets were available for wet-season conditions, a systematic calibration at wet-season conditions was not possible. In total, the northern Door model area is represented by six different model realizations, three dry-season and three wet season. The other models areas (each for 2^{nd} tier sites) each include two model realizations, one dry-season and one wet-season.

Contributing areas for the habitats were estimated in each model realization using reverse particle tracking. GFLOW traces the path of groundwater backwards from a designated point to wherever it entered the aquifer as recharge. By this method it is possible to bound the area in which recharge entering the aquifer may discharge into a discrete habitat area. Figure 2 illustrates the contributing areas predicted for six simulations at the North Bay Marsh habitat. Each area in the figure represents the results of one simulation using different but equally reasonable sets of model parameters. The predicted areas typically varied only slightly between model realizations, with the greatest variation occurring at the upgradient extremes. The estimated contributing areas shown in this report are aggregate areas, encompassing the areas predicted in all model realizations. Figure 2 illustrates the process for designating the aggregate contributing area (shown with dashed line). Aggregate areas encompass the areas predicted in each simulation. Where contributing areas thinned to less than 100 ft in width, the peaks were excluded. Model uncertainty was too great to justifiably include areas at that level of detail. Aggregate contributing areas include the region between the upgradient peaks. We assume that seasonal shifts in water table are gradual and therefore that the upgradient peaks sweep across the upgradient region between the predicted extremes.

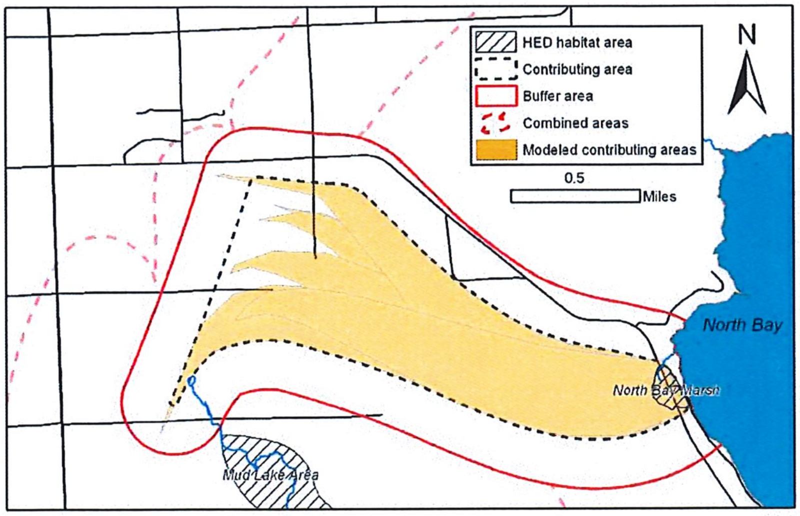

Figure 2. Contributing area for the North Bay site, illustrating the results of several model simulations and aggregated area. See text for details.

Results

Modeling results

The primary product of this study is a series of eleven contributing area maps developed for the Hines emerald dragonfly habitats (Appendix A, figures A1-A11). The areas shown in the appendix figures are also available as GIS files for incorporation into other geographic images. Each figure contains two views of the same region, illustrating different aspects of the study findings. The top views show recharge potential, and the bottom views show water table contours. The following section describes the elements shown in the figures, and discusses how they should be interpreted.

Wetland evaluated (hatched region). The wetland area evaluated is a region containing one or more HED larval habitats, as designated by the WDNR or Dr. Daniel Soluk of the University of South Dakota. Each area contains one or more locations of groundwater discharge, either focused at springs or distributed in wetlands or along streams. In the models, all groundwater flow that enters these areas is considered potential groundwater discharge that may affect HED habitat.

Contributing area (dashed black line). The contributing area is the model-predicted contributing area for a given HED habitat area. It encompasses the regions predicted by all model simulations for that habitat. Water infiltrating into the ground in the contributing area may potentially discharge within the respective HED habitat. Groundwater pumping, bedrock blasting, contaminant release or physical alterations to the hydrologic setting (such as construction projects that may increase impervious area or construction of detention basins) may affect the quantity and quality of water discharging in the HED habitats. Because of model limitations, it cannot be said that all water infiltrating in this region will discharge within the habitat. Though it cannot be quantified, we expect that the closer a location within the area is to the habitat, the more probable it is that infiltration occurring there will impact the habitat.

Buffer areas (solid red line). The buffer area is a region extending 1000 feet beyond the contributing area. Though the area within this buffer was not predicted to be a contributing area by any model simulation, we recommend considering the buffer as potential contributing area. There are two major reasons for creating this buffer: 1) The model is imperfect and may potentially be in error on the scale of 1000 feet; and 2) In many instances rainfall or snowmelt occurring outside the contributing area may travel into the region as runoff (in road ditches, for instance) and infiltrate within the contributing areas.

Combined areas (dashed red line; only present on some figures). The combined areas show the aggregate contributing area and buffer for all HED habitats. The combined area is not present on figures showing isolated habitats, such as the Mink River. In the region between Baileys Harbor and Sister Bay, however, the contributing areas and buffers for the different habitats in that area commonly adjoin or overlap. Overlap occurs because we are including the results of multiple simulations. In these overlapping areas, infiltration may reasonably discharge at more than one habitat.

Recharge potential (color shading in top figure). Recharge potential is a qualitative representation of the recharge model output. Given evenly distributed precipitation and snowmelt, the three levels of recharge potential (high, medium and low) indicate the amount of water that is expected to infiltrate and recharge groundwater. Areas of high recharge potential (orange) are typically areas of thin soil cover, where the greatest infiltration rates are expected. Low recharge potential areas (blue) typically have thicker soil and greater density of vegetation, and therefore are expected to significantly reduce the quantity of groundwater recharge. Medium recharge areas are intermediate. The high/medium/low categories are also intended to rank the particular regions within the contributing areas according to the risk they may pose to the HED habitat.

Water table contours (blue dashed lines in bottom figures). The water table contours show the model-predicted water table from the dry season calibration. For the northern Door County models (from Piel Creek north to Mink River), the water tables are generated from the best of three different models calibrated to dry season targets. Contour elevations are in feet above Mean Sea Level.

The estimated contributing areas varied from as little as 0.4 square miles (Arbter Lake) to 11.4 square miles (Reiboldt Creek and Ridges Sanctuary). Table 2 indicates the size of the contributing areas. Table 2 also gives a qualitative assessment of the variability of the contributing areas between scenarios – the difference in the areas predicted by model scenarios run with dry-season recharge, wet-season recharge, or alternate calibrations. High variability suggests that the predicted result is highly sensitive to seasonal variation or to slight changes in model parameters, and thus carries greater uncertainty than models in which the predicted contributing area remained essentially the same in all model scenarios.

Table 2. Summary of contributing area estimates for HED habitats.

Habitat (contributing area size)	Tier	Scenario variation	Comments
Piel Creek (0.9 square miles)	1	high	The habitat is a wetland at the head of Piel Creek. Though the predicted contributing area is relatively consistent among scenarios, the models frequently predict that the habitat is dry (receives no discharge) in dry seasons. Seasonal variation is great here, and may not be adequately represented by the models.
Mink River Estuary (5.2 square miles)	1	low	The habitat includes a large wetland with many springs. The habitat area was extended to the mouth of estuary based on observations of D. Soluk. The habitat receives surface water from the Mink River north of the contributing area in wet seasons; dry season model scenarios show the river dry north of Highway 42.
Three Springs Creek (1.2 square miles)	1	high	The habitat includes a major spring complex that forms the perennial head of Three Springs Creek. Some model scenarios show all flow entering from the southwest (i.e., the northwest contributing area lobe is absent). The habitat receives surface water from the upper reaches of Three Springs Creek in wet seasons.
North Bay Marsh (0.9 square miles)	1	medium	The habitat includes a wetland adjacent to North Bay. Discharge to this wetland may cease in the driest months. Scenario variation is greatest at the upgradient maximum; near-field estimates are consistent.
Reiboldt Creek and Ridges Sanctuary (11.4 square miles)	1	medium	The habitat includes a large region of spring-fed wetlands containing numerous important HED habitats. Scenario variation is greatest at the upgradient maxima; near-field estimates are more consistent. Most potential surface water inputs are fully contained in the groundwater contributing area.
Ephraim Swamp (1.6 square miles)	2	high	The habitat forms part of the Ephraim Swamp. The hydrologic setting of the habitat is not well understood and may not be adequately represented in the models. Scenarios show greatest variation in the southern lobe of the contributing area.
Baileys Harbor Swamp (3.5 square miles)	1	medium	The habitat is a wetland. Scenario variation is greatest in the southern lobe of the contributing area. Surface water may enter the habitat from the upper reaches of the Baileys Harbor Swamp (west of Highway 57).

Table 2. (continued)

Habitat (contributing area size)	Tier	Scenario variation	Comments
Big & Little Marshes, Washington Island (0.6 square miles)	2	low	The area includes two spring-fed wetland habitats: Big and Little Marshes. The areas are not contiguous, but are treated here as a single habitat for simplicity. There are no surface water inputs to either habitat.
Arbter Lake (0.4 square miles)	2	low	The habitat is a lake in a wetland. Some surface water may enter the habitat through streams entering from north of the lake.
Kelner Fen (0.9 square miles)	2	low	The habitat is a fen. There are no known surface water inputs to the habitat.
Gardner Swamp (9.1 square miles)	2	low	The habitat is within a large wetland complex, and contains a northern region south of Fox Road, and a smaller southern region north of Highway K. The two units are treated as contiguous within the model.

Chemical and isotopic results

Water chemistry. The major-ion water chemistry of the three springs sampled for this project is typical of carbonate-rock terrains, and similar to groundwater in other parts of Door County (Table 3). The water is dominated by calcium, magnesium, and bicarbonate ions, with minor amounts of sodium, potassium, and sulfate. The springs were sampled twice, once in December, 2006 and once in April, 2007. Spring temperatures are typical of Door County groundwater. Minor differences in chemistry between these two sample dates are consistent with the conceptual model of rapid recharge and relatively short flow paths to the springs. Concentrations of most constituents are slightly lower in April than in December, consistent with more rapid recharge and consequent dilution of groundwater in the Spring. The chloride and nitrate levels are worth noting. Chloride levels are higher in December than in April, probably as a result of highway salting for ice removal in December. The presence of nitrate shows that near-surface land use has impacted spring water quality. Nitrate levels are higher in April than in December, possibly a consequence of Spring fertilizer applications. Both these temporal changes suggest rapid recharge and rapid lateral groundwater flow to the springs. This temporal variability shows that the springs are sensitive to changes in local land-use practices.

Isotopes. Analyses of environmental isotopes from water samples collected at three Hine's emerald sites are consistent with the conceptual model of young groundwater moving rapidly along relatively short flow paths. Isotopes of hydrogen (^2H, deuterium; ^3H, tritium) and oxygen (^{18}O, oxygen-18) occur naturally in the environment and are considered to be conservative tracers because they move as part of the water molecule, H_2O. Tritium (^3H) is an unstable radioactive isotope that entered the water cycle in elevated quantities during and following atmospheric atomic weapons testing during the 1960s. Tritium is measured in tritium units, TU. During the 1960s, tritium in precipitation exceeded several thousand TU, and decreased through time due to radioactive decay. Because of its short half-life (12.4 years), tritium has been used to date the "age" (time since recharge) of relatively young (< 50 years) groundwater. Since atmospheric testing ceased, background tritium levels in precipitation have decayed to about 10 TU, and tritium continues to decay once the water enters the subsurface. Accordingly, any groundwater that contains tritium above 1 TU is now considered to be quite young (recharged in less than 10 years), and groundwater that contains tritium near 10 TU must have been recharged in the past one or two years.

Table 3. Major ion and field parameters for springs. Top: field parameters; middle: major cations; bottom; major anions.

location	pH (units)		temperature (°C)		electrical conductivity (uS/cm)	
	Dec	April	Dec	April	Dec	April
Mink River	7.05	7.21	8.4	9.4	678	623
Three Springs	7.09	7.33	9.4	8.7	594	457
Lime Kiln Rd	7.19	7.65	7.5	7.9	592	528

location	K (ppm)		Ca (ppm)		Mg (ppm)		Na (ppm)	
	Dec	April	Dec	April	Dec	April	Dec	April
Mink River	0.9	0.9	82	67	37	33	7.4	4.7
Three Springs	0.9	0.8	67	52	32	26	3.9	2.0
Lime Kiln Rd	1.6	1.5	68	56	32	27	4.1	4.8

location	Cl (ppm)		NO_3 (ppm)		SO_4 (ppm)		Alkalinity (as mg $CaCO_3$/L)	
	Dec	April	Dec	April	Dec	April	Dec	April
Mink River	15.1	10.5	1.7	4.2	14.1	12.8	250	342
Three Springs	10.4	5.8	1.4	6.0	15.7	13.4	225	267
Lime Kiln Rd	10.7	9.8	3.2	4.3	14.2	13.6	250	109

Tritium concentrations at the three springs sampled for this project ranged from 8.9 to 11 TU (Table 4). Differences between the two sampling dates are probably due to seasonal differences in atmospheric tritium input. The range is about what is expected for tritium in recent precipitation, and suggests that water discharging at the springs is very young, certainly no older than 5 years.

Oxygen-18 (^{18}O) and deuterium (^{2}H) are stable isotopes that do not decay radioactively. Instead, the water composition of these isotopes changes by fractional distillation of water vapor as water evaporates or precipitates. Concentrations of ^{18}O and ^{2}H are expressed as del (δ) permil (o/oo) values compared to standard mean ocean water, abbreviated SMOW. Although both isotopes vary seasonally due to temperature and evaporation and precipitation in air masses, the ratio of ^{18}O to ^{2}H in precipitation remains fairly constant. This relationship, called the meteoric water line (MWL), varies slightly from location to location. In general, groundwater recharged directly from precipitation should have an ^{18}O:^{2}H signature that falls on the local meteoric water line. Water samples that plot to the right of the MWL are interpreted as originating from surface water, where free-surface evaporation has occurred. Rayne, Bradbury, and Muldoon (2001) collected isotope data from wells and surface water features in Door County and showed that water from Green Bay and Lake Michigan plotted significantly to the right of the local MWL for their study.

Water from the three springs sampled for the present study plots directly on the local MWL (Figure 3). Lack of deviation from the line suggests that the water discharged from these springs did not originate as surface water in a lake or wetland but instead as direct groundwater recharge. These findings are consistent with our conceptual model of short, rapid flow to the springs.

Table 4. Stable isotope sampling results

Location	Sample ID	Sample Date	Deuterium	Oxygen-18 (δ o/oo)	Tritium (enriched) (TU)		
Mink River	Door - 1	11/30/06	-71.98	-10.40	8.9	±	1
Three Springs	Door - 2	11/29/06	-71.74	-10.36	8.9	±	0.9
Lime Kiln Road	Door - 3	12/01/06	-70.14	-10.30	9.3	±	0.9
Mink River	Door - 1	04/02/07	-74.35	-10.76	10.9	±	0.9
Three Springs	Door - 2	04/02/07	-74.21	-10.83	11.1	±	0.9
Lime Kiln Road	Door - 3	04/02/07	-69.43	-10.15	11	±	0.9

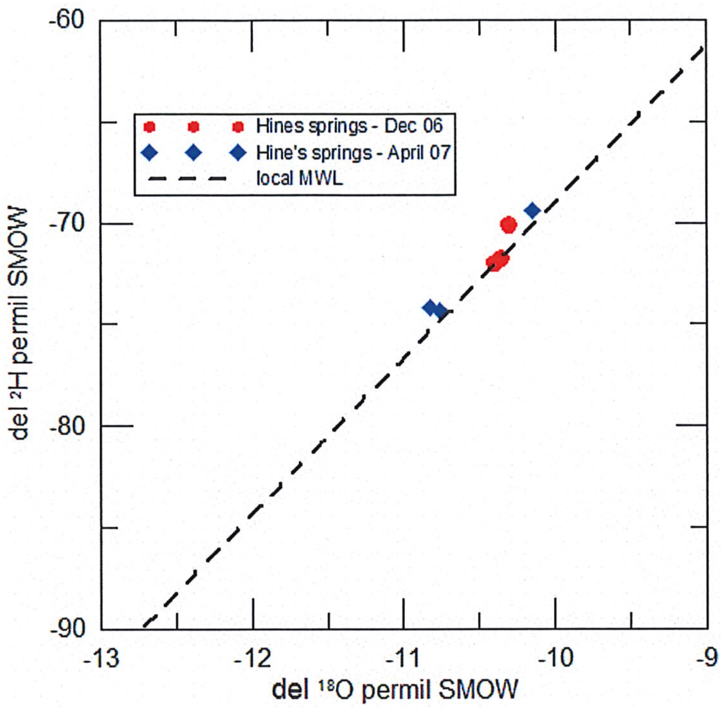

Figure 3. Oxygen-18 versus deuterium contents for water samples collected from springs at three HED sites. All analyses plot along the meteoric water line (MWL), consistent with groundwater recharged directly from recent precipitation.

Estimated groundwater flow rates

Previous studies of groundwater movement in Door County (for example, Rayne, Bradbury, and Muldoon, 2001) have shown that groundwater flow rates are generally rapid, and estimated velocities of 10's of feet per day (ft/day) are not uncommon. The simple groundwater flow models constructed for this study are not intended to be used for transport-time predictions. They simulate the fractured dolomite aquifer in Door County as a porous medium and neglect the rapid and complex groundwater flow paths that undoubtedly occur through fracture conduits and minor karst features. Nevertheless, comparisons of model-simulated flow rates and groundwater travel times with transport data acquired from a recent tracer test in Door County suggest that the models give reasonable estimates of flow rates, and by extension are appropriate tools for delineating contributing areas to the Hine's emerald areas.

In late 2007 a dye tracer test was performed at a site called Plum Bottom, located near Egg Harbor, WI on the western (Green Bay) side of Door County and about equidistant between Sturgeon Bay and Fish Creek. The purpose of the test was to determine the source of contamination of a supply well located at a restaurant. Two different fluorescent dyes were injected into the restaurant's septic system, and dye concentrations were monitored at downgradient wells for several months (Alexander, Green, and Alexander, 2008). The dyes were detected at two wells located 2700 and 3000 feet horizontally downgradient of the injection point. The first detection of the dye in these wells occurred between 83 and 90 days after injection, giving an approximate horizontal groundwater flow rate of 32-33 ft/day. It is important to understand that these numbers apply to the horizontal distance between the injection and detection points and not to the actual complex flow path followed by the water.

For comparison, linear flow velocities predicted by the models developed for this project range from 1 to 43 ft/day, with maximum groundwater travel times from recharge to the HED sites ranging from 260 days to 48 years. At six sites (Washington Island, Mink River, Three Springs, North Bay, Bailey's Harbor Swamp, and Kellner Fen) the estimated maximum travel times are less than two years and estimated horizontal flow velocities are in the range of 10-40 ft/day, similar to the 32 ft/day value from the tracer experiment. These estimates are based on the calibrated hydraulic conductivity and hydraulic gradient obtained from each GFLOW model and use an estimated effective porosity of 0.005, as selected by Rayne, Bradbury, and Muldoon (2001).

Summary and Conclusions

This study has estimated contributing areas for groundwater recharge potentially effecting eleven Hines emerald dragonfly habitats in Door County. The areas range in size from 0.4 to 11.4 square miles, and some areas overlap. The estimated areas are based on relatively simple groundwater models constructed and calibrated using existing information and a small amount of new field data. The scope of this project did not permit extensive new data collection, and the need to evaluate eleven sites prohibited expending substantial resources at any single site. However, the estimated areas in this report are hydrogeologically reasonable and should be considered in future land-use decisions. In particular, the delineated areas provide an outer bound for areas contributing water to each HED site. It is likely that specific points within each area, such as open fractures, shallow bedrock pavements, or small sinkholes, might be critical input points for groundwater flowing to each critical HED habitat, but locating those specific points was beyond the scope of the present study. Geochemical and isotopic data collected from groundwater at three of the HED sites are consistent with the conceptual model of relatively rapid recharge and rapid groundwater movement (10's of ft/day) to the springs. These data reinforce the idea that the springs are vulnerable to local land-use changes.

The area delineations in this report are intended to provide resource managers with a starting point for protecting the downgradient Hine's emerald habitats. Such protection includes maintaining both the water balance and water quality in the areas. New demands on groundwater, or new industry or construction within the contributing areas and buffer zone should be considered to pose a risk to the Hine's emerald dragonfly. Further data collection and modeling may be required to answer specific land-use questions. The models and data generated in this study are intended to provide a resource and starting point for further work of this sort.

References

Alexander, E.C., J.A. Green, and S.C. Alexander. 2008. *Plum Bottom closed depression groundwater trace final report*. Administrative report submitted to the Door County Soil and Water Conservation Department, dated 25 January 2008, 13 p.

Bradbury, K.R., 1989. Door County's groundwater; An asset or a liability? In: Proceedings, Conference on Door County and the Niagara Escarpment: Wisconsin Academy of Sciences, Arts and Letters, p. 36-44.

Bradbury, K.R., and M.A. Muldoon. 1992. Hydrogeology and groundwater monitoring of fractured dolomite in the upper Door priority watershed, Door County, Wisconsin. Open-File Report 1992-02: Wisconsin Geological and Natural History Survey, 83 p.

Doherty, J., 2004. *PEST: Model-independent parameter estimation. Users manual: 5th edition*: Watermark Computing.

Dripps, W.R., and K.R. Bradbury, 2007. A simple daily soil-water balance model for estimating the spatial and temporal distribution of groundwater recharge in temperate humid areas: *Hydrogeology Journal*, v. 15, no. 3, p. 433-444.

Hogler, S, S. Surendonk, and M. Gansberg, 2004. 2003-2004 Door Peninsula Baseline Monitoring Report: Wisconsin Department of Natural Resources Report.

Muldoon, M.A., J.A. Simo, and K.R. Bradbury, 2001. Correlation of hydraulic conductivity with stratigraphy in a fractured-dolomite aquifer, northeastern Wisconsin, USA: Hydrogeology Journal, v. 9, no 6, p. 570-583.

Rayne, T.W., Bradbury, K.R., and Muldoon, M.A., 2001, Delineation of capture zones for municipal wells in fractured dolomite, Sturgeon Bay, Wisconsin, USA: *Hydrogeology Journal,* v. 9, p. 432–450.

Sherrill, M.G., 1978. Geology and ground water in Door County, Wisconsin, with emphasis on contamination potential in the Silurian dolomite: U.S. Geological Survey Water Supply Paper 2047, 38 p.

Appendix A
Maps of HED Sites

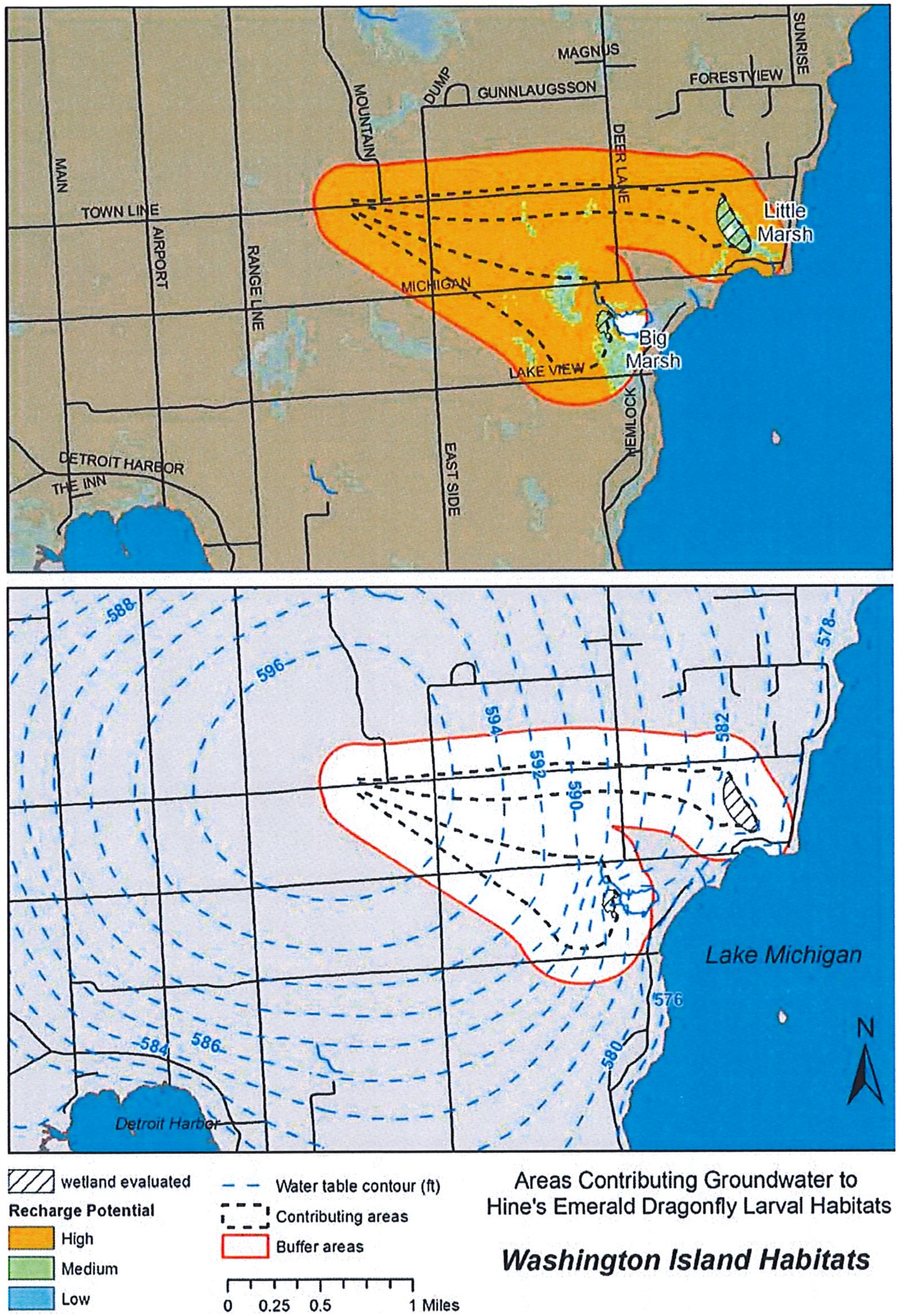

Figure A1. Contributing areas for larval sites on Washington Island.

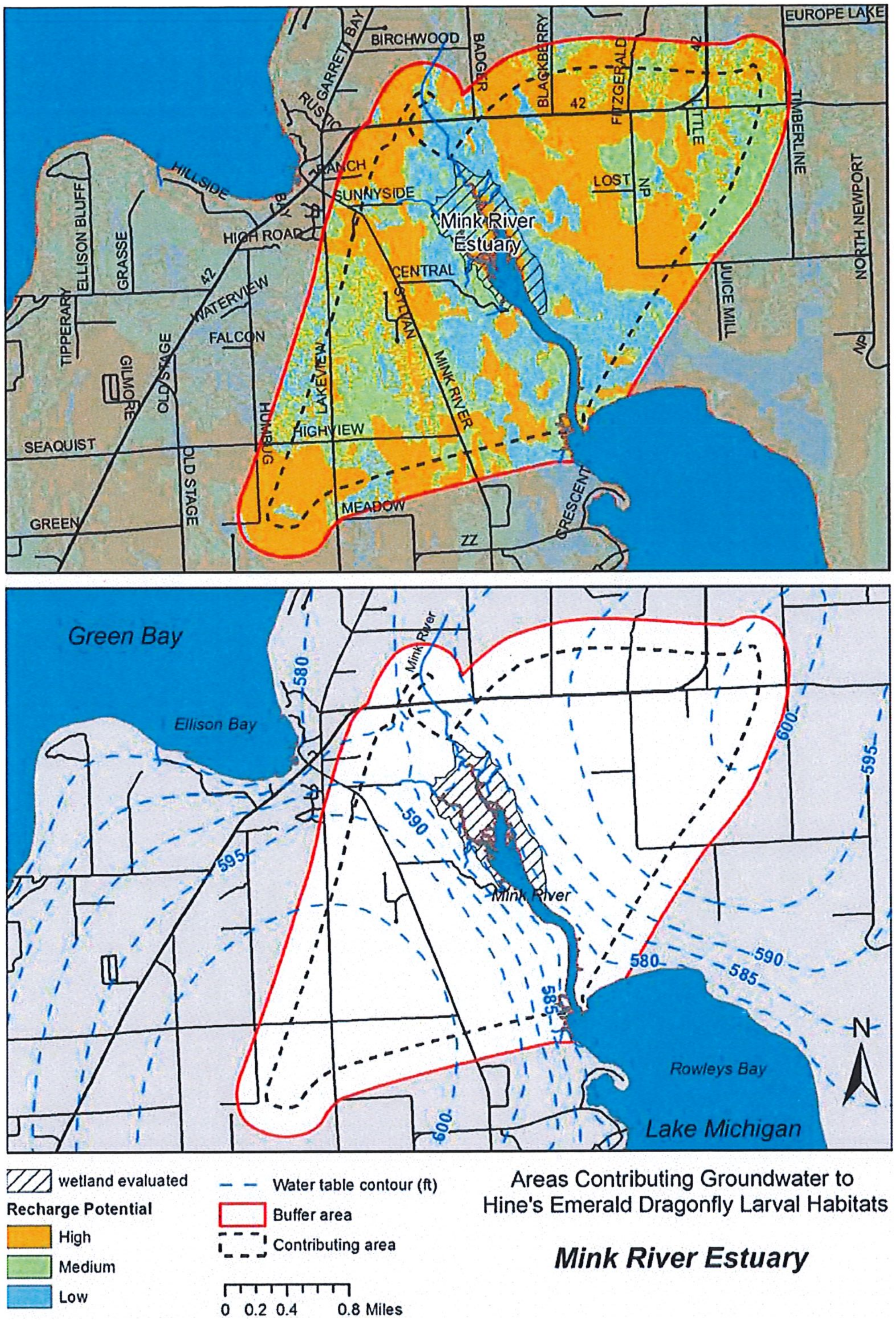

Figure A2. Contributing areas for larval sites along the Mink River

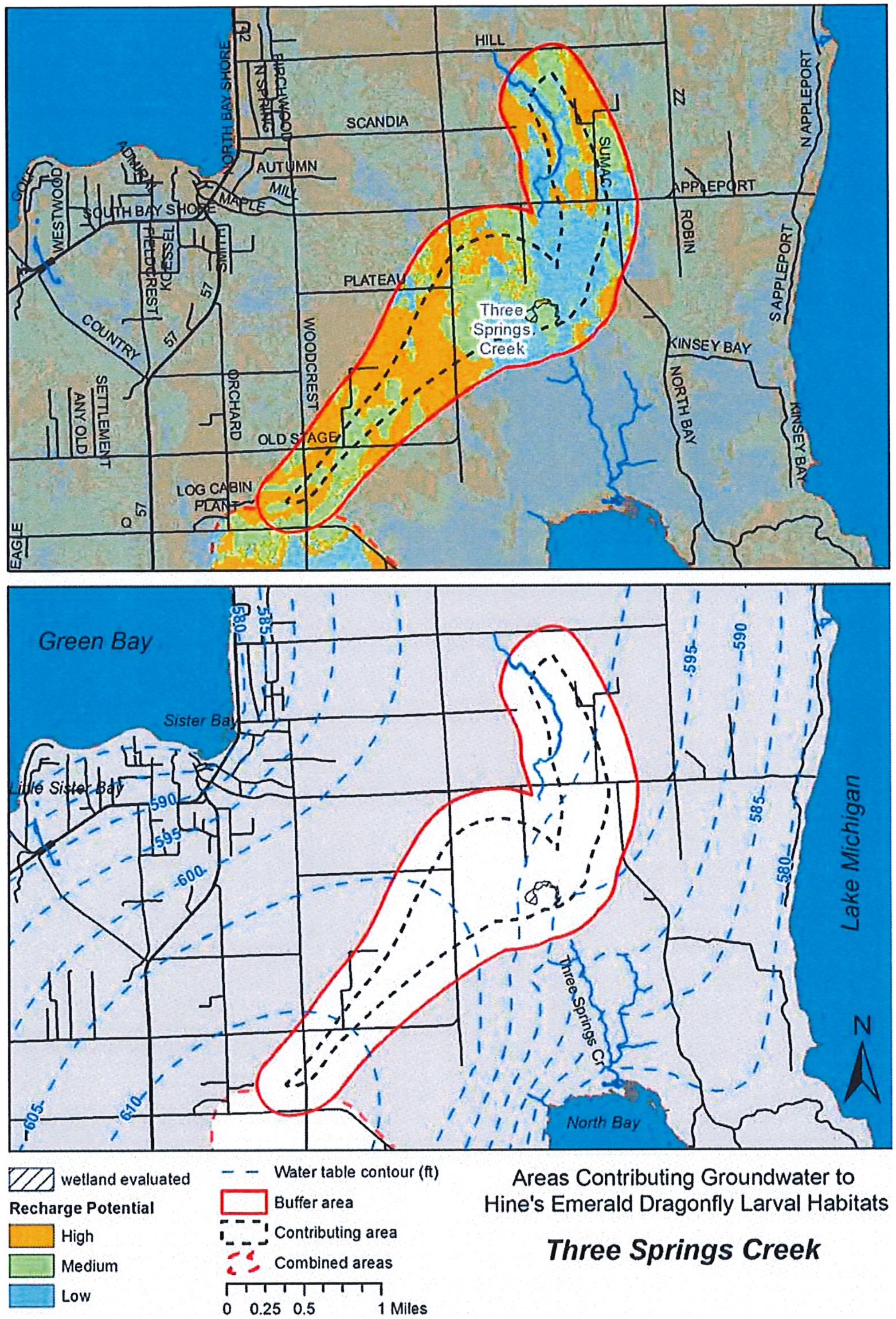

Figure A3. Contributing areas for larval sites along Three Springs Creek

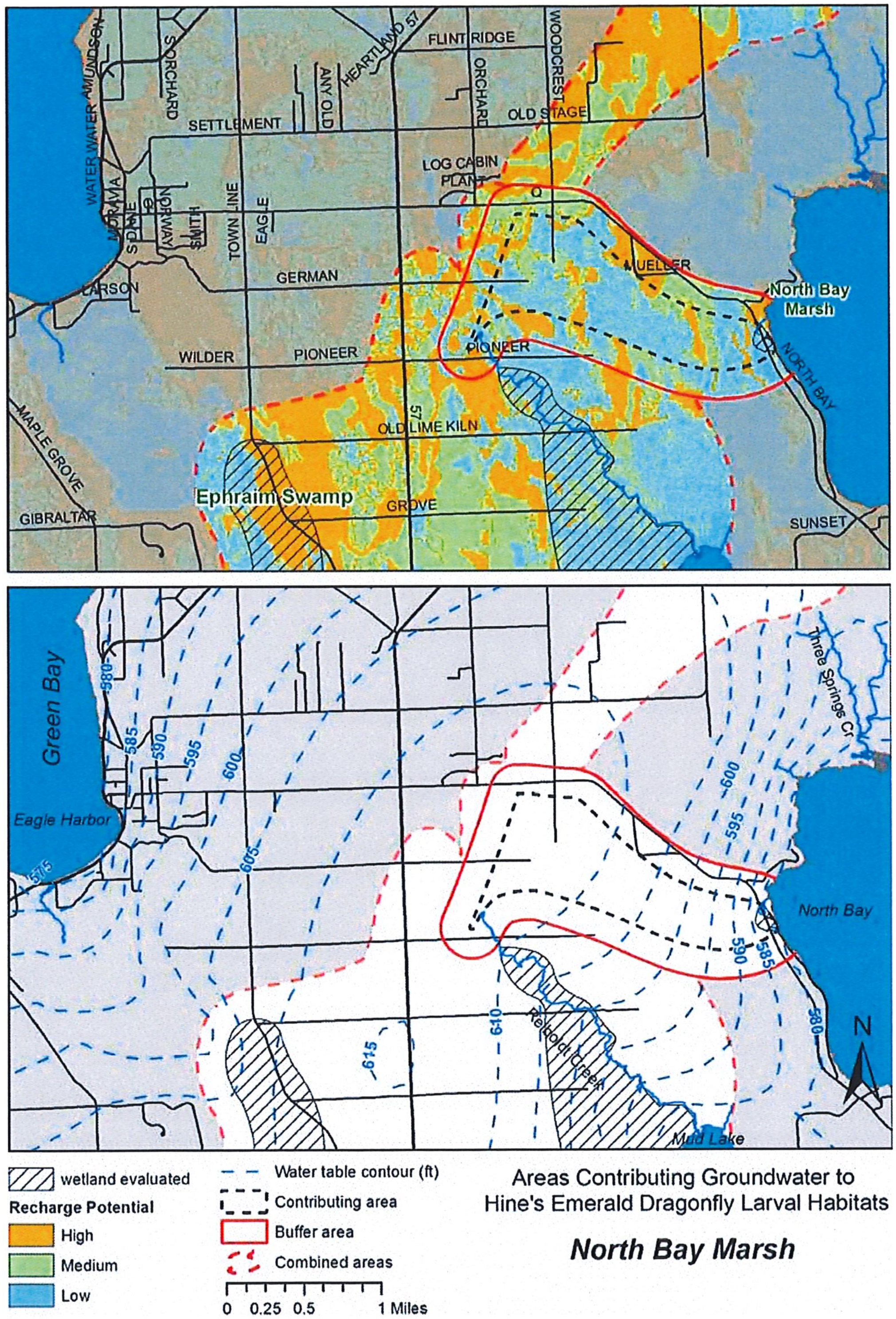

Figure A4. Contributing areas for larval sites near North Bay Marsh

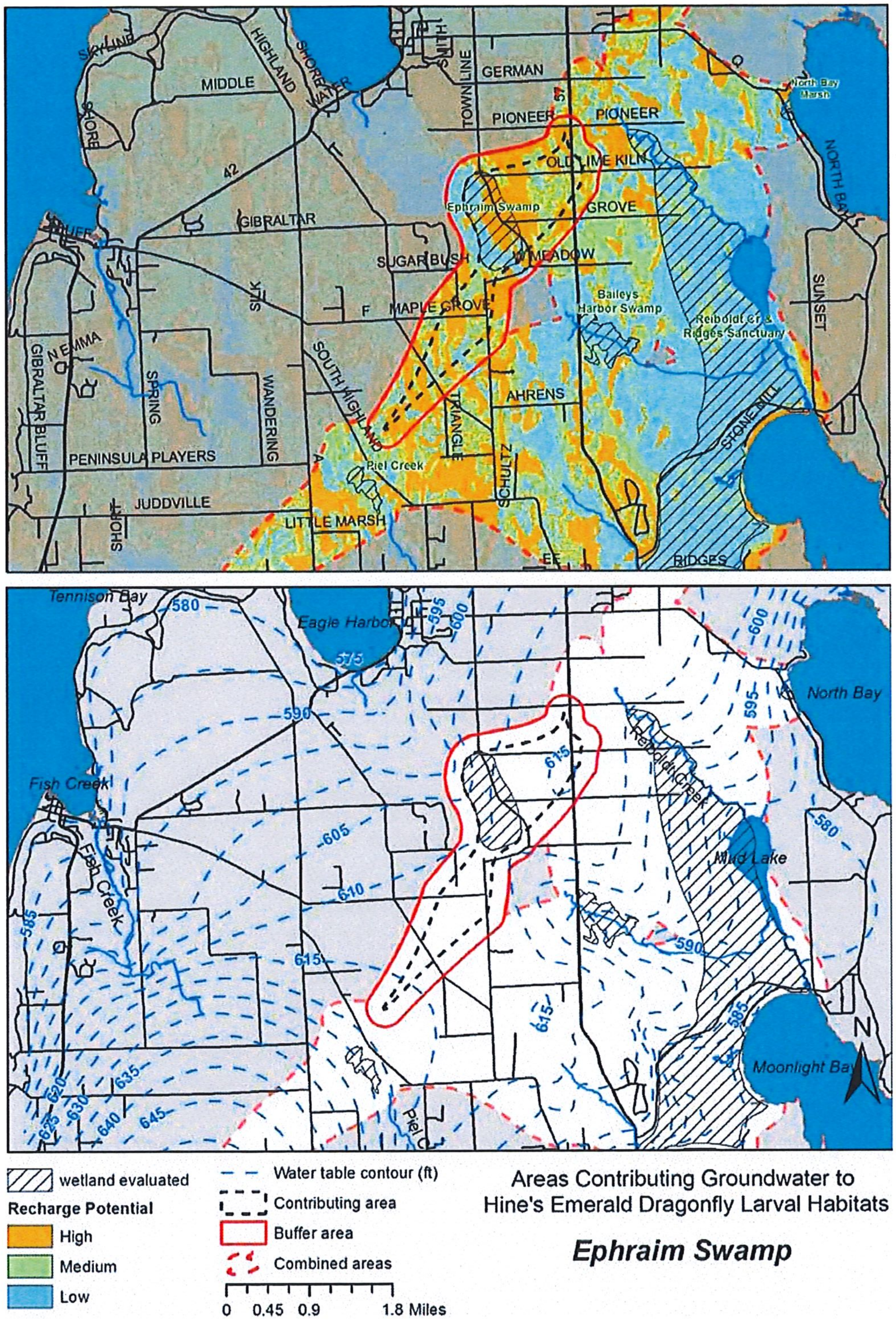

Figure A5. Contributing areas for larval sites near Ephraim Swamp

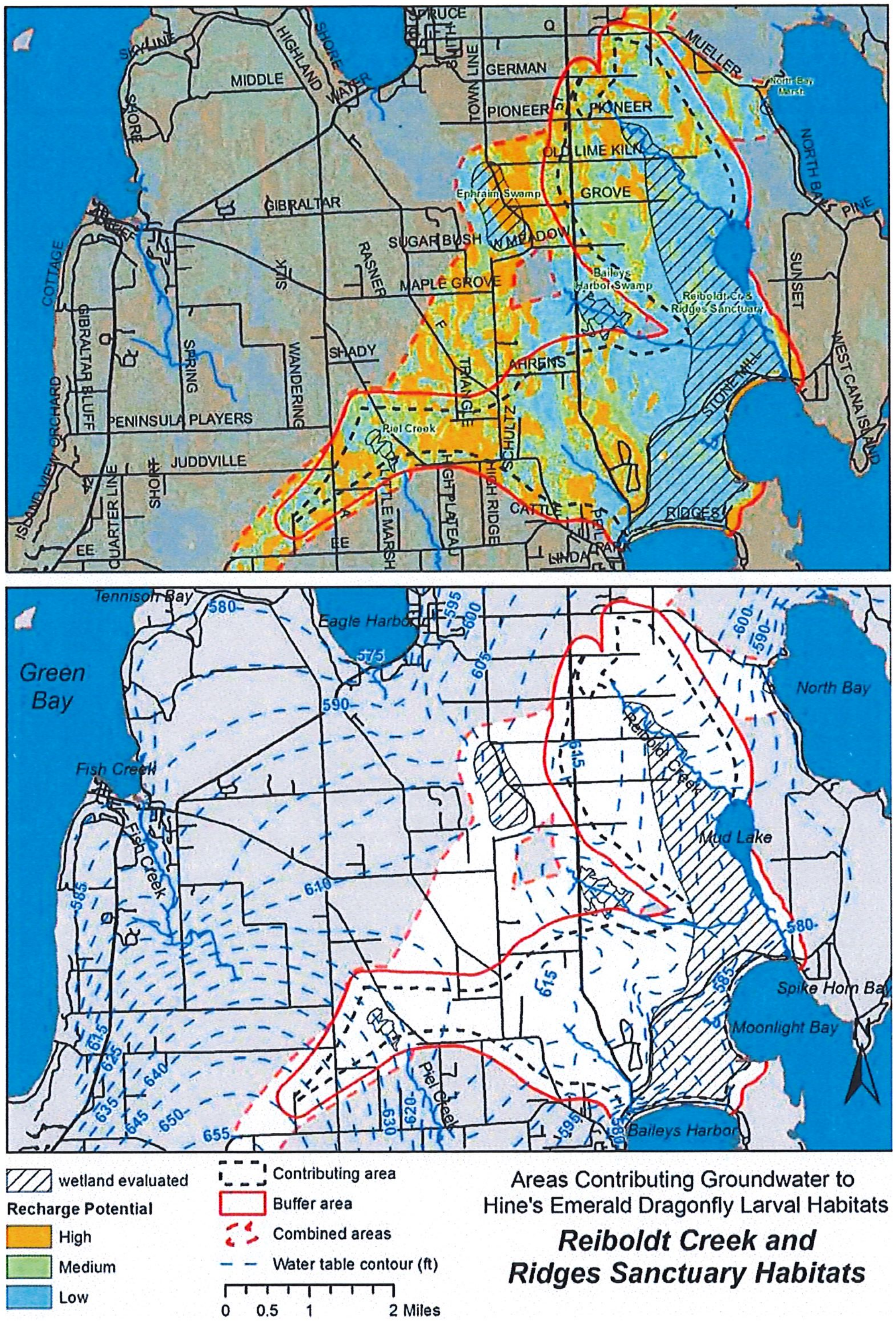

Figure A6. Contributing areas near Reibolt Creek and the Ridges Sanctuary

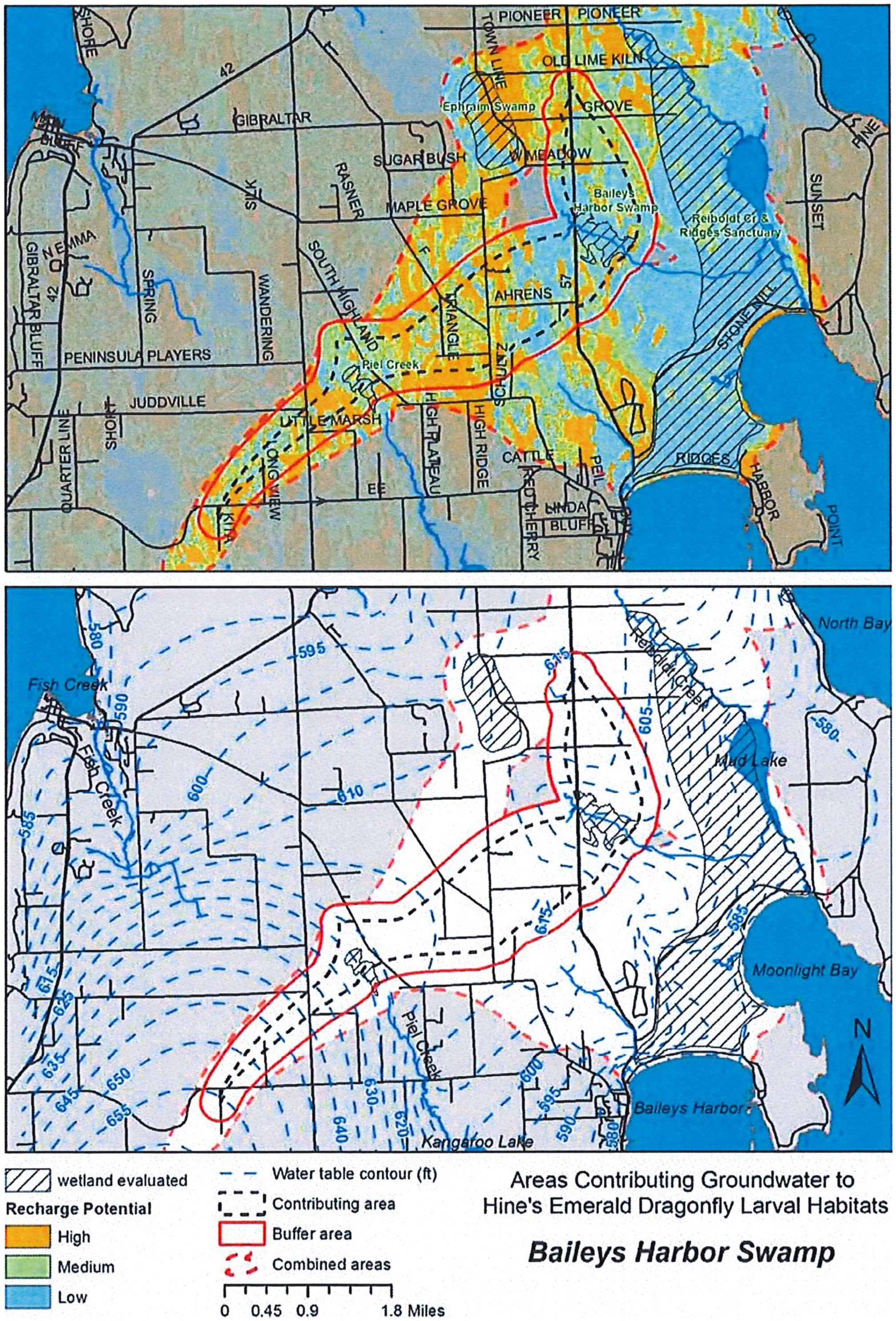

Figure A7. Contributing areas near Baileys Harbor Swamp

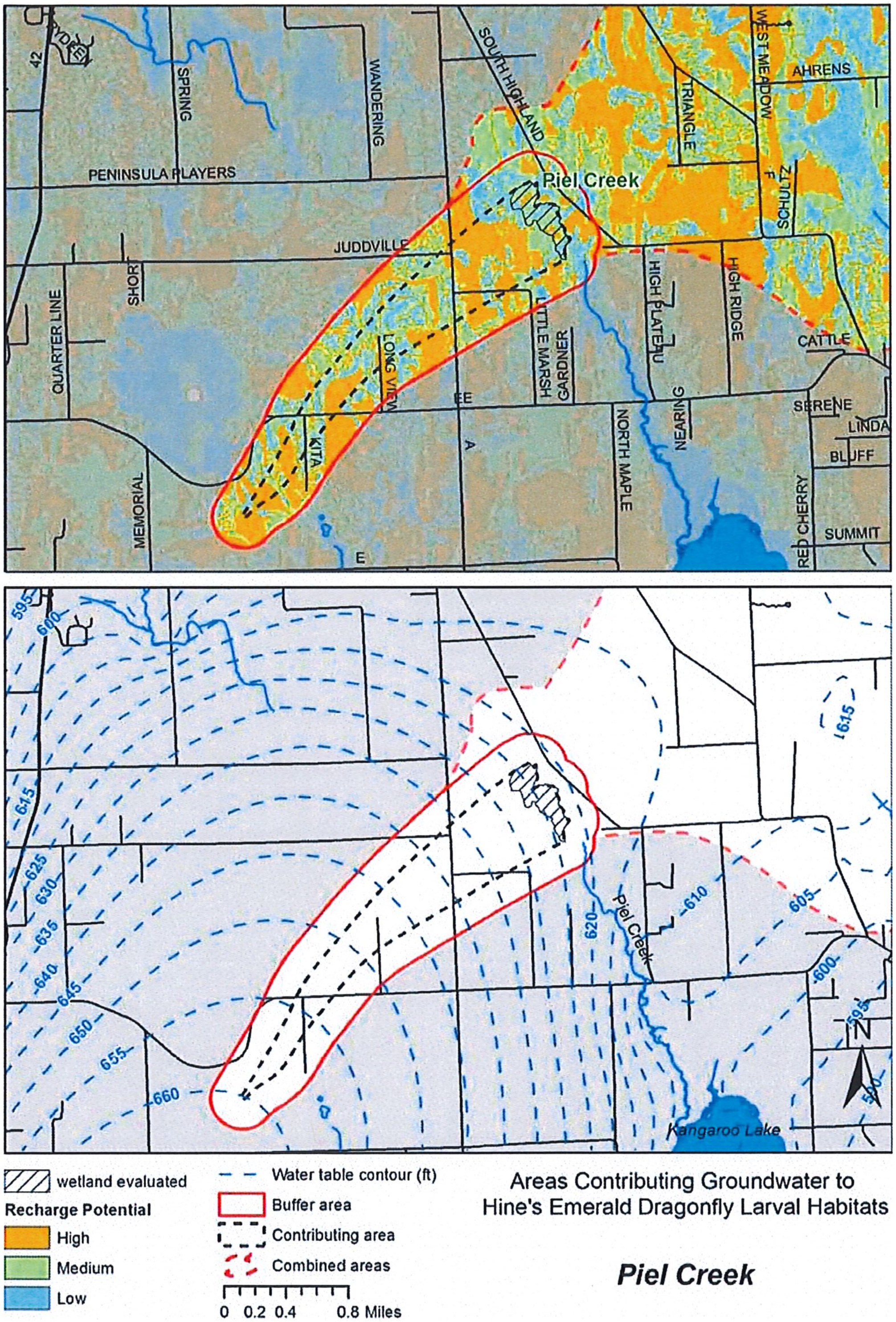

Figure A8. Contributing areas near Piel Creek

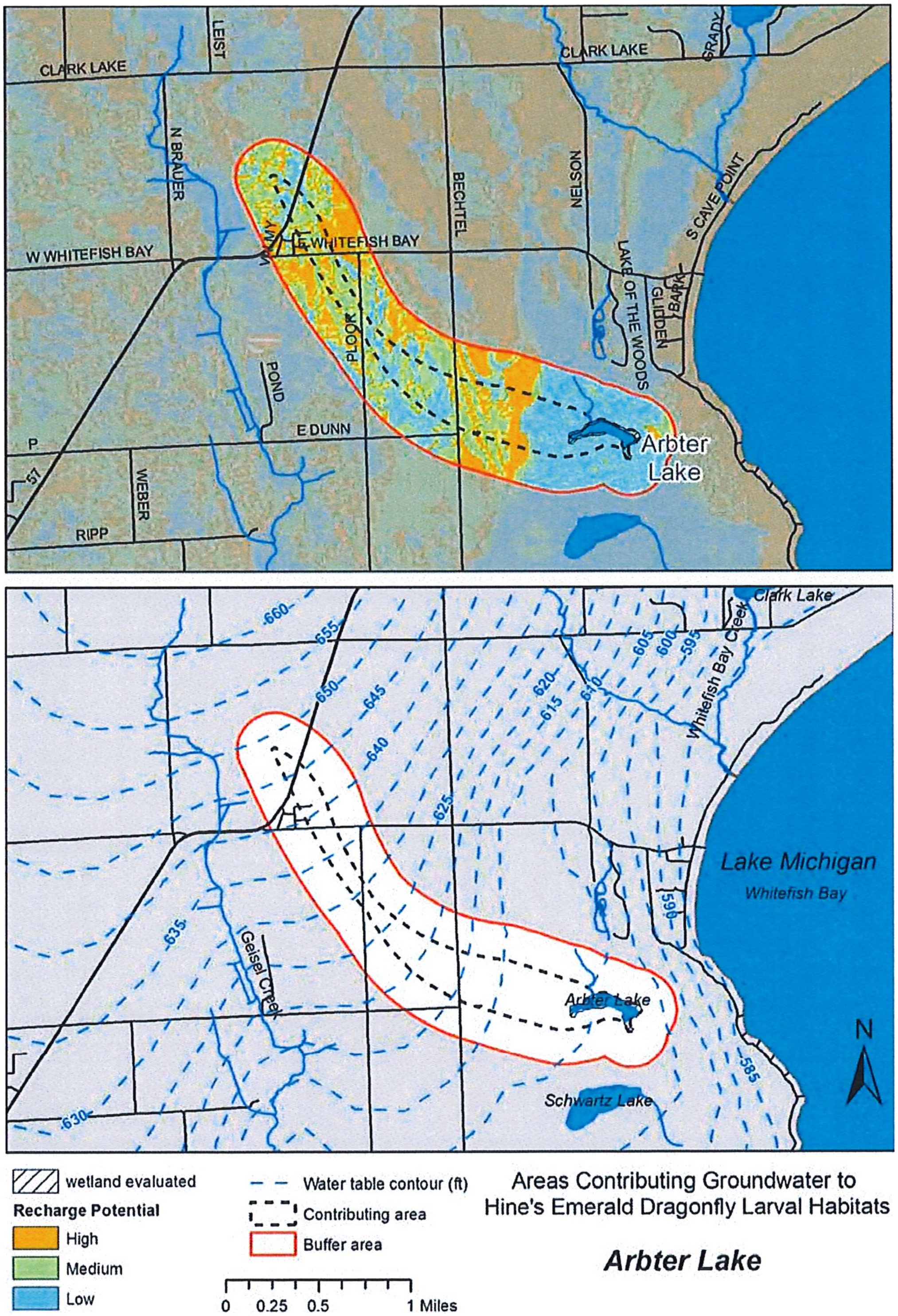

Figure A9. Contributing area for larval sites at Arbter Lake

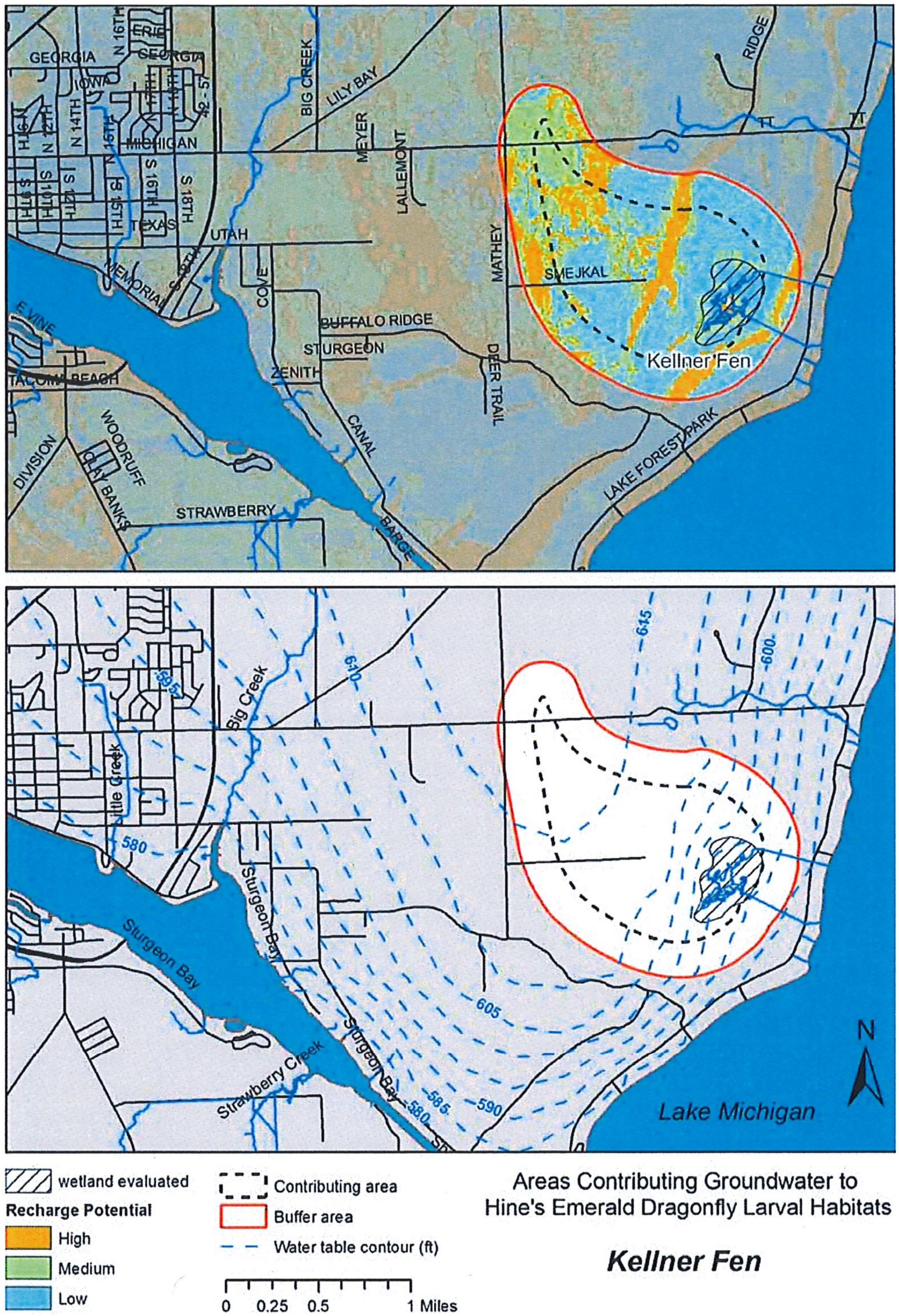

Figure A10. Contributing areas for larval sites near Kellner Fen

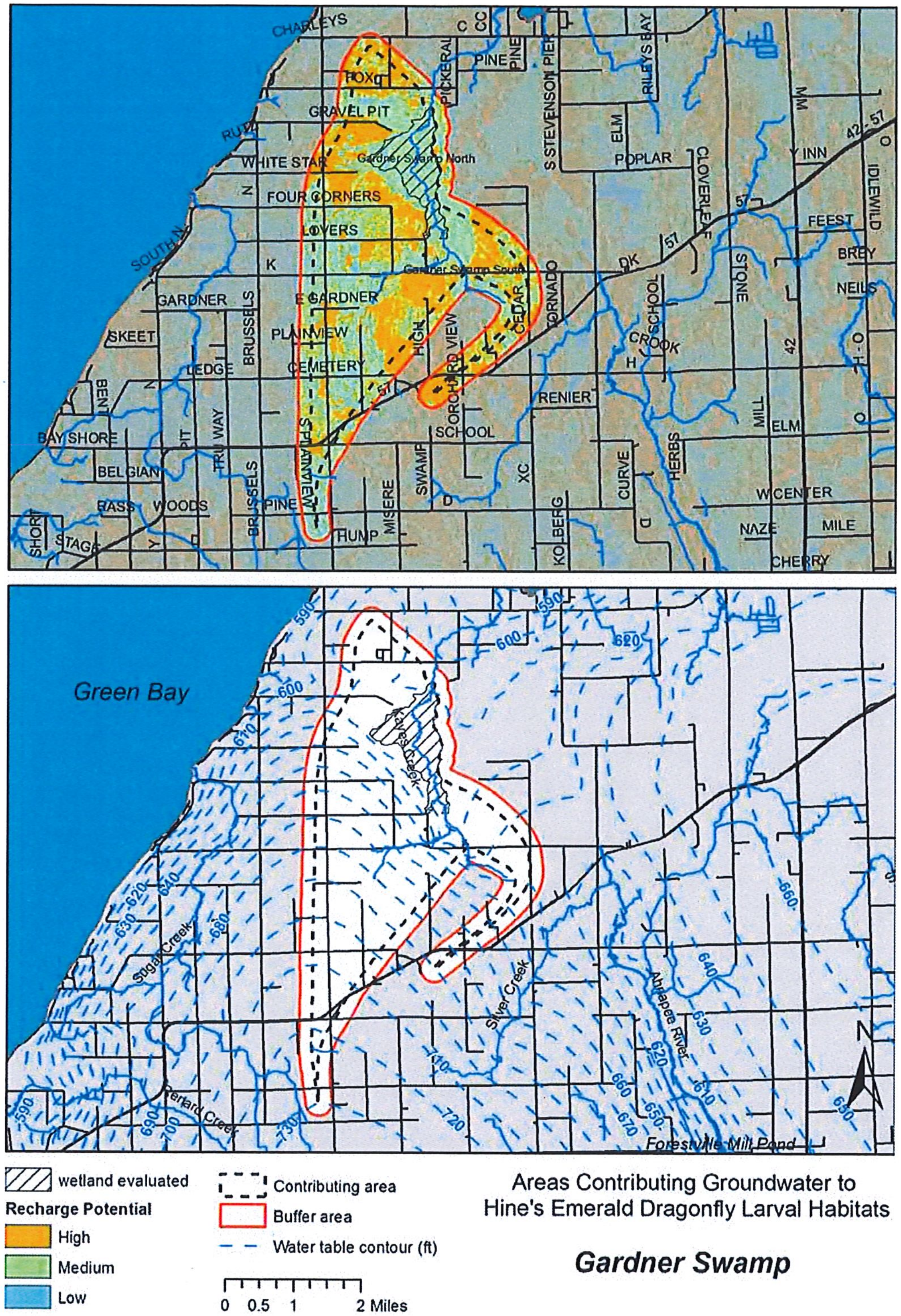

Figure A11. Contributing areas for larval sites near Gardner Swamp

Appendix B: Geophysical Survey

Door County Hine's Emerald Dragon Fly Geophysics Surveys

David Hart – Wisconsin Geological and Natural History Survey
May 24, 2007

Ground Penetrating Radar (GPR)

GPR makes use of electromagnetic pulses that are sent into the ground and waits for responses that arrive in the form of reflected signals. A reflection occurs when the wave crosses a change in dielectric properties such as those found at the water table, bedrock surface, voids or different soil or rock layers. In this study, we sought to identify the bedrock surface. The limitation of this methodology is that the depth of penetration of the electromagnetic wave is controlled by the presence of highly conductive soils (e.g., saturated clays) that absorbs the energy and prevents the generation of reflection signals. Identifying a reflection and correlating it to a surface, such as the bedrock, may also be difficult. There were no good geologic controls available such as borings along the surveys lines and so the results should be verified by drilling if more certainty is required.

For this study, the data were collected using a GSSI SIR-3000 radar system with an 80 MHz antennae towed by hand and behind a pickup (Figure 1). This system gave a depth of penetration of around 30 feet, depending on the sediments and underlying bedrock. We collected data along three transects on Grove, Old Lime Kiln and Pioneer Roads as shown in Figure 2. The data for the three transects were post-processed by applying an automatic gain and distance and elevation corrections (rubberbanding). The reflections interpreted to correspond to the bedrock surface were marked on the three transects with dark lines. That reflection varies in depth from near 0 to over 20 feet in depth. If those reflections accurately represent the bedrock surface, there is significant variation in the depth to bedrock in the study area. A possible correlation between the deep reflection (possibly bedrock surface) and forest cover has been delineated by the lines between the GPR transects and the air photos for reflection "valleys" on Pioneer and Grove Roads.

Figure 1. Photos of the antenna and radar systems.

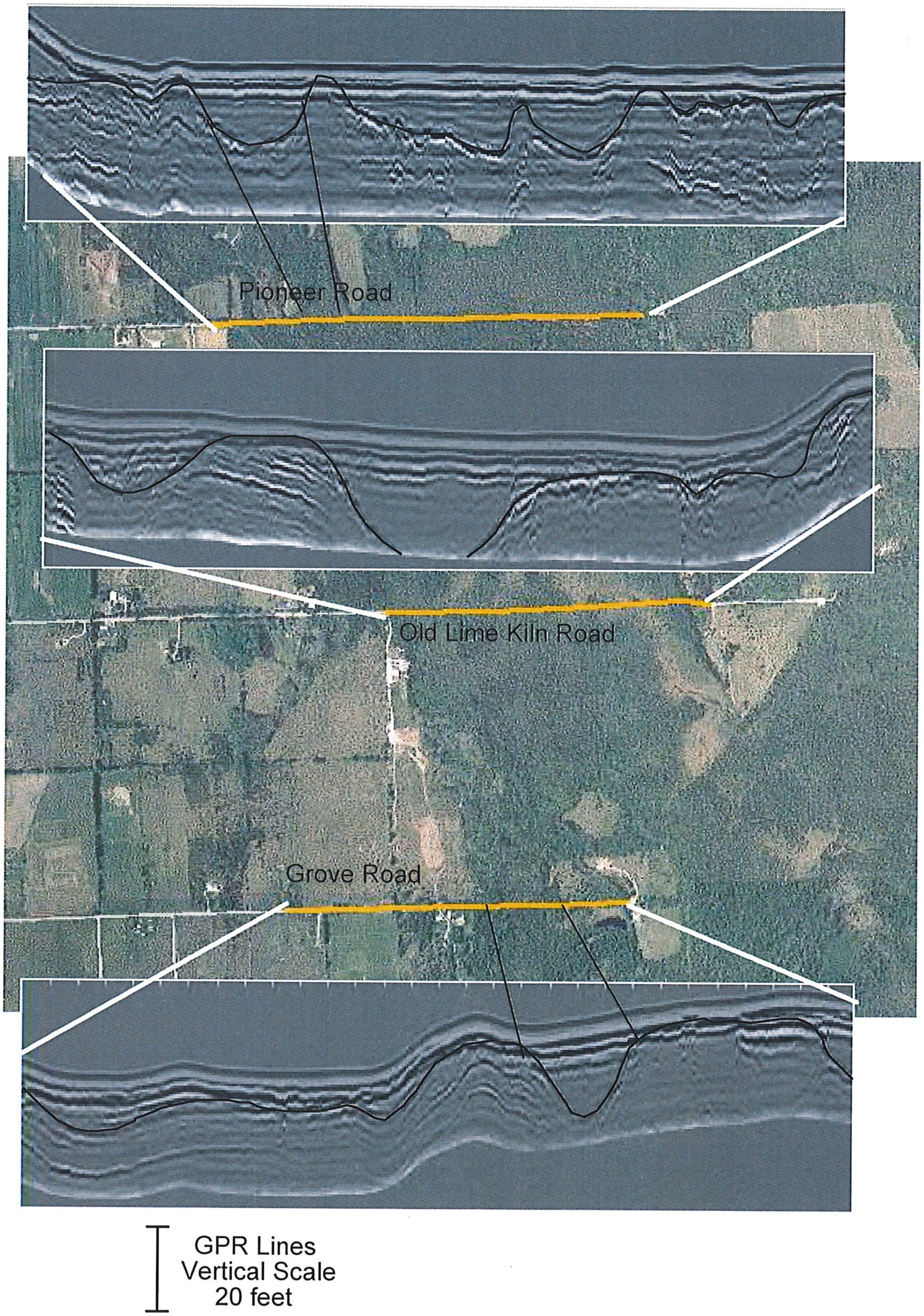

Figure 2. Ground-penetrating radar transects.

Electromagnetic Survey

We also conducted an electromagnetic survey to corroborate the results of the GPR survey. The electromagnetic method induces a current in the ground with a transmitter coil and senses the induced currents with a receiver coil. If the subsurface is a good conductor of electricity, then the induced current is larger and gives a larger signal to the receiver coil. A poor conductor gives a smaller signal to the receiver coil. Saturated soils sands and gravels are good conductors of electricity through the water in their pores. Clays are also very good conductors. Dolomite has few well-connected pores and so is not a good conductor. We made use of this difference of electrical conductivity between the sediment and the dolomite bedrock to provide an independent check on the depth to bedrock predicted by the GPR surveys.

We used an EM-31 conductance meter and recorded the conductance along the Old Lime Kiln Road transect. The EM-31 meter senses and averages the conductivities of all the materials beneath it to a depth of around 20 feet. If there is mostly bedrock beneath the EM-31, then the conductivity will be low, if there is mostly sediment, then the conductivity will be higher. A mix of 10 feet of sediment over bedrock will give an intermediate value. Figure 3 is a plot of the EM-31 measured conductivities along the Old Lime Kiln Road transect. Below that EM-31 plot is the GPR transect for comparison. In general, the agreement is quite good. At around 1000 feet on the transect, the conductivity increases, suggesting a greater depth to bedrock. At the same point, the GPR reflection also decreases to a depth slightly more than 20 feet, also suggesting a greater depth to bedrock. Both the EM-31conductivity and GPR reflection then show a more gradual increase along the transect. The correlation between the EM-31 conductivities and the GPR reflection are not exactly one-to-one because the EM-31 does not linearly average the subsurface conductivities but is most sensitive to the material approximately 1.5 meters below the ground surface.

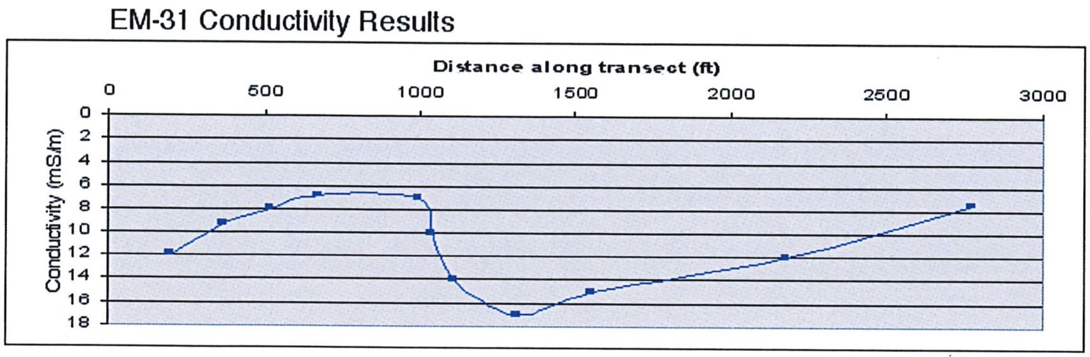

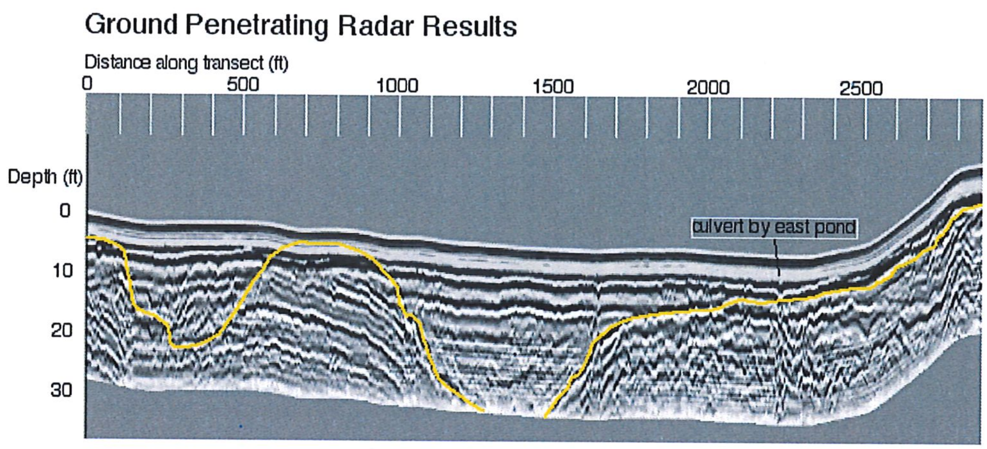

Figure 3. EM-31 conductivity and GPR compared on Old Lime Kiln Road. Both length scales are the same.

Geophysics Conclusions

Ground penetrating radar surveys were conducted on three East-West transects county roads, Pioneer, Old Lime Kiln, and Grove roads. The approximate lengths of the transects were 3000 feet. An electromagnetic survey was conducted along Old Lime Kiln road. The results of that survey support the conclusions of the GPR survey. These surveys all suggest that the depth to bedrock varies along these transects from near 0 to more than 20 feet with sediment filled bedrock valleys. If this conclusion will drive some further investigation or action, we recommend confirmation of the interpreted depths to bedrock by drilling or Geoprobe surveying in selected locations.

USGS
science for a changing world

Potential Environmental Impacts of Quarrying Stone in Karst—A Literature Review

U.S. Geological Survey
Open-File Report OF-01-0484

U.S. Department of the Interior
U.S. Geological Survey

Potential Environmental Impacts of Quarrying Stone in Karst— A Literature Review

By William H. Langer

Open-File Report OF–01–0484

2001

U.S. Department of the Interior
U.S. Geological Survey

U.S. Department of the Interior
Gale A. Norton, Secretary

U.S. Geological Survey
Charles G. Groat, Director

Version 1.0 2002

This publication is only available online at:
http://geology.cr.usgs.gov/pub/ofrs/OFR-01-0484/

Layout and cover design by Carol Quesenberry

Contents

Potential Environmental Impacts of Quarrying Stone in Karst—A Literature Review

By William H. Langer

Introduction

Limestone, dolomite, and marble - the carbonate rocks - are the principal karst-forming rocks. Karst is a type of topography that is formed on limestone, gypsum, and other rocks by dissolution that is characterized by sinkholes, caves, and underground drainage regions. Karst areas constitute about 10 percent of the land surface of the world (fig. 1) (Drew, 1999), and there is widespread concern for the effects that human activities have upon the karst environment. Much of the concern is motivated by the adverse environmental impacts of previous human activities in karst areas and the effects that those impacts have had on the quality of life. Many human activities can negatively impact karst areas, including deforestation, agricultural practices, urbanization, tourism, military activities, water exploitation, mining, and quarrying (Drew, 1999) (fig. 2).

Minerals associated with karst have been exploited for many years. Some carbonate rocks contain valuable supplies of water, oil, and gas, may weather to form bauxite deposits, and are associated with manganese and phosphate rock (guano). Coal is often found within thick carbonate rock sequences. Like other rocks, karst rocks may host ore deposits containing lead, zinc, iron, and gold.

Much of the resource extraction conducted in areas of karst is for the rock itself. Unweathered carbonate rocks provide crushed stone and dimension stone resources. The term "crushed stone" refers to the product resulting from the crushing of rocks such that substantially all faces are created by the crushing operation (ASTM, 2000). The term "dimension stone" is generally applied to masses of stone, either naturally occurring or prepared for use in the form of blocks of specified shapes and sizes, that may or may not have one or more mechanically dressed surface (Bowles, 1939: ASTM, 1998).

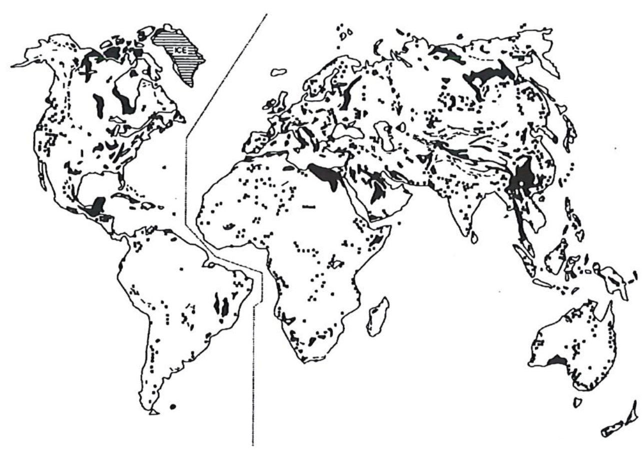

Figure 1. Major worldwide outcrops of carbonate rocks that exhibit at least some karstification *(after Ford and Williams, 1989).*

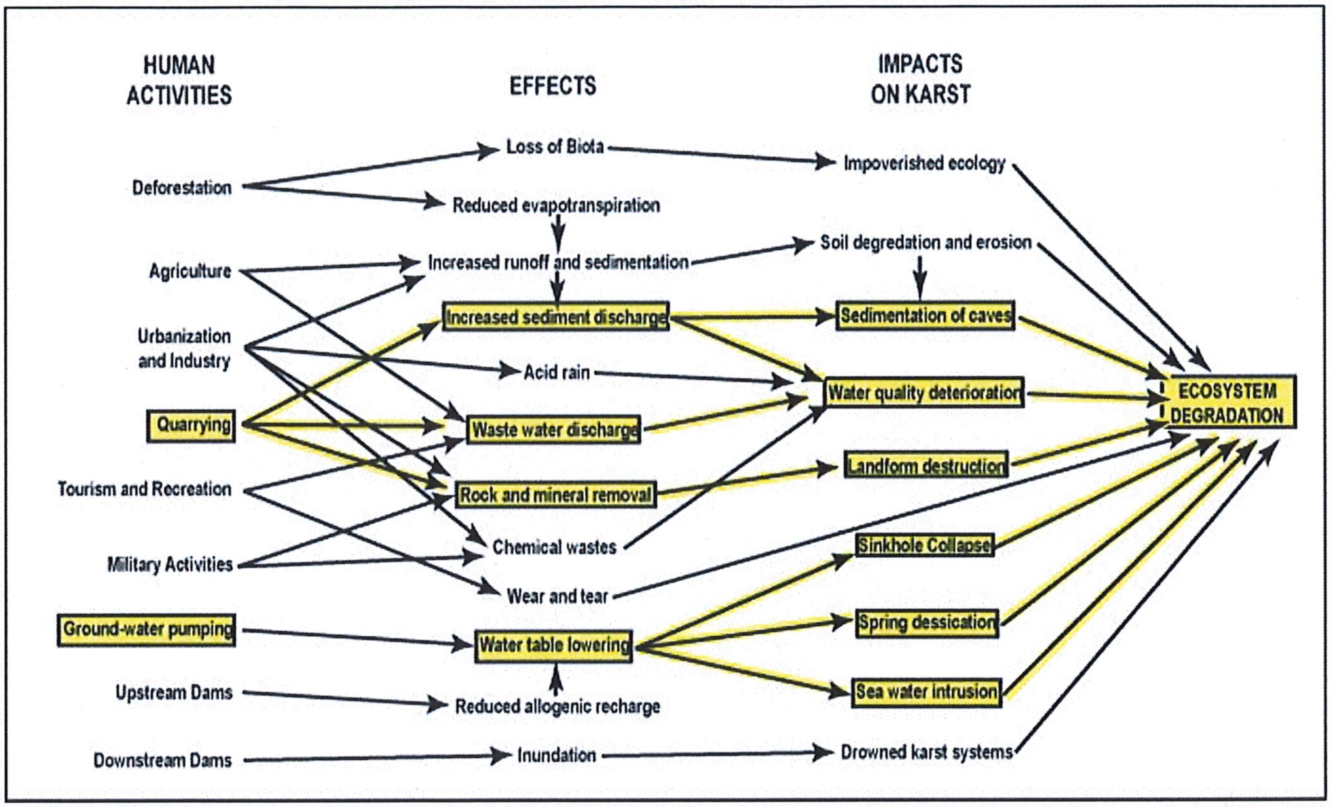

Figure 2. Summary of effects and impacts of various human activities on karst terrains. Effects and impacts from quarrying are highlighted in yellow. *(Modified from Williams, 1993a.)*

Carbonate rocks provide dimension stone, aggregate resources, and raw materials for cement and other industrial and agricultural uses. Over 70 percent of crushed stone produced in the United States is made from carbonate rock. The products derived from carbonate rocks provide essential materials for society –materials that we need to maintain our current standard of living. Quarrying[1] carbonate rocks for use as crushed stone and dimension stone can be accomplished with no significant impacts to the environment, if done carefully and within the limits set by nature. However, if proper precautions are not taken many human activities in karst, including extraction of carbonate rocks, can result in damage to the environment and associated increases in costs for environmental compliance or liability.

Purpose

This report describes the state-of-the-knowledge regarding the environmental impacts from quarrying carbonate rocks in karst. Documentation of the relationships between carbonate rock quarries and environmental problems in karst has existed for nearly fifty years, but is scarce. There are numerous articles in the literature that describe environmental impacts on karst from human activities other than quarrying, but there are relatively few articles that specifically refer to impacts from quarrying.

[1]In this report, the term "quarrying" applies to both surface quarries and underground mines from which cabonate rocks are extracted.

The reported environmental impacts have occurred in a wide variety of karst terrains, under a wide variety of climatic conditions, where the natural systems have been stressed by a wide variety of human activities. It should not be assumed that impacts in one karst terrain under a particular set of natural and man-made conditions will also happen in a different karst terrain with a different set of natural and man-made conditions.

Previous work

In recent years numerous publications have addressed issues related to karst in general, as well as issues specifically related to human impacts on karst. Publications addressing human impacts on karst include a special supplement of the journal Catena entitled Karst Terraines: Environmental Changes and Human Impact (Williams, 1993); a special issue of Environmental Geology with the theme of addressing Environmental Change in Karst Areas (Ford, 1993); a special issue of Engineering Geology with the theme Sinkholes and the Engineering and Environmental Impacts of Karst (Beck, 1999), and the publication Karst Hydrogeology and Human Activities (Drew and Hötzl, 1999). The Florida Sinkholes Research Institute has held symposiums concerned with sinkholes in karst at approximately two-year intervals (Beck, 1984, 1989, 1993; Beck and Pearson, 1995; Beck and Stephenson, 1997; Beck and Wilson, 1987; Beck and others, 1999). The American Geological Institute Environmental Awareness Series 4, Living With Karst, is a non-technical discussion of environmental issues in karst (Veni and DuChene, 2001). Few of the reports in the publications listed above are primarily concerned with quarrying in karst; however, those publications do illustrate the complexities of cause and effects of human activities in karst.

Although a relationship between environmental damage and quarrying of carbonate rock has been well documented for over fifty years (Foose, 1953), there are only a few reports that include major discussions of the environmental impacts of quarrying in karst. These reports include *Development of Sinkholes Resulting from Man's Activities in the Eastern United States* (Newton, 1987), *Ground Subsidence*, which includes a chapter *Sinkholes on Limestones* (Waltham, 1989), and *Karst Hydrogeology and Human Activities* (Drew and Hötzl, 1999), which includes a chapter on *Extractive Industries Impact* (Hess and Slattery, 1999). There are a few individual reports scattered through the literature that address the environmental impacts of quarrying carbonate rocks in karst. In addition, there are reports that describe environmental impacts on karst from mining resources other than carbonate rock. Theories about how extraction of carbonate rock can impact the environment can be extrapolated from some of these reports.

Natural Formation of Karst

There is a tremendous variety of carbonate rocks and these rocks exist in a broad range of climatic situations. Weathering of carbonate rocks produces diverse types of karst landscapes (fig. 3), far too many types to be described here. Instead, this report gives a simplified description of the karst forming processes. Readers interested in learning the details of karst formation are encouraged to consult the numerous textbooks and research reports that describe the geohydrologic and geomorphic processes involved with karst development. For example, Karst Geomorphology (Sweeting, 1981) contains benchmark papers about karst, including excerpts from Das Karstphänomen (Cvijíc, 1893). Process geomorphology (Ritter and others, 1995), a recent textbook, discusses karst from a process / response perspective. Karst Geomorphology (Jennings, 1985) is a technical description of karst written for the non-scientific audience. Karst Lands (White and others, 1995) is a concise article in American Scientist that describes karst formation and hydrology. Sinkholes in Pennsylvania (Kochanov, 1999) is a non-technical description of karst prepared for non-scientific audiences. The International Geographical Union Commission on Sustainable Development and Management of Karst Terrains published eight annotated bibliographies of karst research studies (for example, Urushibara-Yoshino, 2000).

Natural karst processes occur gradually over hundreds to thousands of years. The formation of karst includes interactions between carbonate rocks and slightly acidic water. (Actually karst can form on other soluble rocks such as gypsum; however, this report is restricted to carbonate rocks.) Carbonic acid is a mild acid formed when rainwater and carbon dioxide react. As the rainwater passes through the soil, the water absorbs more carbon dioxide and becomes more acidic. Carbonate rock contains openings between beds of rock and as fractures or joints created when the rocks were uplifted, uncovered, faulted, or folded (fig. 4). The slightly acidic water percolates into the rocks through these openings. The openings are enlarged by solvent action of acidic water. The dissolution process is self-accelerating: openings that are enlarged first will transmit more water, thus increasing the rate that acid is brought into contact with the rock, resulting in additional enlargement of the openings.

As underground flow paths controlled by joints, fractures, and bedding planes continue to enlarge over time, water movement changes from small volumes through many small, scattered openings in the rock to concentrated flow through a few well-developed conduits. As flow paths continue to enlarge, caves, conduits, and sinkholes may be formed (fig. 5). Surface streams may lose water to the subsurface or flow into cave entrances, only to reappear many miles away.

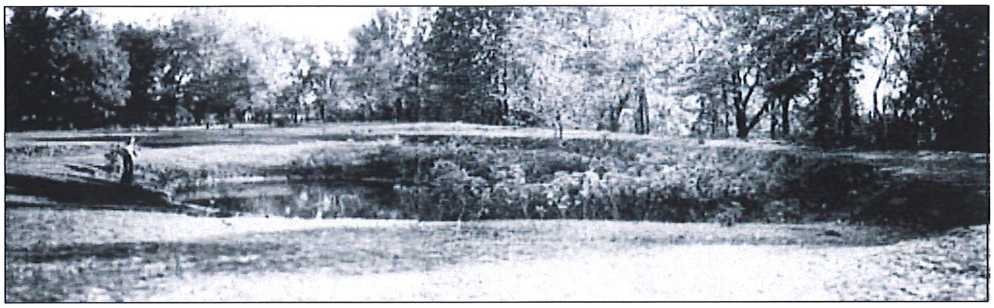

Figure 3. Shallow sinkhole typical of karst terrain in Cherokee County, Kansas. *(USGS photographic library - Pierce # 339, 340.)*

Unusual bedrock surfaces may be created as the carbonate rock is dissolved (fig. 6a and 6b). In temperate climates, some of the surfaces resemble abstract sculptures or contain pointed columns called pinnacles. A residual soil forms over the bedrock because there are minerals within limestone that are not affected by carbonic acid. As the process of dissolution continues, these insoluble minerals collect on top of the bedrock surface as clayey residual material. Some residual material is carried by water into openings in bedrock where they clog the openings. Other material, such as stream alluvium, may overly the clay. Depending on the climate, topography, and type of parent bedrock, soil on the bedrock surface can be non-existent or greater than 50 m thick.

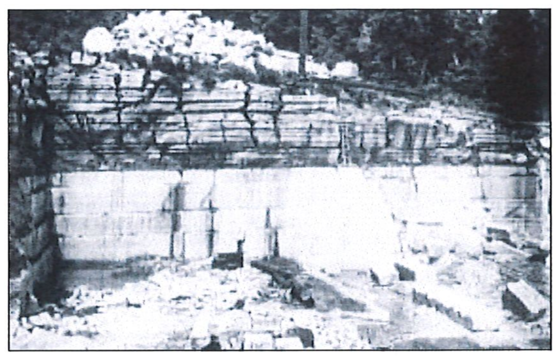

Figure 4. Dimension stone quarry showing weathered outcrop (top) and smooth working face of quarry. Vertical solution channels following fractures and joints in the weathered outcrop extend down into the smooth working face. Horizontal solution features occur between beds of the rock. Notice ladder for scale. *(USGS photographic library - Loughlin 154.)*

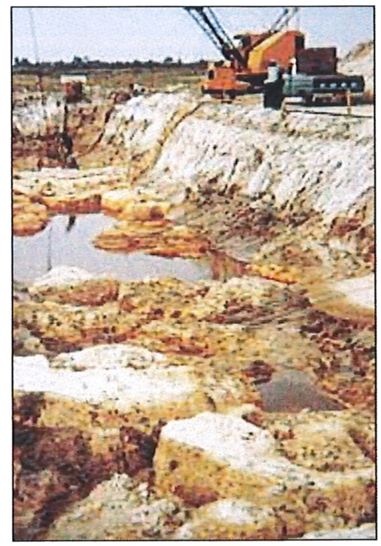

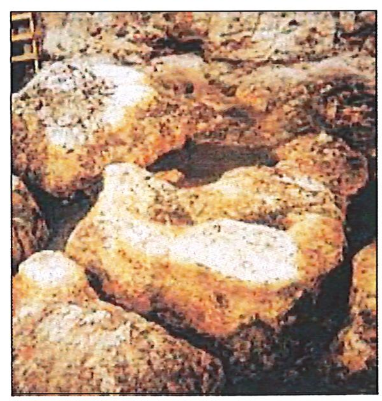

Figure 5 (above). Cave opening in karst terrain, Škocjan Cave, Slovenia.

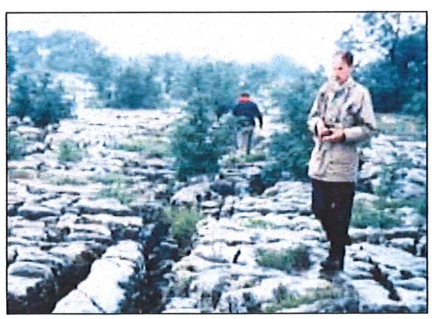

Figure 6-a (right). Limestone surface in karst area with no soil cover.

Figure 6-b (far right, top and bottom). Removal of overburden has exposed the furrowed and pitted surface of carbonate rock. *(Photograph courtesy of Keith Bennett, Williams Earth Sciences, Inc.)*

Quarrying Carbonate Rocks

The general objective of dimension-stone quarrying is to produce large rectangular blocks suitable for cutting into smaller, regularly-shaped products. The quarrying operation cuts a block of stone free from the bedrock mass by first separating the block on all four vertical sides and then undercutting or breaking the block away from the bedrock (fig. 7). Two of the oldest methods for quarrying are channel cutting and drilling and broaching. A channeling machine cuts a channel in the rock using multiple chisel-edged cutting bars that cut with a chopping action. In drilling and broaching, a drilling tool first drills numerous holes in an aligned pattern. The broaching tool then chisels and chops the web between the drill holes, freeing the block. Both channel cutting and drilling and broaching are slow and the cutting tool requires frequent sharpening. Both methods have generally been replaced with other more efficient methods.

Line drilling and sawing are more modern techniques for quarrying. Line drilling (also called slot drilling) consists of drilling a series of overlapping holes using a drill that is mounted on a quarry bar or frame that aligns the holes and holds the drill in position. Sawing can be accomplished with a variety of saws including wire saws, belt saws, and chain saws. The introduction of synthetic-diamond tools during the 1960's revolutionized stone working. A variety of explosive techniques may also be used to quarry dimension stone, but explosives generally are used in very small amounts, if at all, to avoid fracturing the stone block.

The general objective of crushed stone quarrying is to produce relatively small pieces of rock that are suitable for crushing into gravel-sized particles (fig. 8). To produce crushed stone, the rock is first drilled and blasted. Blasting commonly breaks the rock into pieces suitable for crushing. When the blasted material is dry, it can be extracted by using conventional earth-moving equipment, such as bulldozers, front loaders, track hoes, and scraper graders. Rock quarries that do not penetrate the water table, or where discharge from the water table naturally drains from the quarry, is offset by evaporation, or is otherwise insignificant, commonly are mined dry.

Figure 7. Working face of dimension stone limestone quarry in Lawrence County, Indiana, showing smooth surfaces from which large blocks have been removed. *(USGS photographic library – Burchard #556.)*

Where rock quarries penetrate the water table, the quarries commonly are dewatered by collection and pumping of the ground water. The rock is then mined by the procedures used in a dry quarry. Some operators may prefer not to dewater the quarry, or the inflow may be too great to be pumped. In those operations, the quarries are allowed to fill with water. The rock is drilled and blasted, and the rubble is extracted from under the water using draglines, clamshells, or other equipment. The aggregate may be processed wet or may be placed in windrows and allowed to dry before processing.

Carbonate rock is extracted from about 100 underground mines in the United States. Most of these mines are located in the Mid-Continent and produce crushed stone.

Figure 8. Working face of crushed stone operation showing rubble created by blasting. *(Photograph courtesy Luck Stone.)*

Production and Use of Carbonate Rocks

Worldwide production of carbonate rocks ranks third in terms of volume and fourth in terms of value for all non-fuel mineral commodities (fig. 9) (Lüttig, 1994). Over 70 percent of the crushed stone produced in the United States comes from carbonate rock, and about three fourths of that is consumed by the construction industry. Crushed carbonate rock also has numerous agriculture and industrial uses. Agricultural uses include fertilizers and insecticides. Industrial uses include the manufacture of cement, pharmaceuticals, processed food, glass, plastics, floor coverings, paper, rubber, leather, synthetic fabrics, glue, ink, crayons, shoe polish, cosmetics, chewing gum, toothpaste, and antacids. During 1999, over one billion tons of crushed limestone, dolomite, and marble valued at over $5.5 billion were produced from about 2,200 quarries operating in 48 states. The top 10 states (in decreasing order of production) each produced over 45 millions tons of crushed carbonate rocks – Texas, Florida, Illinois, Ohio, Missouri, Pennsylvania, Tennessee, Kentucky, Indiana, and Alabama (Tepordei, 1999). All of these states contain areas of karst.

Dimension stone has a large number of uses ranging from rustic walls and roughly-shaped paving stones to highly polished floor tile, counter tops, and building facades. The final use of the stone, as well as the methods to quarry and mill the stone, depend on the properties of the source rock. Today, stone is considered by many to be the premier building material and is experiencing resurgence in use for commercial and residential construction. During 1999, dimension limestone or dolomite were extracted from 33 quarries in 10 States. Production was 446,000 metric tons valued at $74.9 million. The top five producing states, in descending order by tonnage, were Indiana, Wisconsin, Texas, Minnesota, and Kansas. Other states producing dimension limestone or dolomite include Alabama, Arkansas, California, Ohio, and Vermont. Marble was extracted from 11 quarries in 5 states. Production was 40,300 metric tons valued at $9.5 million. Vermont was the leading producing State, followed by Tennessee, Georgia, Colorado, and Arkansas (Dolley, 1999).

Potential Environmental Impacts

Modern technology and scientific investigation methods have made it possible to reduce environmental impacts associated with extraction of carbonate rocks and manage impacts at acceptable levels that do not cause significant harm to the environment. Nevertheless, carbonate rock resources cannot be obtained from the landscape without causing some environmental impacts.

Engineering Impacts

Some of the environmental disturbance created by quarrying is caused directly by engineering activities during aggregate extraction and processing. The most obvious engineering impact of quarrying is a change in geomorphology and conversion of land use, with the associated change in visual scene. This major impact may be accompanied by loss of habitat, noise, dust, vibrations, chemical spills, erosion, sedimentation, and dereliction of the mined site. Some of the impacts are short-lived and most are easy to predict and easy to observe. Most engineering impacts can be controlled, mitigated, kept at tolerable levels, and restricted to the immediate vicinity of the aggregate operation by employing responsible operational practices that use available engineering techniques and technology (fig. 10). Some reports that generally describe engineering impacts include Barksdale (1991), Kelk (1992), Smith and Collis (2001), Lüttig (1994), Bobrowsky (1998), Primel and Tourenq, (2000) and Langer (2001).

Cascading Impacts

In karst environments, aggregate mining may alter sensitive parts of the natural system at or near the site thus creating cascading environmental impacts (Langer and Kolm, 2001). Cascading impacts are initiated by an engineering activity, such as the removal of rock, which alters the natural system. The natural system responds, which causes another impact, which causes yet another response by the system, and on and on. For example, aggregate mining in some karst might lower the water table, which will remove the buoyant support of rock that overlies water-filled caverns or other solution features, which might result in land collapse, which will create a sinkhole. Cascading impacts may be severe and affect areas well beyond the limits of the aggregate operation. Cascading impacts may manifest themselves some time after mining activities have begun and continue well after mining has ceased. Many of the impacts described below are cascading impacts.

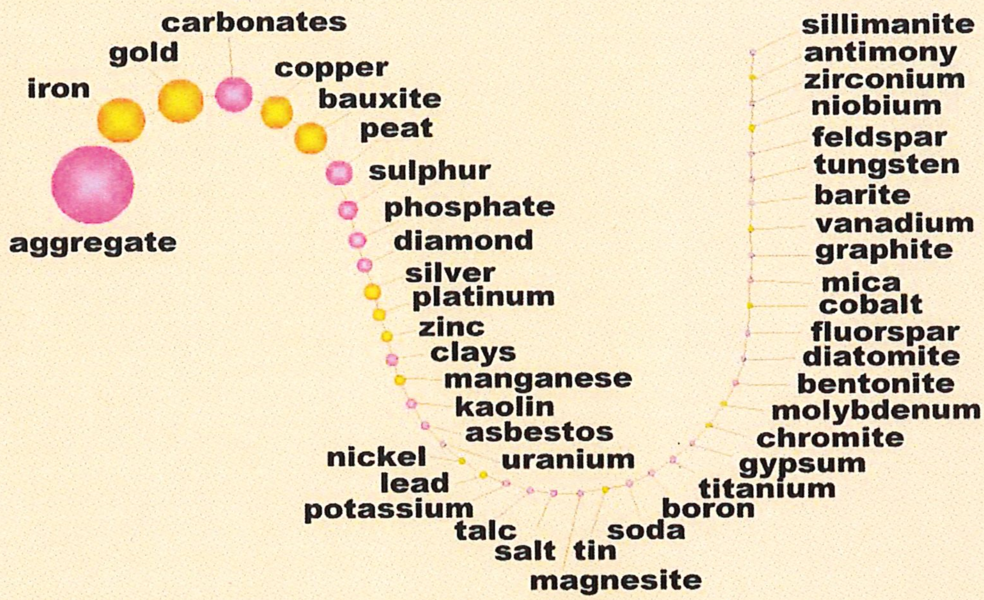

Figure 9. "Resource snake" graph showing relative values of non-fuel mineral resource production *(from Lüttig, 1994).*

Geomorphic Impacts

Quarrying has an associated, often dramatic, visual impact. Karst terrain is commonly considered to be of high scenic value, thus compounding the effects of visual impacts of quarrying. The principal geomorphic impact of quarrying is the removal of stone, which results in the destruction of habitat including relict and active caves and natural sinkholes (Gunn and Gagen, 1987).

The extent of the geomorphic impact is a function of the size of the quarry, the number of quarries, and the location of the quarry, especially with respect to the overall landscape and the local landforms (fig. 11). The influence of quarry size on environmental impact is obvious: all other things being equal, the larger the quarry, the larger the geomorphic impact. The size of quarries has increased over time, and so has their impact.

Great numbers of quarries in a karst region amplifies the geomorphic impact (Sauro, 1993). Stanton (1966) suggested that the disturbance created by numerous smaller quarries is greater than that created by one large quarry and recommended that geomorphic disturbance be minimized by maximizing reserves through deep quarrying. (See section on ground water regarding the impacts of deep quarrying.) Stanton (1990) later suggested that limestone has more value *in situ* as a source of water and for its scenic value than as a source of crushed stone and recommended avoiding extraction of limestone altogether when alternatives are available.

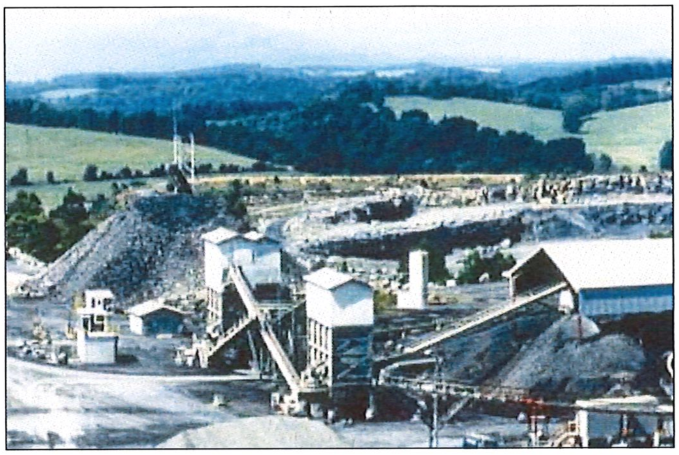

Figure 10. Engineering techniques, such as enclosing equipment and removing dust using vacuums, can mitigate impacts of noise and dust. *(Photograph courtesy of Luck Stone.)*

Figure 11. Quarries can occupy a significant part of the visual landscape.

In broad terms there are three situations where quarries can be located: 1) on flat ground, 2) along or into the side of a valley, and 3) on the side of a hill (Gunn, 1993; Gunn and Bailey, 1993). In most situations, quarries excavated into flat ground have a relatively small impact on geomorphology, which is limited to the removal of sinkholes and cave passageways. Quarries on valley sides can extend laterally along the valley side causing large geomorphic impacts, or they can work back into the valley wall, where the impact is less (Gunn, 1993; Gunn and Bailey, 1993). Quarries on hills generally have a large geomorphic impact. Gunn (1993) reports that crushed stone quarrying has removed an entire karst hill and large portions of other nearby karst hills in the Mendip Hills, UK.

Blasting

One of the most frequent complaints the public makes to the crushed stone industry situated near population centers is about blasting noise (National Academy of Sciences, 1980). Blasting may occur daily or as infrequently as once or twice a year. The blasting techniques used in crushed stone operations are significantly different than those used in dimension stone quarrying. Whereas large amounts of explosives are used in crushed stone operations to produce appropriate-sized rubble (fig. 12), the dimension stone industry uses only small amounts of explosives to loosen large blocks of stone.

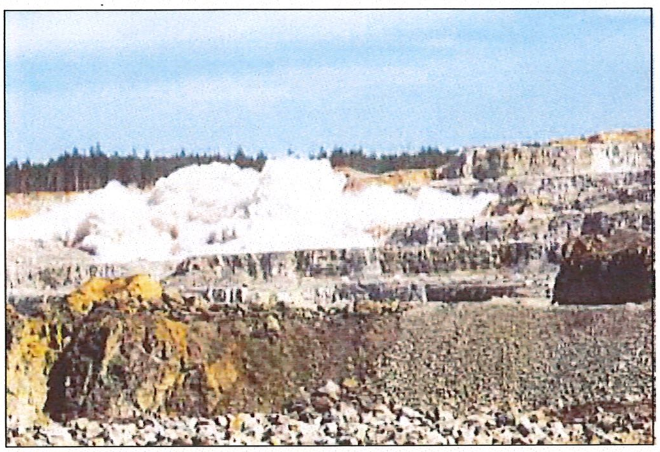

Figure 12. Rock is drilled and blasted for use as crushed stone. In some isolated areas where people are not located nearby, larger amounts of explosives may be used.

Geology, topography, and weather affect the impacts of blasting. Blasting noise generally increases with the amount of explosive, with specific atmospheric conditions, and with proximity to a blast. The area in front of a blast commonly receives more noise than an area behind a blast. People differ greatly in their response to blasting (National Academy of Sciences, 1980).

The technology of rock blasting is highly developed, and when blasting is properly conducted, most environmental impacts should be negligible. By following widely recognized and well-documented limits on ground motion and air concussion, direct impacts from ground shaking and air concussion can be effectively mitigated. Those limits and methods to measure them are discussed in Moore and Richards (1999), Bell (1992), Berger and others (1991), and National Academy of Sciences (1980).

When an explosive is detonated enormous amounts of energy are released. Most of the energy of a properly designed blast works to displace rock from the quarry face. The remaining energy is released as vibrations through and along the surface of the earth and through the air. Most of the energy that goes through the earth comes to the surface within a few meters of the detonation and travels as surface waves, which may cause ground shaking. A small amount of the energy is transmitted through the rocks as shear waves, which commonly are insignificant.

When a blast is detonated, some energy will escape into the atmosphere causing a disturbance in the air. Part of this disturbance is subaudible (air concussion) and part can be heard (noise). Air concussion is most noticeable within a structure, particularly when windows and doors are closed. The air concussion creates a pressure differential between the outside and inside the structure causing it to vibrate.

Poorly designed or poorly controlled blasts may cause rocks to be projected long distances from the blast site (flyrock), which can be a serious hazard. Flyrock is not commonly a problem with carefully designed and executed blasting plans, but is a situation that deserves careful attention. The pinnacled bedrock in karst can complicate blasting, increasing the risks for flyrock.

Blast-induced vibrations and shock waves can cause stalagmites and stalactites to break off and cause cave roofs to crack or collapse. Blasting may cause fracturing of quarry walls, increasing permeability and increasing drainage towards quarry face (Gagen and Gunn, 1987, Gunn and Bailey, 1993). The blast zone beneath the quarry floor in sub-water table quarries may be considered as a separate aquifer with high fracture density, low primary porosity, and negligible conduit development (Smart and others, 1991).

Blasting-induced fracturing or aperture widening may play a role in initiating flooding events.

Lolcama and others (1999) describe a situation where blasting opened a conduit under the floor of a quarry. The conduit was connected to a nearby river and to a local water storage basin. Extensive grouting was required to stop the inflow of water from those sources.

Blasting can negatively impact karst biota and may cause problems with ground-water availability and quality (discussed below).

Noise

The primary source of noise from extraction of aggregate and dimension stone is from earth-moving equipment, processing equipment, and blasting (see above). The truck traffic that often accompanies aggregate mining can be a significant noise source. The impacts of noise are highly dependent on the sound source, the topography, land use, ground cover of the surrounding site, and climatic conditions. The beat, rhythm, pitch of noise, and distance from the noise source affect the impact of the noise on the receiver (Langer, 2001). Topographic barriers or vegetated areas can shield or absorb noise. Sound travels farther in cold, dense air than in warm air and travels farther when it is focused by atmospheric inversions than when inversions are not present.

An important factor in determining a person's tolerance to a new noise is the ambient (background) noise to which one has adjusted. In general, the more a new noise exceeds the existing background noise level, the less acceptable the new noise will be. In an urban or industrial environment, background noise may mask noise from a quarry operation, whereas the same level of noise in a rural area or quiet, residential neighborhood may be more noticeable to people. Furthermore, ambient noise generally is an accumulation of noises and does not have a single, identifiable source. If the mining noise is identifiable, the perception of noise probably will be great. For example, the noise from a single backup alarm can often be picked out from an equally loud engine noise.

Crushed stone operators and dimension stone quarriers are responsible for assuring that the noise emitted from the quarry does not exceed levels set by regulations. The impacts of noise can be mitigated through various engineering techniques. Landscaping, berms, and stockpiles can be constructed to form sound barriers. Noisy equipment (such as crushers) can be located away from populated areas and can be enclosed in sound-deadening structures (fig. 13). Conveyors can be used instead of trucks for in-pit movement of materials. Noisy operations can be scheduled or limited to certain times of the day. The proper location of access roads, the use of acceleration and deceleration lanes, and careful routing of trucks can help reduce truck noise. Workers can be protected from noise through the use of enclosed, air-conditioned cabs on equipment and, where necessary, the use of hearing protectors. Worker safety may include regular health screening.

Noise can negatively impact karst biota (discussed below).

Figure 13. Noisy equipment can be located away from populated areas and can be enclosed in sound-deadening structures. *(Photograph courtesy Luck Stone.)*

Dust

Dust is one of the most visible, invasive, and potentially irritating impacts associated with quarrying, and its visibility often raises concerns that are not directly proportional to its impact on human health and the environment (Howard and Cameron, 1998). Dust may occur as fugitive dust from excavation, from haul roads, and from blasting, or can be from point sources, such as drilling, crushing and screening (Langer, 2001). Site conditions that affect the impact of dust generated during extraction of aggregate and dimension stone include rock properties, moisture, ambient air quality, air currents and prevailing winds, the size of the operation, proximity to population centers, and other nearby sources of dust. Dust concentrations, deposition rates, and potential impacts tend to decrease rapidly away from the source (Howard and Cameron, 1998).

A carefully prepared and implemented dust control plan commonly can reduce impacts from dust (Kestner, 1994). Federal, state, and local regulations put strict limits on the amount of airborne material that may be emitted during site preparation and operation. Controlling fugitive emissions commonly depends on good housekeeping practices rather than control systems. Techniques include the use of water trucks, sweepers, and chemical applications on haul roads, control of vehicle speed, and construction of windbreaks and plantings (fig. 14). The impacts from plant-generated dust commonly can be mitigated by use of dry or wet control systems. Dry techniques include covers on conveyors, vacuum systems, and bag houses, which remove dust before the air stream is released to the atmosphere. Wet suppression systems consist of pressurized water (or surfactant treated water) sprays located at dust generating sites throughout the plant. Fugitive dust from blasting can be controlled by proper design and execution of blasts. Workers are protected from dust through the use of enclosed, air-conditioned cabs on equipment and, where necessary, the use of respirators. Worker safety may include regular health screening.

In some situations, dust on quarry floors and nearby areas can clog pores in the ground (fig. 15), thus altering recharge rates. In other situations, dust can enter conduits and smaller openings, and can be transported and deposited into caves (Gunn and Hobbs, 1999).

Dust can negatively impact karst biota (discussed below).

Habitat and Biota

Caves develop one of the most peculiar terrestrial ecosystems. One determining factor for life in karst solution features is the lack of light. The karst environment can be divided into four zones based on the degree of darkness (Vermeulen and Whitten, 1999): 1) The twilight zone, near the entrance where light intensity, humidity, and temperature vary and a large and varied fauna are found, 2) The transition zone of complete darkness, variable humidity and temperature where a number of common species live, some of which make sorties to the outside world, 3) The deep zone of complete darkness, almost 100 percent humidity, and constant temperature where fully cave-adapted species that never venture outside the cave live, and 4) The stagnant zone of complete darkness, 100 percent humidity, where there is little air exchange and carbon dioxide concentrations may become high.

Many species of bats, including nectar-feeding bats and insectivorous bats, roost in the twilight zone or transition zone of caves. Insectivorous bats make up the largest known colonies of mammals in the world (Veni and DuChene, 2001). Birds, other animals, and plants also inhabit these zones.

To cope with the permanent darkness, extreme scarcity of food, and relatively constant climate of the underground voids in the deep and stagnant zones, animals have developed physiological, behavioral, and morphological adaptations (fig. 16), losing many of the essential functions of aboveground species. Eyes are reduced or absent, and they have little or no pigment. These animals are able to cope with the highly alkaline environment created by the abundance of soluble calcium carbonate. They have developed means of expelling water in 100 percent humidity without losing body salts. If their ancestors had wings, cave animals have lost them. Diurnal rhythms are lost. Their life span increases and their fertility decreases dramatically. These adaptations have confined cave species to their habitat; they cannot survive elsewhere (Vermeulen and Whitten, 1999).

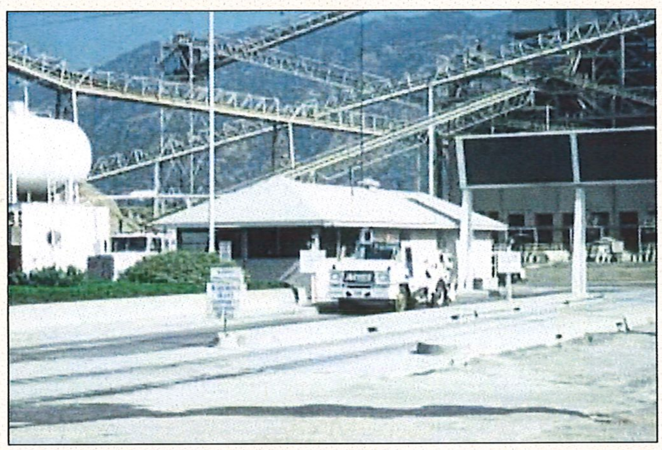

Figure 14. Dust control techniques include the use of water trucks and sweepers on haul.

Figure 15 (right). Dust on quarry floors can clog pores in the ground, thus altering ground-water. recharge.

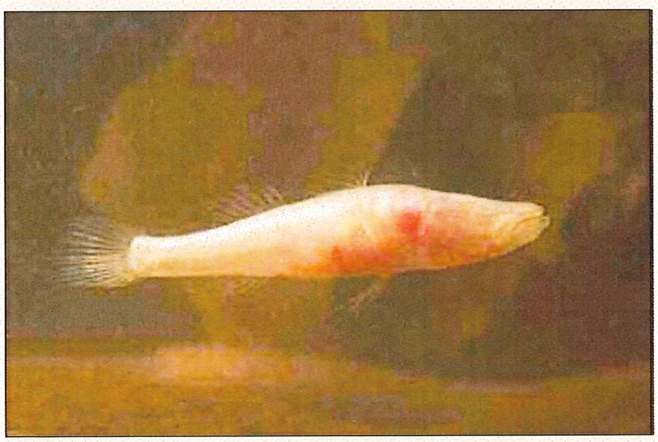

The biodiversity of karst ecosystems is highly restrictive. Some species are restricted to single cave systems and are little known. For example, about 47 species of aquatic and terrestrial invertebrates have been collected from the Movile Cave and nearby springs in southern Romania. Thirty of the 47 species were previously unknown and appear to be endemic to the system (White and others, 1995).

As rock is removed by quarrying, any cave passage is destroyed, along with any sediments it may have contained. The habitat provided by the caves and passages will cease to exist. Animals that inhabit the twilight or transition zone, and are mobile and able to find new homes, might survive; the rest will die. Creatures that have adapted to the deep and stagnant zones will perish.

Figure 16a (top left). Karst inhabitant – Bamazomus. *(Photograph courtesy Elery Hamilton-Smith.)*

Figure 16b (bottom left). Karst inhabitant – Milyeringa. *(Photograph courtesy Elery Hamilton-Smith.)*

Quarrying may intersect active ground-water conduits, or cause their blockage, with adverse consequences for aquatic communities. Ground-water withdrawal and diversion of surface water may cause aboveground and underground hydrologic systems to dry up. Water bodies, which may be inhabited by small, site-endemic fish and snail species, will disappear and with them, the species. Alterations of flow volumes and patterns and the availability of nutrients can profoundly change the limestone environment and may lead to the extinction of whole communities (Vermeulen and Whitten, 1999). Lowering the water table will increase the thickness of the unsaturated zone, which can change the pH of the water in the unsaturated zone, which will change the biotic environment in small voids in the rock, which will kill species that live there.

Blasting can negatively affect karst habitat and biota. Blast-induced vibrations and shock waves can cause cave roofs to crack or collapse, and karst environmental conditions can be altered by just one new crack. Light may enter an otherwise dark cave or passage, or streams and ponds may suddenly drain into a new crack in the floor. Either situation can result in the death or displacement of cave communities (Vermeulen and Whitten, 1999).

Noise and air concussion may disturb colonies of bats and swiftlets, causing them to leave their roosting sites. This type of disturbance can occur as far away as 1,500 meters from the quarry if the opening of the roosting cave happens to be facing in the direction of the blast (Vermeulen and Whitten, 1999). Noise can adversely affect wildlife by interfering with communication and masking the sounds of predators and prey, and in the extreme, result in temporary or permanent hearing loss (Fletcher and Busnel, 1978).

Dust, if uncontrolled, may spread over the surroundings during dry weather, leach into the soil during storms, and create harmful conditions for the flora and fauna (Vermeulen and Whitten, 1999). When dust smothers leaf surfaces, vegetation can be damaged through the blocking of leaf stomata, thus inhibiting gas exchange and reducing photosynthesis (Howard and Cameron, 1998).

Changes in the humidity of karst openings, presence of water, and quality of water (see below) can all impact karst biota. The impacts of quarrying on surface water and ground water (see below) can impact wetland riparian, and aquatic habitat which, in turn, can impact biota.

Water Quality

Karst systems have very low self-purification capabilities (Kresic and others, 1992), which makes karst water very susceptible to pollution. A major concern is that polluted materials, including pathogens, can be carried long distances without being filtered because of high flow velocities (several hundreds of thousands of meters per day) (Assad and Jordan, 1994).

The sources of pollutants do not necessarily have to be man-made; there also are natural sources of pollution (Kresic and others, 1992). Generally, karst occurs in areas that contain large amounts of organic material and bacteria, which can naturally degrade water quality. Erosion, especially at boundary areas between karst and nonkarst areas, and washout of terra rossa and clay residue from fissures can cause increased turbidity at karstic springs. Ground-water drainage from ore deposits act as natural pollutants.

Quarrying can substantially modify the routing of recharge and water quality may be degraded (Gunn and Hobbs, 1999). Commonly the first impact of quarrying is to remove the overlying vegetation and soil. In temperate areas removing vegetation and soil reduces evapotranspiration and increases the effective rainfall. Unless measures are taken to control runoff and sedimentation, deterioration of ground water is likely. In some karst areas the soil overlying the rock normally is a zone of filtration and water purification (Gunn and Hobbs, 1999). In aggregate mining, the target limestone, if unsaturated, may also act as a protective cover for the underlying aquifer. If the protective soil cover or unsaturated rock is removed, the hole created by the mining may focus surface water to the ground-water system. If the surface water is contaminated, the ground water can quickly become polluted (Hobbs and Gunn, 1998; Ekmekçi, 1993).

Quarrying can cause sinkhole collapse, which can result in capture of surface water. In the Tournaisis area, southern Belgium, about thirty sinkholes opened up along the Escaut River downstream from the city of Tournai. As a consequence, the ground water was polluted by an extensive loss of contaminated river water into the karst aquifer (Kaufmann and Quinif, 1999).

Dust can enter conduits and smaller openings and can be transported by ground water (Gunn and Hobbs, 1999). The fine debris produced by the cutting of marble can be worked through the ground-water system during storm events (Drysdale and others, 2001).

Blasting may cause problems with ground-water quality, but may also be erroneously identified as a cause of problems. Spigner (1978) reported that shock waves from blasting operations loosened clay particles from solution cavities causing "muddying" of the ground water. Elsewhere, Moore and Hughes (1979) investigated the impact of quarry blasting on ground-water quality and determined there was no relationship between blasting and quality of water in wells in the situation that they studied.

The risk of ground-water pollution may increase if the direction of ground-water flow is modified. New source areas of recharge may be introduced, and those sources may contain contaminated water. This situation can arise because of ground-water pumping (Adamczyk and others, 1988; Sedam and others, 1988) or can occur if old choked passages are flushed and become operational again. Ekmekçi (1993) reported that blasting associated with quarrying may close existing karst ground-water passages, or may open up new passage, resulting in a change in direction of ground-water flow.

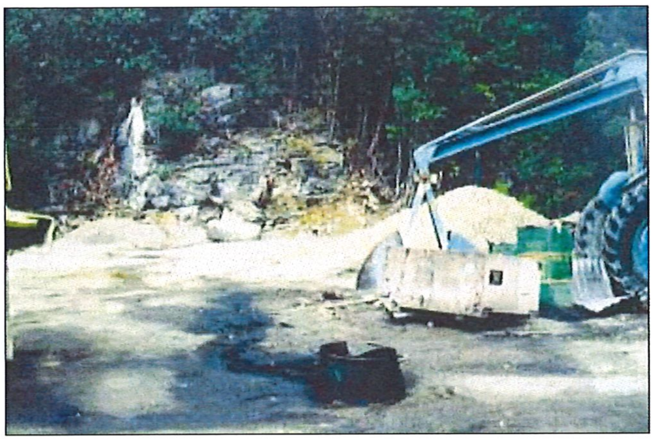

Figure 17a. Fuel oil spills can rapidly contaminate karst aquifers. *(Photograph courtesy Elery Hamilton-Smith.)*

Figure 17b. Properly constructed containment facilities can protect the aquifer from potential fuel spills. *(Photograph courtesy Lafarge.)*

Large amounts of silt and other effluents from quarries (waste, fuel, oil) may pollute rivers as well as underground water bodies within and far beyond the boundaries of the limestone area (fig. 17a and b). Rivers in Indo-China, for example, host hundreds of species of large freshwater clams and snails, many of which are site endemic to a section of one stream. Development puts great pressure on these animals, which are very vulnerable because they are easily smothered in mud or killed by chemical pollution when silt is allowed to seep into a river. Fish communities are equally vulnerable (Vermeulen and Whitten, 1999).

Surface Water

Engineering activities associated with quarrying can directly change the course of surface water. Sinkholes created by quarrying (see below) can intercept surface water flow. Conversely, ground water being pumped from quarries changes streams from gaining streams to loosing streams and can drain other nearby surface water features such as ponds and wetlands. Similarly, blasting (see above) can modify ground-water flow, which ultimately can modify surface water flow. Discharging quarry water into nearby streams can increase flood recurrence intervals.

Ground Water

Overall, quarrying in the unsaturated zone is likely to result in relatively local impacts such as increased runoff, reduced water quality, rerouting of recharge water through the aquifer, and localized reduction in ground-water storage. In karst areas, the unsaturated zone commonly contains only a small percentage of storage, and where the unsaturated zone is thin, impact on ground-water quantity generally is minimal (Hobbs and Gunn, 1998). However, Smart and Friederich (1986), Dodge (1984), and Gunn (1986) all describe areas where a thick, well-developed unsaturated zone is present. In those areas, the unsaturated zone may store significant quantities of water. Following rainfall, water may be collected and temporarily stored in the unsaturated zone, until it subsequently joins the ground-water system.

The major impact of quarrying in the karst saturated zone relates to quarry dewatering and the associated decline of the water table. It should be noted that there are many human activities other than quarrying that can affect ground-water levels, including municipal, industrial, and private ground-water withdrawals, irrigation, use of ground water for freeze protection, and mine drainage from other mineral resource extraction activities. Drought is a natural cause for water table declines. Many of the reports of dramatic declines of the water table refer to underground mines, rather than surface quarries.

If quarrying intersects a phreatic conduit (a conduit in the saturated zone), the water-transporting function of that conduit will be severely impacted. Dye studies have demonstrated that, even without intersecting conduits, quarry dewatering can affect the function of a conduit by inducing leakage into diffuse flow zones (Edwards and others, 1991; Sedam and others, 1988). In cross section, the path of a conduit often has a wave shape. If the water table is lowered to where at least the crests of the waves no longer contain water, water will be trapped in the troughs of the waves and the conduits will no longer be able to transmit water.

If a quarry intersects the water table, ground water commonly will flow out of the rock into the quarry. Water may just trickle into the quarry or it may flow into the quarry at a rate of hundreds or thousands of liters per second (L/s), especially if quarrying intercepts a phreatic conduit. Foose (1953) reported an inrush of 500 to 630 L/s that occurred when an underground limestone quarry intersected a conduit, and Lolcama and others (1999) reported a flow of about 2,525 L/s when a surface quarry intersected a conduit that was in hydraulic connection to a nearby river. In some situations, it may be necessary to drain or pump the water from the quarry to protect people, quarry workings, and equipment.

Pumping from a quarry will reduce hydraulic head and, thus, draw down water levels in the rock draining into the quarry. In the simplest case, the part of the water table impacted by quarry dewatering would look like a downward-pointing cone that has been depressed into the water table, thus its name – cone of depression. If the quarry were the only major source of ground-water draw down in the area, it would be located over the apex of the cone of depression.

The actual shape of a cone of depression depends on many factors including the direction, volume, and velocity of water moving past the site; rock properties, including permeability of rock layers, attitude of rock layers, amount of fractures in the rock, size of fractures, fracture orientation, continuity of fractures, and regional stresses keeping fractures open or closed; other sources of ground-water withdrawals, natural or manmade discharge points, recharge points, conduits, whether conduits recharge or drain aquifer, and so forth. Homogeneous rocks yield a classic circular cone of depression, but the anisotropic nature of most limestones produces an irregular zone of depression, with preferential development along zones of highest permeability (Gunn and Hobbs, 1999). Depending on local conditions and quarrying practices, cones of depression can be almost as small as the quarry itself, or can be as large as 25 km^2.

Figure 18. Natural sinkhole near Ste. Genevieve, Missouri *(USGS photographic library-Shaw #891).*

Water pumped from a quarry is likely to be lost from the local groundwater system. Within the cone of depression, wells, springs, and streams can go dry or have their flows significantly reduced, and the overall direction of ground-water flow may be changed (Hobbs and Gunn, 1998). It is within this cone of depression that many human-induced sinkholes are formed.

Karst aquifers are often separate from overlying shallow surficial aquifers. Fraser and Grapes (1998) determined that a shallow aquifer in drift and the underlying karstic limestone aquifer in South Wales are separate hydraulic systems with distinct water chemistries and distinct responses to hydraulic stress. They determined that dewatering the deep aquifer would not affect plant communities supported by the shallow aquifer.

Sinkhole Collapse

Sinkholes are depressions formed in karst by either slow, downward solution or rapid collapse of the land surface. Sinkholes in carbonate rocks occur world wide, with notable concentrations in the eastern USA, southeast Asia, and parts of Europe. Sinkholes can occur naturally or can be induced by activities of man (Newton, 1976).

Figure 19. Human-induced sinkholes formed during the development of an irrigation well affected a 20-acre area and ranged in size from less than 1 foot to more than 150 feet in diameter. *(Photograph courtesy Ann Tihansky, USGS.)*

Natural sinkholes (fig. 18) can form through the dissolution of rock (solution sinkhole) or through the failure of a bedrock roof overlying a cavern (collapse sinkhole). The formation of both of these types of sinkholes occur over periods of geologic time, not within a human lifetime. The solution of rock has little to do with the final cause of sinkhole collapse, however, it can set the stage for some human-induced event in the future (Thorpe and Brook, 1984; White and White, 1995). Of an estimated 4,000 sinkholes formed in Alabama between 1900 and 1976, only 50 were natural collapses (Newton, 1976).

Human-induced sinkholes are those caused or accelerated by human activities and commonly are characterized by catastrophic subsidence (Newton, 1976; LaMoreaux and Newton, 1986; LaMoreaux, 1997). If human activities had not taken place, these sinkholes would not have occurred, would not have occurred when they did, or, under natural conditions, would have occurred as subsidence, not rapid collapse (Newton, 1987). Human-induced sinkholes (fig. 19) commonly form as a result of ground-water withdrawal, construction activities, or a combination of both.

Ground-Water Withdrawal

Human-induced sinkholes in karst commonly are caused by human activities that lower the water table below the rock/soil interface (fig. 20). Many human activities, in addition to quarrying, can lower the ground-water table. While quarrying commonly is restricted to relatively small areas, other activities tcan be spread out, which may increase their relative impacts on the environment. Regardless, in some situations quarrying includes ground-water withdrawals and should be carefully addressed.

A classic case of sinkhole development caused by dewatering an underground limestone quarry occurred in the Hershey Valley, Pennsylvania (Foose, 1953, 1969; Foose and Humphreville, 1979). In 1949, increased pumping from the quarry created a cone of depression covering 600 hectares. Nearly 100 subsidence sinkholes formed above the cone of depression within three months of the increased pumping. Sinkhole development ceased after quarrying dewatering stopped and the water table returned to normal.

Figure 20a. Hypothetical cross section showing karst area under conditions prior to quarry development. The water table (1) is generally above the soil / bedrock contact. Natural ground-water discharges to a spring (2), and a perennial stream (4), which support a wetland (3) and a riparian woodland (5). The surface of the bedrock is highly irregular (6), and is referred to as pinnacled bedrock. A natural sinkhole occurs where the water table is below the soil / bedrock contact (7).

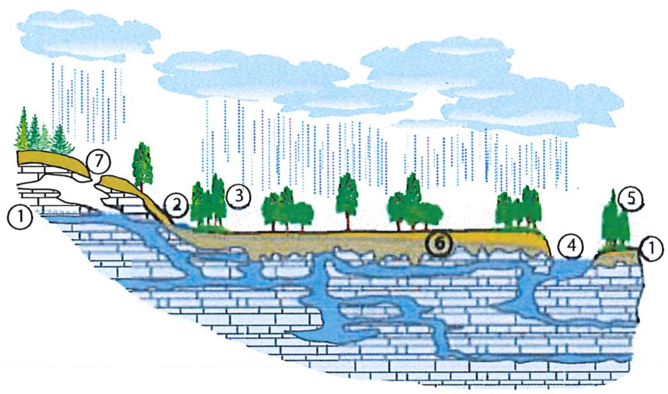

Figure 20b. Hypothetical cross section showing karst area under worst-case conditions after quarry development. Under actual conditions, none, some, or all of these conditions may exist. Quarry dewatering has lowered the water table (1) below the soil / bedrock contact. Natural ground-water discharge to a spring (2) and perennial stream (4) has stopped, resulting in destruction of the wetland (3), drying up of the stream (4) and destruction of the riparian woodland (5). Underground cavities formed in the soil in the area of the pinnacled bedrock due to loss of buoyant support and piping (6). The ground above the cavity has subsisded, resulting in the formation of a wet area, and the tilting of fence posts or trees (7). Ultimately these cavities could collapse, creating a collapse sinkhole (8).

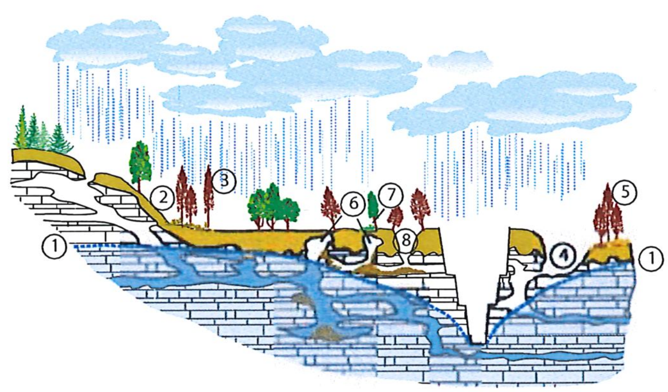

LaMoreaux and Newton (1986) document a similar occurrence in the Dry Valley area of Alabama where several thousand sinkholes formed above a cone of depression in the period 1967 – 1984. Ground-water withdrawals from two quarries in the Jamestown, South Carolina, area resulted in the formation of 42 sites of subsidence and collapse from 1976 – 1978 (Spigner, 1978; Newton, 1987). Ground-water withdrawal caused by limestone quarrying appears to be the cause of sinkhole collapse at Railtown in northwestern Tasmania (Kiernan, 1989). Other areas of sinkhole collapse related to quarry dewatering have been described by Newton (1976, 1986, 1987), and Newton and Hyde (1971).

Sinkhole collapse related to ground-water pumping can also result from some other dewatering activity in combination with quarrying. A number of sinkhole collapses near Calera, Alabama, occurred in an area dewatered by wells, quarries, and an underground mine (Warren, 1976). Intense pumping for domestic and industrial water supply, combined with dewatering of deep limestone quarries, has caused sinkhole development in the Tournaisis area, Belgium, since the beginning of the 20th century (Kaufmann and Quinif, 1999).

Quarrying begins at the top of bedrock and deepening occurs over a period of years. Sinkhole development may begin after quarrying penetrates the water table (fig. 20). When the depth below the water table is shallow, sinkhole development generally is confined to the vicinity of the quarry. As the quarry is deepened, the cone of depression enlarges and sinkholes occur further away (Newton, 1987). Sinkhole development following dewatering associated with subsurface mining commonly occurs more rapidly than that resulting from surface quarrying because the depth of dewatering and cones of depression are relatively large (Newton, 1987).

Triggering Mechanisms

The act of lowering the water table commonly does not by itself create a sinkhole. Most often land subsidence will occur only if support to overlying unconsolidated material is removed (Foose, 1967) and some other activity commonly "triggers" sinkhole formation. Triggering mechanisms include: 1) water level fluctuations, 2) loss of buoyant support by the water, 3) volume shrinkage, 4) piping or induced recharge, and 5) increased gradient and water velocity (fig. 21) (Newton and Hyde, 1971; Newton, 1987).

Subsidence or collapse of soil overburden into the fissures and caves of an underlying limestone creates subsidence sinkholes without involving failure of the rock (Waltham, 1989). Bedrock caves do exist beneath some sinkholes, but their role is merely to swallow the debris. Almost all sinkholes occur where cavities develop in unconsolidated deposits overlying solution openings in carbonate rocks (LaMoreaux and Newton, 1986), and given sufficient time, sinkholes can develop above bedrock containing only narrow rock fissures (Waltham, 1989).

Water Level Fluctuations

Pumping of ground water, particularly in seasonally-operated quarries, may result in ground-water fluctuations that are of greater magnitude than fluctuations that occur under natural conditions. The magnitude of fluctuation principally depends on the amount and duration of pumping and on the transmissivity and storage coefficient of the aquifer. The unconsolidated material bridging bedrock pinnacles can be weakened by the alternate wetting and drying, lubrication, and addition or subtraction of buoyant support brought about by fluctuating water levels (Newton and others, 1973).

Loss of Buoyancy Support

In some karst areas residual clay soil spans or fills space between bedrock pinnacles. If the soil is saturated, about 40% of the weight of the residual clay soil overlying a bedrock opening is supported by ground water (Newton and Hyde, 1971; Newton, 1987). When the ground-water level is lowered, buoyant support is lost (fig. 21, block B). The loss of buoyant support can trigger sinkhole collapse (fig. 21, block D) or cause spalling that ultimately trigger collapse. (Newton, 1984a, 1984b, 1984c, 1987).

In artesian areas, hydrostatic pressure provides support to the confining bed and to overlying material (Newton, 1987). Weakening of buoyant support in artesian carbonate rocks may be caused by a decline of piezometric levels of the confined aquifer system. A one meter decline in piezometric level corresponds to a 1 ton/m^2 increase of effective loading of overburden. Local or distant withdrawals of karst aquifer could cause such a decline (Prokopovich, 1985).

Volume Shrinkage

As ground water is lowered in areas of pinnacle weathering, volume shrinkage due to compaction of the unconsolidated debris takes place. If two pinnacles are less than 10 – 15 m apart, the weight of the sediment load between the pinnacles can be carried as an arch (Foose, 1967). As spalling occurs, the cavity grows upward, enlarging the vaulted roof. There is a limit to the weight that the arch can hold, and when the ability of the arch to hold the load is exceeded, rapid upward propagation of the arch by continuous spalling results in sudden collapse of the surface.

Soils with low cohesive strength, such as dry sands, tend not to form a stable arch. There is a continuous flow of soil down the drain (raveling) and instead of an abrupt collapse, the sinkhole forms by a process of continuous subsidence. Human influences, particularly dewatering, can greatly modify the rate of soil transport (Newton and others, 1973).

Piping or Induced Recharge

When cavities in the soil or bedrock are filled with ground water (fig. 21, block A), surface water cannot flow into the cavities. When the water table is lowered, the cavities drain, thus allowing the inflow of surface water. Surface water passes through the residual soil, eroding it and carrying it downward into the air-filled cavities by a process called piping or subsurface mechanical erosion (LaMoreaux, 1997) (fig. 21, block C). Soil is piped down into the bedrock creating a void within the soil mantle. As time passes, more and more soil is piped down the drain and the void grows with an arched roof held up only by the cohesive strength of the soil. Eventually, the void becomes too large for the soil arch to support its own weight and there is a collapse (fig. 21 block D). The fallen roof may obscure the bedrock surface and the drain. The freshly-formed sinkhole is usually roughly circular in outline and has near vertical walls (Lolcama and others, 1999; White and White, 1995). Piping is well-documented by observations of the pumping of "muddy water" during quarry dewatering (Foose, 1953, 1967). Piping is most active during periods of heavy or prolonged rainfall.

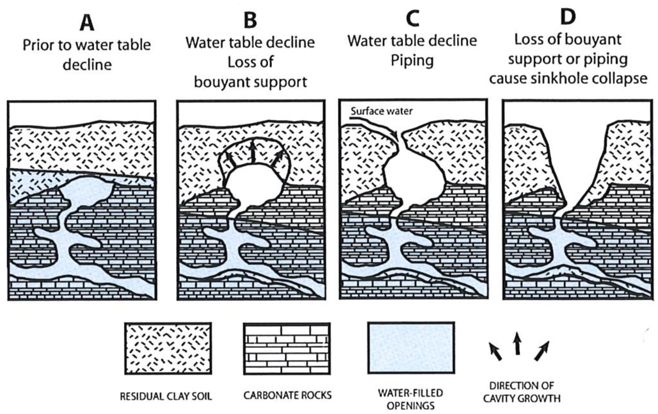

Figure 21. Diagram showing mechanics of sinkhole development.

Increased Velocity of Ground Water

Surface structures, such as storm drains, parking lots, and roof drains, concentrate recharge into a single inlet point in the carbonate rock, thus encouraging piping. Construction activities of various kinds can also raise hydraulic heads, increase velocities in the drain, and thus also enhance the rate of sediment transport leading to accelerated sinkhole development (Newton, 1986).

Ground-water withdrawal creates an increased hydraulic gradient, which results in an increased velocity of ground-water movement. Increased water velocity results in flushing of sediments filling openings in cavity systems. In turn, downward movement of overburden sediments into newly created bedrock openings, results in a sinkhole (Newton, 1976, 1984a, 1984b, 1984c).

A decline in potentiometric surface under artesian conditions produces increased head differential, which results in increased velocity of recharge through the confining bed. The energy of this movement is diffuse, and unless the confining bed is breached, will not be expected to contribute to sinkhole development (Newton, 1987).

Figure 22. "A giant sink hole opened up on Thursday, September 19 [1975] at a drilling site near Tampa, Florida and swallowed up a well-drilling rig, a water truck, and a trailer loaded with pipe all valued at $100,000. The well being drilled was down 200 ft when the ground began to give way to what turned out to be a limestone cavern. Within 10 minutes all the equipment was buried way out of sight in a crater measuring 300 ft deep, and 300 ft wide. Fortunately, the drilling crew had time to scramble to safety and no one was hurt." -from National Water Well Association newsletter. *(Photograph courtesy Tom Scott.)*

Construction Activities

Some sinkhole failures are induced by construction activities and are of major significance because they directly affect the site being developed, either immediately or some years later. Construction activities that can trigger sinkholes include 1) diversion or impoundment of drainage, 2) removing overburden, 3) drilling, augering, or coring 4) blasting, 5) loading, and 6) removal of vegetation. A lowered water table may leave sections of ground in a critical state awaiting construction activity to triggers their failure; however, even without a water-table decline, the same activity may prompt failure, but statistically less often.

Diversion or Impoundment of Drainage

A major influence from construction is the diversion of natural drainage. Concentration of drainage at the surface, such as leaking pools, impoundments, pipes, canals, and ditches, can all create point discharge into the soil, inducing ground water to move through overburden into bedrock. This can result in an increased velocity of ground water, piping, saturation of overburden, and loss of cohesiveness of unconsolidated deposits (LaMoreaux, 1997). These effects can result in collapse of the overburden into openings below.

Runoff from roads or buildings commonly is disposed of into ditches, soakaway drains, or dry wells in soil over carbonate rock. Ditches and drainage wells cased into the limestone should perform safely, but, if poorly installed, leakage may cause adjacent or nearby failures (Crawford, 1986). In Pennsylvania, 7 km of highway induced 184 sinkholes along its associated drainage channels within 12 years (Meyers and Perlow, 1984).

Removing Overburden

Excavation of part of a soil cover may thin the roof of a soil cavity to a point of failure. Removal of a clay soil may permit drainage through previously sealed sands. Some Missouri railroads stand on banks made from soil excavated adjacent to them, and the marginal hollows frequently develop sinkholes (Aley and others, 1972).

Drilling, Augering, or Coring

These activities cause erosion of overburden into underlying openings. Unsealed boreholes can allow surface water to gain new access to the subsurface or may allow a perched soil aquifer to drain into a bedrock cavity. Drilling has resulted in collapses at or near working drill rigs (fig. 22) or the holes created (LaMoreaux, 1997). During 1960 an USGS driller was killed when a sinkhole formed around a test hole in Florida (Newton, 1987). Installation of wells at Westminster, Maryland, in 1940 and 1948 was associated with nearby sinkhole collapse (Newton, 1987). A sinkhole collapsed next to a USGS test well near Dickson, Tennessee, in May 1981 (Newton, 1987).

Blasting

Explosives create vibrations that can disturb the overburden and trigger its downward movement into solution openings in bedrock (Stringfield and Rapp, 1976; Ekmekçi, 1993; LaMoreaux, 1997). The village of Liangwu, in southern China, was abandoned when nearby blasting triggered 40 sinkholes, and another 100 followed soon after in an area 1800m long (Yuan, 1987).

Loading

Heavy construction equipment and other traffic can disturb the overburden and trigger its downward movement into solution openings in bedrock (LaMoreaux, 1997). The weight of construction alone can trigger sinkholes (Newton, 1976).

Removal of Vegetation

The removal of vegetation permits increased infiltration and also deprives the soil of its root mat. In Alabama, sinkholes are more common in the parts of Dry Valley where timber has been cut (LaMoreaux and Newton, 1986) and failures occurred on a Birmingham, Alabama, construction site when foundation trenches stripped areas of topsoil (Newton and Hyde, 1971). Modern sinkhole development in Tasmania has been attributed to timber cutting and pasture development (Kiernan, 1989).

Analysis of Triggering Mechanisms

Two independent studies, one in Missouri and one in Florida, indicate that altered drainage is the triggering mechanism responsible for over half of the sinkhole collapses. Williams and Vineyard (1976) conducted a study of 46 reported sinkhole collapses in Missouri and determined the cause of collapse to be; altered drainage (52 percent, water impoundments (22 percent), dewatering (15 percent), highway construction (7 percent), and blasting (4 percent). The Florida Department of Transportation analyzed 96 roadway-related collapses and determined the triggering mechanisms to be related to; heavy rainfall (58 % percent), construction (11 percent), lowering of the water table (8 percent), blasting (5 percent), drilling (5 percent), and other (11 percent). (Numbers do not add to 100 due to rounding.) Runoff collected during heavy rainfall is concentrated by highway drainage, thus supporting the findings of Williams and Vineyard (1976) that altered drainage is the dominant triggering mechanism for collapse (Thorpe and Brook, 1984).

Sinkhole Size, Occurrence, and Area Impacted

Collapse sinkholes in fissured bedrock occur in the soil overlying cavernous bedrock, and the depth, therefore, is limited to the thickness of the soil. In cavernous bedrock the depth of collapse sinkholes is limited to the combined depth of the soil and the cavern. The width of a collapse sinkhole near the surface depends on the thickness of the soil and on the slope stability, which, in turn, relates to the cohesiveness of the soil (Waltham, 1989). Geometry dictates that thick soils develop sinkholes with greater diameters than thin soils (White and White, 1995). Cohesive clayey soils maintain steeper slopes that sandy soils with low cohesiveness and, consequently, maintain wider sinkholes.

Size

Data relating to the size of sinkholes resulting from ground-water withdrawals are limited and not all the figures below refer to sinkholes related to quarrying. Sinkhole collapses in general range from 1 m to 145 m in their longest dimension. One of the largest sinkholes resulting from the withdrawal of ground water from carbonate rocks in Alabama is about 145 m long, 115 m wide, and 50 m deep (LaMoreaux and Warren, 1973) (fig. 23). A study of an area in the Birmingham, Alabama, containing over 200 sinkhole collapses (Newton and Hyde, 1971) reported that the average sinkhole was 3.7 m long, 3 m wide, and 2.4 m deep. A similar study of an area near Greenwood, Alabama, containing over 150 sinkholes (Newton and others, 1973) reported that the average elongated sinkhole was about 6.1 m long, 4 m wide, and 2.1 m deep. Some sinkholes near Sylacauga, Alabama, (Newton, 1986) had surface diameters of 9 to 30 m. In Shelby County, Alabama, (Newton, 1986) six collapses had diameters approaching or exceeding 30 m. Collapse sinkholes near Orlando, Florida, have a mean diameter of 9.4 m and a mean depth of 4.7 m (Wilson and Beck, 1992). A collapse sinkhole in central

Figure 23. The "December giant," a large sinkhole, developed rapidly in Shelby County, Alabama, in December 1972. The sinkhole measures 145 m long, 115 m wide, and 50 m deep. *(USGS Photographic Library-USGS #140.)*

Maryland (Martin, 1995) was approximately 9 m in diameter and 6-7 m deep. Collapse sinkholes resulting from quarry dewatering in North Carolina are up to 5 m in diameter and 3 m deep (Strum, 1999). Sinkholes in Pennsylvania (Kochanov, 1999) generally range from 1.2 m to 6.1 m in diameter and have approximately the same range in depth. In Hershey Valley, Pennsylvania, (Foose, 1953) 100 new sinkholes were reported to be 0.3 to 6.1 m in diameter and 0.6 to 3 m deep. The largest of 42 sinkhole collapses described in South Carolina (Spigner, 1978) was over 8 m in diameter and the greatest depth exceeded 3 m. The largest of 64 sinkhole collapses near Tampa, Florida, also has these same dimensions (Sinclair, 1982).

Occurrence

The numbers of collapse sinkholes that occur in an area and the size of the effected area varies from a single sinkhole in (about 1 m) to about 1,000 sinkholes in area of about 45 km2. Seven sinkholes developed at a distance of 600 m from a quarry in North Carolina (Strum, 1999). Newton (1986) similarly reports that most induced sinkholes in Alabama related to quarry operations were found within 600 m of the point of withdrawal. In contrast, Sowers (1976) reports that quarries less than 60 m deep near Birmingham, Alabama, have been related to sinkhole development as far away as 1.6 km. Sinclair (1982) also reports that 64 collapses occurred within a 1.6 km radius of a well field near Tampa, Florida. In one area in Alabama, an estimated 1,700 collapses or related features have occurred in five areas with a combined area of 36 km2 (Newton, 1976). In another area of Alabama, it was estimated that 1,000 collapses or other related features formed in an area of about 41.5 km2 (Warren and Wielchowsky, 1973). Near Jamestown, South Carolina, 42 collapses occurred within a cone of depression (Spigner, 1978). In Pennsylvania, about 100 collapses occurred in a cone of depression near Hershey where the ground-water surface had been lowered in an area greater than 25.9 km2. Impacts were observes 2.4 km from the point of dewatering (Foose, 1969; Foose and Humphreville, 1979). At Friedensville, Pennsylvania, 128 sinkholes formed from 1953-57 in an area around the point of withdrawal at a zinc mine, and 25 new sinkholes were recorded during a four-month period ending January 1971 (Newton, 1987; Metsger, 1979). Sites of similar intense development, in addition to those described above, were identified in Alabama, Georgia, Maryland, North Carolina, Pennsylvania, South Carolina, and Tennessee (Newton, 1986).

Area Impacted

The size of the impacted areas varies with the amount of ground-water withdrawal. Rates of withdrawal at the Friedensville zinc mine were between 440 and 1,310 liters per second (L/s), and the cone of depression covered an area exceeding 10.3 km2 (Newton, 1987; Metsger, 1979). Pumping by wells, quarries, and an underground mine west of Calera, Alabama, exceeded 883 L/s, creating a cone of depression of about 26 km2 (Newton, 1976, 1987; Warren, 1976). Ground-water withdrawal from two quarries with a combined rate in excess of 1,575 L/s has lowered water levels in wells over 2.4 km from the quarries (Spigner, 1978). Near Hershey, Pennsylvania, an average of 347 L/s of water was pumped from the underground quarry, impacting areas 2.4 km away (Foose, 1953, 1969). In Craven County, North Carolina, a quarry pumped at a rate of about 440 L/s, which resulted in sinkholes 600 m away (Strum, 1999).

Predicting Collapse Sinkholes

It is only possible to predict sinkhole subsidence events in the broadest of terms. However, it is possible to identify zones where sinkhole risk is increased. A number of researchers have identified specific karst features that are diagnostic in pinpointing areas having a likelihood of collapse and subsidence. Williams and Vineyard (1976) cited nine features that can foretell of collapse or subsidence in karst terrain. Foose (1969) lists seven conditions that are common in areas of karst topography subject to collapse. Aley and others (1972) described seven features of karst terrain where catastrophic collapse had occurred, although they were primarily concerned with collapses induced by construction of impoundments.

The indicators cited may have limited regional usefulness because of the tremendous number of variables among various karst terrains and the various climatic conditions in those terrains. While this report is not intended to challenge the significance of the indicators, it is important to remember that the physical properties of karst are the result of local conditions.

Guidelines that repeatedly emerge from case studies is that sinkhole development most commonly occurs where four conditions exist: 1) residual soil overlies pre-existing fractures or cavities in pinnacled carbonate bedrock; 2) a solutionally widened fracture or shaft leading down into bedrock can act as a drain to transport sediment; 3) there is some provision to store or remove soil from the drain; and 4) the water table has declined past the bedrock/soil contact (Waltham, 1989; White and White, 1995).

Collapse sinkholes form most often where and when the water table first declines past the bedrock/soil contact. This condition occurs where the water level, previously above the bedrock/soil contact during all or most of the year, is maintained below the contact by ground-water withdrawal (Waltham, 1989; Newton, 1987; LaMoreaux and Newton, 1986; Foose, 1969). All the mechanisms that trigger sinkhole development in unconsolidated deposits can be activated by the decline in water table (LaMoreaux and Newton, 1986).

LaMoreaux and Newton (1986) state that sinkholes will not occur in areas where the water table was below the bedrock/soil contact prior to dewatering. However, Foose (1969), states that sinkholes have formed where the original water table was below the bedrock/soil contact as a consequence of flushing out underlying bedrock openings during ground-water lowering.

Wilson and Beck (1992) relate sinkhole occurrence in Florida to declines in the potentiometric surface. When the surface declines 3 m below its mode, more than 10 times as many collapse sinkholes as expected per unit of time begin to occur.

Many authors also pointed out that sinkholes occur where the bedrock weathering is irregular, where the bedrock is pinnacled, or where there are extensive cavernous openings and major structural elements in the underlying bedrock (Foose, 1968; Newton, 1984a, 1984b, 1984c; Waltham, 1989).

The thickness of the residual soil has some control on the likelihood of collapse sinkholes, although the actual values appear to be site and soil-type dependent. Williams and Vineyard (1976) pointed out that sinkhole collapses are more likely to occur in residual soil ranging in thickness from 12 to 30 m. Foose (1969) observed that few sinkholes occur where the overburden is less than 10 m thick. Waltham (1989) states that the most hazardous zone is where the soil is 2 to 20 m thick. Sinclair and Stewart (1985) state sinkhole collapses are rare where limestone is at surface or the ground is thinly covered with soil; sinkhole collapse is common where overlying material is 5-50 m thick, especially between 5 and 25 m thick; sinkhole collapses are found but are rare in areas of soil cover over 50 m thick. Williams and Vineyard (1976) pointed out that sinkhole collapses are more likely to occur in residual soil that retains the fabric of the parent material and in soil where the clay fraction has low plasticity common to kaolinitic and halloysitic clays.

Geomorphology influences collapse sinkhole formation. Newton (1984a) reports induced sinkhole formation is most common in terrain that is geomorphically youthful, exhibits little karstification, is usually a lowland area, has a water table above or near the top of bedrock, and contains perennial or near-perennial streams. Williams and Vineyard (1976) found that collapses are more likely to take place in valleys with losing streams and watersheds than in gaining ones. Waltham (1989) states that the most hazardous zone is a valley floor. Many collapse sinkholes occur where concentrations of surface water are greatest, such as streambeds, natural drains, or poorly drained areas. Wilson and Beck (1992) report that near Orlando, Florida, 85 percent of new sinkholes occur over high recharge areas on slightly elevated, sandy ridges. Few or no sinkholes occur in discharge areas where net downward erosion of surficial sediment is very unlikely. Kaufmann and Quinif, (1999) related sinkhole orientation in southern Belgium to structure, and reported that almost every sinkhole they investigated lies in three parallel linear zones that reflect the orientation of a shear fault about 1 km away.

Hobbs and Gunn (1998) outline a method to characterize the nature of a karst aquifer in terms of the likelihood of impacts from carbonate rock extraction on the ground water. They classify carbonate aquifers into four groups based on storage, type of flow, and type of recharge. Storage ranges from high to low; flow ranges from conduit to diffuse, and recharge ranges from concentrated to dispersed.

- Group 1 represents aquifers with high storage, conduit flow, and variable recharge. Predicting the impact of quarry dewatering is very difficult and is dependent on the likelihood of the workings intersecting an active conduit.
- Group 2 represents aquifers with low storage, conduit flow, and variable recharge. Predicting the impact of quarry dewatering is very difficult, but with low storage, the number of water supplies and size of springs supported by the aquifer is likely to be small.
- Group 3 represents aquifers with low storage, diffuse flow, and dispersed recharge. These are thin limestones with seasonal springs and typically are minor or non-aquifers. These aquifers present no problem from a geohydrologic point of view, and the potential impact can easily be predicted by treating them as homogenous aquifers.
- Group 4 represents aquifers with high storage, diffuse flow, and variable recharge. These aquifers provide a useful resource and may support moderately large springs that may, in turn, provide stream base flow. The potential impact can easily be predicted by treating them as homogenous aquifers.

A holistic systems analysis technique to investigate impacts of aggregate extraction on the environment is described by Langer and Kolm (2001). The method requires analyzes of various systems making up the environment, including land surface, geomorphic, subsurface, and ground-water systems (Kolm, 1996). After system characterization is complete, the method focuses on risk analysis techniques for identifying and evaluating potential environmental impacts to determine acceptable mining strategies (Langer, in press).

There may be warning signs of impending sinkhole collapse. There may be slow localized subsidence and, although new depressions may be hard to identify, the depressions may be enhanced by the ponding of water. Circular cracks may appear in the soil or pavement. Fence posts or other objects may be tilted from the vertical. Vegetation may be distressed due to lowering of the water table. Muddy water in wells may indicate the early stages of a nearby developing sinkhole.

Reclamation

Reclamation commonly is considered to be the start of the end of environmental impacts from mining. The development of mining provides an economic base and use of a natural resource to improve the quality of human life. Equally important, properly reclaimed land can also improve the quality of life. Wisely shaping mined out land requires a design plan and product that responds to a site's physiography, ecology, function, artistic form, and public perception.

There are numerous examples of successfully reclaimed aggregate quarries, including residential, commercial, recreational, and natural uses (Arbogast and others, 2000). Many of the examples are independent of rock type. However, there are a few studies that relate specifically to reclamation of carbonate rock quarries to near natural conditions.

The oldest design approach around is nature itself. Given enough geologic time, a suitable small site scale, and stable adjacent ecosystems, disturbed areas may recover without mankind's input. Ursic and others (1997) studied the Niagara Escarpment and recognized natural cliffs as special places that provide refuge for rare species of plants and animals. They also inventoried vegetation on the walls of 18 carbonate rock quarries abandoned from 20 to 100 years ago and discovered that many of the older quarry walls naturally revegetated in such a way as to replicate the biodiversity of natural landforms.

In other areas, long-term natural recovery alone may not bring about the specific changes people find desirable. The natural reclamation process of abandoned quarries can be accelerated through a process called landform replication. Through carefully designed blasting, referred to as restoration blasting, talus slopes, buttresses, and headwalls of carbonate rock quarries can be created that can be revegetated to produce landform and plant assemblages similar to those that occur on natural valley sides (fig. 24) (Gunn and Bailey, 1993; Gunn and others, 1997).

Gillieson and Houshold (1999) describe reclamation projects in Australia that are specifically designed to return carbonate rock quarries to as close as possible to their original state. The key issues were the integrity of the underground drainage, its water quality, and the cave invertebrate populations.

Legal Aspects

The legal situation concerning induced sinkholes and other environmental impacts in karst is reviewed by Quinlan (1986), LaMoreaux (1997), and LaMoreaux and others (1997).

Quinlan (1986) summarizes case law, legal concepts of ground water and surface water, liability, and law review articles. He reviews the rationales of plaintiffs and defendants, including the allegations that serve as the basis of liability for damages and the defenses against those allegations.

LaMoreaux (1997), and LaMoreaux and others (1997) primarily discuss regulatory standards and the geologic and hydrologic conditions that lead to legal disputes. The authors point out that nearly every State in the United States has implemented legislation, rules, and regulations that apply in part or totally to karst terrain and give examples of State and local laws.

An example of the difficulties in determining the proximate cause of a sinkhole is demonstrated by the investigation of a catastrophic sinkhole that occurred near Westminster, Maryland (Gary, 1999). On March 31, 1994, a sinkhole opened up in the middle of a State road. The sinkhole measured approximately 8 m by 6 m, and was 4.5 m deep. A man drove into the sinkhole and was killed. An active quarry operation was located about 600 m away, and two municipal water supply wells were within 1.6 km of the sinkhole. An isolated pinnacle of limestone occurred in the center of the roadway alignment. A dye trace was conducted to determine if there was a hydraulic connection between the sinkhole and the quarry or other pumping locations. Sampling stations were placed throughout the surrounding valley and in the nearby quarry. There was no dye recovered in the sample sites, therefore, there was no conclusive evidence that quarry dewatering was the cause for the sinkhole.

Figure 24. Face of limestone quarry after restoration blasting and habitat reclamation. *(Photograph courtesy John Gunn.)*

Case Studies

There are numerous causes of environmental damage in karst, many that do not relate to quarrying. These case studies are primarily those directly related to quarrying or engineering activities, such as drilling and blasting, that are used by a number of activities, including quarrying. Units of measurements in case studies are as reported by the original authors.

Blasting - A sinkhole collapse occurred in 1983 while blasting for new highway construction near Erwin in Unicoi County, Tennessee (Newton and Tanner, 1987).

Blasting - A number of rural residents near Oxford, Alabama, reported recurring problems in turbidity of water from their individual water-supply wells and, occasionally, decreases in yield. Many residents associated the problems with blasting operations in a local rock quarry. Research identified no relationship between blasting events and the quality of water in wells. Most turbidity problems occurred during the dry period of the year (October—December) when water levels in some wells are as much as 40 feet lower than during summer months. Turbid or muddy water in some wells resulting from heavy rainfall and heavy use of ground water, particularly during extended dry periods, contributes significantly to the problem (Moore and Hughes, 1979).

Blasting - Collapse sinkholes formed at a quarry (location not given) in Paleozoic dolomitic limestone following a routine blasting event. Ground water entered through the floor of the quarry from an unsuspected conduit. The conduit connected the quarry with a karst cavern network that extended to a nearby river. Immediately following the blasting event, water flowed into the quarry at a rate of about 15,000 gpm, carrying with it eroded karst-fill from the cavern. For the first few weeks, the inflow decreased in response to a rapid decline of the water table within the karst aquifer. The drainage may have led to enlargement of subsurface voids, creating a continuous connection between the river and the quarry. Subsequent river inflow to the pit further eroded fill material from the conduit and the rate of inflow increased over the next several months to over 40,000 gpm (Lolcama and others, 1999).

Drilling - Collapse at a U.S. Geological Survey test well near Keystone Heights, Florida, in 1959-60 buried a driller's helper to a depth of 30 feet and partially buried the geologist at the site. Drilling was at a depth of about 80 feet near the contact between the unconsolidated surficial material and the underlying limestone aquifers. Water level in the shallow aquifer was reportedly higher than in underlying aquifer. The well being drilled was a replacement for another recently completed and abandoned well about 12 feet away. Blasting in the abandoned well to increase yield had damaged the bottom of the casing set at depth of about 80 feet. The casing was removed prior to drilling the new well (Newton, 1987).

Drilling - Installation of wells at Westminster, Maryland, in 1940 was associated with nearby sinkhole collapse. In 1948, the well was replaced by two new wells. During a 72-hour test, the two wells were pumped at a combined rate of 950 to 1050 gpm. A sinkhole formed near the wells and cracks reportedly formed in two nearby buildings (Newton, 1987).

Drought - As many as 40 collapses sinkholes formed in downtown Sylacauga, Alabama, during a prolonged drought in 1953-56. The largest sinkhole was as much as 30 to 40 feet in diameter and 30 to 40 feet in depth. Collapses occurred under streets, water lines, drains, and other structures including a church and football field. Sinkhole activity ceased with recovery of the water table at the end of the drought. Limited activity occurred briefly in 1981 during similar decline in water table. Some water withdrawals contributed to declines during both periods (Newton, 1987)

Freeze Protection – Collapse sinkholes formed near Pierson, Florida, during the period 1973-1979 in the cone of depression created by ground-water withdrawals. Most of the sinkholes are known to have occurred during periods of drawdown caused by irrigation for freeze protection. The remainder formed in secluded locations, but were discovered soon after periods of freeze protection pumping (Rutledge, 1982).

Mine - Many sinkholes developed coincidently with major dewatering (started 1960) of a portion of the Far West Rand mining district near Johannesburg, South Africa. Between December 1962 and February 1966, eight sinkholes greater than 50 m in diameter and 30 m in depth formed. The area is characterized by deep weathering and a thick mantel of surficial material. The depth to bedrock is as much as 400 m and commonly is about 100 m. Ground water was lowered from about 100 m below surface to 550 m below surface in July of 1966. Eight large sinkholes formed after ground water was lowered to 160 m or more. Smaller sinkholes formed in the outer part of the cone of depression where the drawdown was between 60 and 160 m. Several sinkholes formed where rapid seepage of water from the surface hastened the process of roof spalling and cavern enlargement. The largest of the sinkholes formed after a few days of torrential rainfall (Foose, 1967).

Mine - Dewatering a zinc mine near Friedensville, Pennsylvania began in 1953. Active sinkhole collapse occurred in an area of large ground-water withdrawals. Records indicate that 128 sinkholes formed around the dewatering site during period 1953-57. Twenty-five new sinkholes occurred from October 1970 to January 1971. The number of sinkholes occurring during the intervening 13 years was not inventoried. The water table in lowland areas prior to withdrawals was generally at a depth of less than 30 feet. Depth to top of bedrock exceeds 30 feet in numerous areas. Rates of withdrawal between 1953 and 1977 varied between 10 and 30 million gallons per day. The cone of depression in 1967 exceeded 4 mi^2 in area (Metsger, 1979).

Multiple Causes - Collapse sinkholes have been reported since the beginning of the 20th century in the Tournaisis area, southern Belgium. The sinkholes developed from reactivated paleokarsts. Intensive pumping for domestic and industrial water supply, combined with the dewatering due to deep limestone quarries, resulted in the lowering of ground-water levels. This triggered the reactivation of paleokarstic systems resulting in sinkhole collapse (Kaufmann and Quinif, 1999).

Multiple Causes – An estimated 1,000 collapses west of Calera, Alabama include sites of subsidence, fracturing, and significant piping. One collapse, the "December Giant" (fig. 23), measures 145 m long, 115 m wide, and 50 m deep (LaMoreaux and Warren, 1973). The area was dewatered by wells, quarries, and an underground mine. The cone of depression in October 1973 was about 10 mi^2 (26 km^2) in area. Pumpage at that time exceeded 14,000 gallons per minute (883 liters per second). Significant sinkhole development began about 1964. The greatest hazards in this ural area were collapses beneath highways and major gas pipelines. Sinkholes in part of the area were still active in 1981 (Newton, 1976, 1987; Warren, 1976).

Multiple Causes - More than 150 sinkholes, depressions, and related features formed in and adjacent to the proposed right-of-way of Interstate Highway 459 near the community of Greenwood in Bessemer, Alabama. Sinkhole collapse began about 1950 and continued through March 1972. A general lowering of the water table occurred during the early 1950's, or the preceding decade de to large withdrawals of ground water from more than 1,070 wells (1,500 gpm) and deep mines (9,500 gpm), compounded with a prolonged drought during the 1950's (Newton and others, 1973).

Quarry and underground mining - Quarry and mine dewatering extended to within 1.5 miles (2 km) of Farmington, Missouri. Collapses were recorded at least 30 years prior to quarrying and mining and have continued for 10 years subsequent to the completion of mining activities. Although deep mines exist in areas subject to catastrophic collapse in Missouri, and continuous dewatering is required for mining, only minor surface effects have been noted (Williams and Vineyard, 1976).

Quarry and underground quarry, Hershey, Pa. – A series events in surface and underground quarrying near Hershey, Pennsylvania, between 1946 and 1953 altered ground-water levels over an area of 10 mi. About 100 new sinkholes formed within the area where there was a drastic lowering of the water table. Recovery of water levels to nearly normal conditions in 1950 was accompanied by a cessation of sinkhole development (Foose, 1953, 1969).

A blast of August 1946, Hershey, Pa. - Blast in the hanging wall of the underground quarry near Hershey, Pa. exposed a 6-inch-wide solution channel about 275 or 375 feet below the surface. Water flowed at 8,000 to 10,000 gpm, flooding the quarry in one day. Near-by wells dried up, ground-water seepage into a nearby quarry ceased, Derry Spring 1½ miles to the southwest dried up on second day, and water in two nearby wells at the Hershey Chocolate Corporation (1½ miles northeast) rapidly declined. After many months the opening was sealed. Adjacent wells had water in them again, and flow at spring and water levels in corporate wells were restored (Foose, 1953, 1969).

Pumping Test of August 1948, Hershey, Pa. - From August 30 to September 4, 1948, an average of 5,500 gpm was pumped from the underground quarry near Hershey, Pa. as a test preliminary to permanent installation of pumps for deeper quarry operations. The water level was maintained at about 200 feet below the quarry floor. On September 2 the newly drilled Derry Spring well 1½ miles southwest (yield of 2100 gpm) dried up; water level fell from an elevation of 355 ft to 313 ft, which was below the pump intake. On September 8, water level began to rise, and within a couple of days normal pumping operations resumed (Foose, 1953, 1969).

Increased pumping during May 1949, Hershey, Pa. - The quarry operation near Hershey, Pa. inaugurated its new pumping program at about 6,500 gpm normal discharge from pumps with the intake at 340 ft. below the land surface. Derry Spring well dried up. Spring Creek dried up. Many wells throughout the valley went dry. During the second month of the new pumping program, sinkholes began to form in the valley of Spring Creek. The size of the sinkholes ranged from 1 to 20 ft in diameter and 2 to 10 ft deep. Nearly 100 sinkholes formed. More new sinkholes formed during the late summer of 1949 than had previously existed in the areas. During February and March of 1950, grouting in the underground quarry reduced flow into the quarry (flow had reached 8,000 gpm). Springs began to flow again, wells could be pumped, and Spring Creek began to flow. In 1953, the quarry was allowed to flood and became a water storage reservoir. Sinkhole formation ceased after dewatering stopped and the water table had recovered (Foose, 1969).

Quarry - In 1950, a quarry at Pelham, Alabama, was in its early stages of development and sinkholes were not actively occurring. As the excavation progressed, it became necessary to dewater. In 1959, 11 open collapses were observable on aerial photographs and by 1967 34 open collapses were observable. The total distance of sinkhole migration was about 0.4 mile. At some time prior to October 1967, the quarry was abandoned and ground-water pumping stopped, along with sinkhole formation (Newton, 1976).

Quarry - More than 18 sinkhole collapses occurred along a planned highway corridor near Castle Hayne, North Carolina in 1980-81. These sinkholes were under the pavement of an existing road and in or adjacent to its right-of-way near a dewatered quarry. Four sinkholes were triggered by torrential rains in August 1981 (Newton, 1987).

Quarry - In August and September 1994, seven sinkholes up to 5 m in diameter and 3 m deep developed at a residential property adjacent to a limestone quarry in Craven County, North Carolina. The quarry operates about 600m southeast of the sinkholes and pumps water at a rate of 38 million liters per day. Water levels in wells on the perimeter of the quarry site have declined by as much as 5 meters below pre-pumping conditions. Large changes in hydraulic head were observed in monitoring wells at the quarry as the active pit was developed across the quarry site. The collapse of the sinkholes concurrent with large changes in water levels at the quarry suggests that head changes in the limestone aquifer may have been a triggering mechanism for sinkhole collapse (Strum, 1999).

Quarry - In about 1986, a limestone quarry in the Valley and Ridge Province in the southeastern United States began expansion by deepening the quarry to a new level about 60 m (200 ft) below the original water table. Extensive dewatering triggered sinkhole development in a nearby town and along a local railroad track. The ground-water surface was depressed in and around the quarry and appeared to affect the ground-water flow regime in and around the quarry and town. Ground-water levels were lowered 18 to 24 m (60 to 80 ft) at a distance of about 0.8 km (one half mile) from the quarry. Collapse sinkholes began to develop around the quarry, occurring as much as 1.6 km (one mile) from the quarry. A perennial stream was captured by a sinkhole, a sinkhole drained a local wastewater treatment pond, and sinkholes and ground subsidence began to threaten the local railroad track. The summer of 1987 was a drought year for the region, and the likely impact of the drought on sinkhole development in the area was investigated. The investigation concluded that quarry dewatering related to quarry expansion was the primary cause of the sinkholes and subsidence that occurred around the town that year. A few years after the expansion, quarry operations ceased and the quarry naturally filled with water. The writers did not document any further sinkhole or subsidence activity since that time (Kath and others, 1995).

Quarry - Artificial drawdown is the probable cause of a sinkhole problem at Railton in northwestern Tasmania where limestone is excavated from a deep quarry on the floor of a broad valley beneath about 20m of overburden. Prior to quarrying there was little evidence of sinkholes. Local anecdotes suggest minor sinkhole problems arose during the early years of the operation. A new bench was developed in the quarry during the early-mid 1980's, deepening the quarry by 15-20m, and sinkhole collapses increased. The sinkholes appeared to occur within a cone of ground-water depression around the quarry. The town sewage main was ruptured by one sinkhole. A nearby abandoned water-filled quarry drained rapidly. Other sinkholes appeared in pasture close to the quarry and in the backyards of at least two village dwellings. Exposures in the quarry reveal that the limestone surface beneath the overburden consists of pinnacles with a relief of 10 – 15 m. At least two small caves and one major spring were encountered at depth in the quarry. Artificial lowering of the ground-water table due to the quarrying together with differential settlement of the overburden between the limestone pinnacles was reported as the most likely cause of the problem. Inadequate drainage of runoff from the roofs of houses and outbuildings contributed to at least one collapse (Kiernan, 1989).

Quarry - Numerous sinkholes and sites of subsidence developed in a borrow pit area near Andrew Johnson Highway west of Morristown, Tennessee. The borrow pit was active as early as April 1976. Most sinkholes occurred between 1983 and 1986. The site exhibits three distinct levels of excavating with sinkholes occurring on all levels. Ten sinkholes occurred on the lower level, two sinkholes on the middle level, and one sinkhole on the upper level. The number of sinkholes occurring on each level was correlative with amounts of drainage received by each. Three additional sinkholes occurred across a road adjacent to the borrow pit, and collapses in the road have reportedly occurred on more than one occasion (Newton and Tanner, 1987).

Quarries – Ground-water withdrawals from two quarries in the Jamestown, South Carolina area resulted in 42 sites of subsidence and collapse in 1976-78. Collapses range in size from less than 1 ft to over 24 ft in diameter. Most dramatic collapses occur within 5,000 ft of, the point of largest ground water withdrawal. About 20 feet of unconsolidated sands and clays overlie the cavernous limestone that was being quarried. Pumpage was estimated to periodically be in excess of 36 million gallons per day, causing a water level decline of over 35 feet. Water levels in wells over 1.5 miles from the center of pumping have been affected. Blasting has caused "muddying" of water (Spigner, 1978).

Quarries – Ground-water withdrawal from two deep quarries in Birmingham, Alabama, resulted in two overlapping cones of depressions, with apexes being at quarries. More than 200 sinkholes formed in an area of less than 0.5 mi^2 during a period of about 8 years. The formation of many of the sinkholes coincided with periods of heavy rain. Movement of water to one quarry was verified by dye tests. Estimated total average discharge from both quarries exceeds 1.0 mgd. Withdrawals from other sources were not identified (Newton and Hyde, 1971).

References

Adamczyk, A.F., Motyka, Jacek, Wilk, Zbigniew, and Witczak, Stanislaw, 1988, Mine drainage of a karstic aquifer and the related protection problems – Olkusz Mining District, Poland: Proceedings if the IAH 21st Congress, Guilin, China, Geologic Publishing House, Bejing, China, pp. 1097-1104.

Aley, T.J., Williams, J.H., and Massello, J.W., 1972, Groundwater contamination and sinkhole collapse induced by leaky impoundments in soluble rock terrain: Missouri Geological Survey Engineering Geology Series 5, 32 p.

Arbogast, B.F., Knepper, D.H., Jr., and Langer, W.H., 2000, The human factor in mining reclamation: U.S. Geological Survey Circular 1191, 28 p.

Assad, F.A., and Jordan, H., 1994, Karst terranes and environmental aspects: Environmental Geology, v. 23, pp. 228 – 237.

ASTM, 1998, Standard terminology relating to dimension stone, American Society of Testing and Materials Designation C 119-98: American Society of Testing and Materials Annual Book of ASTM Standards, v. 04.07, pp. 6-9.

ASTM, 2000, Standard terminology relating to concrete and concrete aggregates, American Society of Testing and Materials Designation C 125-00: American Society of Testing and Materials Annual Book of ASTM Standards, v. 04.02, pp. 60-63.

Barksdale, R.D., ed., 1991, The aggregate handbook: National Stone Association, 717 p.

Bates, R.L., and Jackson, J.A., eds., 1987, Glossary of Geology: American Geological Institute, 788 p.

Beck, B.F., ed., 1984, Sinkholes - Their geology, engineering and environmental impact: Proceedings of the First Multidisciplinary Conference on Sinkholes, A.A. Balkema, 429 p.

Beck, B.F., ed., 1989, Engineering and environmental impacts of sinkholes and karst: Proceedings of the Third Multidisciplinary Conference on Sinkholes and the Engineering and Environmental Impacts of Karst, A.A. Balkema, 384 p.

Beck, B.F., ed., 1993, Applied karst geology: Proceedings of the Fourth Multidisciplinary Conference on Sinkholes and the Environmental Impacts of Karst, A.A. Balkema, 295 p.

Beck, B.F., ed., 1999, Sinkholes and the Engineering and Environmental Impacts of Karst: Engineering Geology, v. 52, nos. 1-2, 152 p.

Beck, B.F., and Pearson, F.M., eds., 1995, Karst geohazards – Engineering and environmental problems in karst terrane: Proceedings of the Fifth Multidisciplinary Conference on Sinkholes and the Environmental Impacts of Karst, A.A. Balkema, 581 p.

Beck, B.F., and Stephenson, J.B., eds., 1997, The engineering geology and hydrogeology of karst terranes: Proceedings of the Sixth Multidisciplinary Conference on Sinkholes and the Engineering and Environmental Impacts of Karst, A.A. Balkema, 516 p.

Beck, B.F., and Wilson, W.L., eds., 1987, Karst hydrology: Engineering and environmental applications: Proceedings of the Second Multidisciplinary Conference on Sinkholes and the Environmental Impacts of Karst, A.A. Balkema, 467 p.

Beck, B.F., Pettit, A.J., and Herring, J.G., eds., 1999, Hydrogeology and engineering geology of sinkholes and karst: Proceedings of the Seventh Multidisciplinary Conference on Sinkholes and the Engineering and Environmental Impacts of Karst, A.A. Balkema, 478 p.

Bell, F.G., 1992, Open excavation in rock masses, *in*, Bell, F.G., ed., Engineering in rock masses: Buterworth, Heinemann, Oxford, England, p. 400-422.

Berger, P.R., Ford, W.C., Graham, E.K., Long, J.F., Jr., Rohrs, D.M., West, J.R., and Willard, R.B., 1991, Environmental and community concerns, *in* Barksdale, R.D., The Aggregate Handbook: National Stone Association, p. 5-1 – 5-59.

Bobrowsky, P.T., ed., 1998, Aggregate resources - A global perspective: A.A. Balkema, Rotterdam, Netherlands, 470 p.

Bowles, Oliver, 1939, The Stone Industries: McGraw Hill Book Company, 519 p.

Crawford, N.C., 1986, Karst hydrological problems associated with urban development – ground water contamination, hazardous fumes, sinkhole flooding and sinkhole collapse in the Bowling Green area, Kentucky: Field Trip Guide Book, Centre for Cave and Karst Studies, Western Kentucky University, 86 p.

Cvijíc, J., 1893, Das karstphanomen: Versuch einer morphologischen Monographie, Geographische Abhandlungen herausgegeben von A Pench, Bd., V. H, 3. Wien.

Dodge, E.D., 1984, Les characteristiques hydrogeoloqigues des aquifers kartisques du Causse Comtal (Aveyron, France): Hydrogeologie-Geologie de l'ingenieur, v. 3, pp. 241-252.

Dolley, T.P., 1999, Crushed stone: U.S. Geological Survey Minerals Yearbook, pp. 73.1-73.11.

Drew, David, 1999, Chapter 1 – Introduction, *in* Drew, David, and Hötzl, Heinz, eds.: Karst hydrology and human activities – Impacts, consequences and implications, A.A. Balkema, pp. 3-12.

Drew, David, and Hötzl, Heinz, eds., 1999: Karst hydrology and human activities – Impacts, consequences and implications, A.A. Balkema, 322 p.

Drysdale, R., Pierotti, L., and Baldacci, F., 2001, Suspended sediments in karst spring waters near Massa (Tuscany), Italy: Environmental Geology, v. 40, pp. 1037-1050.

Edwards, A.J., Hobbs, S.L., and Smart, P.L., 1991, Effects of quarry dewatering on a karstified limestone aquifer; a case study from the Mendip Hills, England, *in* Proceedings of the Third Conference on Hydrogeology, ecology, monitoring and management of groundwater in karst terranes, National Water Well Association, pp. 77-91.

Ekmekçi, M., 1993, Impact of quarries on karst groundwater systems, *in* Günay, G., Johnson, A.I., and Back, W., eds, Hydrogeological processes in karst terranes: Proceedings of the Antalya Symposium and Field Seminar, October 1990, IAHS Publication no. 207, p. 3-6.

Fletcher, J.L., and Busnel, R.G., 1978, Effects of noise on wildlife: Academic Press, New York.

Foose, R.M., 1953, Ground-water behavior in the Hershey Valley, Pennsylvania: Geological Society of America Bulletin, v. 64, pp. 623-646.

Foose, R.M., 1967, Sinkhole formation by groundwater withdrawal; Far West Rand, South Africa: Science, v. 157, pp. 1045-1048.

Foose, R.M., 1969, Mine dewatering and recharge in carbonate rocks near Hershey, Pennsylvania, *in* Kiersch, G.A., Cleaves, A.B., Adams, W.M., Pincus, H.J., and Ferguson, H.F., eds., Legal aspects of geology in engineering practice: Geological Society of America, Engineering Geology Case Histories no. 7, pp. 46-60.

Foose, R.M., and Humphreville, J. A., 1979, Engineering geological approaches to foundations in the karst terrain of the Hershey Valley: Bulletin of the Association of Engineering Geologists, v. 16, no. 3, pp. 355-381.

Ford, D.C., ed., 1993, Environmental change in karst areas: Environmental Geology, v. 21, no. 3, pp. 107-200.

Ford, D.C., and Williams, P.W., 1989, Karst geomorphology and hydrology: Unwin-Hyman, London, 601 p.

Fraser, Hannah, and Grapes, Tim, 1998, Impact of quarry dewatering on a water dependent conservation site, *in* Van Brahana, John, Eckstein, Yoram, Ongley, L.K., Schneider, Robert, and Moore, J.E., eds., Gambling with groundwater – Physical, chemical, and biological aspects of aquifer-system relations: American Institute of Hydrology, pp. 469-474.

Gagen, Peter, and Gunn, John, 1987, A geomorphological approach to restoration blasting in limestone quarries, *in* Beck, B.F., and Wilson, W.L., eds., Karst hydrology: Engineering and environmental applications: Proceedings of the Second Multidisciplinary Conference on Sinkholes and the Environmental Impacts of Karst, A.A. Balkema, pp. 457-461.

Gary, M.K., 1999, Maryland's zone of dewatering influence law for limestone quarries, *in* Beck, B.F., Pettit, A.J., and Herring, J.G., eds., Hydrogeology and engineering geology of sinkholes and karst – 1999: Proceedings of the Seventh Multidisciplinary Conference on Sinkholes and the Engineering and Environmental Impacts of Karst, A.A. Balkema, pp. 273-277.

Gillieson, David, and Houshold, Ian, 1999, Chapter 6.3 – Rehabilitation of the Lune River Quarry, Tasmanian Wilderness World Heritage Area, Australia: *in* Drew, David, and Hötzl, Heinz, eds. Karst hydrology and human activities – Impacts, consequences and implications, A.A. Balkema, pp. 201-205.

Gunn, John, 1986, A conceptual model for conduit flow dominated karst aquifers, *in* Günay, Gültekïn, and Johnson, A.I., eds., Karst water resources: IAHS Publication 161, pp. 587-596.

Gunn, John, 1993, The geomorphic impacts of limestone quarrying, *in* Williams, P.W., ed., Karst terrains – Environmental changes and human impact: Catena Supplement 25, Catena Verlag, Cremlingen, pp. 187-197.

Gunn, John, and Bailey, Debra., 1993, Limestone quarrying and quarry reclamation in Britain: Environmental Geology, v. 21, pp. 167 – 172.

Gunn, John, Bailey, Debra, and Handley, John, 1997, The reclamation of limestone quarries using landform replication: Department of Geographical & Environmental Sciences, University of Huddersfield, Queensgate, Huddersfield, U.K., 176 p.

Gunn, John, and Gagen, Peter, 1987, Limestone quarrying and sinkhole development in the English Peak District, *in* Beck, B.F., and Wilson, W.L., eds., Karst hydrology: Engineering and environmental applications: Proceedings of the Second Multidisciplinary Conference on Sinkholes and the Environmental Impacts of Karst, A.A. Balkema, pp. 121-125.

Gunn, John, and Hobbs, S.L., 1999, Chapter 6.2 Limestone quarrying: hydrogeological impacts, consequences, implications: *in* Drew, David, and Hötzl, Heinz, eds.: Karst hydrology and human activities – Impacts, consequences and implications, A.A. Balkema, pp. 192-201.

Hess, J.W., and Slattery, L.D., 1999, Chapter 6.1 Overview of extractive industries impact, *in* Drew, David, and Hötzl, Heinz, eds.: Karst hydrology and human activities – Impacts, consequences and implications, A.A. Balkema, pp. 187-192.

Hobbs, S.L., and Gunn, John, 1998, The hydrogeological effect of quarrying karstified limestone: options for protection and mitigation: Quarterly Journal of Engineering Geology, v. 31, pp. 147-157.

Howard, Bob, and Cameron, Ian, 1998, Dust control: Best Practice Environmental Management in Mining, Environment Australia, 73 p.

Jennings, J.N., 1985, Karst geomorphology: Bell and Bain Ltd., Glasgow, 293 p.

Kath, R.L., McClean, A.T., Sullivan, W.R., and Humphries, R.W., 1995, Engineering impacts of karst: Three engineering case studies in Cambrian and Ordovician carbonates of the Valley and Ridge Province, *in* Beck, B.F., and Pearson, F.M., eds., Karst geohazards – Engineering and environmental problems in karst terrane: Proceedings of the Fifth Multidisciplinary Conference on Sinkholes and the Environmental Impacts of Karst, A.A. Balkema, pp. 469-457.

Kaufmann, Oliver, and Quinif, Yves, 1999, Cover-collapse sinkholes in the "Tournaisis" area, southern Belgium: Engineering Geology, v. 52, nos. 1&2, pp. 15-22.

Kelk, B., 1992, Natural resources in the geological environment, *in* Lumsden, G.I., 1992, ed. Geology and the environment in Western Europe: Oxford University Press, New York, p. 34 – 138.

Kestner, M., 1994, Developing a dust control plan: Stone Review v.10, no. 1, p. 22-23.

Kiernan, Kevin, 1989, Sinkhole hazards in Tasmania, *in* Beck, B.F., ed., Engineering and environmental impacts of sinkholes and karst: Proceedings of the Third Multidisciplinary Conference on Sinkholes and the Engineering and Environmental Impacts of Karst, A.A. Balkema, pp. 123-128.

Kochanov, W.E., 1999, Sinkholes in Pennsylvania: Pennsylvania Geological Survey, 4th Series, Educational Series 11, 33 p.

Kolm, K.E., 1996, Conceptualization and characterization of ground-water systems using geoscientific information systems, *in* May, J. and Kolm, K. E., eds, 1996, Special Issue: Advanced Techniques for Solving Groundwater Contaminant Problems: Engineering Geology, Vol. 42; Nos. 2 - 3, Elsevier Publishers, p. 111 - 118.

Kresic, Neven, Papic, Petar, and Golubovic, Radosav, 1992, Elements of groundwater protection in a karst area: Environmental geology Water Science, v. 20., no. 3, pp. 157-164.

LaMoreaux, P.E., 1997, Legal aspects of karst and insurability, *in* Günay, Gültekin, and Johnson, A.I., eds., Karst waters & environmental impacts: Proceedings of the 5th International Symposium and Field Seminar on Karst Waters and Environmental Impacts, Antalya, Turkey, A.A. Balkema, pp. 11-17.

LaMoreaux, P.E., Powell, W.J., and LeGrand, H.E., 1997, Environmental and legal aspects of karst areas: Environmental Geology, v. 29, no. 1/2, pp. 23 – 36.

LaMoreaux, P.E., and Newton, J.G., 1986, Catastrophic subsidence: An environmental hazard, Shelby County, Alabama: Environmental Geology Water Science, v. 8, no. 1/2, p. 25-40.

LaMoreaux, P.E., and Warren, W.M., 1973, Sinkhole: Geotimes, v. 18, no. 3, p. 15.

Langer, W.H., 2001, Environmental impacts of mining natural aggregate, *in* Bon, R.L., Riordan, R.F., Tripp, B.T., and Krukowski, S.T., eds., Proceedings of the 35th Forum on the Geology of Industrial Minerals—The Intermountain West Forum: Utah Geological Survey Miscellaneous Publication 01-2, p. 127-138.

Langer, W.H., in press, Environmental Risk Analysis and Aggregate Mining, *in* Proceedings of the 37th Forum on the Geology of Industrial Minerals, 2001: British Columbia Ministry of Energy and Mines.

Langer, W.H., and Kolm, K.E., 2001, Hierarchical systems analysis of potential environmental impacts of aggregate mining: Society for Mining, Metallurgy, and Exploration, Inc., Annual Meeting, 2001, Preprint No. 01-103, 10 p.

Lolcama, J.L., Cohen, H.A., and Tonkin, M.J., 1999, Deep karst conduits, flooding and sinkholes: Lessons for the aggregates industry, *in* Beck, B.F., Pettit, A.J., and Herring, J.G., Hydrogeology and engineering geology of sinkholes and karst – 1999: Proceedings of the Seventh Multidisciplinary Conference on Sinkholes and the Engineering and Environmental Impacts of Karst, A.A. Balkema, pp. 51–55.

Lüttig, G.W, 1994, Rational management of the geo-environment – A view in favour of "geobased" planning – with special reference to aggregate resources, *in* Lüttig, G.W., ed., Aggregates -- Raw materials' giant: Report on the 2nd International Aggregate Symposium, Erlangen, 346 p.

Martin, A.D., 1995, Maryland Route 31 sinkhole, *in* Beck, B.F., and Pearson, F.M., eds., Karst geohazards – Engineering and environmental problems in karst terrane: Proceedings of the Fifth Multidisciplinary Conference on Sinkholes and the Environmental Impacts of Karst, A.A. Balkema, pp. 331-334.

Metsger, R.W., 1979, Mining problems in a karst valley – Technical and social: Bulletin of the Association of Engineering Geologists, v. 16, n. 3, pp. 427-447.

Meyers, P.B., Jr., and Perlow, M., Jr., 1984, Development, occurrence, and triggering mechanisms of sinkholes in the carbonate rocks of the Lehigh Valley, eastern Pennsylvania, *in* Beck, B.F., ed., 1984, Sinkholes - Their geology, engineering and environmental impact: Proceedings of the First Multidisciplinary Conference on Sinkholes, A.A. Balkema, pp. 11-15.

Moore, J.D., and Hughes, T.H., 1979, Effect of quarry blasting on ground-water quality in a limestone terrane in Calhoun County, Alabama: Water Resources Research Institute Bulletin 38, Auburn University, 72 p.

Moore, A.B., and Richards, A.J., 1999, Blast vibration assessment for planning and control: Quarry, v.7, no. 4, p. 28-32.

National Academy of Sciences, 1980, Surface mining of non-coal minerals - Appendix I - Sand and gravel mining, and quarrying and blasting for crushed stone and other construction minerals: National Academy of Sciences, Washington, D.C., 91 p.

Newton, J.G., 1976, Induced sinkholes – A continuing problem along Alabama highways, *in* International Association of Hydrologic Sciences, Land Subsidence Symposium: Proceedings of the Second International Symposium on Land Subsidence held at Anaheim, California, IAHS-AISH Publication no. 121, pp. 453-463.

Newton, J.G., 1984a, Review of induced sinkhole development, *in* Beck, B.F., ed., Sinkholes: Their geology, engineering and environmental impact: Proceedings of the First Multidisciplinary Conference on Sinkholes, A.A. Balkema, pp. 3-9.

Newton, J.G., 1984b, Sinkholes resulting from ground-water withdrawals in carbonate terranes-an overview, *in* Holzer, T.L., ed., Man-induced land subsidence: Geological Society of America, Reviews in Engineering Geology, v. 6, pp. 195-202.

Newton, J.G., 1984c, Case History No. 9.11. Alabama, U.S.A., *in* Poland, J.F., ed., Guidebook to studies of land subsidence due to ground-water withdrawal: UNESCO, pp. 245-251.

Newton, J.G., 1986, Natural and induced sinkhole development in the eastern United States, *in* Johnson, A.I., Carbognin, Laura, and Ubertini, L., eds., Land Subsidence: Proceedings of the Third International Symposium on Land Subsidence held in Venice, Italy, IAHS Publication No. 151, pp. 549-564.

Newton, J.G., 1987, Development of sinkholes resulting from man's activities in the Eastern United States; U.S. Geological Survey Circular 968, 54 p.

Newton, J.G., Copeland, C.W., and Scarbough, L.W., 1973, Sinkhole problem along proposed route of Interstate Highway 459 near Greenwood, Alabama: Alabama Geological Survey Circular 83, 53 p.

Newton, J.G., and Hyde, L.W., 1971, Sinkhole problem in and near Roberts Industrial Subdivision, Birmingham, Alabama – A reconnaissance: Geological Survey of Alabama Circular 68, 42 p.

Newton, J.G., and Tanner, J.M., 1987, Case histories of induced sinkholes in the eastern United States, *in* Beck, B.F., and Wilson, W.L., eds., Karst hydrology: Engineering and environmental applications: Proceedings of the Second Multidisciplinary Conference on Sinkholes and the Environmental Impacts of Karst, A.A. Balkema, pp. 15-23.

Primel, Louis, and Tourenq, Claude, 2000, eds., Aggregates: Balkema, 590 p.

Prokopovich, N.P., 1985, Development of karst sinkholes and fluctuations of aquifer levels, *in* Günay, Gültekïn, and Johnson, A.I., eds., Karst water resources: IAHS Publication 161, pp. 387-397.

Quinlan, J.F., 1986, Legal aspects of sinkhole development and flooding in karst terranes - 1. Review and synthesis; Environmental Geology and Water Sciences, v. 8, nos. 1/2, pp. 41-61.

Ritter, D.F., Kochel, R.C., and Miller, J.R., 1995, Process geomorphology – Third edition: Wm C. Brown Publishers, Chicago, 546 p.

Rutledge, A.T., 1982, Hydrology of Floridian aquifer in northwest Volusia County, Florida: U.S. Geological Survey Water-Resources Investigations Open-File Report 82-108, 116 p.

Sauro, U., 1993, Human impact on the karst of the Venetian Fore-Alps, Italy: Environmental Geology, v. 21, pp. 115-121.

Sedam, A.C., Eberts, S.M., and Bair, E.S., 1988, Ground-water levels, water quality, and potential effects of toxic-substance spills or cessation of quarry dewatering near a municipal ground-water supply, southern Franklin County, Ohio: U.S. Geological Survey Water-Resources Investigations report 88-4138, 93 p.

Sinclair, W.C., 1982, Sinkhole development resulting from groundwater withdrawal in the Tampa area, Florida: U.S. Geological Survey Water Resources Investigation 81-50, 19 p.

Sinclair, W.C., and Stewart, J.W., 1985, Sinkhole type, development, and distribution in Florida: Florida Bureau of Geology, Map series No. 110.

Smart, P.L., Edwards, A.J., and Hobbs, S.L., 1991, Heterogeneity in carbonate aquifers: Effects of scale, fissuration, lithology and karstification,*in* Proceedings of the Third Conference on Hydrogeology, ecology, monitoring and management of groundwater in karst terranes: National Water Well Association, pp. 373-388.

Smart, P.L., and Friedrich, H., 1986, Water movement and storage in the unsaturated zone of a maturely karstified carbonate aquifer, Mendip Hills, England, *in* Proceedings Environmental Problems in Karst Terranes and Their Solutions Conference: National Water Well association, 59-87.

Smith, M.R., and Collis, L., eds., 2001, Aggregates -- Sand, gravel and crushed rock aggregates for construction purposes, 3rd Edition: Geological Society of Engineering Geology Special Publication No. 17, London, The Geological Society, 339 p.

Sowers, G.F., 1976, Mechanisms of subsidence due to underground openings, *in*, National Academy of Science, Subsidence over mines and caverns, moisture and frost actions, and classification: Transportation Research Record 612, pp. 2-8

Spigner, B.C., 1978, Land surface collapse and ground-water problems in the Jamestown area, Berkley County, South Carolina: South Carolina Water Resources Commission Open-File Report 78-1, 99 p.

Stanton, W., 1966, The impact of quarrying on the Mendip Hills, Somerset: Proceedings of the University of Bristol Speleological Society, v. 11, p. 54-62.

Stanton, W., 1990, Hard limestone – Too valuable to quarry: Minerals Planning, v. 43, pp. 3-9.

Stringfield, V.T., and Rapp, J.R., 1976, Land subsidence resulting from withdrawal of ground water in carbonate rocks, *in* International Association of Hydrologic Sciences, Land Subsidence Symposium: Proceedings of the Second International Symposium on Land Subsidence held at Anaheim, California, IAHS-AISH Publication no. 121, pp.447-452.

Strum, Stuart, 1999, Topographic and hydrogeologic controls on sinkhole formation associated with quarry dewatering, *in* Beck, B.F., Pettit, A.J., and Herring, J.G., Hydrogeology and engineering geology of sinkholes and karst – 1999: Proceedings of the Seventh Multidisciplinary Conference on Sinkholes and the Engineering and Environmental Impacts of Karst, A.A. Balkema, pp. 63 – 66.

Sweeting, M.M., 1981, Karst Geomorphology: Benchmark Papers in Geology / 59, Hutchinson Ross Publishing Company, Stroudsburg, Pennsylvania, 427 p.

Tepordei, V.V., 1999, Crushed stone: U.S. Geological Survey Minerals Yearbook, pp. 72.1-72.32

Thorp, M.J.W., and Brook, G.A., 1984, Application of double Fourier series analysis to ground subsidence susceptibility mapping in covered karst terrain, *in* Beck, B.F., ed., Sinkholes: Their geology, engineering and environmental impact: Proceedings of the First Multidisciplinary Conference on Sinkholes, A.A. Balkema, pp. 197-20?.

Ursic, K.A., Kenkel, N.C., and Larson, D.W., 1997, Revegetation dynamics of cliff faces in abandoned limestone quarries: Journal of Applied Ecology, v. 34, pp. 289-303.

Urushibara-Yoshino, K., 2000, Newsletter on annotated bibliography, No. 8: International Geographical Union, Department of Geography, Hosei University, Tokyo, 71 p.

Veni, George, and DuChene, Harvey, eds., 2001, Living with karst: American Geological Institute Environmental Awareness Series, 4, 64 p.

Vermeulen, Jaap, and Whitten, Tony, 1999, Biodiversity and cultural property in the management of limestone resources: World Bank, Washington, D.C., 120 p.

Waltham, A.C., 1989, Ground subsidence: Blackie & Son Limited, London, 195 p.

Warren, W.M., 1976, Sinkhole occurrence in western Shelby County, Alabama: Geological Survey of Alabama Circular 101, 45 p.

Warren, W.M., and Wielchowsky, C.C., 1973, Aerial remote sensing of carbonate terranes in Shelby County, Alabama: Ground Water, v. 11, no. 6, p. 14-26.

White, W.B., and White, E.L., 1995, Thresholds for soil transport and the long term stability of sinkholes, *in* Beck, B.F., and Pearson, F.M., eds., Karst geohazards – Engineering and environmental problems in karst terrane: Proceedings of the Fifth Multidisciplinary Conference on Sinkholes and the Environmental Impacts of Karst, A.A. Balkema, pp.73-78.

White, W.B., Culver, D.C., Herman, J.S., Kane, T.C., and Mylroie, J.E., 1995, Karst lands: American Scientist, v. 83, pp. 450-459.

Williams, J.H., and Vineyard, J.D., 1976, geologic indicators of subsidence and collapse in karst terrain in Missouri, *in*, National Academy of Science, Subsidence over mines and caverns, moisture and frost actions, and classification: Transportation Research Record 612, pp. 31-37.

Williams, P.W., ed., 1993, Karst terrains – Environmental changes and human impact: Catena Supplement 25, Catena Verlag, Cremlingen, 268 p.

Wilson, W.L., and Beck, B.F., 1992, Hydrogeologic factors affecting new sinkhole development in the Orlando area, Florida: Ground Water, v. 30, no. 6, pp. 918-930.

Yuan, Daoxian, 1987, Karst hydrology: Engineering and environmental applications, *in* Beck, B.F., and Wilson, W.L., eds., Proceedings of the Second Multidisciplinary Conference on Sinkholes and the Environmental Impacts of Karst: A.A. Balkema, pp.1-11.

An Assessment of the Economic Impact of the Proposed Stoneco Gravel Mine Operation on Richland Township

August 15, 2006

George A. Erickcek
Senior Regional Analyst
W.E. Upjohn Institute for Employment Research

An Activity of the W.E. Upjohn Unemployment Trustee Corporation

W.E. Upjohn Institute for Employment Research

300 South Westnedge Avenue • Kalamazoo, Michigan 49007-4686 • U.S.A.
Telephone (269) 343-5541 • FAX (269) 342-0672

An Assessment of the Economic Impact of the Proposed Stoneco Gravel Mine Operation on Richland Township

George A. Erickcek
Senior Regional Analyst
W.E. Upjohn Institute for Employment Research

Executive Summary/Introduction

This report, which was completed at the request of the Richland Township Planning Commission, provides an estimation of the economic impact of the proposed Stoneco Gravel Mine Operation on Richland Township.[1] The following impacts are assessed in this study:

1. The potential impact on residential property values in Richland Township.
2. The potential employment impact of the proposed gravel mine on the area's economy.

In addition, we carefully reviewed the economic impact reports provided by Stoneco for consideration.

In the preparation of this impact analysis we used nationally-recognized modeling techniques that are the standard for academic research.

We estimate that the proposed gravel mine will have a significant negative impact on housing values in Richland Township. Once in full operation, the gravel mine will reduce residential property values in Richland and Richland Township by $31.5 million dollars, adversely impacting the values of over 1,400 homes, which represent over 60 percent of the Richland residences.

In addition, the mining operation will have an insignificant impact on area employment and personal income. At most, we estimate that only 2 additional jobs will be created in Kalamazoo County due to the mining operation. The mining operation serves the local market, and analysis based on the Institute's econometric regional model for the Kalamazoo region shows that it will bring in an insignificant amount of new income into the area's economy, $58,000. Although the mine will employ an estimated 5 to 10 workers and require drivers to haul an estimated 115 to 120 truck loads of gravel per day,

[1] The report was completed without charge as part of the W.E. Upjohn Institute's community service commitment. The Institute has prepared requested reports and analyses for the City of Kalamazoo, theCity of Hastings, the City of Battle Creek, the City of Grand Rapids as well as other local governmental units and school districts.

most all of these jobs would simply "displace" any employment growth in the county's 15 existing gravel pits.

Stoneco has not established a need for new aggregate capacity. Kalamazoo County is currently serviced by 15 gravel operations, and in recent years, employment in the county has been shrinking and the population has been stagnant. Consequently, there is no *prima facie* case that new capacity is needed. To definitively determine whether such a need exists, we would need to have information on projected demand for aggregated material in the county and capacity of the gravel pits currently servicing the county.

Finally, a careful evaluation of the five impact studies presented by the Stoneco finds that their methodologies are seriously flawed, and thus conclusions drawn from the analyses are invalid.

Qualifications

The W.E. Upjohn Institute for Employment Research is an internationally-recognized independent, non-profit economic research organization established in 1945 for the sole purpose of conducting research into the causes and effects of unemployment and measures for the alleviation of unemployment. The Institute currently has a staff of 60 including 10 senior-level economists, and its research agenda includes issues on the international, national, state, and local levels.

For the past 20 years the W.E. Upjohn Institute has maintained a strong research focus on west Michigan which includes

- The publication of its quarterly economic report: *Business Outlook for West Michigan.*
- The preparation of short- and long-term employment forecasts for all of the metropolitan areas in west Michigan including Kalamazoo, Battle Creek, Grand Rapids, Muskegon, and Holland.
- The completion of numerous economic impact reports and economic development strategies for communities in Michigan.

George Erickcek, the Institute's Senior Regional Analyst, was the lead researcher for this study. He received his Masters of Economics at the University of Pittsburgh and has been with the Institute since 1987. George has prepared numerous economic impact, benchmarking, and forecasting studies for the west Michigan region, and has conducted research on the national and international level.

Methodological Approach to Estimating the Impact on Housing Values of the Proposed Gravel Mine

Many factors influence housing prices. These include, of course, the characteristics of the house or dwelling unit, such as size, age, lot size, number of bedrooms and bathrooms, as well as its upkeep. In addition, the house's proximity to amenities such as a lake or pleasing neighborhood or "disamenities" (e.g. landfills, pollution sites) can have a substantial impact on its price.[2]

Economists have found that "hedonic pricing models" are extremely useful in isolating the contribution of specific factors on the price of housing, as well as other goods. First developed by University of Chicago economist Sherwin Rosen in 1974, hedonic pricing models use a statistical regression technique that allows the researcher to estimate the impact of one factor, e.g. the proximity of a neighborhood park, on the value of a house while holding all of the other factors impacting the house's value constant. There is an extensive literature applying hedonic pricing models to study the effects of environmental disamenities on residential property values. These studies generally show that proximity to landfills, hazardous waste sites, and the like has a significant negative effect on the price of a residential property.[3]

Professor Diane Hite, an economist who has published widely in the area of property value impact analysis, has recently applied hedonic pricing methodology to study the effects of a gravel mine on nearby residential values. This appears to be the only rigorous study to date of gravel mine impacts on property values.[4] Her study is based on detailed data from Delaware County, Ohio that were collected by the Ohio State University for the purposes of studying land use planning.

Hite examines the effects of distance from a 250-acre gravel mine on the sale price of 2,552 residential properties from 1996 to 1998. Her model controls for a large set of other factors that determine a house's sale price, including number of rooms, number of bathrooms, square footage, lot size, age of home, sale date, and other factors specific to the locality, so that she can focus solely on the effect of proximity to the gravel mine on house values. She finds a large, statistically significant effect of distance from a gravel mine on home sale price: controlling for other determinants of residential value, proximity to a gravel mine reduces sale price. Specifically, Hite reports that the elasticity of house price with respect to distance from a gravel mine is .097, implying that a 10 percent increase in distance from the gravel mine is associated with slightly less than a 1 percent increase in home value, all else the same (Appendix A).[5] Conversely, the closer the house to the proximity to the mine, the greater the loss in house value.

---

[2] In a recent study of the impact of housing programs in the City of Kalamazoo, we found that moving a house from one neighborhood to another can add or subtract as much as $20,000 from its value.

[3] For reviews of some of this literature, see Arthur C. Nelson, John Genereux, and Michelle Genereux, "Price Effects of Landfills on House Values," *Land Economics*, 1992 68(4): 359-365 and Diane Hite, Wen Chern, Fred Hitzhusen, and Alan Randall, "Property-Value Impacts of an Environmental Disamenity: The Case of Landfills," *The Journal of Real Estate Finance and Economics* 22, no. 2/3 (2001): 185-202

[4] Diane Hite, 2006. "Summary Analysis: Impact of Operational Gravel Pit on House Values, Delaware County, Ohio," Auburn University.

[5] This estimate is based on a constant elasticity model specification. At the Upjohn Institute's request, Professor Hite tested the sensitivity of these findings to model specification, and in all specifications finds a large, statistically significant negative effect of proximity to gravel pit on house prices. The simulations for Richland Township reported below are based on the estimates from the constant elasticity specification and yield slightly lower estimated negative property value impacts than those based on models using other functional forms. We consider this number to be a conservative estimate.

Figure 1 displays the estimated effects of distance from the gravel pit on house price. A residential property located a half mile from the gravel mine would experience an estimated 20 percent reduction in value; one mile from the mine, a 14.5 percent reduction; 2 miles from the mine, an 8.9 percent reduction; and 3 miles from the mine, a 4.9 percent reduction. These estimates are similar to estimates published in academic journals on the effects of landfills on nearby property values.

Figure 1: Impact of Gravel Pit on Residential Property Values:
(Percent Reduction by Distance from Mine)

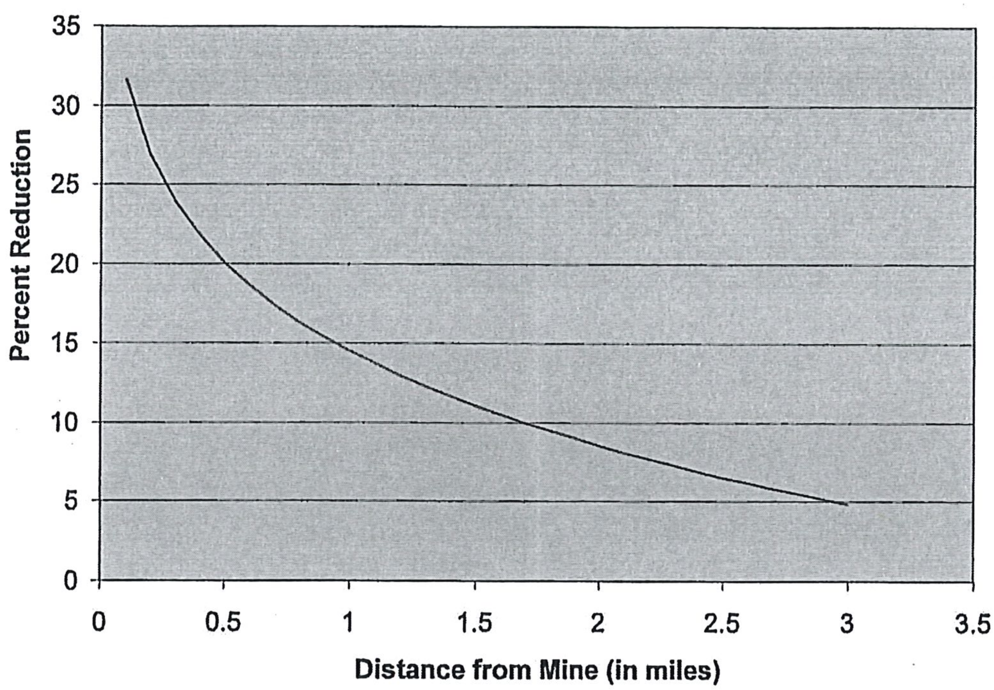

The loss in property value results from the negative consequences of the mining operation and reflects the deterioration in the area's quality of life due solely to the operation of the gravel mine. In other words, the loss in house value is a way to quantify in dollars the deterioration in quality of life, as capitalized in the price of the house. It captures the price reduction the homeowner would have to offer to induce a new buyer to purchase the property. Even if homeowners do not move as a result of the gravel mine, they will lose homeowner equity as the potential sale price of their house is less.[6] Therefore, regardless of whether or not a person actually sells their property, it measures

[6] Only those owning property at the time of the establishment of the gravel mine would experience a loss in equity. Those purchasing property near an established mine would not experience an equity loss because any negative effects from the mine's operation would have been incorporated into the purchase price. By implication, few property owners near long-established mines could claim loss of property value from the mine because few would have owned the properties at the time the mine went into operation.

the adverse effects in their quality of life in being subjected to the disamenities introduced into the area by the gravel mine.

The policy implications of Hite's study are clear: because property value losses are higher the closer to the gravel mine, all else the same, new sites should be located far from existing residences so as to minimize adverse consequences for homeowners.

Simulation of Gravel Mine on Residential Property Values in Richland

Utilizing the estimates from the Hite study and data on 2006 assessed values provided by Richland Township, the Upjohn Institute simulated the effects of the proposed gravel mine on residential property values in Richland Village and Richland Township. Our analysis is based on 2005 assessed values of single-family homes in Richland Township and Richland Village obtained from the Township's assessor office in June and July. In total 2,319 single-family homes, 88.7 percent of all single-family residences in the township and village, were geo-coded using the ArcView© mapping program, manually matched using Yahoo© maps and, finally, through drive-by inspection of addresses. Once all of the homes were mapped, the distance between each of the residences and the closest boundary of proposal Stoneco gravel mine was determined.

As shown in Table 1, more than 1,400 homes will be negatively impacted by the proposed gravel mine with the total cost reaching $31.5 million dollars.

Table 1
Estimated Impact on Housing Values of the Proposed Stoneco Gravel Mine

Distance (miles from Stoneco Site)	Number of Houses Affected	Estimated Loss in Value	Distance (miles from Stoneco Site)	Number of Houses Affected	Estimated Loss in Value
0.1	2	$211,703	1.6	73	$1,207,011
0.2	3	$106,428	1.7	128	$2,500,456
0.3	2	$134,894	1.8	99	$1,630,149
0.4	9	$522,981	1.9	70	$1,146,761
0.5	3	$389,319	2	34	$633,720
0.6	8	$598,518	2.1	105	$952,068
0.7	24	$831,338	2.2	98	$1,311,040
0.8	25	$798,108	2.3	99	$2,843,845
0.9	27	$1,085,190	2.4	72	$2,699,584
1	22	$918,374	2.5	34	$912,133
1.1	75	$2,428,602	2.6	12	$377,548
1.2	62	$1,688,031	2.7	23	$373,873
1.3	45	$1,146,920	2.8	80	$939,861
1.4	32	$824,928	2.9	55	$944,061
1.5	30	$712,731	3	70	$655,846
			Total	1,421	$31,526,020

While Hite's original study covered a 5-mile radius from the gravel mine in Ohio, we chose to examine only a 3-mile area from the boundaries of the proposed Stoneco site.[7] Only properties located in Richland and Richland Township are included. Property values in other townships, notably Prairieville Township, also could be adversely affected by the location of a gravel mine near its border with Richland Township but were not included in the study. In addition, the analysis does not consider possible effects on commercial property. Our estimates do not factor in the likely negative impact on property values along the truck routes used for the mine. Finally, although Stoneco has proposed to reclaim some of the land for a lake and residential development, its proposed timeframe for this development would occur too far into the future to mitigate adverse property value impacts for current Richland area residents.

Employment and Personal Income Impact

Stoneco estimates that 5 to 10 permanent jobs will be created at the proposed mine. In addition, truck drivers will be required for the 115 to 120 truck loads of gravel that will be hauled from the mine daily.

To measure the potential employment and income impact of the gravel mine, we used the Institute's econometric regional model of the Kalamazoo area.[8] Because of its weight and low-value, gravel is hauled for only short distances. It is not a part of the area's economic base that brings new monies into the area. Therefore, it is an activity that does not generate any significant new income or employment opportunities. We estimate that only 2 additional new jobs will be created in Kalamazoo County due to the gravel mine and personal income in the county will increase by only $58,000. In short, the jobs created at the gravel mine will displace jobs elsewhere in Kalamazoo County or the immediate region. The proposed mine would not result in any significant net benefit to the area from job or income creation.

Need for the Proposed Mine

Adverse economic effects of the proposed gravel mine to the Richland community must be balanced against the county's broader needs for aggregate material for road construction. Currently, 15 gravel mines operate in Kalamazoo County according to the Kalamazoo County Planning Department (Table 2). Stoneco's application materials do not provide any evidence for the need for additional capacity. Statistics were cited on projected needs, but no evidence was presented as to whether existing capacity could cover anticipated needs.

The need for additional capacity of gravel production is not supported by current and projected population or employment trends in Kalamazoo County. Population growth in Kalamazoo County has been modest during the past five years, and well below the national rate. From 2000 to 2005, population in the county increased annually at a rate of

---

[7]Hite's statistical analysis intentionally includes homes at a distance deemed unaffected by the gravel operation. Our choice to study the impacts up to 3 miles is based on Nelson, et al. (1992) and the fact that estimated impacts for individual homeowners are still relatively large out to three miles in all of Hite's models.

[8] The Upjohn Institute maintains a regional economic impact and forecasting model for the Kalamazoo metropolitan area which was built by Regional Economic Models Incorporated (REMI) especially for the Upjohn Institute. The REMI modeling approach, which incorporates an input-output model with a forecasting model and a relative cost of production model, has been repeatedly reviewed and upheld as the industry standard.

below 0.2 percent, compared to 0.9 percent nationwide.[9] An analysis of the individual components of population change—births, deaths, net migration—shows that individuals and households, on net, are leaving the county. From 2000 to 2005, the county's population increased by 6,342 individuals due to number of births surpassing the number of deaths. However, on net, 4,150 individuals moved out of the county.[10]

Table 2

Kalamazoo County Gravel Pits

Owner Name	Site Address	Site Township
Aggregate Industries	C Ave. Near 6th St	Alamo
Art Austin	6287 K Avenue	Comstock
Triple B Aggregates	2702 Ravine Rd.	Kalamazoo
Thompson McCully Co	3800 Ravine Rd.	Kalamazoo
Byholt, Inc.	1600 Sprinkle Rd.	Brady
Byholt, Inc.	4th St	Prairie Ronde
Fulton Brothers Gravel	4th St	Prairie Ronde
Balkema Excavating	8964 Paw Paw Lk.	Prairie Ronde
Balkema Excavating	6581 E. K Ave	Comstock
Balkema Excavating	4274 Ravine Rd	Kalamazoo
Balkema Excavating	40th St. & I-94	Charleston
Balkema Excavating	14500 E. Michigan	Charleston
Balkema Excavating	15600 E. Michigan	Charleston
Consumer Concrete	10328 East M-89	Richland
Consumer Concrete	700 Nazareth Rd	Kalamazoo

Source: Kalamazoo County Planning Department July 2006

During the same time period, employment declined by 3.4 percent, a loss of 5,000 jobs. The Michigan Department of Labor and Economic Growth estimates that from 2002 to 2012, total employment in Kalamazoo and St. Joseph counties will increase at a rate of 0.8 percent—substantially below the 1.3 percent rate of growth projected for the nation as a whole. If this rate of employment growth holds true for the future, it will be not until 2010 that the county will reach its 2000 employment level.

Thus, economic projections do not, in and of themselves, indicate a need for expanded aggregate capacity. However, we emphasize that any definitive determination of need would require information on the capacity and life expectancy of existing area gravel pits, to which the Institute does not have access.[11]

Review of Stoneco's Property Value Impact Analysis

The Environmental Study submitted by Stoneco in connection with its special use permit application concludes that gravel mining operations have no adverse impact on the value of nearby properties. This conclusion is based on five reports included in Appendix J of Stoneco's Environment Study:

---

[9] U.S. Census Bureau.

[10] U.S. Census Bureau. Furthermore, Internal Revenue Service (IRS) data from 2000 to 2004 shows that the majority of the individuals leaving the county are moving outside the greater Kalamazoo region.

[11] Note that whether there is a public need for additional capacity and whether it is in Stoneco's interest to develop a new mine are distinctly different issues. Stoneco has indicated that it would reduce its transportation costs by operating at the proposed Richland location. The degree to which any lower transportation costs translate into lower prices of aggregate material—and hence broadly benefit the public—versus increased company profits will depend on the competitive structure of the industry in this region.

1. "Impacts of Aggregate Mine Operations: Perception or Reality?" Anthony Bauer, 2001.[12]

2. "Social, Economic, and Legal Consequences of Blasting in Strip Mines and Quarries," Bureau of Mines, 1981.

3. "Impact of Rock Quarry Operations on Value of Nearby Housing," Joseph Rabianski and Neil Carn, 1987.

4. "Impacts of Rock Quarries on Residential Property Values, Jefferson County, Colorado," Banks and Gesso, 1998.

5. "Proposed Fuquay-Varina Quarry: Analysis of Effect on Real Estate Values," Shlaes & Co., 1998.

These reports, in fact, fail to show that mining operations have no adverse impact on property values. None uses the standard methodology (the hedonic pricing model, described above) for evaluating property value impacts. Four of the five reports are based on flawed logic (as explained below) and hence cannot be used to draw any conclusions about property value effects. Only one report, commissioned by the U.S. Bureau of Mines, used a defensible methodology, although this report also suffers from serious limitations. Notably, this study found some evidence of adverse impacts of gravel mining operations on property values in six out of the seven sites examined.

The Bauer, Rabianski and Carn, Banks and Gesso, and Shlaes & Co. reports rely on one or both of the following types of observations to argue that gravel mining operations have minimal adverse impact on nearby property values:

- Over time, housing and commercial developments have moved closer to and sometimes adjacent to aggregate mine operations.
- For property values in the vicinity of mining operations that have existed for many decades, the rate of growth in property values does not increase with distance from the mining site.

In neither case do such observations have any bearing on the impact of aggregate mine operations on nearby property values.

1. Residential and commercial developments have located closer to and sometimes adjacent to mines over time.

   Economic or real estate analysis does not predict that properties near mines have no value or no development potential. Rather, one would expect that nearby property values would be lower to compensate for any costs (e.g. noise, pollution, unsightly landscapes, and traffic congestion) associated with the mine. This reflects the common sense observation that property that is near sources of noise, pollution, traffic congestion, and blight will (all other things being equal) be less valuable. Of course, these lower property values, in turn, will help lure development, especially

[12] Bauer (2001) is a two-page statement that in large part summarizes the results of a 1984 study by a Michigan State University student.

over time, but the development more than likely will include non-residential activities, which are not affected by the disamenities generated by the mine.

Two studies (Bauer 2001; Banks and Gesso 1998) examined aerial photographs taken over the course of several decades that showed housing and commercial developments moving closer to mining operations. As the population has expanded, land values near central cities have increased, and transportation infrastructures have improved, development has fanned out all across the country. Any study would inevitably find that over the course of the last 20, 30, or 40 years, housing developments have moved closer to mines (and any other less desirable location), and such observations have no relevance to the question posed by Stoneco's application—whether the establishment of mining operations will lower nearby property values.

2. Near well-established mines, the year-to-year change of property values is no less for properties located close to mines than for those located somewhat farther away from mines.

The adverse impact that a mine will have on nearby property values will occur within a short period of time following the establishment or announcement of the mine. After the adverse effects of being located near a mine have been capitalized into the property value—that is, after the negative effects of being close to a mine operation has resulted in a decrease in property values—we would not expect the <u>future</u> rate of change of nearby properties to be different from those of other properties, all else the same.

The analyses in Rabianski and Carn (1987), Shlaes & Co. (1988), and Banks and Gesso (1998) look at whether the relative difference in property values between properties close to and farther from a mine continue to widen 30, 50, even 100 or more years after the mine was established. All of these studies conclude that because we do not see continued widening of these differentials many decades after the establishment of mines, mines have no adverse effect on property values. This argument makes no sense: the adverse impact on property values would have occurred decades before. These studies shed no light on possible adverse impacts of mining operations on property values.

Figure 2 illustrates this point. This figure depicts the prices of two hypothetical homes over a 20-year period. Home B is affected by the opening of a gravel mine in the middle of the time period; otherwise the homes are identical. Except in the year when the gravel mine is introduced, the annual *percentage changes* in the prices of the two homes are the same. The methodology used in the reports cited in the Stoneco environmental study compared the percentage change of homes near the gravel mine (percent change from B to B′ in Figure 2) to the percentage change in home prices farther from the gravel pit (percent change from A to A′ in Figure 2). But even with adverse property value effects, these percentage differences should be approximately equal. To capture any adverse impact, one must measure the difference in values of otherwise comparable properties close to and farther from the gravel mine at a point in time. In Figure 2, the difference between points A and B or between A′ and B′ measure the true property value impact, which conceptually is what is measured in the hedonic pricing model used in the analysis reported above.

Figure 2: Methodology for Evaluating Gravel Mine Impact on House Prices: Hypothetical Case

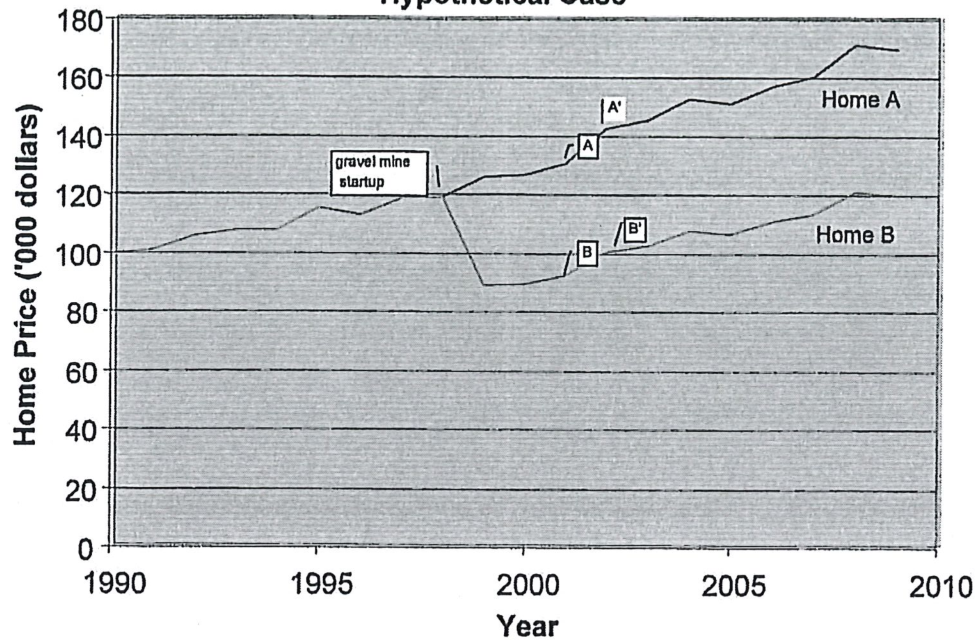

Only the study commissioned by the U.S. Bureau of Mines attempted to assess how the value of comparable homes varied with distance from the mine. However, the Bureau of Mines study suffered from several serious shortcomings:

- The sample size at each of seven sites was very small, and hence no statistically valid conclusions could be drawn.
- Homes were classified into rough typologies, and hence controls for other factors affecting home prices were crude.
- The study was based on assessed values rather than on more accurate sale price data.
- The study only examined potential property value impacts within approximately a half mile of the mine site. More recent research shows that property value effects may be significant up to two or three miles from such sites.[13] Limiting analysis to properties within a half mile of the mine site could lead to a significant understatement of any property value impacts.
- Researchers used subjective assessments to discount findings of adverse impacts on property values.

With these shortcomings in mind, the Bureau of Mines study found some evidence that the value of comparable homes increased with distance from the mine site in six of the report's seven case-study sites. In some cases, the differences in values were described as large.

[13] See, for example, Arthur C. Nelson, John Genereux, and Michelle Genereux, "Price Effects of Landfills on House Values," *Land Economics,* 1992 68(4): 359-365.

Appendix A

This report's estimation of the potential impact on residential property values in Richland Township of a proposed gravel mine is based on the following regression model developed by Diane Hite, Professor of Economics, Auburn University. The model is based on a study of 2,552 homes in Delaware County, Ohio.

The results of the model are shown below. It is important to note that the model controls for house characteristics—bath, rooms and age, as well as location from the gravel pit.

Effect of Gravel Mine Operation on House Values Less than 5 Miles Delaware County, OH 1998--Log Distance Specification

Nonlinear OLS Summary of Residual Errors								
Equation	DF Model	DF Error	SSE	MSE	Root MSE	R-Square	Adj R-Sq	Label
PRICE	8	2544	25816929	10148.2	100.7	0.2564	0.2544	PRICE

Nonlinear OLS Parameter Estimates					
Parameter	Estimate	Approx Std Err	t Value	Approx Pr > |t|	Label
a0	4.981671	2.2279	2.24	0.0254	Intercept
a1	0.097358	0.0162	6.00	<.0001	log(Miles from Gravel Pit)
a2	0.00045	0.000056	8.00	<.0001	Sale Date
a3	0.03527	0.00594	5.94	<.0001	Distance to Delaware City
a4	-4.67E-6	4.204E-6	-1.11	0.2664	FAR (House Size/Lot Size)
a6	0.248225	0.0384	6.47	<.0001	Total Baths
a7	0.078881	0.0139	5.69	<.0001	Total Rooms
a9	-0.00376	0.00110	-3.43	0.0006	Year Built

Number of Observations		Statistics for System	
Used	2552	Objective	10116
Missing	0	Objective*N	25816929

The key finding of the model is **a1** which can be interpreted as showing that a 10 percent increase in distance from the gravel mine is associated with slightly less than a 1 percent (0.97358) increase in home value, all else the same. Moreover the parameter is highly statistically significant. In other words, the chance of the gravel mine not having an adverse effect on housing values is one in a thousand.

Text Amendments to Ch. 14
Correspondence in Opposition

Bay Point Inn

From: Bay Point Inn <stay@baypointinn.com>
Sent: Sunday, May 31, 2020 9:26 AM
To: 'iriemer@co.door.wi.us'
Subject: BROADBAND TOWER TESTIMONY

this address didn't work ??

I SUPPORT THE REMOVAL OF BROADBAND TOWERS FROM CHAPTER 14 TO FACILITATE EXPANSION OF INTERNET SERVICE THROUGHOUT THE PENINSULA

Expansion of Broadband to the entire Peninsula is a critical need for the following reasons:

Many people cannot take jobs in Door County because their spouse has employment that relies on internet service
Workers who live in areas that don't have high speed internet can't work from home which is a critical need at this time.
Shut in seniors often do not have any internet service for recreation or medical needs.
Internet service is an essential need for any disaster event.
Many times disabled people can remain at home if cameras can be viewed remotely by caregivers.

Myles Dannhausen, Sr.
Egg Harbor town resident
Egg Harbor Town Supervisor
Egg Harbor Historical Society, President

mrdannhausen@gmail.com
9204210790

RECEIVED
JUN 01 2020
DOOR COUNTY
LAND USE SERVICES DEPARTMENT

Riemer, Linda

From: Paul Schwengel <igofishn.paul@gmail.com>
Sent: Monday, June 1, 2020 11:36 AM
To: Riemer, Linda
Subject: Tower ordinance, amendment, Chap 14, RPC meeting June 4th

Please support and encourage broadband internet expansion, not discourage it. The county must do better. One short term option would be to exempt fixed wireless broadband towers not more than 200 feet tall from the Chapter 14 regulations. Don't compare these 200' broadband towers to cell towers.
Thank You,
Paul Schwengel
Liberty Grove Plan Commison member
824 Top o the Thumb la
Ellison Bay, WI

RECEIVED
JUN - 1 2020
DOOR COUNTY
LAND USE SERVICES DEPARTMENT

Pioneering the Next Generation

PIONEERS

School District of Sevastopol

4550 Highway 57 • Sturgeon Bay, WI 54235 • 920-743-6282 • Fax: 920-743-4009
www.sevastopol.k12.wi.us

June 1, 2020

Dear Door County Resource Planning Committee;

I would like to address the committee on the agenda item pertaining to zoning ordinance as it relates to communications support structures and related facilities. Thank you for taking the time to read my letter.

As you are all well aware, in March our school buildings were closed for attendance. Educating our students did not stop. Instead it changed gears dramatically. Sevastopol was fortunate to have enough devices for all of our students in grades 7 through 12. Our elementary teacher held group and individual class meetings via Google. Various teachers utilized YouTube videos for instruction. Emails were not only used for communication but for students to submit homework. None of these steps taken by our teachers matter if a student did not have internet access. Our teachers did provide alternate means to educate the children without available technology. It wasn't the same type of education.

We found that this access or lack of access placed students into two groups. The haves and the have nots. Public education is based on providing for *all* students. Our students without internet were placed and still are at a disadvantage. We found over 20% of our students had little to no internet service available. This was 76 of our 348 families. As we move forward with uncertainty for fall, the realization is that public education will be dependent on remote learning on some level.

I understand fully that you have a difficult task at hand and it is a balancing act. As you take action please consider the students of our county.

Yours in Education,

Kyle Luedtke
Superintendent
School District of Sevastopol

5343 South Lake Road
Sturgeon Bay WI 54235

June 2, 2020

Re: Testimony in opposition to Door County Comprehensive Zoning Ordinance Chapter 14 Amendments as currently written

To David Enigl, Vinni Chomeau, Ray Englebert, Ken Fisher, and Richard Virlee

Thank you for your service to our Door County community. We have been full-time Door County residents for several years and strongly support all efforts to secure the best available technology in affordable high speed internet for all Door County. It needs to be a county-wide approach that encompasses all townships, allowing them to reach this attainable goal, without having to opt out of the County Ordinances individually.

We are requesting that the members of the RPC vote **against** the amendments to the Chapter 14 ordinance as proposed. The current ordinance and proposed amendments as written will do nothing to improve high speed internet access to all of Door County, particularly its more rural areas. In fact, these regulations discourage any broadband expansion. We are asking instead that the Chapter 14 ordinance be amended such that **ALL BROADBAND TOWERS** which are self-supported structures 125 feet or less in height and guywire-supported structures 200 feet or less in height **be exempt** from the ordinance as written.

If the members of RPC feel it is necessary, we support making this amendment a 12-month automatically renewable exemption, unless complaints have been submitted to the RPC relating to broadband towers in the prior year.

Our regulations need to encourage development of more widely distributed better high speed internet access for multiple reasons, specifically:

--Strong economic development: current businesses need internet access for growth and new businesses will not locate here without it

--K through 12 education and beyond: learning is being done via the internet and each child needs reliable high speed internet to compete in today's world.

--Safety: home security systems and access to urgent/emergency information is important for homeowners and businesses as has been elucidated with the current COVID-19 pandemic

--Property values and tax base: high speed internet access will sustain, if not increase, current home values and future development as reliable high speed internet is now often viewed as a "utility" like electricity and water.

--An informed electorate: people use the internet daily to access news and community information. They want this service fast, dependable, and affordable.

It is vitally important for all of Door County to move forward by expanding high speed internet services for everyone. We strongly encourage you to vote to create an exemption for broadband towers in the Chapter 14 ordinance.

We appreciate your time in considering this very important issue that affects all of Door County now and in the future.

Respectfully,
Gwenn and Joseph Graboyes

RECEIVED
JUN 02 2020
DOOR COUNTY
LAND USE SERVICES DEPARTMENT

RECEIVED
JUN 3 2020
DOOR COUNTY
LAND USE SERVICES DEPARTMENT

Town of Sevastopol
Door County, Wisconsin

June 3, 2020

Re: Broadband Access

Resource Planning Committee:

The Town of Sevastopol supports the removal of the 50-foot limit on broadband tower heights. Given the limited coverage that exists for our townspeople, we must support this action. Our desire to keep our electorate better informed and productive will leave us little choice but to remove ourselves from the County ordinance, should such restrictions prevail.

We have been one of the most proactive towns with respect to transparency of government. We were the first to have a website, and the second community in the County to have made a commitment for a PEG channel (Public Access TV station). We are currently striving to increase our ability to broadcast more of our meetings live through the internet. High speed access is needed; it is a requirement!

In addition, the school children of our community need access, and given the recent demands placed on the school system by the Covid-19 virus, the issue of increasing connectivity is especially important to their education.

Please support changing this facet of the ordinance. The need is great and the companies that want to provide the service are willing. I suspect that all of you on the committee currently have high speed access at your home or at work. I ask you to recall what it was like when you all you had dialup service!

We are doing a disservice to our community by forcing arbitrary restrictions on the expansion of broadband.

Dan Woelfel

Town of Sevastopol Chairman

danwoelfel@townofsevastopol.com

To the Door County Resource Planning Committee:

I am in opposition to the ordinance as sponsored.

I recommend the following amendment be made to Door County Chapter 14 Communications Support Structures and Related Facilities.

Add 14.04(9) (d) as follows:

> ***(d) For the purposes of Section 14.04, the language in 14.01(4) (e) shall be replaced with the following language: support structures 125 feet or less in height which do not require guy wires and support structures 200 feet or less in height which are supported with the aid of guy wires.***

The intent of this amendment is, for the purposes of Section 14.04, to replace the exemption defined in 14.01(4) (e) "Support structures 50 feet or less in height." with wording that would allow fixed wireless broadband towers as defined to be constructed without being subject to the same regulations as the much larger cell phone towers.

Statements have been made that such an exemption would make these towers unregulated. That is not correct. Their construction and placement would still be subject to all the standard building codes and other restrictions, local, county and state, to which structures are subject.

The establishment of adequate, reliable broadband service with access to the Internet is critical to the economic health of Door County, the quality of life of our residents and the satisfaction of our visitors. A wide range of experiences during the pandemic has made this painfully apparent.

This ordinance change by itself will not solve our internet access problems, but it will permit fixed wireless service to expand throughout the County. Fixed wireless technology is critical to providing broadband service in rural areas where service is currently lacking. If we continue to regulate the small fixed wireless towers with the same rules, regulations and construction requirements as we use to regulate the 20 times larger cell towers, internet access in rural Door County internet will not improve.

Eliminating this regulatory roadblock to current broadband service options will allow Door County to begin seeking federal grant opportunities as a whole county with the goal of developing adequate, reliable, high speed internet access across the County. Otherwise grant funding agencies will look at us and decide that if we don't care to help ourselves, why should they help us?`

RECEIVED

JUN 3 2020

DOOR COUNTY
LAND USE SERVICES DEPARTMENT

Sincerely,

David A. Studebaker
11823 Timberline Road #215
Ellison Bay, WI 54210
920-854-9490 (land) or (779) 245-0201 (cell)

Speaking regarding agenda item *6.1 Zoning ordinance text amendment petition. Resource Planning Committee; amend Door County Comprehensive Zoning Ordinance Chapter 14, Communications Support Structures and Related Facilities*
In opposition

From the Spring 2020 Gibraltar School News

Published May 29, 2020

Description of some of the challenges of teaching over the Internet in Door County

Who Are the Heroes?

By Bridget Schopf

Reading Specialist & Literacy Instructional Coach

Living in the middle of Door County, away from the highways, under the shelter of trees is a beautiful thing until you need a reliable internet to meet face to face with students 6-7 hours each day.

"I can't hear you. Are you talking?" "Your voice is lagging." "It's glitchy." "You sound like a robot." "You're frozen!" These are all things I've heard my students say over the course of this remote learning adventure. Being a person who plans and over plans, when things do not go as I had intended, I have been known to shed some tears.

What I've learned from my students during these trying times is flexibility. It was an elementary student whom I could not hear that started typing in the chat box in order to communicate with me and finish the lesson. It was an elementary student who said, "Let me try a different room, maybe the internet will be better." It was an elementary student who said, "I can meet with you later, maybe it will be better then." Flexibility, that's what I've learned from these courageous, persistent, hard-working students.

Every day, across media sources, we hear about heroes. Heroes who are helping us to get through this pandemic. My heroes are the students in front of me who help to problem solve while still working hard to learn. I am blessed to teach and learn from these remarkable young people every day!

RECEIVED

JUN 3 2020

DOOR COUNTY
LAND USE SERVICES DEPARTMENT

Published May 31, 2020

DCEDC "supports removal of Broadband towers from regulation under Chapter 14 of the Zoning Ordinance."

DOOR COUNTY
Economic Development Corporation
Business by Nature

Non-Traditional Finance | Business Assistance | Workforce Development

Economic Developments

May 31st, 2020

Critical Broadband Public Hearing

The Door County Resource Planning Committee (RPC) in January and then again on May 7th discussed potential amendments to the county's communication tower regulations (Chapter 14 of the zoning ordinance). The RPC voted to sponsor for public hearing the amendments to the chapter as presented.

The public hearing will be held using virtual technology on June 4th at 1:00 pm.

One issue concerning Broadband service in rural Door County revolves around regulation of towers in the County. Broadband towers are smaller and less intrusive than cell towers and larger antennas but are controlled the same under Chapter 14 of the Zoning Ordinance making it difficult to site Broadband towers.

If you are experiencing inadequate Broadband service, it will be important to make a statement during this virtual hearing. The DCEDC supports the removal of Broadband towers from regulation under Chapter 14 of the Zoning Ordinance.

Today, Broadband service is a public need and necessity that is essential for small businesses, remote workers, telehealth, and education. Inadequate or the total absence of Broadband service has a profound impact on every resident and the local economy.

Riemer, Linda

From: MAR C <micarson4524@gmail.com>
Sent: Tuesday, June 2, 2020 6:33 PM
To: Riemer, Linda; Mickie Rasch
Subject: Testimony for Enhanced Broadband Opportunities

Hello - my name is Mary Carson, and I have a home at 1254 Garrett Bay Road in Ellison Bay, WI. DC Broadband came out today to install wifi, however, because I don't have a straight view at Washington Island's tower, I have no chance of getting a signal. My neighbors on either side are also affected, and I would guess anyone north of me would be included in that dead zone.

I am writing to request your group to support and encourage broadband internet expansion. To that end, I would like your group to exempt fixed wireless broadband towers not more than 200 feet tall from the Chapter 14 regulations, so I and my neighbors and broader community can gain access to the Internet.

Unless you do, we'll all be resigned to driving back and forth to town 2-3 times a day...or more...to stay in touch with the world. There's no reason this simple fix can't be adopted, and hopefully it can happen sooner than later.

Thank you.

Mary Carson
414-339-3334

RECEIVED
JUN 3 2020
DOOR COUNTY
LAND USE SERVICES DEPARTMENT

Riemer, Linda

From: James Schuessler <jshusss@gmail.com>
Sent: Tuesday, June 2, 2020 6:40 PM
To: Riemer, Linda
Subject: Fwd: Door County Zoning Regulation 14

Please include this letter as testimony for the upcoming RPC hearing. Thank you.

I hope this email finds you safe and well. Who knew just a few months ago that a health emergency would occur that would demonstrate just how important broadband access would be to *each* household in Door County--not just those fortunate to be connected by Spectrum or in reach of existing tower infrastructure?

Although I have moved from Door County, this issue, especially at this time of health emergency, has remained in my thoughts. All citizens of Door County deserve access.

The proposed changes to the zoning regulation do not solve the problems that are constricting broadband access for Door County citizens. I believe you send a positive message to citizens without access to broadband that the county is serious about solving this issue by making revisions that reflect the distinction between cell towers and much smaller broadband towers. The health and safety of residents, especially those that make their home in Door County year-round, depends upon it.

Without making suitable corrections to Regulation 14, Door County is not likely to see significant investment to solve the problem of access to broadband.

Kindest regards,
James G. Schuessler

#OnWisconsin

RECEIVED
JUN 3 2020
DOOR COUNTY
LAND USE SERVICES DEPARTMENT

--
Jim Schuessler, CEcD, EDFP
Executive Director
Yuma Multiversity Campus
YumaMultiversity.com
c/o Gowan Building
370 South Main Street
Yuma, AZ 85364
928-210-5013

Southern Door County School District
2073 County Highway DK, Brussels, WI 54204
ENGAGE · EMPOWER · EXCEL

DISTRICT
920-825-7311; 920-825-7155 (Fax)

Patricia Vickman, Superintendent

Mark Logan, Business Manager
David Desmond, Director of Pupil Services
Dan Viste, Maintenance/Transportation

HIGH SCHOOL
920-825-7333; 920-825-1490 (Fax)
Steve Bousley, Principal

ELEMENTARY/MIDDLE SCHOOL
920-825-7321; 920-825-7692 (Fax)
Cory Vandertie, Elementary Principal
Brenda Shimon, Middle Principal

April 28, 2020

Mariah Goode, Director
Door County Land Use Services Department
Door County Government Center
421 Nebraska Street
Sturgeon Bay, WI 54235
mgoode@co.door.wi.us

RECEIVED
JUN 3 2020
DOOR COUNTY
LAND USE SERVICES DEPARTMENT

Dear Director Goode:

This is a letter of support for the modification of the current County Chapter 14 Tower Ordinance to exempt all fixed wireless broadband transmission or reception towers regardless of height. The district wrote letters of support for the successful applications of the town of Nasewaupee's Broadband Expansion grant application, as well as one for South Lake Michigan Drive. As a school district with many of our students and families residing in this area, we are pleased with the proactive steps taken by these two areas of our district to improve the accessibility to high-speed internet.

The use of technology as a tool to engage students in their learning has become an important part of today's education. This need became even more critical during the current COVID-19 challenge this spring, when the district had to provide remote learning to over 1029 students, due to the closure of school facilities from March 18, 2020 through the end of the school year. One of the biggest challenges the District faced was the availability of functional internet service for students and staff. In fact, the district needed to purchase over 150 hot spots to ensure that students had access to the virtual instruction taking place. This was due largely to limited service (internet access in the home only on phones) to insufficient service (unable to handle more than one device) to absolutely no service at all. A heat spot map of where hot spots needed to be deployed was created just this month with all the addresses of our students affected by accessibility issues.

The reality encountered by our families in Southern Door this spring, validates a 2017 Bright Bytes survey of our PreK-12 families which indicated that a majority of parents felt their Internet connection was under-connected, constrained due to service interruptions, so slow in speed that multiple users could not be accommodated, or limited to mobile-only access (smartphones) – all a result of the lack of broadband connectivity in their locations. While the District has worked with the County of Door to increase our broadband through governmental access, the reality is that for rural areas like our school district, reliable home Internet remains a challenge for Southern Door students, families, staff, and businesses in Southern Door.

Even when school is in session in our facilities, high-speed home Internet is no longer viewed as a luxury but a necessity for students' access to learning. Our district recently became a 1:1 district with each student having access to a device to assist them in their learning. A majority of the curriculum materials now consists of digital textbooks, google classroom applications, and online strategies which allow students to collaborate together. While there are workaround solutions for students without home Internet such as downloading items onto a USB drive, these are all time-consuming measures for both teachers and students that impact efficiency. More importantly, students' ability to complete meaningful online work, or have access to virtual instruction is compromised when there is such inequity as to which students have access and which ones do not. In more urban settings, such limitations may be addressed by accessing Wi-Fi hotspots at local restaurants and libraries; however, these are not feasible options in rural communities.

While many rural districts face the complications of increased weather compromised days during the winter months, we now know that there may be other crises spanning over months that affect when school can't be safely held in session. The current broadband landscape of unreliable, inconsistent and limited internet conductivity in Southern Door is not a plausible solution for students and staff. This results in our students and families not having the equity of resources at their disposal to keep abreast of their peers in other more strongly connected areas in the state, whether it is for blended learning when school is on site, during remote learning times like this spring, or when parents find it necessary to work from home.

Lastly, high-speed Internet is a huge factor in families and businesses relocating to this rural area. Three years ago, a new family chose our community as a place to raise their children and one in which they hoped to continue their international business from home. After a year of frustration with the lack of internet accessibility, they left the area and moved to the Fox Valley area in order to sustain their livelihood. Realtors have also shared that the lack of internet access in the area has also negatively impacted home sales for young families looking to move into our school district.

As an education institution, our mission is to prepare our students to be productive citizens in today's society. Greater access to high-speed internet in our district's homes and businesses will help address our educational goal for students and attract more families and businesses to the area for a more viable, thriving community.

As a district, we applaud the county for its consideration to modify the current County Chapter 14 Tower Ordinance to provide townships and municipalities with greater flexibility to make accessible, high-quality internet service a priority, particularly for our students, staff, families, and businesses. The assistance of government, broadband providers, businesses, and schools all pitching in to do their part is the only way we will close the digital-use gap that currently exists between the citizens in rural communities and their urban peers. I strongly recommend your consideration of the proposal to modify the Chapter 14 Ordinance.

Sincerely,

Patricia Vickman

Patricia Vickman, Superintendent

RECEIVED

JUN 3 2020

DOOR COUNTY
LAND USE SERVICES DEPARTMENT

Riemer, Linda

From: Dona Anderson <donacanderson@gmail.com>
Sent: Wednesday, June 3, 2020 1:00 PM
To: Lienau, David; Riemer, Linda; Gauger, Elizabeth
Subject: Broadband Tower issues

I feel that all residents of Door County should have high speed internet access, and the amendments to the Chapter 14 Ordinance as proposed would interfere with those process. Please consider a plan that would allow coordinated efforts to provide service to all of the county.

Dona Anderson
Jacksonport, WI

Riemer, Linda

From: Phil Klink <phil.klink@att.net>
Sent: Wednesday, June 3, 2020 2:28 PM
To: Riemer, Linda; Riemer, Linda
Cc: Melissa Klink
Subject: Door county broadband

Thank you for reviewing our internet challenges in Door County. My wife and I bought a second home on Clark lake in 2017. My wife's parents have had a place on the lake my wife's entire life. This is where we want to be and would like to spend as much time as possible there.

We have 3 children ages 24,18 and 16. We do not get to spend as much time as we like with our children's schedules, but would like to be there every chance we get.

I have a finance /accounting background and work for FIS. My wife stays busy with taking care of our kids and household.

With the current Covid-19 situation it has presented us with an opportunity to spend more time there. Our kids finishing school online and me working remote. We were fortunate that our internet worked well enough for our kids to do most of their schooling. They did have challenges with video calls.

My wife and two younger kids stayed up there for the better part of 2 months but I was not as lucky as our internet solution was not enough for me to work remote. Any conference calls thru Teams or other programs were not good as the internet speed was not enough to support the program and there was a delay of 3-5 seconds which made calls bad.

In the 3 years we have owned this property we have tried 4 different internet services.

1) HughesNet was our first program. It worked generally fine But was very slow, expensive and with data limits.

2) About a year in, we got wind of a possible solution with US Cellular WiFi service. We signed up for the service and worked better in the beginning, but as leaves grew on trees the service got gradually worse and would not support our security cameras. We ended up switching back to Hughes net. Cellular service is still very spotty at best in our area. Somewhat of a concern if emergency arises.

3) In 2020 during Covid, we got wind that we might be a candidate for Door County Broadband. They came out to the house and tried to find a signal, they were unable to get a strong enough signal to proceed with install (interestingly my father in law who lives 100 feet to the south had them out the same day and they found a signal and he was able to get setup). The installer suggested we try Viasat satellite internet.

4) So a couple months age we had Viasat installed. It has been better than HughesNet, is less expensive and has more high speed data. It performs slightly better for my remote work needs but is still not enough where I could work regularly remote from here.

During these last several months, my family has lived up in door county and I would go back and forth every week to Hartford to work remote from our house there and then go back up to Clark Lake every weekend.

My family is very interested in improving our internet options up there as it would allow us to lead our normal lives from there, seeing as my long term ability to work from home looks to continue. This would allow us to be up there more often enjoying our place and supporting the Door County economy.

Thank you

Phil and Melissa Klink

Sent from my iPhone